Liver and Gallbladder Morphology of the juvenile Nile crocodile, *Crocodylus niloticus* (Laurenti, 1768)

by

ERNA VAN WILPE

Submitted in partial fulfilment of the requirements for the degree MSc

DEPARTMENT OF ANATOMY AND PHYSIOLOGY

FACULTY OF VETERINARY SCIENCE

UNIVERSITY OF PRETORIA

2012

Supervisor: Professor H.B. Groenewald

Department of Anatomy and Physiology

Faculty of Veterinary Science

University of Pretoria

Pretoria

DECLARATION

I declare that the dissertation which I hereby submit for the degree MSc at the University of Pretoria is my own work and has not been submitted by me for a degree at another university.

To my husband Deon, for your support and patience

To my Pa, wish you were here....

CONTENTS

ACKNOWLEDGEMENTS

SUMMARY

Liver and Gallbladder Morphology of the juvenile Nile crocodile, *Crocodylus niloticus* (Laurenti, 1768)

by

ERNA VAN WILPE

SUPERVISOR: Professor Herman B. Groenewald

DEPARTMENT: Department of Anatomy and Physiology, Faculty of Veterinary Science, University of Pretoria, Private Bag X04, Onderstepoort, 0110, Republic of South Africa.

Degree: MSc (Veterinary Science)

This investigation illustrates the topography, gross anatomy, histology and ultrastructure of the liver and gallbladder of the Nile crocodile in order to fill the gap that exists in the literature regarding this important crocodilian. For the topographical and macroscopical descriptions the livers and gallbladders were obtained from the carcasses of slaughtered juvenile Nile crocodiles. Perfusion and immersion fixation of tissues for histology and transmission electron microscopy were performed on juvenile Nile crocodiles donated to the university. Published descriptions of other vertebrates were inevitably relied upon for comparison due to the lack of information on these two organs of the Nile crocodile.

The liver was located in its own coelomic cavity with the post-pulmonary and the post-hepatic membranes intimately associated with the cranial and caudal surfaces of the bi-lobed liver respectively. The right lobe was larger than the left lobe and they were located at the level of the third to seventh intercostal spaces with their extremities extending to the ninth intercostal space. The triangular shaped liver lobes were joined dorso-medially by a narrow isthmus consisting of liver tissue. The liver was covered by Glisson's capsule.

Central veins, sinusoids and portal tracts were distributed haphazardly with no visible lobulation. The parenchymal component occupied the largest part of the liver and was formed by anastomosing and branching cell cords consisting of two-cell-thick plates in the longitudinal sectional plane and at least five hepatocytes in the cross-sectional plane. Central bile canaliculi contained microvilli originating from apical hepatocyte surfaces and were sealed off by junctional complexes. Hemosiderin granules, bile pigments, melanin pigments, lipid droplets, cholesterol ester slits and glycogen granules were observed in addition to the normal hepatic cytoplasmic organelles.

Non-parenchymal cells consisted of endothelial cells, Kupffer cells, stellate cells and pit cells localized in and around the angular sinusoids. The space of Disse existed between endothelial cells and the base of the hepatocytes which was lined by microvilli. Endothelial cells were flat cells with long fenestrated cytoplasmic extensions that lined the sinusoidal wall and contained numerous endocytotic vesicles and many lysosomes. Pleomorphic Kupffer cells were located in the sinusoidal lumen, in the space of Disse and within groups of hepatocytes. They were often situated between groups of hepatocytes, connecting two adjacent sinusoids. Large phagosomes were present in the Kupffer cells and contained a combination of melanin and hemosiderin granules as well as ceroid. Phagocytosis of apoptotic and dying cells was evident. Conspicuous groups of membrane-bound tubular organelles with a filamentous or crystalline interior were present in the Kupffer cells. Stellate cells occupied a subendothelial position in the space of Disse and contained prominent lipid droplets that indented the nuclei. A solitary cilium was infrequently found projecting into the space of Disse. Myofibroblastic cells were found in the same region as stellate cells. Pit cells with indented eccentric nuclei were found in the sinusoidal lumen and in close contact with endothelial and Kupffer cells. Numerous small electron-dense membrane-bound cytoplasmic granules were present. Occasional intercalated cells

resembling lymphocytes were seen in the space of Disse and forming part of the groups of hepatocytes.

Glisson's capsule extended collagenous trabeculae into the parenchymal interior and variably sized trabeculae randomly traversed the liver tissue. Portal tracts were enmeshed by a collagenous network that contained fibroblasts, lymphocytes, plasma cells and phagocytes. Portal triads consisted of branches of the portal vein, hepatic artery and bile duct with lymphatic vessels sometimes in accompaniment. Reticular fibres were positioned around hepatocyte tubules and a basal lamina supported the hepatocytes adjacent to Glisson's capsule. Occasional unmyelinated nerve axons were present. The isthmus contained liver tissue with similar parenchymal and a non-parenchymal components.

Three anatomical zones were identified in the pouch-like gallbladder that was attached caudally to the right liver lobe in the dorso-medial region. The gallbladder wall consisted of pseudostratified columnar epithelium, a *lamina propria,* a *muscularis externa* and a serosal layer. The accumulation of apical secretory granules, apical bulging, exocytosis of mucous granules and the desquamation of the apical portions of the epithelial cells into the lumen indicated different stages of the mucus secretory cycle.

CHAPTER 1
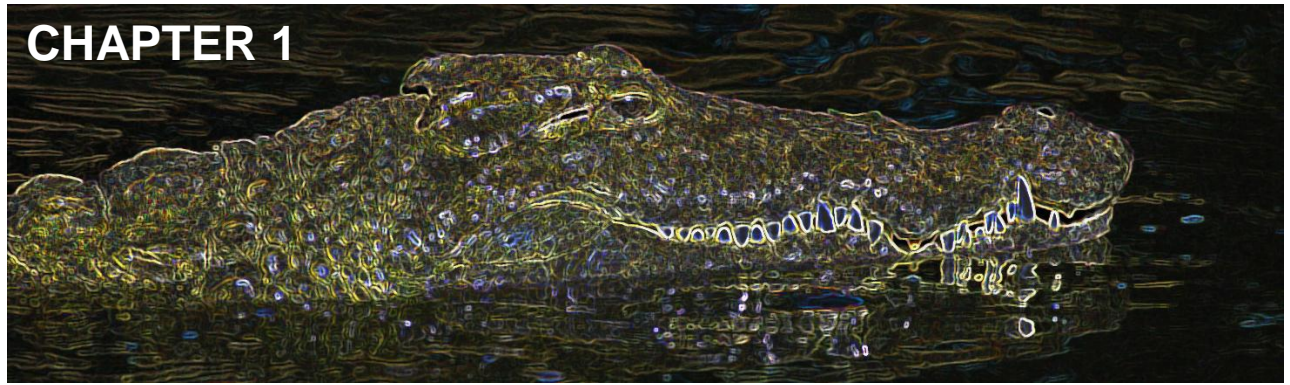
GENERAL INTRODUCTION

Modern crocodiles descended from ancestors about 225 million years ago in the late Triassic period in Europe, South America and South Africa (Seymore *et al.* 2004; Summers 2005). According to Trutnau & Sommerlad fossil records of the Nile crocodile found in North and East Africa date back 2.5 to 3.5 million years (2006, cited in http://library.sandiegozoo.org/factsheets/nile_crocodile/crocodile.htlm).

The Nile crocodile belongs to the class Reptilia, the order Crocodylia, the suborder Eusuchia (modern crocodiles), the family Crocodylidae and the subfamily Crocodylinae. (http://library.sandiegozoo.org/factsheets/nile_crocodile/crocodile.htlm). The Crocodylinae includes the genera *Osteolaemus* and *Crocodylus.* Crocodiles are diapsid ("two arched") reptiles (Benton 1985) and the diapsids are subdivided into Lepidosauria (lizards & snakes) and Archosauria that include modern birds and crocodiles.

The scientific name *Crocodylus niloticus* is derived from the Greek *kroko* (meaning "pebble") referring to the rough texture of the skin, and *deilos* (meaning "worm"). (http://library.sandiegozoo.org/factsheets/nile_crocodile/crocodile.htlm). *Niloticus* means "of the Nile River". The Nile crocodile is the largest crocodile in Africa with total body lengths of between 2 and 5 m and a mass of up to 1000 kg having been recorded (Pooley & Gans 1976).

Crocodile farming is a niche farming industry with approximately 40 farms still viable in South Africa and Zimbabwe. The commercial importance of crocodiles lie in their skin and meat and the Chinese population use certain organs for medicines (Putterill 2002). It has been reported that the Nile crocodile has been one of the top commercially utilized species of crocodiles in the world (Ross 1998).

The liver is the largest internal organ in the reptilian body and has many complex functions that are vital for metabolism and homeostasis. Major metabolic functions include carbohydrate (energy storage), protein (plasma proteins, peptide hormones) and lipid metabolism (bile salts) (McClellan-Green, Celander & Oberdörster 2006). As such the liver also stores vitamins and iron and is involved in glucose, lipid and cholesterol metabolism, the synthesis of amino acids and the degradation of toxins. The hepatic enzymes are responsible for the metabolism of xenobiotic substances, for example pollutants. The antioxidant defense system in the liver through its enzymes manages the elimination of the reactive oxygen species, namely hydroxyl radicals, superoxide radicals and hydrogen peroxide. The melanin in reptilian livers acts additionally as a free radical trap for superoxide.

The morphology of the mammalian liver has been studied extensively (Elias & Bengelsdorf 1952; Elias 1955; Schaffner 1998). Elias & Bengelsdorf (1952) also noted the liver morphology of alligators, birds and lizards. Beresford & Henninger (1986) tabulated the microscopical variations in livers of mammals, birds, fishes and reptiles. Crocodiles were not included in these comparative studies. Ultrastructural features of the livers of various animals were described by Kalashnikova (1996), but crocodiles were excluded.

An overview of the anatomy and histology of the reptilian liver was given by Jacobson (2007), with McClellan-Green *et al.* (2006) covering the basic anatomy and fine structure of the same. The liver morphology of the freshwater turtle was described by Moura *et al.* (2009) and that of the Newt by Goldblatt *et al.* (1987), while Marycz & Rogowska (2007) discussed the general liver topography of terrestrial tortoises. Many articles concentrate only on specific constituents of the liver, for example, Ito cells, Kupffer cells, sinusoids or the perisinusoidal space, and not on the liver architecture as a whole (Purton 1976; Aterman 1986; De Brito Gitirana 1988; Kalashnikova 1992; Geerts, Bouwens & Wisse 1998; Ghoddusi & Kelly 2004). The liver of reptiles differs in size, shape and appearance among species (Schaffner 1998) and although liver cells in the different classes of animals share common organelles, the cell structure varies both between and within classes (Kalashnikova 1996). Divers & Cooper (2000) stated that there was a lack of knowledge of hepatic metabolism and the pathogenesis of hepatic disease in the reptilian liver. McClellan-Green *et al.* (2006) commented on the lack of documented neoplastic diseases in reptiles and the need to form a link between liver disease and exposure to specific chemicals. Ganser, Hopkins, O'Neil, Hasse, Roe & Sever (2003) found a definite

connection between liver tissue damage and dietary contamination in their study on the liver of the Southern Watersnake. Schaffner (1998) mentioned that regarding the reptilian liver the two main routes of investigation have been its metabolic function and its place in the structural evolution of the organ in vertebrates. Hopkins (2000) stated that "Reptiles are the least studied group of vertebrates with regard to environmental contaminants".

General descriptions of the crocodilian liver can be found in Huchzermeyer (2003) and Schaffner (1998). The macroscopic anatomy of the abdominal organs of the Nile crocodile was documented by Van der Merwe & Kotzé (1993) and the serous cavities by Mushonga & Horowitz (1996). Light microscopical and ultrastructural findings on the liver of immature West African crocodiles *Osteolaemus tetraspis* were published by Storch, Braunbeck & Waitkuwait (1989). The general anatomy of the liver of the saltwater crocodile *Crocodylus porosus* was discussed by Richardson, Webb & Manolis (2002) and the occurrence of fibrous trabeculae in the American alligator *Alligator mississipiensis* liver was described by Beresford (1993).

The gallbladder functions as an auxiliary organ of the digestive tract that stores diluted bile received from the hepatic duct via the cystic duct (Oldham-Ott & Gilloteaux 1997; Ross, Kaye & Pawlina 2003; Fried 2008). It concentrates the bile by reabsorbing water and replacing electrolytes through an active sodium chloride pump. The presence of fat in the proximal duodenum triggers hormones that effect smooth muscle contraction of the gall-bladder with resulting secretion of the concentrated bile into the duodenum. The gallbladder therefore plays a significant role in controlling the flow of bile to the intestine when needed.

The anatomy of the reptilian and crocodilian gallbladder is briefly mentioned by Richardson *et al.* (2002), Huchzermeyer (2003) and Jacobson (2007). Xu, Elsey, Lance, Javors, Chen, Salen, & Tint (1997) studied the biliary ductal system and the bile fistula in the American alligator. A comparative morphological study of the gallbladder and biliary tract of vertebrates was done by Oldham-Ott & Gilloteaux (1997). There was no specific mention of the Nile crocodile gallbladder.

The aims of the study are to describe:

- the topography of the liver and gallbladder
- the macroscopic appearance of the liver and gallbladder.
- the histology of the liver and gallbladder.
- the ultrastructural features of the liver and gallbladder.

Benefits

Ecologists have considered the Nile crocodile as an important keystone species for aquatic biodiversity in Africa (Pooley, 1969; Tinley, 1976, cited in Ashton 2010) and also specifically for the Olifants River in South Africa (Joubert 2007, cited in Ashton 2010). Nile crocodile mortalities along the Olifants River between 2008 and 2009 amounted to almost 200 carcasses with the histolopathogical examination finding pansteatitis as the cause of death (Ashton 2010). Polluted freshwater ecosystems were possibly responsible for the demise of the animals.

The literature review clearly shows that data on the normal liver and gallbladder morphology of the Nile crocodile are virtually non-existent, which means that there is no reference baseline information to compare with diseased livers.

An in-depth study of the topography, anatomy, histology and ultrastructure of the Nile crocodile liver and gallbladder will enhance our understanding of the normal morphology of these organs. Knowledge of the normal micro-morphology of the liver is essential for the pathological evaluation of disease. Baseline data will be established for comparative liver and gallbladder studies.

1.1 <u>REFERENCES</u>

ASHTON, P.J. 2010. The demise of the Nile crocodile (*Crocodylus niloticus*) as a keystone species for aquatic ecosystem conservation in South Africa: The case of the Olifants River. *Aquatic Conservation: Marine and Freshwater Ecosystems*, 20: 489–493.

ATERMAN, K. 1986. The parasinusoidal cells of the liver: a historical account. *Histochemical Journal,* 18: 279-305.

BERESFORD, W.A. & HENNINGER, J.M. 1986. A tabular comparative histology of the liver. *Archivum Histologicum Japonicum,* 49: 267-281.

BERESFORD, W.A. 1993. Fibrous trabeculae in the liver of alligator (*Alligator mississipiensis*). *Annals of Anatomy,* 175: 357-359.

DE BRITO GITIRANA, L. 1988. The fine structure of the fat-storing cell (Ito cell) in the liver of some reptiles. *Zeitschrift Mikroskopish- Anatomische Forschung,* 102: 143-149.

DIVERS, S.J. & COOPER, J.E. 2000. Reptile hepatic lipidosis. *Seminars in Avian and Exotic Pet Medicine*, 9:153-164.

ELIAS, H. & BENGELSDORF, H. 1952. The structure of the liver of vertebrates. *Acta Anatomica,* 15: 297-337.

ELIAS, H. 1955. Liver morphology. *Biological Reviews,* 30: 263-310.

FRIED, G.H. 2008. Liver, in *AccessScience*, ©McGraw-Hill Companies.
http://www.accessscience.com

GANSER, L.R., HOPKINS, W.A., O'NEIL, L., HASSE, S., ROE, J.H. & SEVER, D.M. 2003. Liver histopathology of the Southern Watersnake, *Nerodia fasciata fasciata*, following chronic exposure to trace element-contaminated prey from a coal ash disposal site. *Journal of Herpetology,* 37: 219–226.

GEERTS, A., BOUWENS, L. & WISSE, E. 1998. Ultrastructure and function of hepatic fat-storing and pit cells. *Journal of Electron Microscopy Technique,* 14: 247-256.

GHODDUSI, M. & KELLY, W.R. 2004. Ultrastructure of *in situ* perfusion-fixed avian liver, with special reference to structure of the sinusoids. *Microscopy Research and Technique,* 65: 101-111.

GOLDBLATT, P.J., HAMPTON, J.A., DIDIO, L.N., SKEEL,K.A. & KLAUNIG, J.E. 1987. Morphologic and histochemical analysis of the Newt (*Notophthalmus viridescens*) liver. *The Anatomical Record,* 217: 328-338.

HOPKINS, W.A. 2000. Reptile toxicology: challenges and opportunities on the last frontier in vertebrate ecotoxicology. *Environmental Toxicology and Chemistry,* 19: 2391-2393.

HUCHZERMEYER, F.W. 2003. Crocodiles and alligators, in *Crocodiles: biology, husbandry and diseases,* edited by F.W. Huchzermeyer. Cambridge: CABI Publishing, pp. 1-52.

JACOBSON, E.R. 2007. Overview of reptile biology, anatomy, and histology, in *Infectious diseases and pathology of reptiles,* edited by E.R. Jacobson. CRC Press, Taylor & Francis Group, 6000 Broken Sound Parkway NW, Suite 300, Boca Raton, FL 33487-2742, pp. 1-130.

KALASHNIKOVA, M.M. 1992. Erythrophagocytosis and pigmented cells of the amphibian liver. *Bulletin of Experimental Biology and Medicine,* 113: 82-84.

KALASHNIKOVA, M.M. 1996. Liver cells in a comparative morphological series of animals: ultrastructural features and their significance. *Bulletin of Experimental Biology and Medicine,* 6: 543-548.

MARYCZ K., ROGOWSKA K. 2007. The liver morphology and topography of Horsfield's (*Testudo horsfieldi*) and Hermann's (*T. Hermanni*) terrestrial tortoises. *Electronic Journal of Polish Agricultural Universities,* 10: 1-9.

MCCLELLAN-GREEN, P., CELANDER, M. & OBERDÖRSTER, E. 2006. Hepatic, renal and adrenal toxicology, in *Toxicology of reptiles,* edited by S.C. Gardner & E. Oberdörster. CRC Press, Taylor & Francis Group, 6000 Broken Sound Parkway NW, Suite 300, Boca Raton, FL 33487-2742, pp. 123-148.

MOURA, L.R., SANTOS, A.L.Q., BELLETI, M.E., VIEIRA, L.G., ORPINELLI, S.R.T. & DE SIMONE, S.B.S. 2009. Morphological aspects of the liver of the freshwater turtle *Phrynops geoffroanus* Schweigger, 1812 (Testudines, Chelidae). *Brazilian Journal of Morphological Science,* 26: 129-134.

MUSHONGA, B. & HOROWITZ, A. 1996. Serous cavities of the Nile crocodile (*Crocodylus niloticus). Journal of Zoo and Wildlife Medicine,* 27: 170-179.

OLDHAM-OTT, C.K. & GILLOTEAUX, J. 1997. Comparative morphology of the gallbladder and biliary tract in vertebrates: variation in structure, homology in function and gallstones. *Microscopy Research and Technique,* 38: 571-597.

POOLEY, A. & GANS, C. 1976. The Nile crocodile. *Scientific American,* 234: 114-124.

PURTON, M.D. 1976. Extravascular cells within the perisinusoidal space of the avian liver. *Cellular and Molecular Life Sciences,* 32: 737-739.

PUTTERILL, J.F. 2002. A morphological study of the oral cavity, pharyngeal cavity and the oesophagus of the Nile crocodile, *Crocodylus niloticus* (Laurenti, 1768). MSc thesis, University of Pretoria.

RICHARDSON, K.C., WEBB, G.J.W. & MANOLIS, S.C. 2002. Digestive system, in C*rocodiles: inside out,* edited by K.C. Richardson. Australia: Surrey Beatty & Sons, pp. 89-94.

ROSS, J.P. 1998. *Status Survey and Conservation Action Plan,* edited by J.P. Ross. Switzerland: IUCN-SSG/CSG **http://www.iucncsg.org/ph1/modules/Publications/action_plan1998/plan1998a.htm#Contents**

ROSS, M.H., KAYE, G.I. & PAWLINA, W. 2003. *Histology: a text and atlas.* 4th ed. Lippincott Williams & Wilkens, Baltimore, USA.

SCHAFFNER, F. 1998. The hepatic system, in *Biology of reptilia: volume 19, Morphology G: Visceral organs,* edited by C. Gans & A.B. Gaunt. Missouri: Society for the Study of Amphibians and Reptiles, pp. 485-531.

SEYMOUR, R.C., BENNETT-STAMPER, S., JOHNSTON, D., CARRIER, D. & GRIGG, G. 2004. Evidence of endothermic ancestors of crocodiles at the stem of archosaur evolution. *Physiology Biochemistry Zoology,* 77: 1051-1067.

STORCH, V., BRAUNBECK, T. & WAITKUWAIT, W.E. 1989. The liver of the West African crocodile *Osteolaemus tetraspis.* An ultrastructural study. *Submicroscopical Cytology and Pathology,* 21: 317-327.

SUMMERS, A. 2005. Warm-hearted crocs. *Nature,* 434: 833-834.

VAN DER MERWE, N.J. & KOTZÉ, S.H. 1993. The topography of the thoracic and abdominal organs of the Nile crocodile *(Crocodylus niloticus). Onderstepoort Journal of Veterinary Research,* 60: 219-222.

XU, G., ELSEY, R.M., LANCE, V.A., JAVORS, B., CHEN, T.S., SALEN, G. & TINT, G.S. 1997. A study on the biliary ductal system and bile fistula in the American alligator, *Alligator mississipiensis. The Journal of Experimental Zoology,* 279: 554-561.

WWW Site reference:

http://library.sandiegozoo.org/factsheets/nile_crocodile/crocodile.htlm

CHAPTER 2
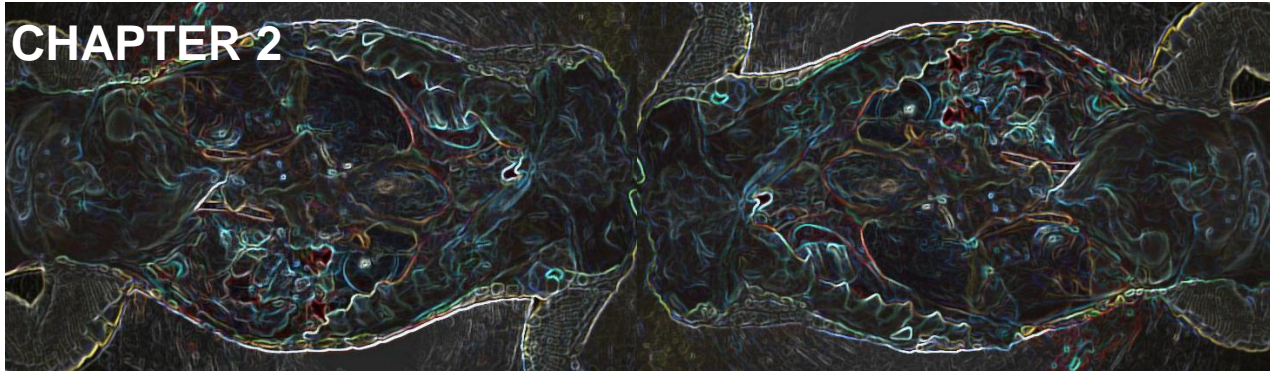
TOPOGRAPHY OF THE LIVER AND GALLBLADDER

2.1 INTRODUCTION

The variety of forms of the reptilian liver have long been recognized (Owen 1866). The topography of this organ has received moderate attention in the literature with authors giving consideration mostly to testudines, lizards, alligators, snakes and crocodiles. The liver of reptiles have unusual shapes because they conform to the shape of the coelomic cavity of the species in which it is found, for example, it is elongated and slim in snakes (Schaffner 1998). Goldblatt *et al.* (1987) described the gross morphology of the Newt liver, Marycz and Rogowska (2007) explained the liver topography of Horsfield's and Hermann's tortoises and Moura *et al.* (2009) described the coelomic cavity and identified four liver lobes in the freshwater turtle. A short discussion of the topography of the liver of three species of the family Alligatoridae was given by Romão, Santos, Lima, De Simone, Silova, Hirano, Vieira & Pinto (2011). Richardson *et al.* (2002) reported on the positioning of the liver and its adjacent structures in the Saltwater crocodile *Crocodylus porosus*. The anatomical relationship of the crocodilian liver with other organs and the location of the crocodilian liver in the coelomic cavity was noted briefly by Schaffner (1998), Huchzermeyer (2003) and Jacobson (2007).

Two articles have referred specifically to the topography of the Nile crocodile liver. One described the hepatic coelom and provided a schematic drawing depicting the position of the liver in relation to heart, stomach and duodenum (Van der Merwe & Kotzé 1993). The other article described the right and left hepatopulmonary bursae which included detailed topography of the liver (Mushonga & Horowitz 1996).

The topography of the gallbladder is briefly mentioned in most of the referenced literature above, as well as by Owen (1866). In addition Oldham-Ott & Gilloteaux (1997) reviewed

the morphology of the gallbladder and biliary tract in fish, reptiles, amphibians, birds and mammals. Xu *et al.* (1997) demonstrated the potential anatomical variations of the biliary ductal system in the American alligator *Alligator mississippiensis.*

2.2 MATERIALS AND METHODS

The carcasses of three 1-year old juvenile Nile crocodiles that were slaughtered for their skins at the Le Croc Crocodile Breeding Farm near Brits in the North West Province were used for the topographical description of the liver and gallbladder. The ventral body wall, the ribs and fat layer were removed to expose the abdominal organs *in situ.* The organs were photographed with a Canon 5D Mark II camera using a 28-135mm zoom lens.

2.3 RESULTS

The liver was located in a cavity between the thoracic and abdominal organs. It was surrounded cranially by the post-pulmonary membrane and caudally by the post-hepatic membrane (Fig. 2.1). The liver, in relation to the ribcage, was located between the third and seventh intercostal spaces with its margins spreading to the ninth intercostal space. The liver was bi-lobed with the right lobe being larger than the left lobe (Fig. 2.2). The right lobe was associated caudally with the double-looped duodenum via the hepatoduodenal ligament and the left lobe was attached to the cranial surface of the stomach by the gastrohepatic ligament. A narrow isthmus, situated dorso-medially, connected the two liver lobes. The heart, in its pericardial sac, was connected to both liver lobes by the coronary ligament with the apex lodged ventrally to the isthmus between the two liver lobes.

The empty gallbladder had a flattened sac-like shape and was attached caudally to the dorso-medial aspect of the right liver lobe by the hepatocystic ligament. When fully distended the gallbladder had the form of a blind-ending pouch with its body lodged ventromedially between the duodenum on the right and the stomach on the left (Fig. 2.3).

2.4 DISCUSSION

This study confirms the description by Van der Merwe & Kotzé (1993) that the Nile crocodile liver is located in its own coelomic cavity with the post-pulmonary and the post-hepatic membranes being intimately associated with the cranial and caudal surfaces of the bi-lobed liver respectively. The findings also endorse the topographical description of the Nile crocodile liver given by Mushonga & Horowitz (1996) who note that the right lobe is larger than the left lobe and that they are found at the level the third to the seventh intercostal spaces with their extremities extending to the ninth intercostal space.

Schaffner (1998) concurred that the crocodilian liver occupies a large portion of the coelomic cavity and is situated under the posthepatic septum. Richardson *et al.* (2002) also stated that the large bilobed liver of crocodilians lies transversely across the junction of the thoracic and abdominal regions and that the visceral surface is associated with the stomach on the left and the duodenum on the right. He also found that the Saltwater crocodile was almost unlobed with just an indentation indication the beginning of a division. Huchzermeyer (2003) described the crocodilian bi-lobed liver as occupying the hepatic coelom between two transverse membranes with the lobes being of almost equal size, in contrast to the findings of this study where the right lobe is larger than the left lobe. Romão *et al.* (2011) commented on a direct connection of the liver to the pancreas in one alligator specie (*Paleosuchus palpebrosus*), but a similar connection was not found in the Nile crocodile.

This study also confirms that the Nile crocodile liver lobes are joined in the middle by a narrow isthmus (Mushonga & Horowitz 1996). Richardson (2002) described the hepatic isthmus as being dorsally located between the two lobes in crocodiles. Some crocodile species have two separate liver lobes with other species' lobes linked by a dorsal bridge (Huchzermeyer 2003). Chiasson (1962) noted briefly that the bi-lobed liver of alligators were connected by a "middle constricted portion". Van der Merwe & Kotze (1993) and Romão *et al.* (2011) did not mention the existence of a liver isthmus in the Nile crocodile or in three alligator species respectively.

The liver topography of other reptiles differs significantly from crocodilians, for example, Goldblatt *et al.* (1987) and Moura *et al.* (2009) described four liver lobes in *Notophthalmus viridescens* (Newt) and *Phrynops geoffroanus* (freshwater turtle) respectively. Machado

Júnior, Sousa, Carvalho *et al.* (2005, cited by Moura *et al.* 2009) found five lobes in *Kinosternon scorpioides* (scorpion mud turtle) and Ells (1954) discovered three lobes in the lizard *Sceloporus occidentalis biseriatus.* As already mentioned, the livers in snakes are elongated, but are also unlobed and in some lizards only a deep indentation defines a form of lobation (Guibe 1970, cited by Oldham-Ott & Gilloteaux 1997). In Chelonians the liver is a large, saddle-shaped organ filling the abdominal region under the lungs (McClellan-Green *et al.* 2006) with the left lobe being considerably smaller than the right lobe (Jacobson 2007). In 2009 Kassab *et al.* stated that the left lobe of the Desert tortoise (*Testudo graeca*) liver was larger than the right lobe which opposes what was found in the Nile crocodile. Lizards lack a posthepatic septum (Schaffner 1998) which contrasts with the caudal presence of this membrane around the liver of the Nile crocodile.

Regarding the Nile crocodile gallbladder, Van der Merwe & Kotzé (1993) stated only that it is located to the right of the midline within the hepatic coelom. Mushonga & Horowitz (1996) found that the gallbladder was situated at the caudal surface of the right liver lobe at its ventromedial angle. The current study also describes the gallbladder as being located caudal to the right liver lobe in the ventromedial position, but the neck area is attached to the right liver lobe through the hepatocystic ligament in the dorso-medial position.

In crocodilians in general, the gallbladder is 'held close' to the right liver lobe by a fibrous ligament (Richardson *et al.* 2002) or lies between the two lobes (Huchzermeyer 2003). Romão *et al.* (2011) in their study of the digestive system of three alligator species placed the gallbladder's location dorso-medially and caudal to the right liver lobe. Richardson *et al.* (2002) in their illustration of the Saltwater crocodile showed the gallbladder to be attached caudally to the liver by a fibrous ligament in the dorso-medial region.

The position of the gallbladder varies among reptilian species. In testudines, chelonians and some lizards the gall bladder is embedded in the right lateral lobe, with the scorpion mud turtle being the exception by having its gall bladder located in the middle of the right lateral and medial lobes (Moura *et al.* 2009; Jacobson 2007). The gallbladder of the lizard *Sceloporus* is located in the middle liver lobe (Ells 1954). Snakes have their gall- bladders separate but related caudally to the liver (Owen 1866; Moura *et al.* 2009). In the newt with its four liver lobes the gallbladder lies dorsally on the liver surface between the right upper and lower lobes (Goldblatt *et al.* 1987).

2.5 REFERENCES

CHIASSON, R.B. 1962. Digestive system, in *Laboratory anatomy of the alligator.* USA: WM.C. Brown, pp. 36-37.

ELLS, H.A. 1954. The gross and microscopic anatomy of the liver and gall bladder of the lizard, *Sceloporus occidentalis biseriatus* (Hallowell). *The Anatomical Record,*119: 213-229.

GOLDBLATT, P.J., HAMPTON, J.A., DIDIO, L.N., SKEEL,K.A. & KLAUNIG, J.E. 1987. Morphologic and histochemical analysis of the Newt (*Notophthalmus viridescens*) liver. *The Anatomical Record,* 217: 328-338.

HUCHZERMEYER, F.W. 2003. Crocodiles and alligators, in *Crocodiles: biology, husbandry and diseases,* edited by F.W. Huchzermeyer. Cambridge: CABI Publishing, pp.1-52.

JACOBSON, E.R. 2007. Overview of reptile biology, anatomy, and histology, in *Infectious diseases and pathology of reptiles,* edited by E.R. Jacobson. CRC Press, Taylor & Francis Group, 6000 Broken Sound Parkway NW, Suite 300, Boca Raton, FL 33487-2742, pp.1-130.

KASSAB, A., SHOUSHA, S. & FARGANI, A. 2009. Morphology of blood cells, liver and spleen of the Desert Tortoise (*Testudo graeca*). *The Open Anatomy Journal,* 1*:* 1-10.

MARYCZ K., ROGOWSKA K. 2007. The liver morphology and topography of Horsfield's (*Testudo horsfieldi*) and Hermann's (*T. Hermanni*) terrestrial tortoises. *Electronic Journal of Polish Agricultural Universities,* 10: 1-9.

MCCLELLAN-GREEN, P., CELANDER, M. & OBERDÖRSTER, E. 2006. Hepatic, renal and adrenal toxicology, in *Toxicology of reptiles,* edited by S.C. Gardner & E. Oberdörster. CRC Press, Taylor & Francis Group, 6000 Broken Sound Parkway NW, Suite 300, Boca Raton, FL 33487-2742, pp. 123-148.

MOURA, L.R., SANTOS, A.L.Q., BELLETI, M.E., VIEIRA, L.G., ORPINELLI, S.R.T. & DE SIMONE, S.B.S. 2009. Morphological aspects of the liver of the freshwater turtle

Phrynops geoffroanus Schweigger, 1812 (Testudines, Chelidae). *Brazilian Journal of Morphological Science,* 26: 129-134.

MUSHONGA, B. & HOROWITZ, A. 1996. Serous cavities of the Nile crocodile (*Crocodylus niloticus). Journal of Zoo and Wildlife Medicine,* 27: 170-179.

OLDHAM-OTT, C.K. & GILLOTEAUX, J. 1997. Comparative morphology of the gall bladder and biliary tract in vertebrates: variation in structure, homology in function and gallstones. *Microscopy Research and Technique,* 38: 571-597.

OWEN, R. 1866. Fishes and reptiles, in *Anatomy of vertebrates,* Longmans, Green, and Co., London, pp. 448-451.

RICHARDSON, K.C., WEBB, G.J.W. & MANOLIS, S.C. 2002. Digestive system, in C*rocodiles: inside out,* edited by K.C. Richardson. Australia: Surrey Beatty & Sons PTY LIMITED, pp. 89-94.

ROMÃO, M.F., SANTOS, A.L.Q., LIMA, F.C., DE SIMONE, S.S., SILVA, J.M.M., HIRANO, L.Q., VIEIRA, L.G., PINTO, J.G.S. 2011. Anatomical and topographical description of the digestive system of *Caiman crocodilus* (Linnaeus 1758), *Melanosuchus niger* (Spix 1825) and *Paleosuchus palpebrosus* (Cuvier 1807). *International Journal of Morphology,* 29: 94-99.

SCHAFFNER, F. 1998. The hepatic system, in *Biology of reptilia: volume 19, Morphology G: Visceral organs,* edited by C. Gans & A.B. Gaunt. Society for the Study of Amphibians and Reptiles, Missouri, pp. 485-531.

VAN DER MERWE, N.J. & KOTZE, S.H. 1993. The topography of the thoracic and abdominal organs of the Nile crocodile *(Crocodylus niloticus). Onderstepoort Journal of Veterinary Research,* 60: 219-222.

XU, G., ELSEY, R.M., LANCE, V.A., JAVORS, B., CHEN, T.S., SALEN, G. & TINT, G.S. 1997. A study on biliary ductal system and bile fistula in the American alligator, *Alligator mississipiensis. The Journal of Experimental Zoology,* 279: 554-561.
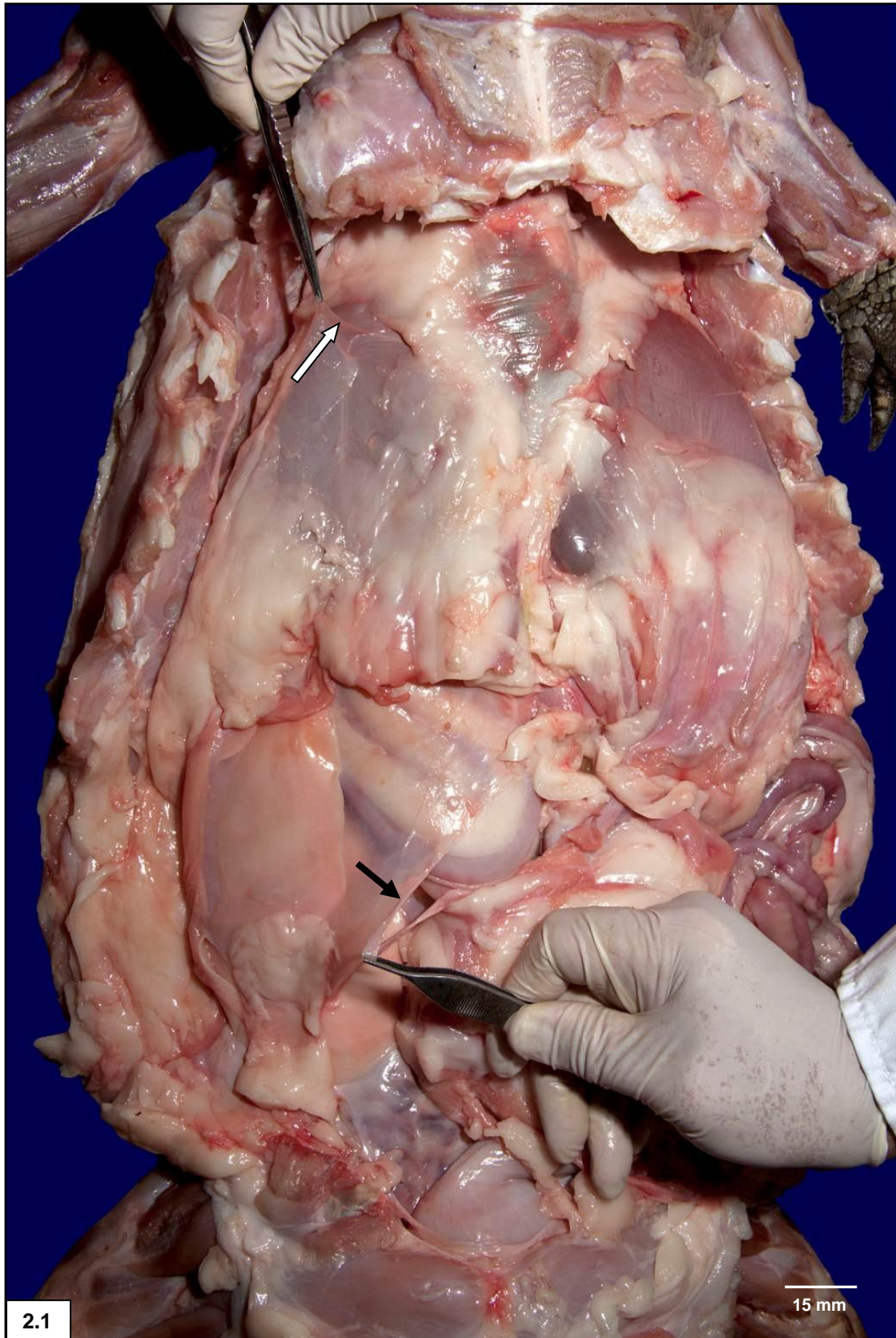
Figure 2.1: Ventral view of the liver *in situ* showing the post-pulmonary membrane (white arrow) and the post-hepatic membrane (↑).
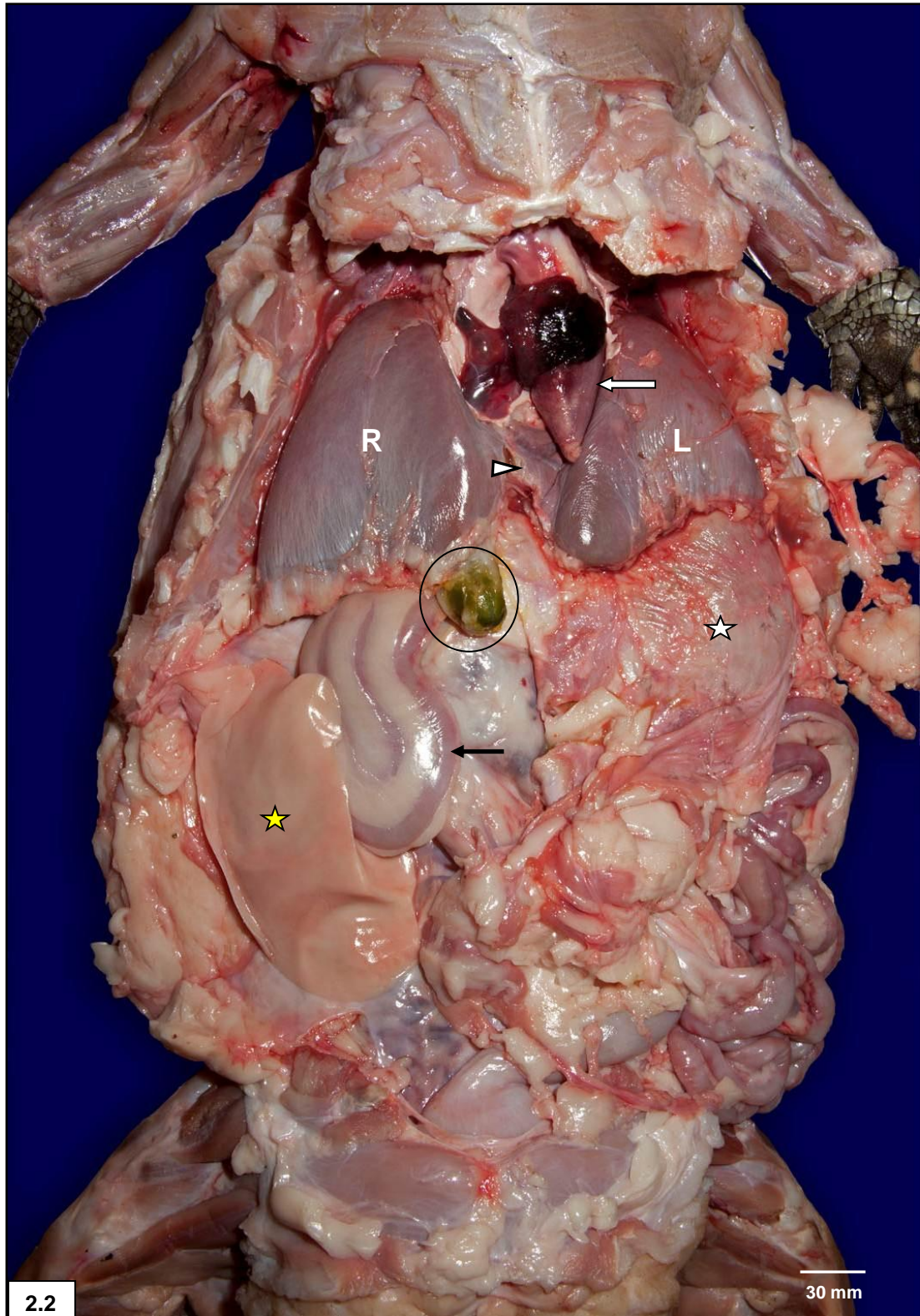
Figure 2.2: Ventral view of the liver showing the right (**R**) and left (**L**) liver lobes with the heart (white arrow) nestled in between, ventral to the isthmus (white arrowhead), and their association with the stomach (white star), the duodenum (black arrow) and the gallbladder (circled). Note the fat body (yellow star).
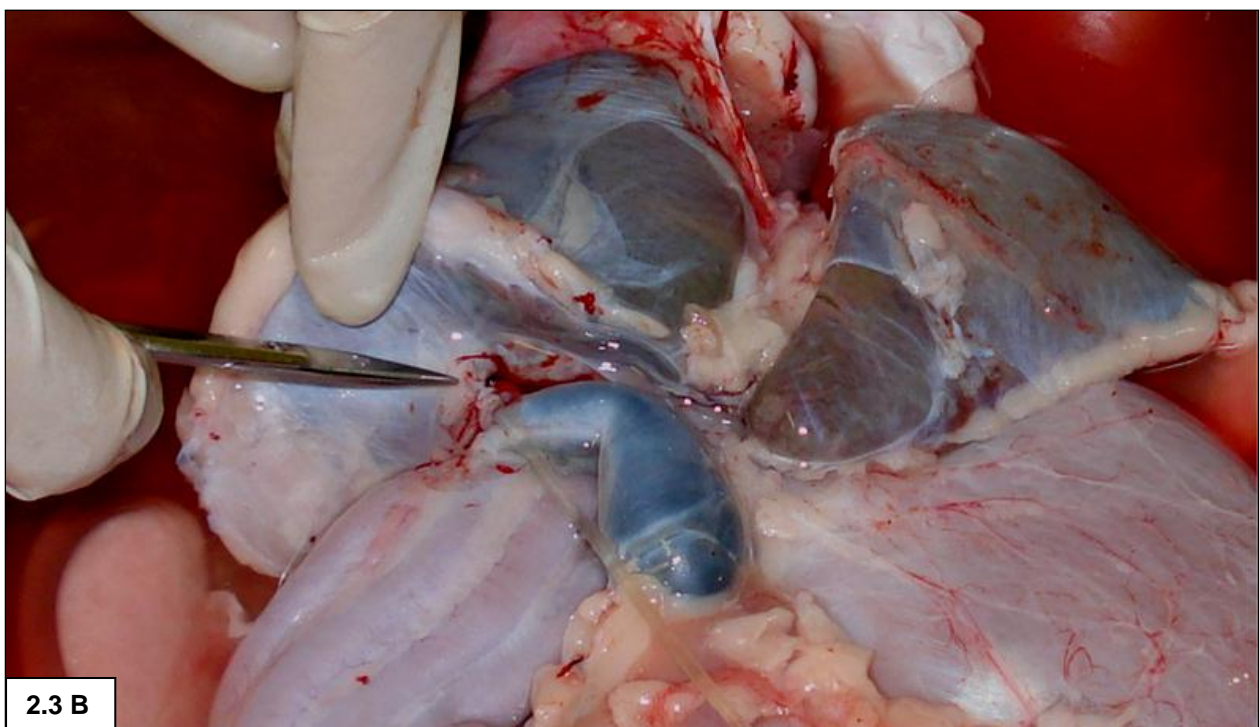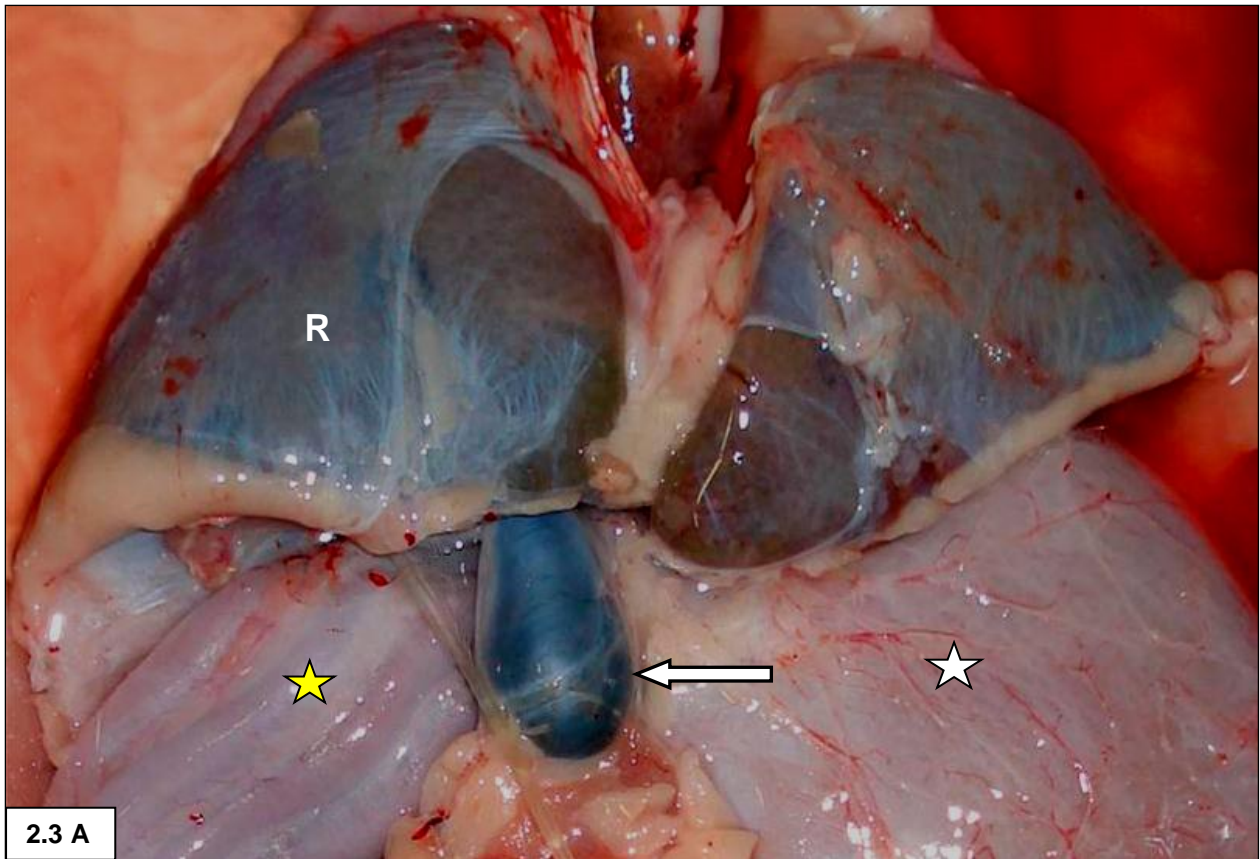
Figure 2.3: A - Ventral view of the pouch-like gallbladder (white arrow) positioned caudally to the right liver lobe (**R**) at the ventromedial aspect. Duodenum (yellow star); stomach (white star).

Figure 2.3: B - Partial reflection of the right liver lobe showing the dorso-medial attachment of the gallbladder to liver.

17
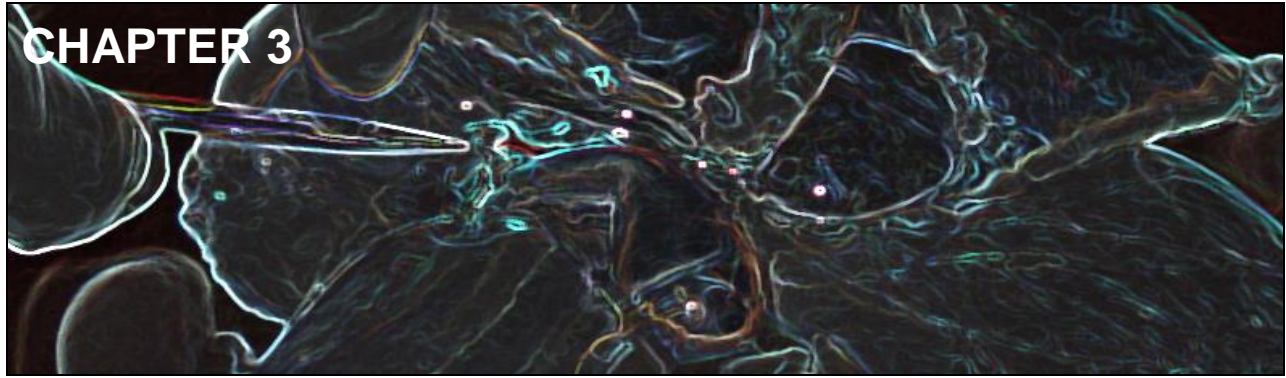
GROSS ANATOMY OF THE LIVER AND GALLBLADDER

3.1 INTRODUCTION

There is a shortage of information regarding the macroscopic features of the liver and gallbladder of crocodilians and particularly that of the Nile crocodile. Two publications gave anatomical descriptions of the liver and gallbladder of *Crocodylus niloticus* (Van der Merwe & Kotzé 1993; Mushonga & Horowitz 1996). Richardson *et al.* (2002) illustrated the liver and gall- bladder of the Saltwater crocodile (*Crocodylus porosus*). Romão *et al.* (2011) included a brief anatomical explanation of the liver and gallbladder in their discussion of the digestive system of alligators. Divers and Cooper (2000) stated, "We remain ignorant of the specific features of liver anatomy of many reptiles".

3.2 MATERIALS & METHODS

After the topographical description was completed, the intact liver with the gallbladder attached was removed from the body cavity and the ventral and dorsal aspects photographed with a Canon 5D Mark II camera using a 28-135mm zoom lens.

3.3 RESULTS

The livers were a dark reddish-brown colour, were covered by capsules and weighed 98 g, 165 g and 215 g. It consisted of two lobes with the right lobe being the largest. Both lobes had the shape of a triangular prism with a caudal base and a blunt cranial apex (Fig. 3.1). Each liver lobe exhibited dorsal, ventral and lateral borders with the caudal, cranial and lateral surfaces being rounded and not flattened. The two lobes were joined by a narrow, flattened isthmus, measuring approximately 7 x 2.5 x 1 cm and apparently composed of

liver tissue. The isthmus was located in the medial dorsal region between the two lobes (Fig. 3.2).

The distended pouch-like gallbladder measured approximately 5 x 2 x 2 cm and was enclosed by a thin wall. Three anatomical zones could be identified, namely, a long narrow neck closest to the hepatocystic ligament, a middle area constituting the body of the organ, and the blind end or fundus. The distended gallbladder was filled with around 5 ml of green mucoid bile contents and in one crocodile the gallbladder displayed a curved appearance.

3.4 DISCUSSION

The present study agrees with the findings of Mushonga & Horowitz (1996) that the right liver lobe of the Nile crocodile is larger than the left lobe, that the two lobes are joined by an isthmus and that the gall bladder is attached caudally to the right liver lobe. Van der Merwe & Kotze (1993) concurred with the previous statement, but did not mention an isthmus. The Caiman liver and gall bladder descriptions were identical to that of the Nile crocodile, but again an isthmus was not referred to (Romão *et al.* 2011). *Crocodylus porosus* differs in that this Saltwater crocodile displayed an unlobed liver with only a short indentation in the medial region (Richardson *et al.* 2002). The macroscopic appearance of the isthmus in the current study gave the impression that it was composed of liver tissue. In other reptiles, for example tortoises, the isthmus was described as a "narrow band of connective tissue" (Marycz & Rogowska 2007; Kassab *et al.* 2009). Some reptiles differ in respect of liver lobe sizes, for example, Kassab *et al.* (2009) found the left liver lobe of the Desert tortoise to be larger than the right lobe.

Many publications fail to comment on the form of the gallbladder. The shape of the gallbladder however varies between reptile species: oval in the desert tortoise (Penninck *et al.* 1991, cited in Oldham-Ott & Gilloteaux 1997); oblong or piriform in alligators (Xu *et al.* 1997; Romão *et al.* 2011) and pouch-like when full in the Nile crocodile (current study). The illustration of the Saltwater crocodile liver and gallbladder given by Richardson *et al.* (2002) also depicted the gall bladder's shape as pouch-like. As in the present study the gallbladder of alligators were also described as having a thin wall (Xu *et al.* 1997). The division of the Nile crocodile gallbladder into three anatomical zones has also been noted in the snake *Bothrops jararaca* gallbladder (Silveira & Mimura 1999).

3.5 REFERENCES

DIVERS, S.J. & COOPER, J.E. 2000. Reptile hepatic lipidosis. *Seminars in Avian and Exotic Pet Medicine*, 9:153-164.

KASSAB, A., SHOUSHA, S. & FARGANI, A. 2009. Morphology of blood cells, liver and spleen of the Desert Tortoise (*Testudo graeca*). *The Open Anatomy Journal,* 1*:* 1-10.

MARYCZ K., ROGOWSKA K. 2007. The liver morphology and topography of Horsfield's (*Testudo horsfieldi*) and Hermann's (*T. Hermanni*) terrestrial tortoises. *Electronic Journal of Polish Agricultural Universities,* 10: 1-9.

MUSHONGA, B. & HOROWITZ, A. 1996. Serous cavities of the Nile crocodile (*Crocodylus niloticus). Journal of Zoo and Wildlife Medicine,* 27: 170-179.

OLDHAM-OTT, C.K. & GILLOTEAUX, J. 1997. Comparative morphology of the gallbladder and biliary tract in vertebrates: variation in structure, homology in function and gallstones. *Microscopy Research and Technique,* 38: 571-597.

RICHARDSON, K.C., WEBB, G.J.W. & MANOLIS, S.C. 2002. Digestive system, in C*rocodiles: inside out,* edited by K.C. Richardson. Australia: Surrey Beatty & Sons, pp. 89-94.

ROMÃO, M.F., SANTOS, A.L.Q., LIMA, F.C., DE SIMONE, S.S., SILVA, J.M.M., HIRANO, L.Q., VIEIRA, L.G., PINTO, J.G.S. 2011. Anatomical and topographical description of the digestive system of *Caiman crocodilus* (Linnaeus 1758), *Melanosuchus niger* (Spix 1825) and *Paleosuchus palpebrosus* (Cuvier 1807). *International Journal of Morphology,* 29: 94-99.

SILVEIRA, P.F. & MIMURA, O.M. 1999. Concentrating ability of the *Bothrops jararaca* gallbladder. *Comparative Biochemistry and Physiology,* Part A, 123: 25–33.

VAN DER MERWE, N.J. & KOTZE, S.H. 1993. The topography of the thoracic and abdominal organs of the Nile crocodile *(Crocodylus niloticus). Onderstepoort Journal of Veterinary Research,* 60: 219-222.

XU, G., ELSEY, R.M., LANCE, V.A., JAVORS, B., CHEN, T.S., SALEN, G. & TINT, G.S. 1997. A study on biliary ductal system and bile fistula in the American alligator, *Alligator mississipiensis. The Journal of Experimental Zoology,* 279: 554-561.
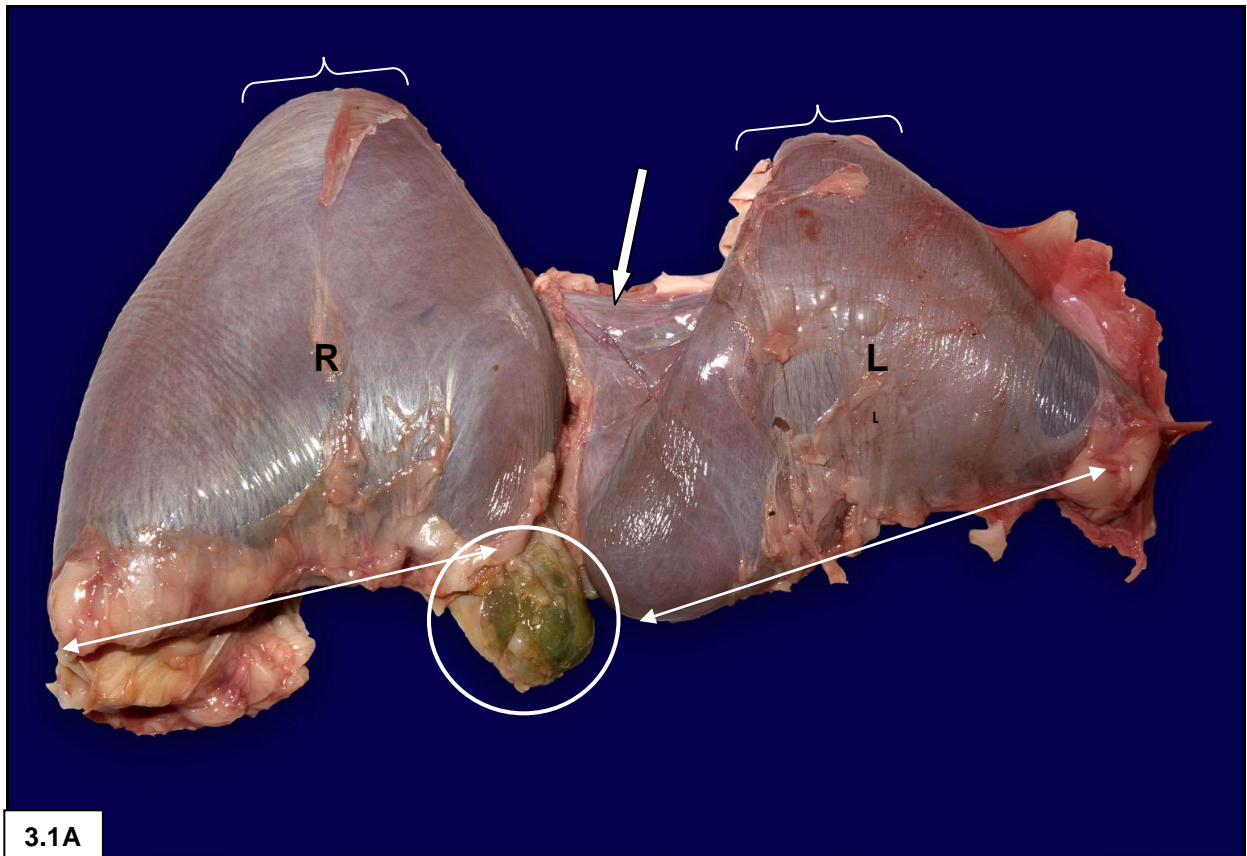
Figure 3.1: A & B- Ventral view showing the difference in size and the shape of the two liver lobes, the position of the gallbladder (encircled) and the isthmus (white arrow) between the right (**R**) and left (**L**) lobes. Base (double arrows), apex (brackets)
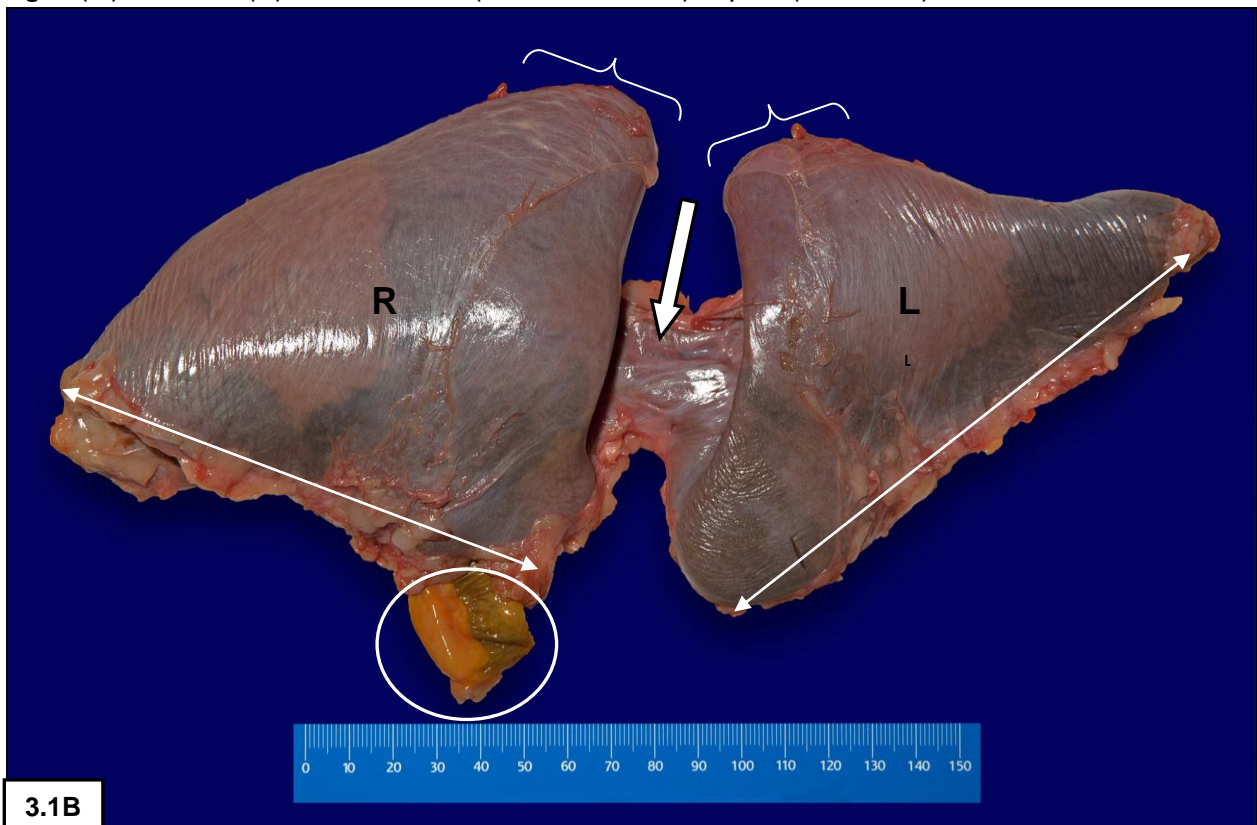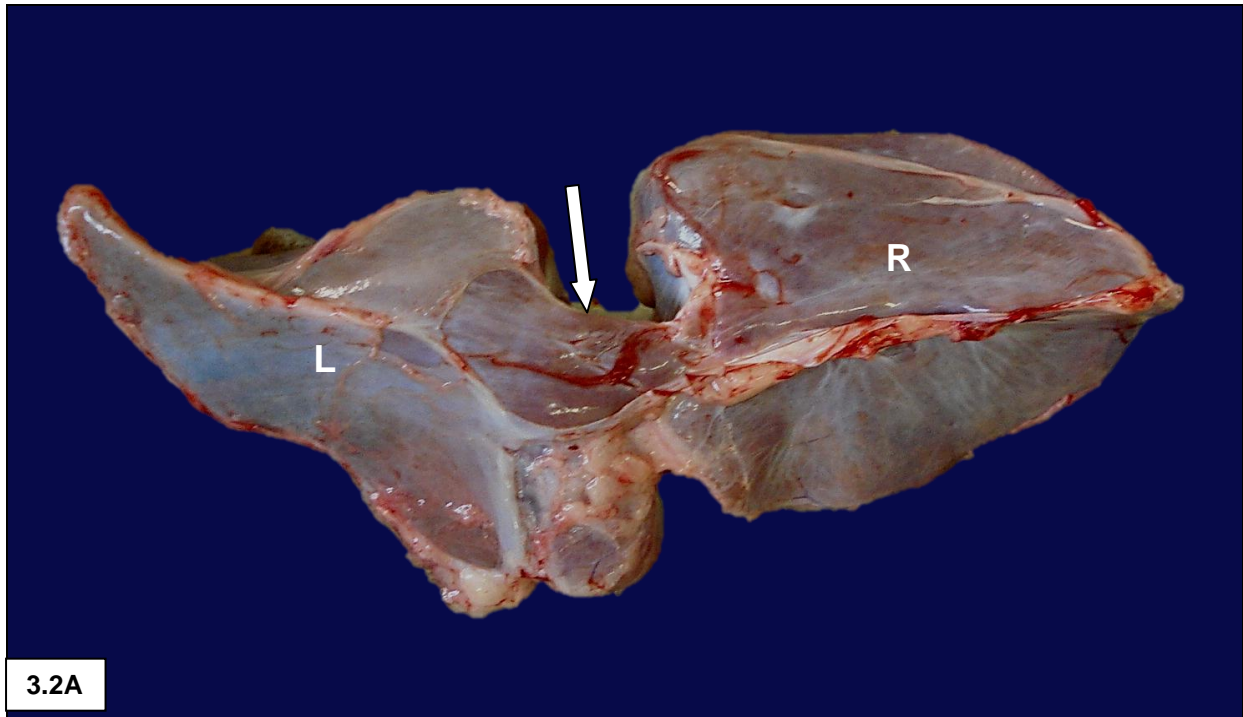
Figure 3.2: **A & B-** Dorsal view of the right (R) and left (L) liver lobes showing their prismatic appearance, the isthmus (white arrow) and the position of the gallbladder (star).
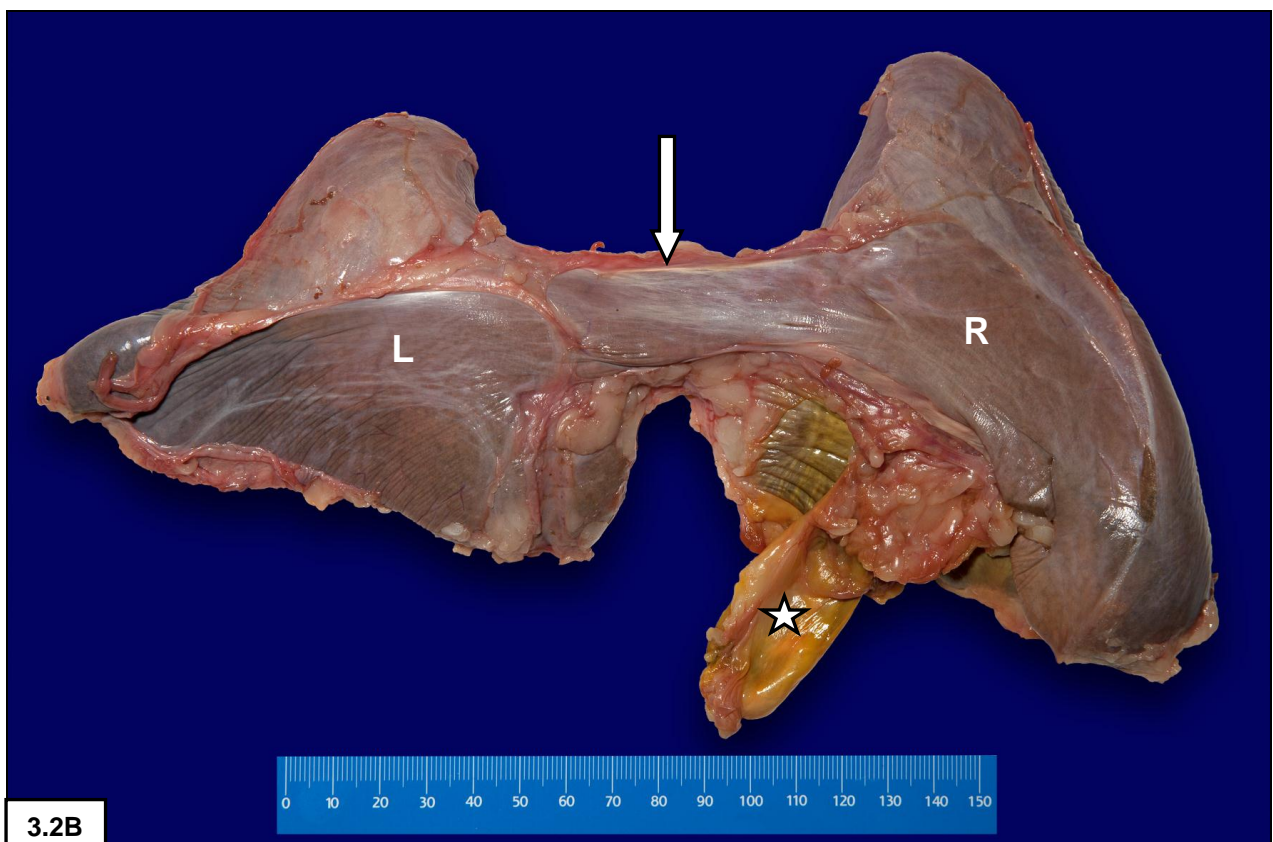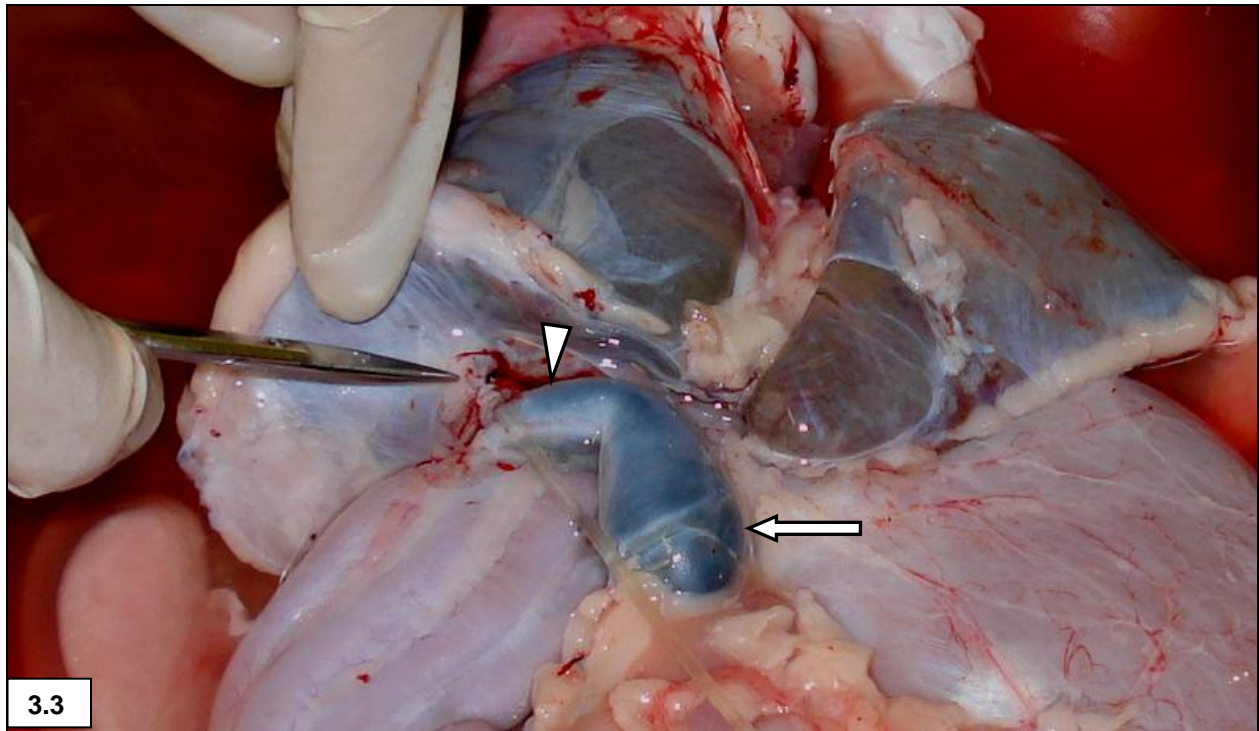
Figures 3.3: Dorso-medial view of the blind-ending pouch-like gallbladder (arrow), curving at the body-neck juncture, and a narrowed neck area (arrowhead).

Figure 4.1: Lateral incision facilitating removal of the skin, ventral body wall and ribs.
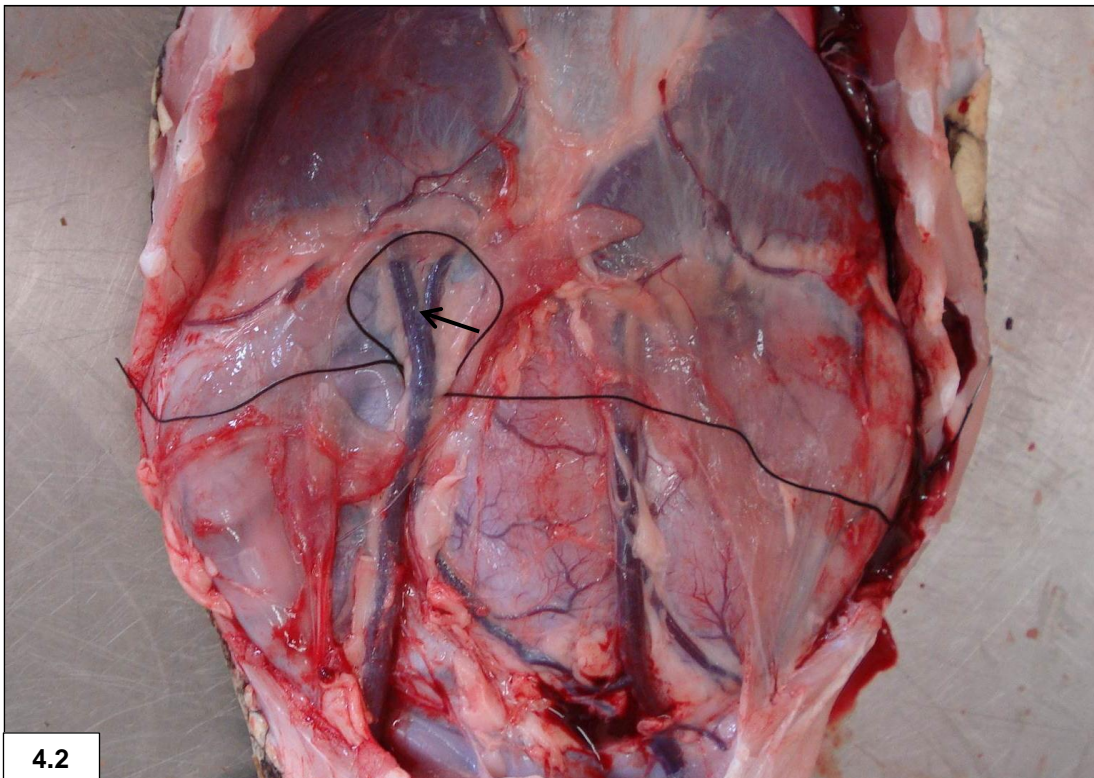
Figure 4.2: The portal vein to the liver was tied off *in situ.* Note the branching of the blood vessel (arrow).

Figure 4.3: The liver was removed from the body cavity and connected to a peristaltic pump.

Figure 4.4: A pale discoloration of the liver tissue indicated successful perfusion.
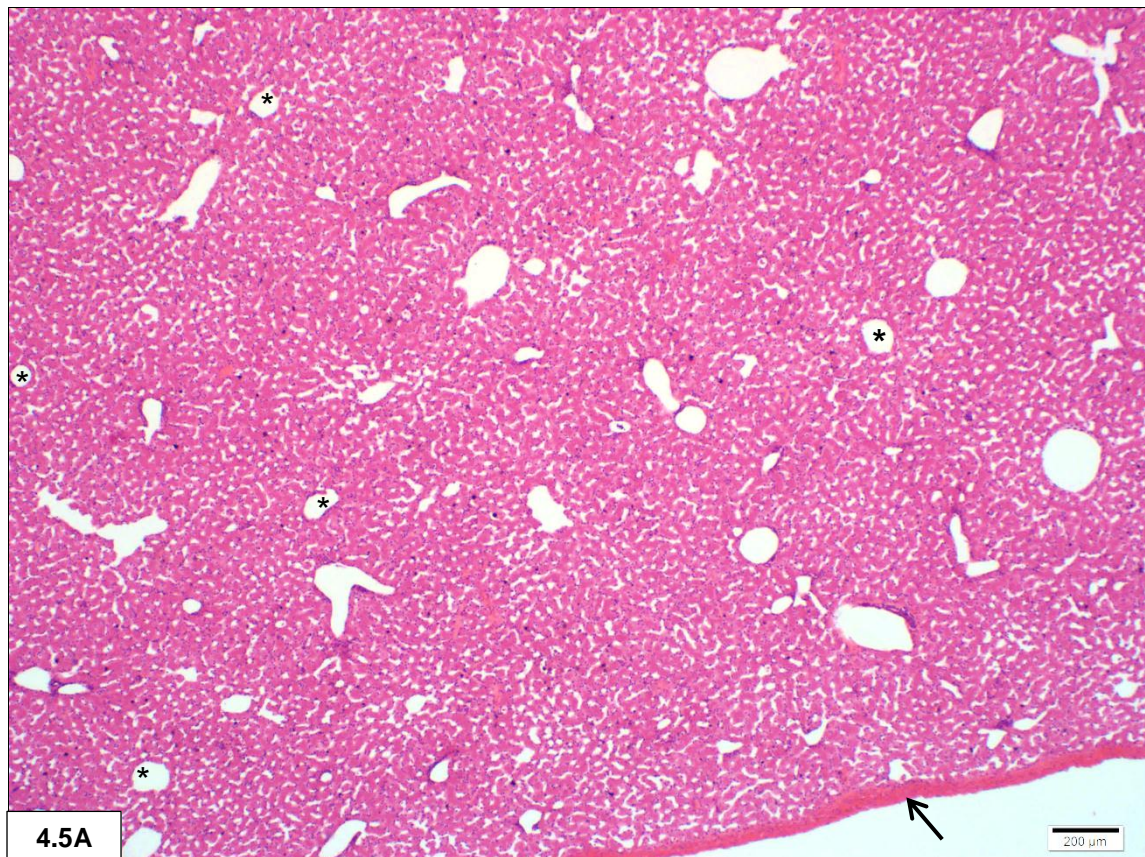
Figure 4.5 A & B: Haphazard arrangement of central veins (stars) and portal tracts surrounded by plates of hepatocytes. Note Glisson's capsule (arrows).

4.6A
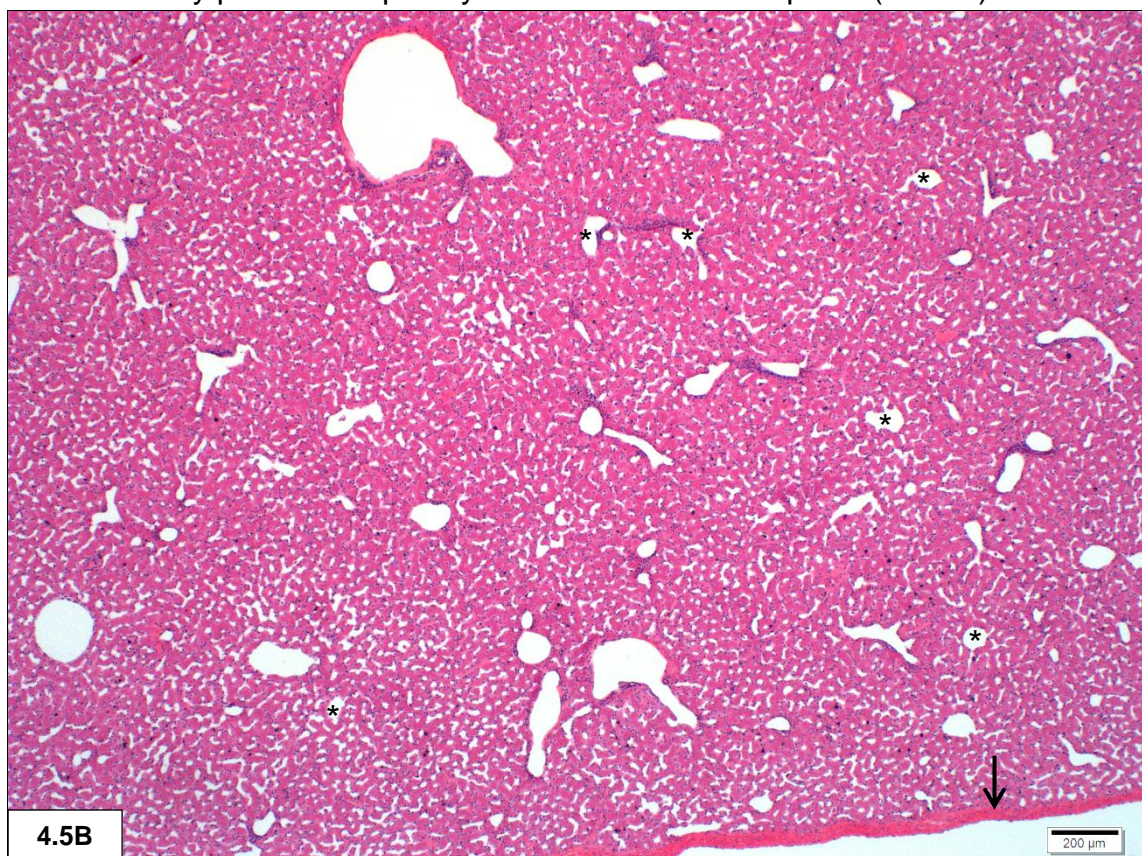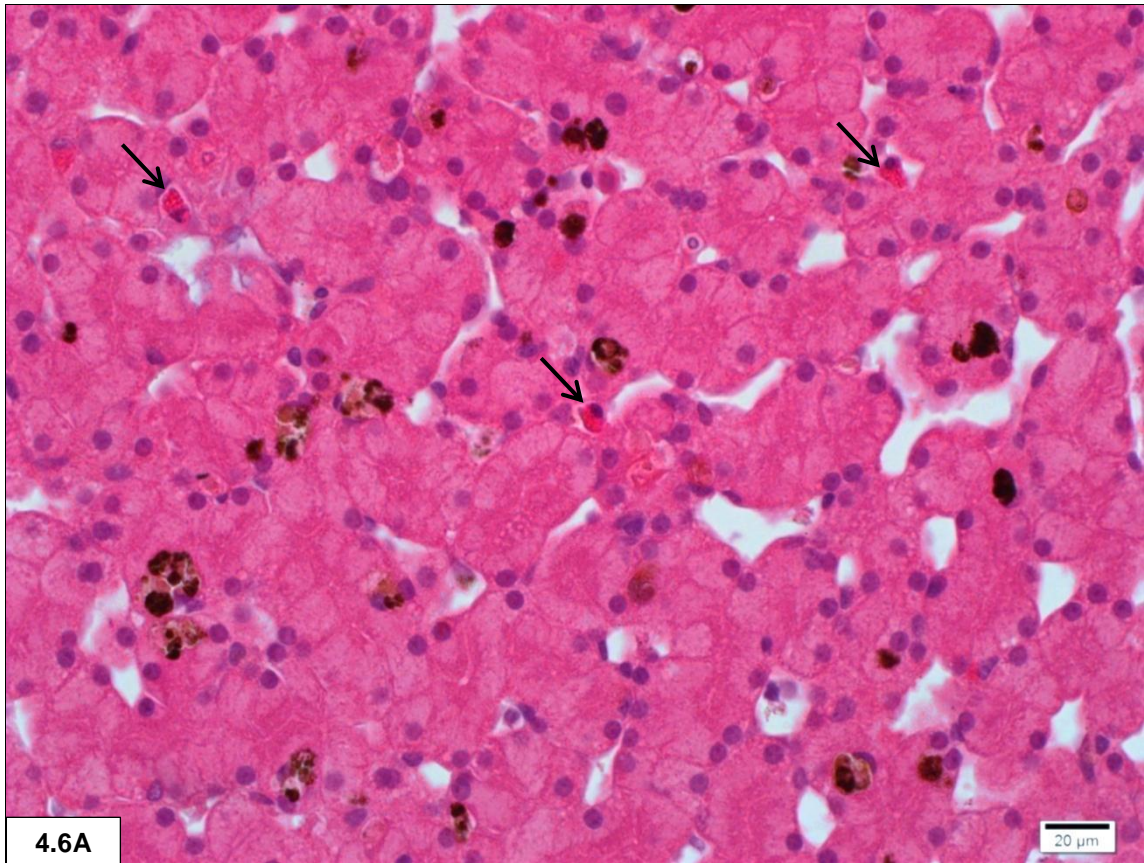
Figure 4.6 A & B: Eosinophilic hepatocyte cytoplasm with blue-staining basal nuclei next to the sinusoids. Distinctive pink-staining apical cytoplasmic inclusions are seen next to the bile canaliculi. Note brownish cytoplasmic inclusions in Kupffer cells. Note eosinophils (arrows in **A**).

4.6B
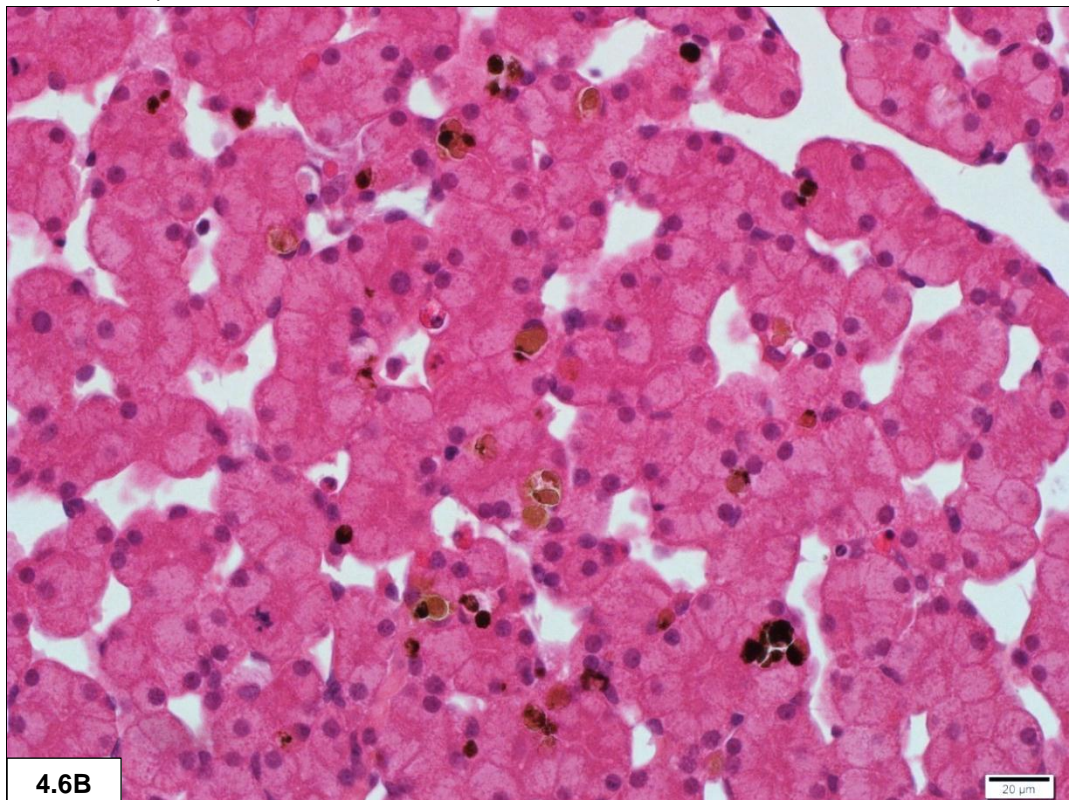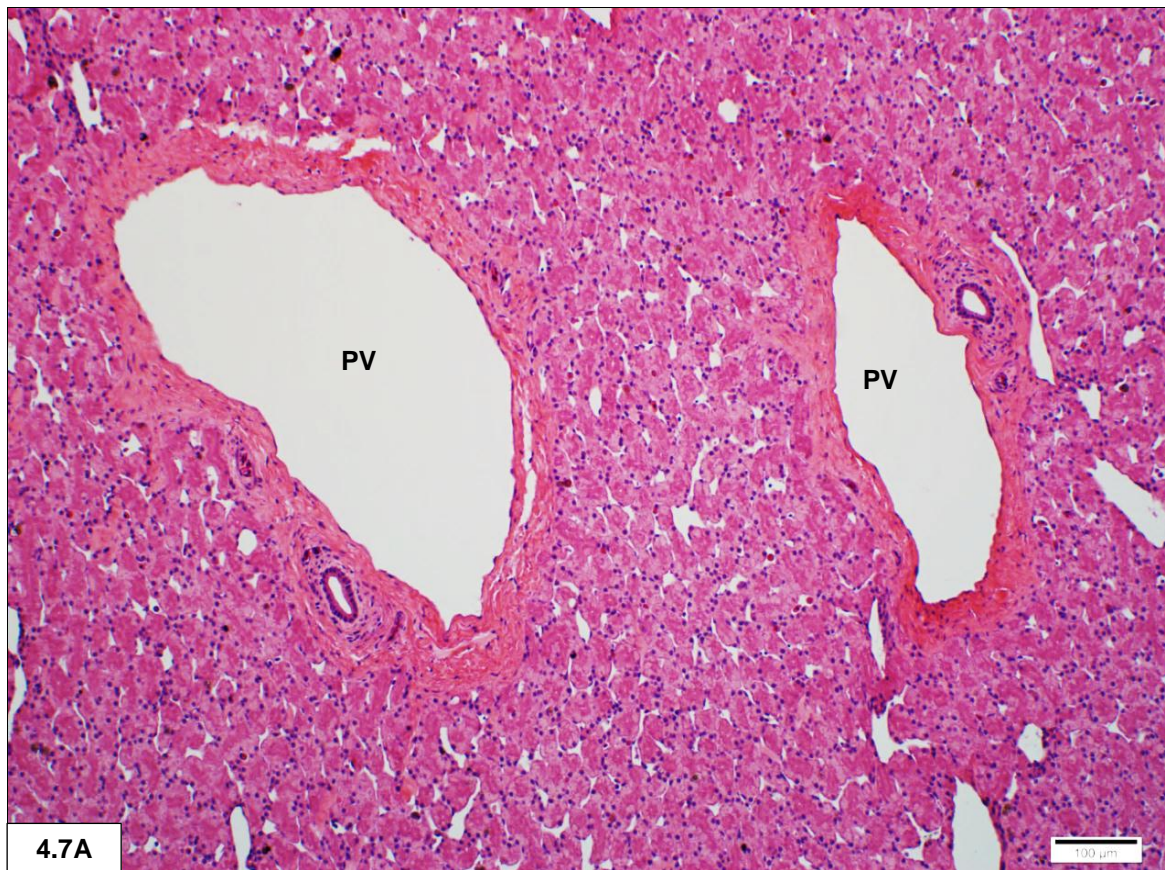
Figure 4.7 A: Two large branches of the portal vein (PV).
B: Portal triad consisting of a bile duct (bd), artery (a) and venule (v) next to a portal vein (PV).
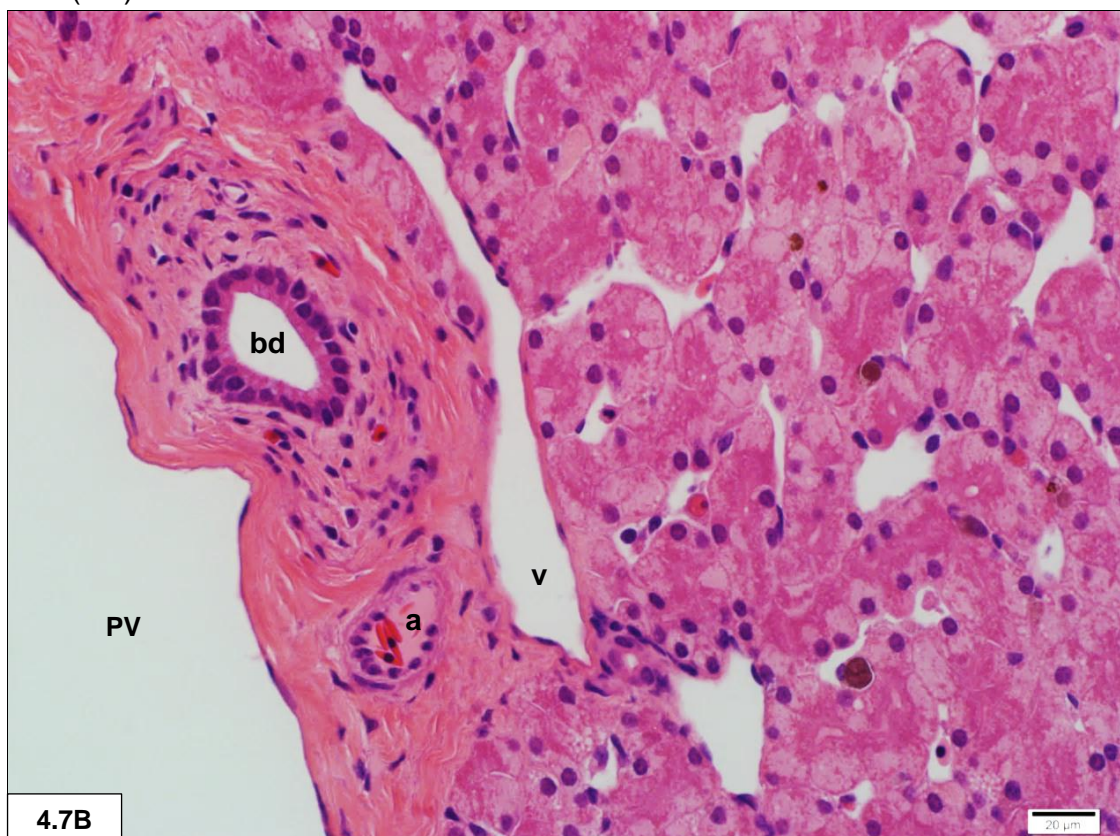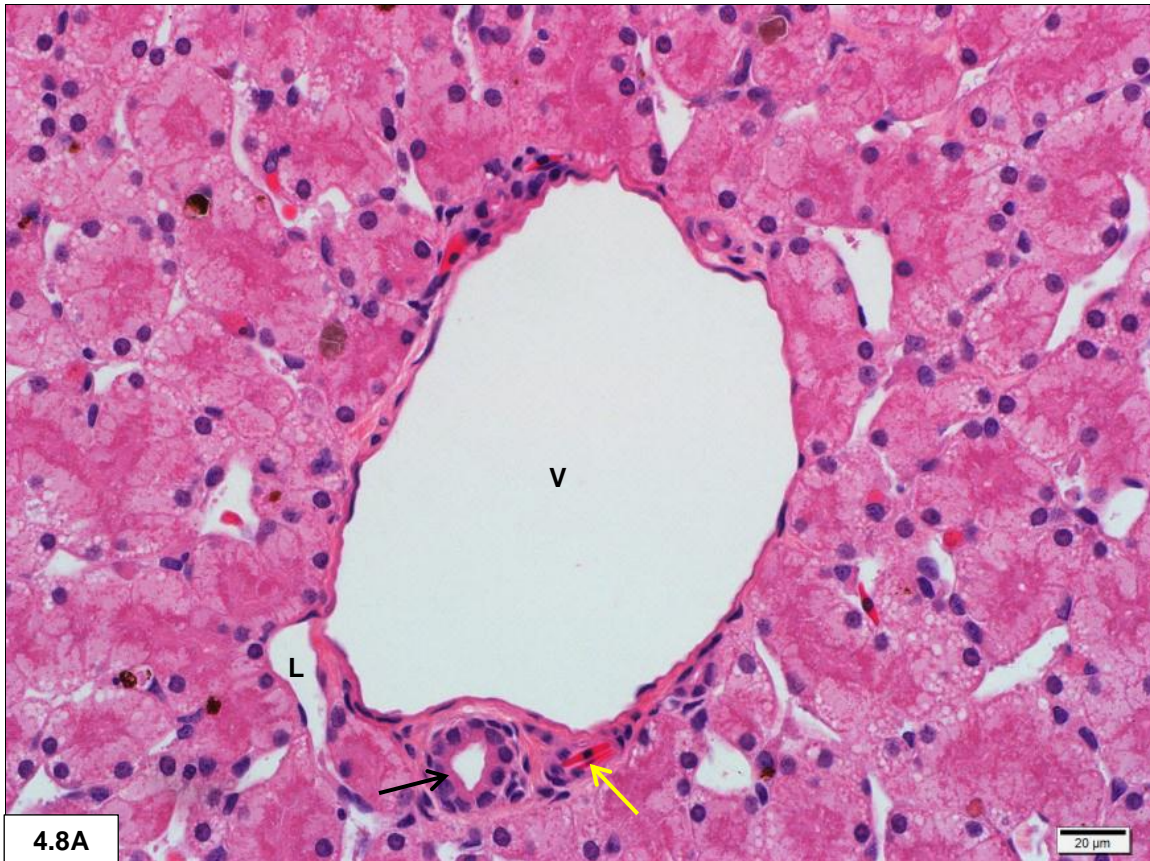
Figure 4.8 A & B: Portal triad – vein (V), artery (yellow arrow), bile duct (black arrow). Note lymphatic vessel (L in **A**) and frothy hepatocytes. H/E. **B:** Note pale vacuoles and collagen surrounding the portal triad. TB.
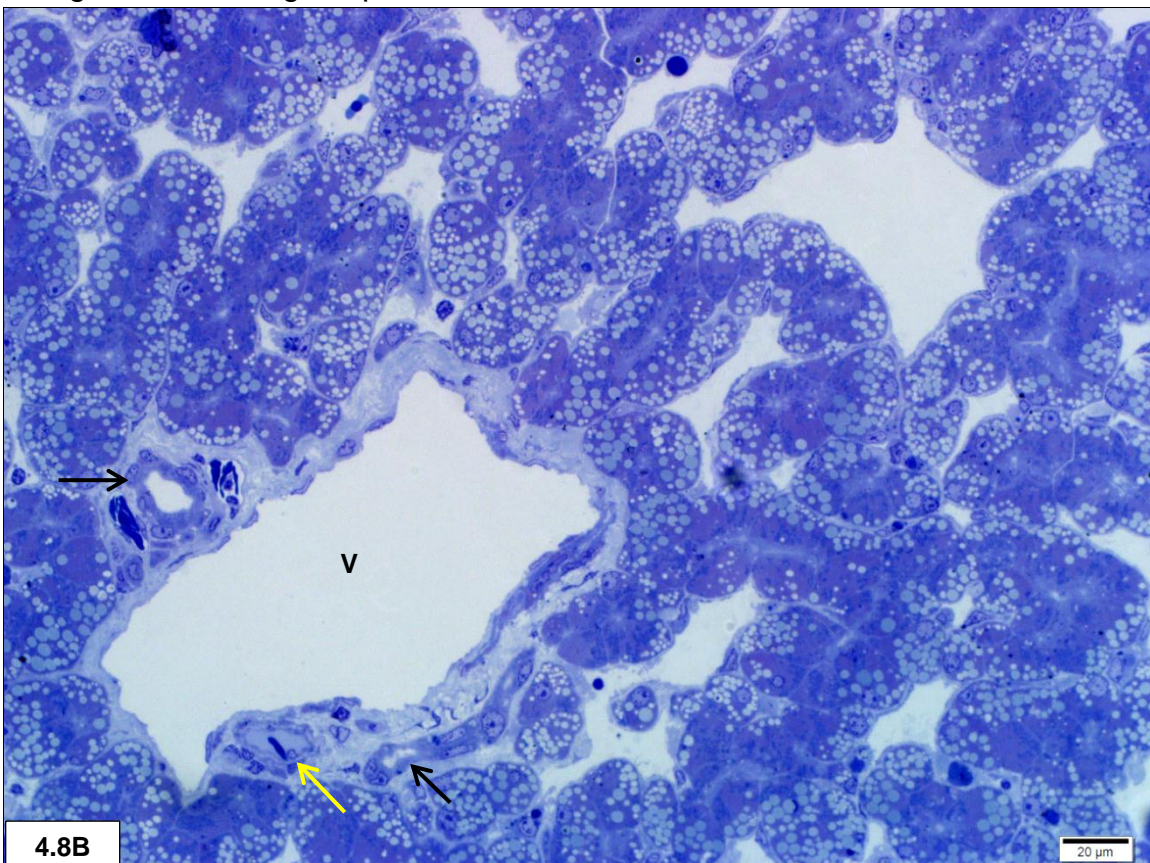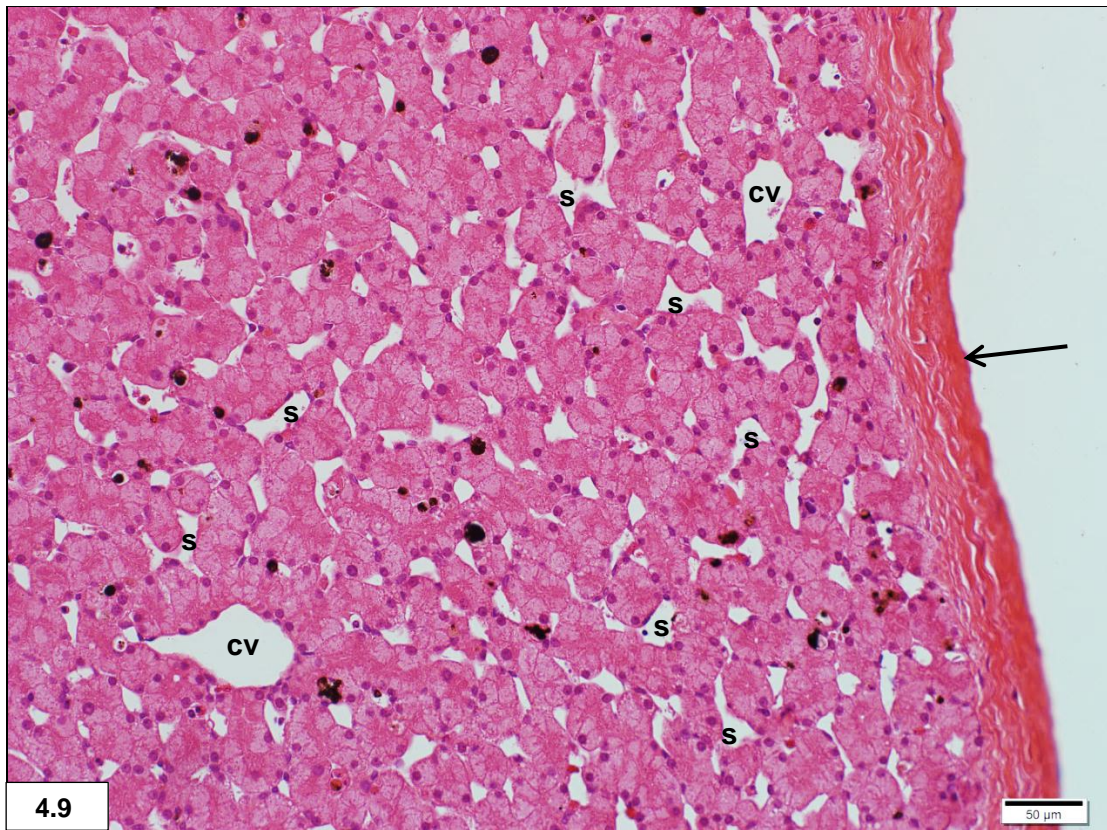
Figure 4.9: Glisson's capsule (arrow), central veins (**cv**) and sinusoids (**s**).
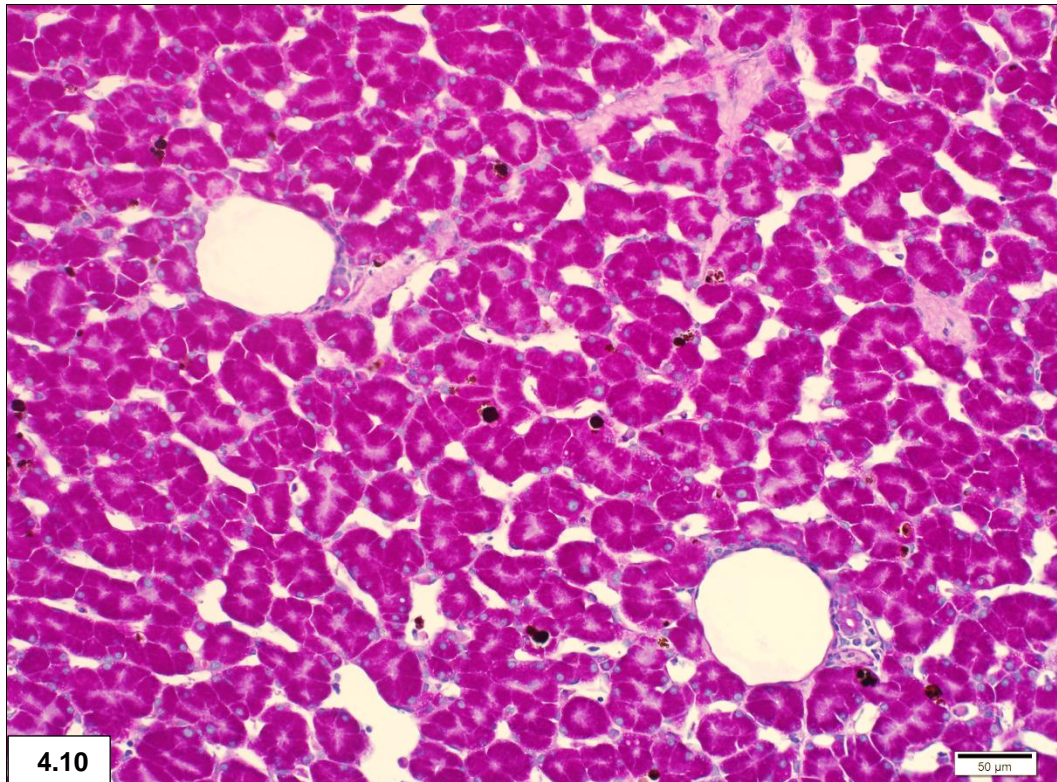
Figure 4.10: PAS **-** magenta cytoplasmic positivity indicating the presence of carbodydrates.
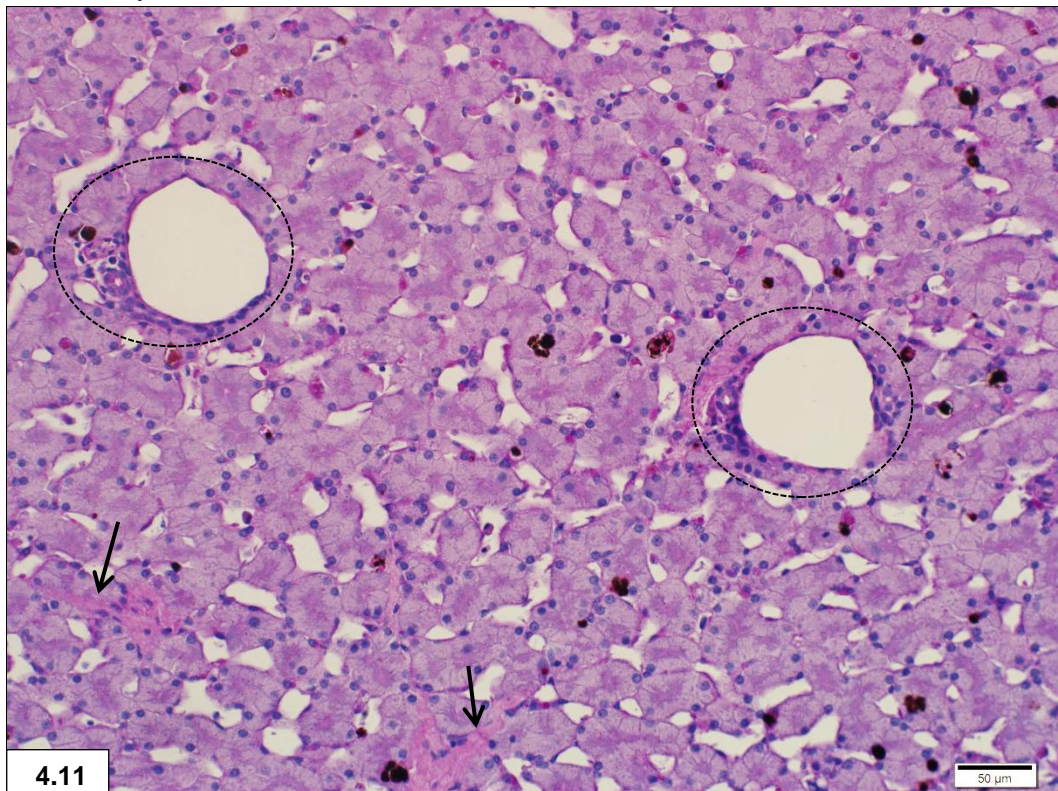
Figure 4.11: PAS-D - elimination of the magenta positivity by diastase digestion indicating the presence of glycogen. Note portal triads (dashed lines) and collagen trabeculae (arrows).
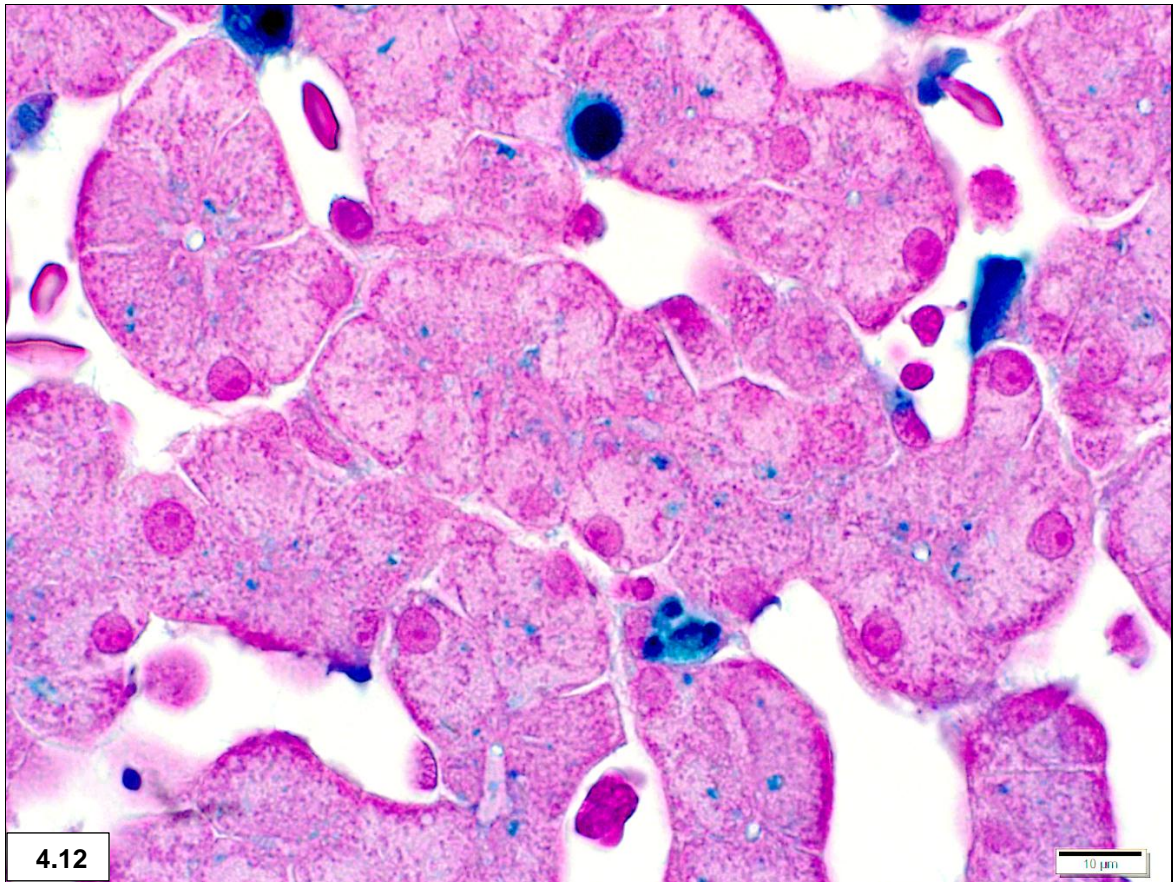
Figure 4.12: Perls' Prussian blue stain demonstrating fine blue peribiliary hemosiderin granules.
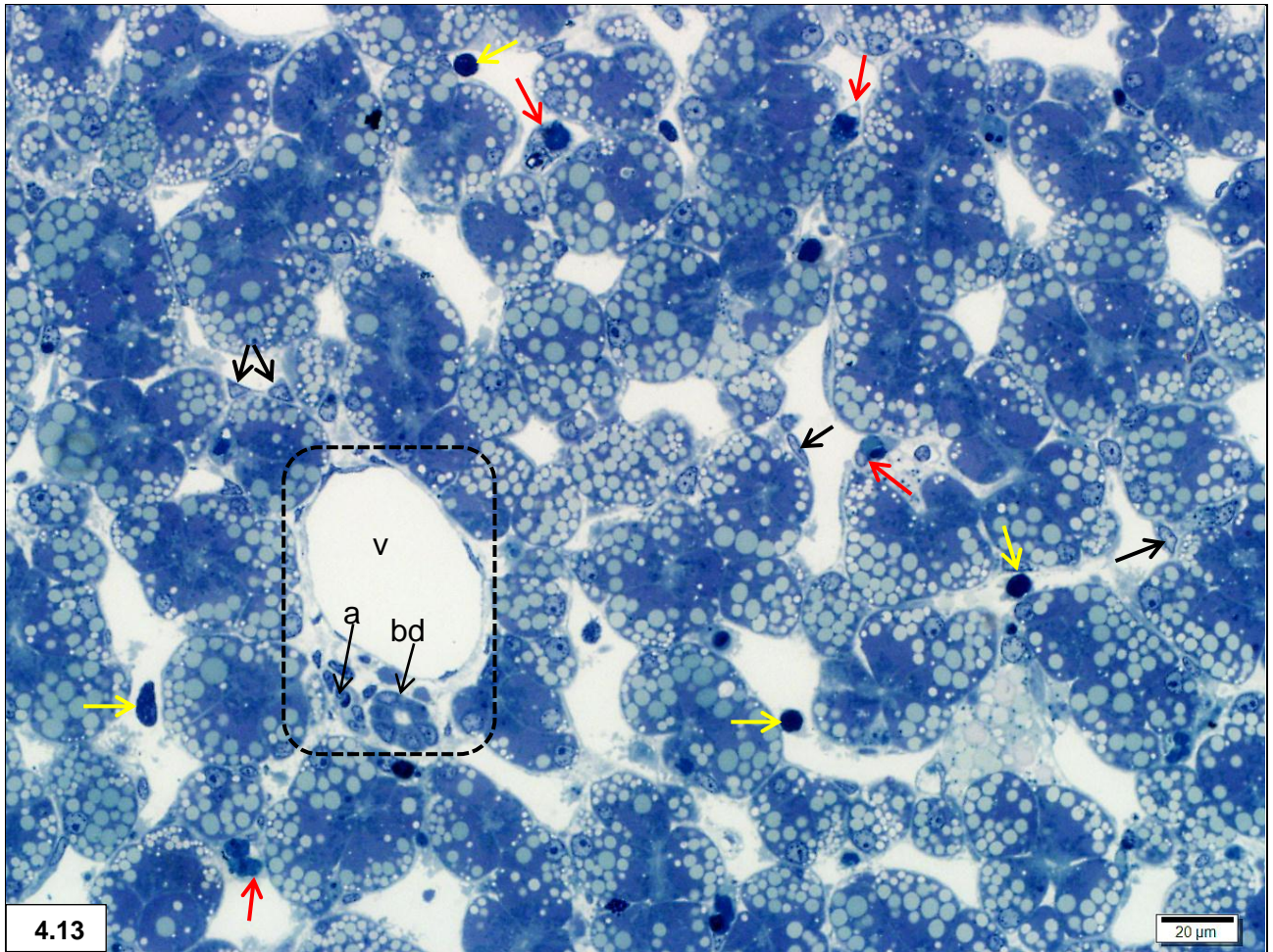
Figure 4.13: Toluidine Blue – endothelial cells (black arrows), Kupffer cells (red arrows), blood cells (yellow arrows). Note portal triad (dashed line) consisting of a vein (v), artery (a) and bile duct (bd) and variably sized pale vacuoles in the hepatocytes indicating lipid droplets. The basal nuclei of the hepatocytes have a pale blue colour with distinctive dark blue nucleoli.
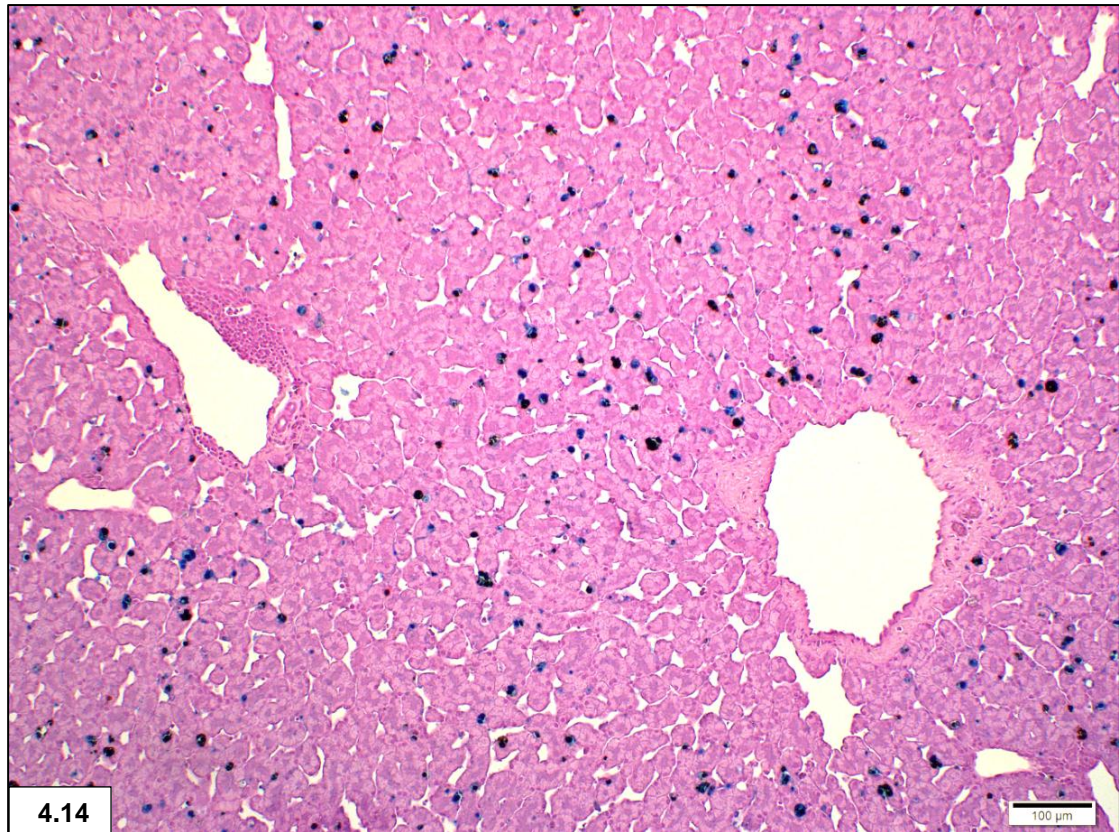
Figure 4.14: Perls' Prussian blue – blue positivity for iron deposits in Kupffer cells.
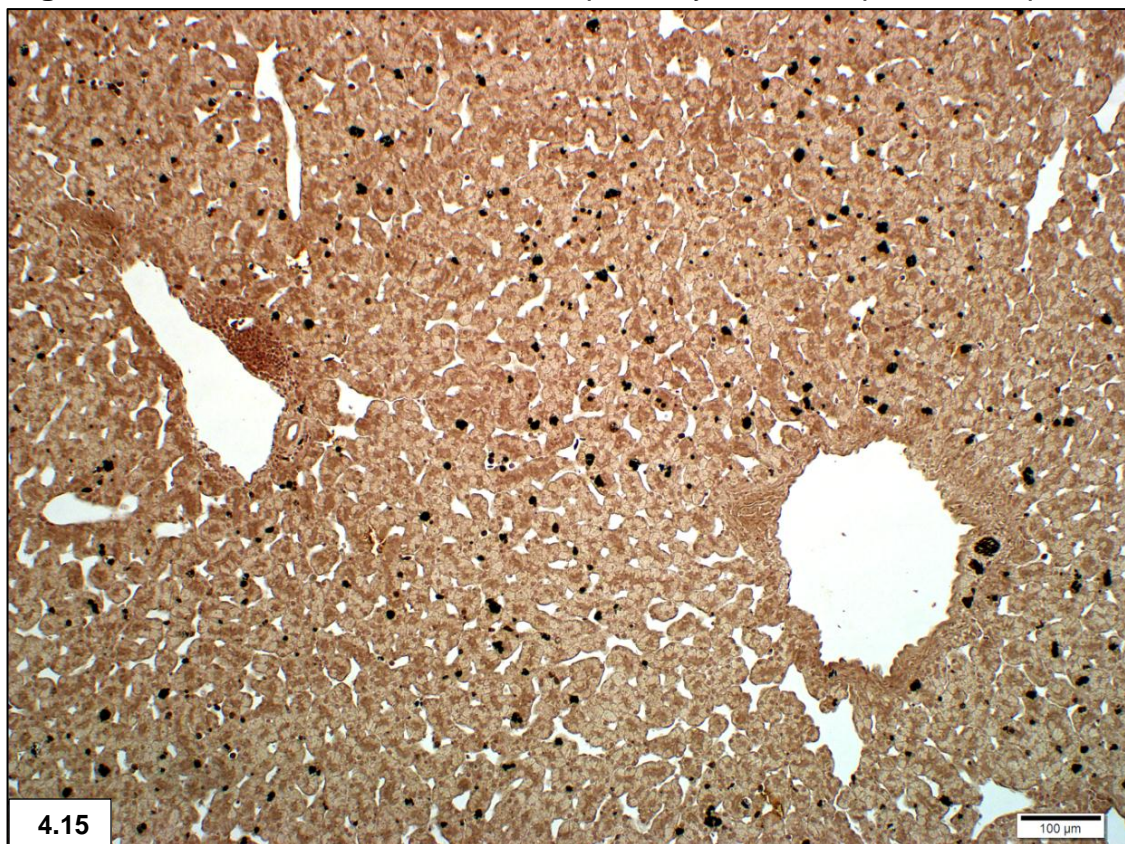
Figure 4.15: Masson-Fontana – black positivity for melanin in Kupffer cells .
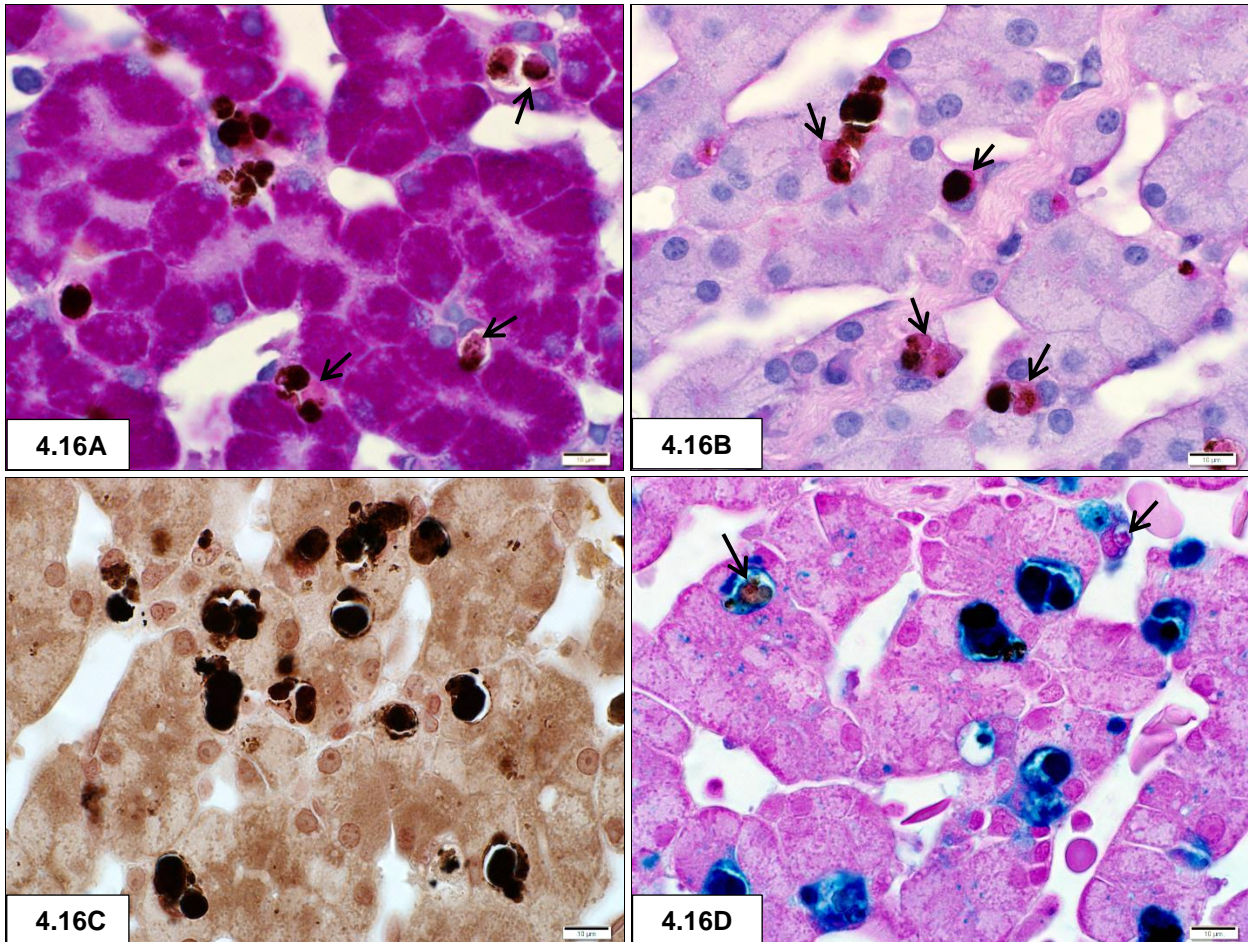
Figure 4.16: A-D – Granule comparison with different staining methods to show variable contents of the granules in Kupffer cells. **A** – PAS; **B** – PAS-D; **C** – Masson-Fontana; **D** - Perls' Prussian blue.

In **A** & **B** the granules are brownish-black with a pinkish component (ceroid or lipofuscin - arrows) in some granules. Note pink outline of some of the hepatocyte groups in **B** indicating a putative basal lamina. In **C** there are distinctive black granules (melanin) mixed with a brownish component. **D** shows partially blue granules (hemosiderin) mixed with a black (melanin) and in some a pink (ceroid or lipofuscin - arrows) component. Note the fine blue peribiliary granules indicating the presence of hemosiderin in the hepatocytes.
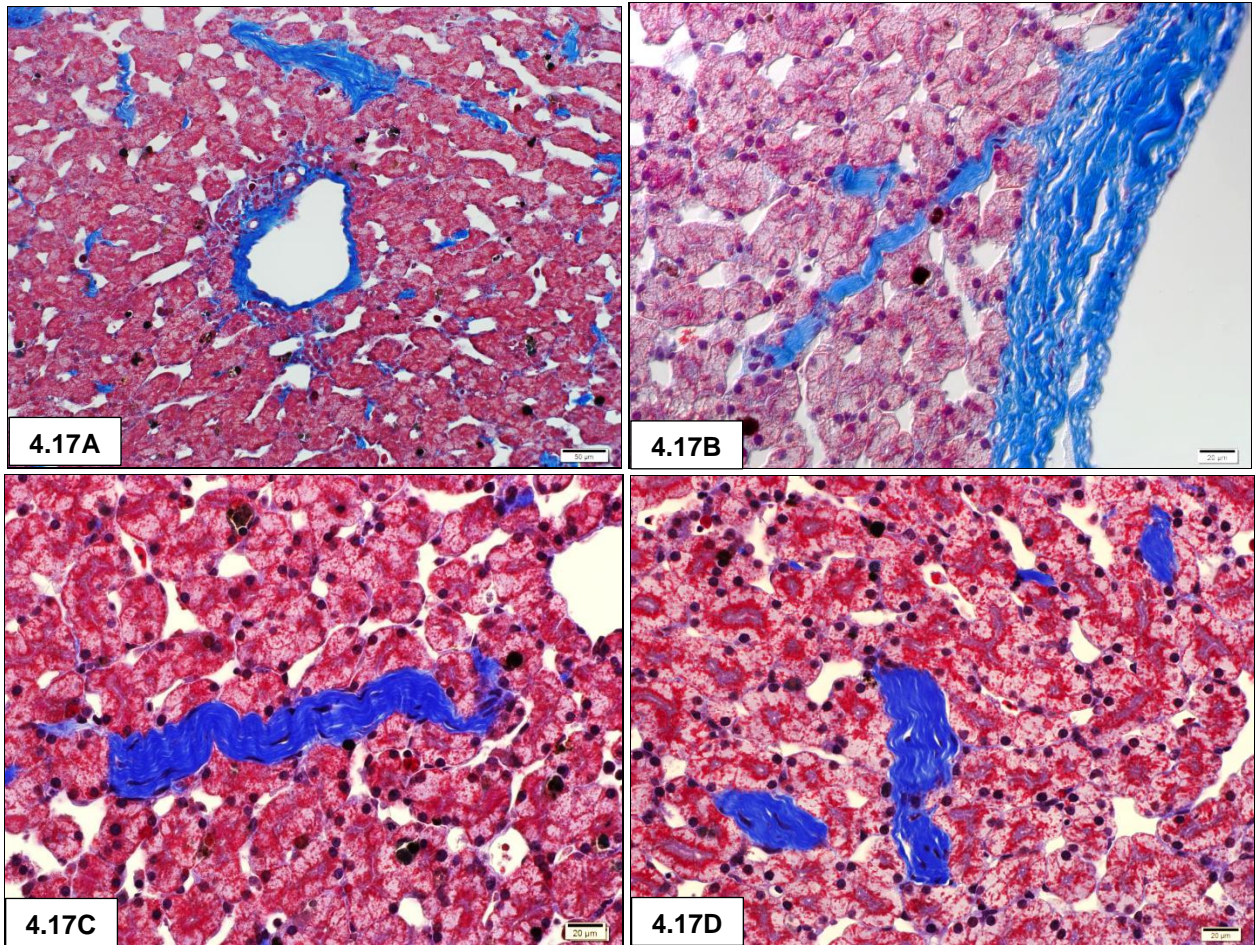
Figure 4.17 A – D: Masson trichrome stain for collagen.
B – Differential interference contrast.

Note collagen network around portal triad in **A,** collagen extending from Glisson's capsule in **B** and prominent collagen fibres between hepatocytes in **C** & **D.**
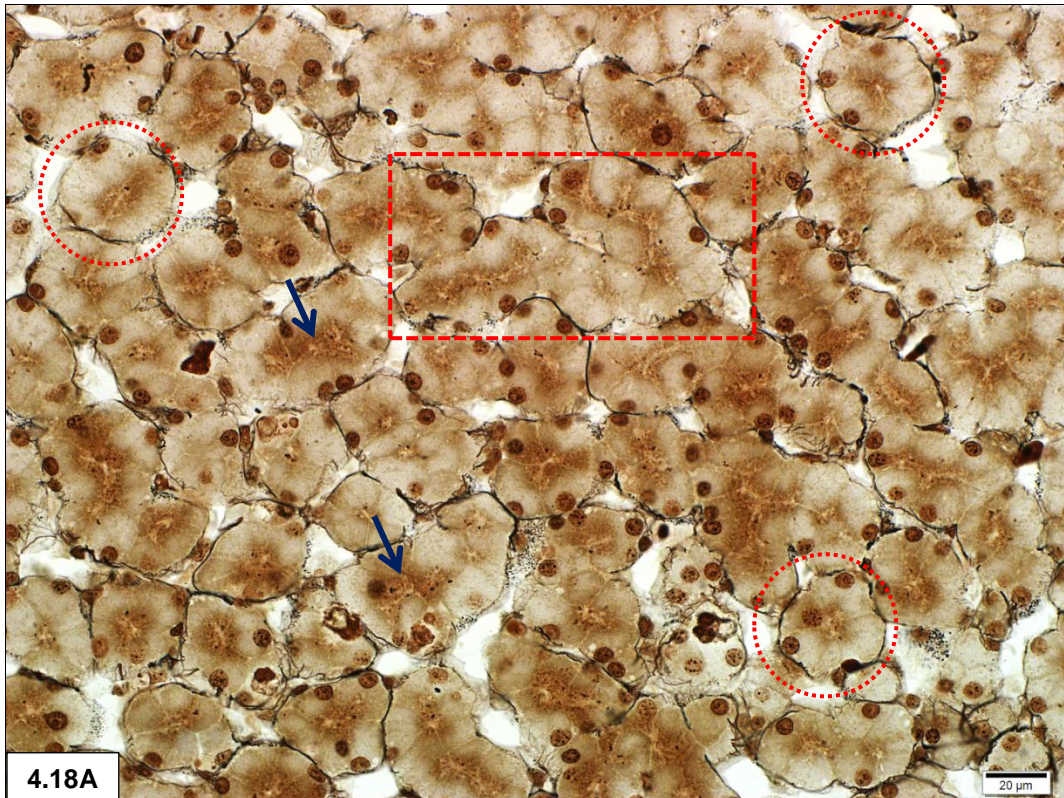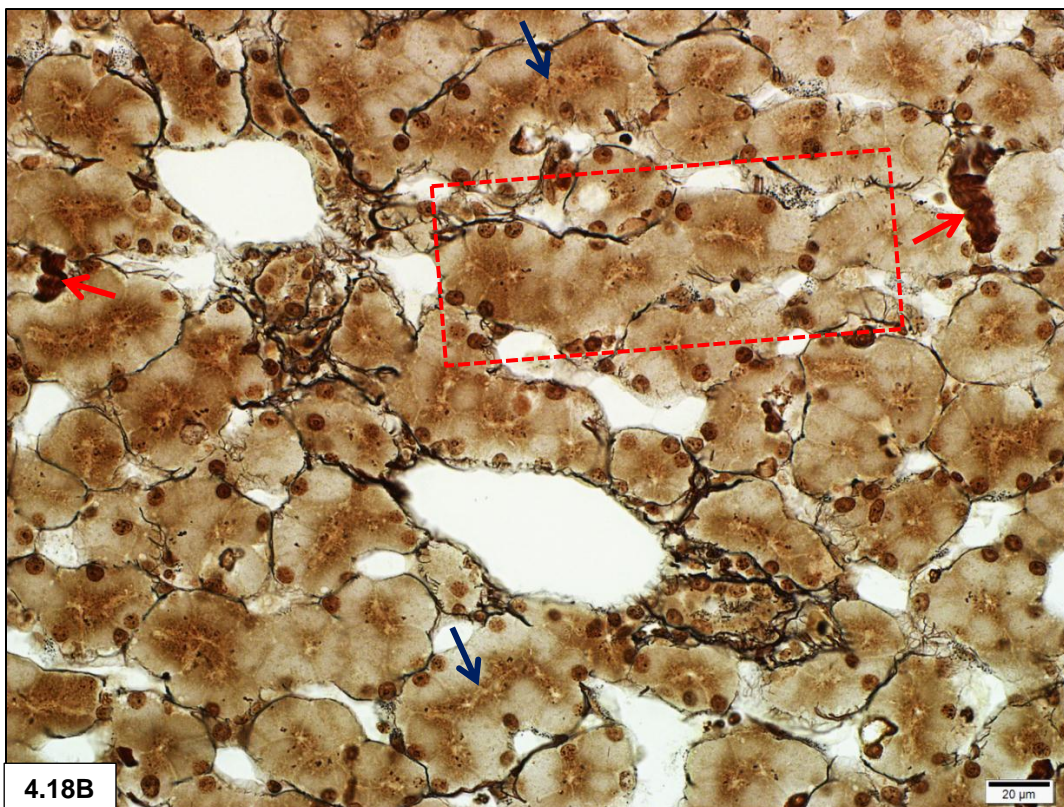
Figure 4.18 A & B: Gordon & Sweet's stain demonstrating the fine black reticular fibre network around groups of hepatocytes, sinusoids and portal tracts. The transverse (dashed circles) and longitudinal hepatocyte groups (dashed squares), basal nuclei and central bile channels (blue arrows) are well illustrated. Note brown collagen fibers (red arrows) in **B.**
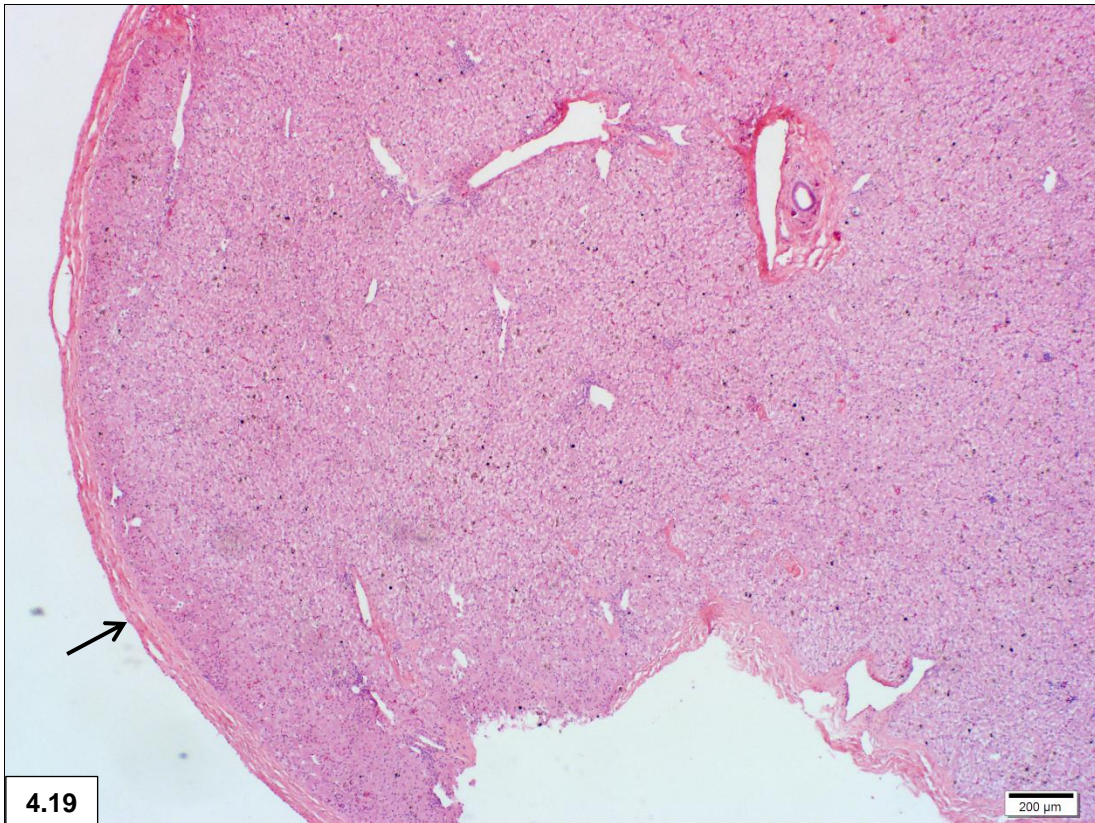
Figure 4.19: Low power view of the general architecture of the **isthmus** enclosed by Glisson's capsule (arrow). H/E.
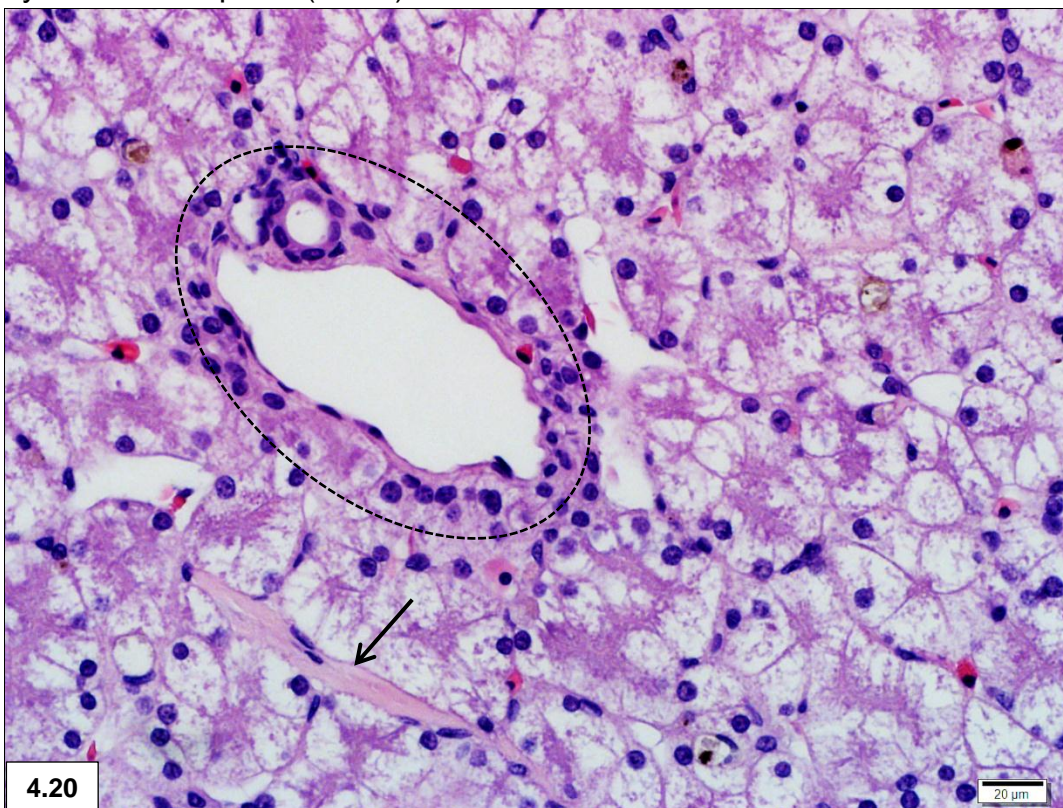

Figure 4.20: Isthmus - Portal triad (dashed lines) and hepatocytes exhibiting a clear cytoplasm. Hepatocyte tubular structures are evident. Note collagen trabecula (arrow). H/E.
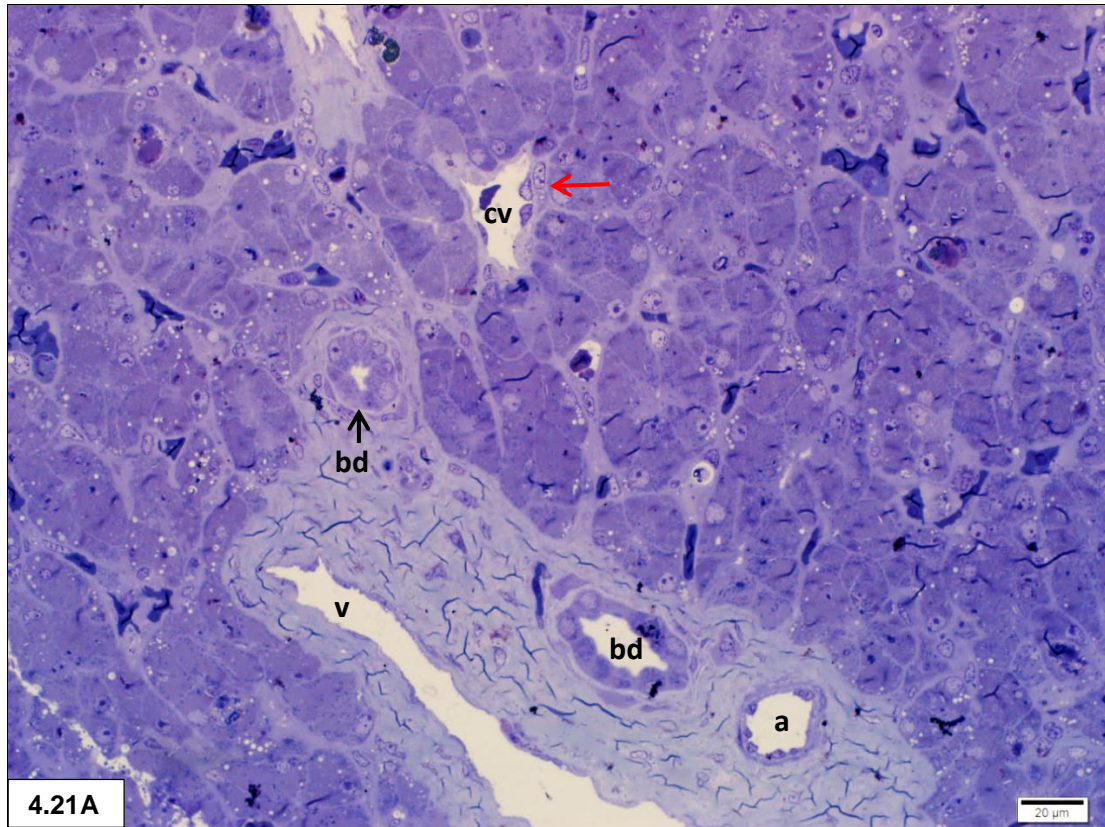
Figure 4.21: A – Isthmus - ** Portal triad enmeshed in collagen. Note central vein and stellate cell (red arrow) with underlying endothelial cells. Vein **(v); bile duct **(bd)**; artery **(a)**
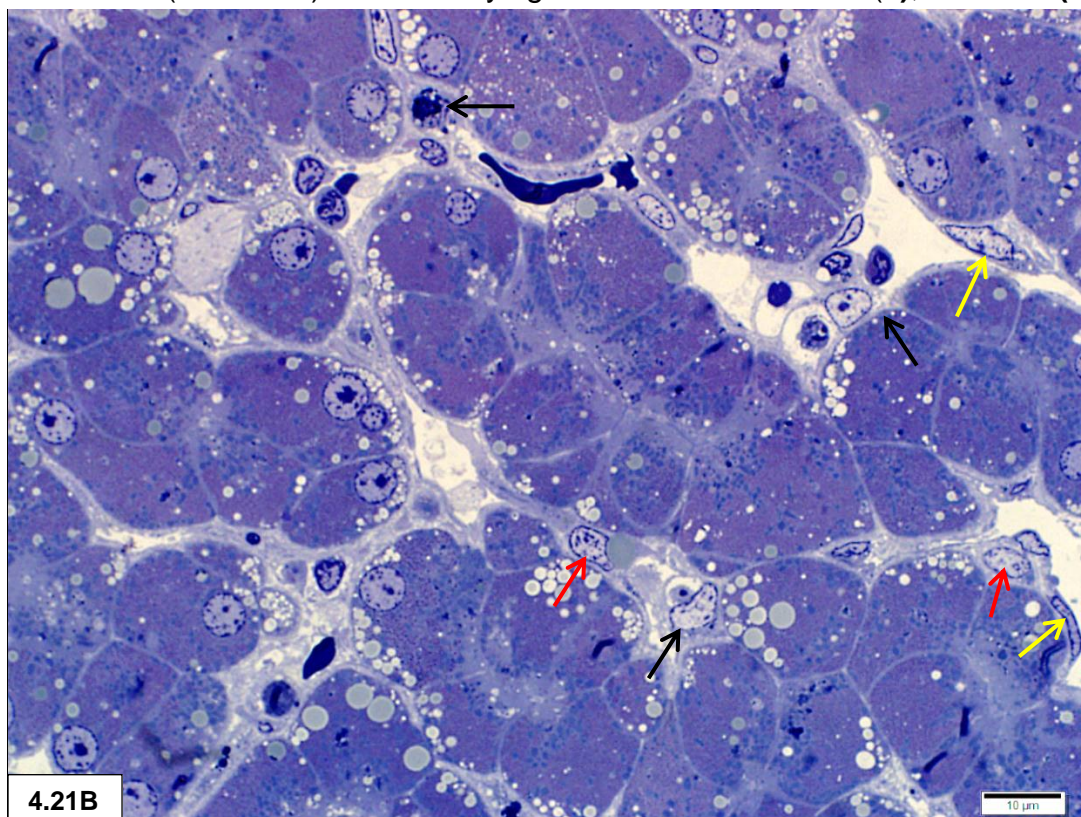

**Figure 4.21: B – ** Note stellate (red arrows), endothelial (yellow arrows) and Kupffer cells (black arrows). A few blood cells are evident. Note pinkish metachromasia indicating glycogen. TB.
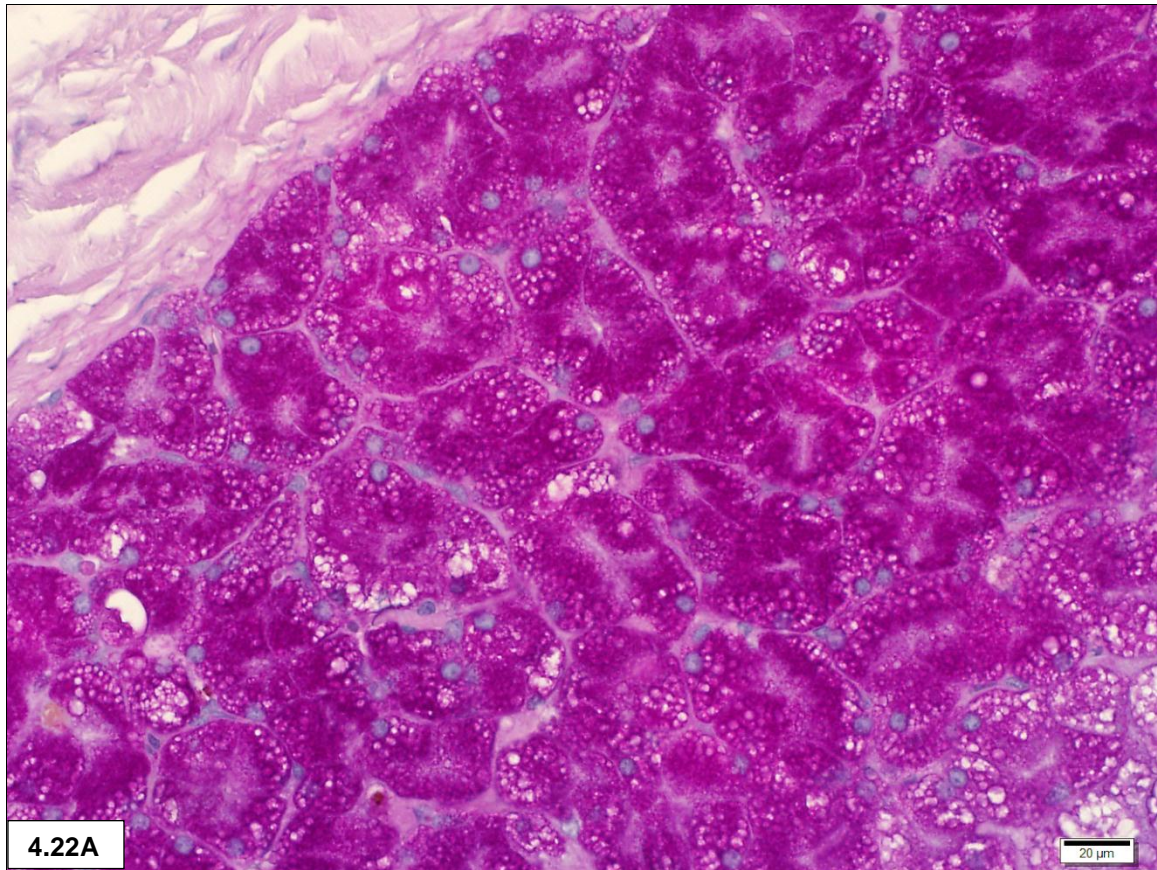
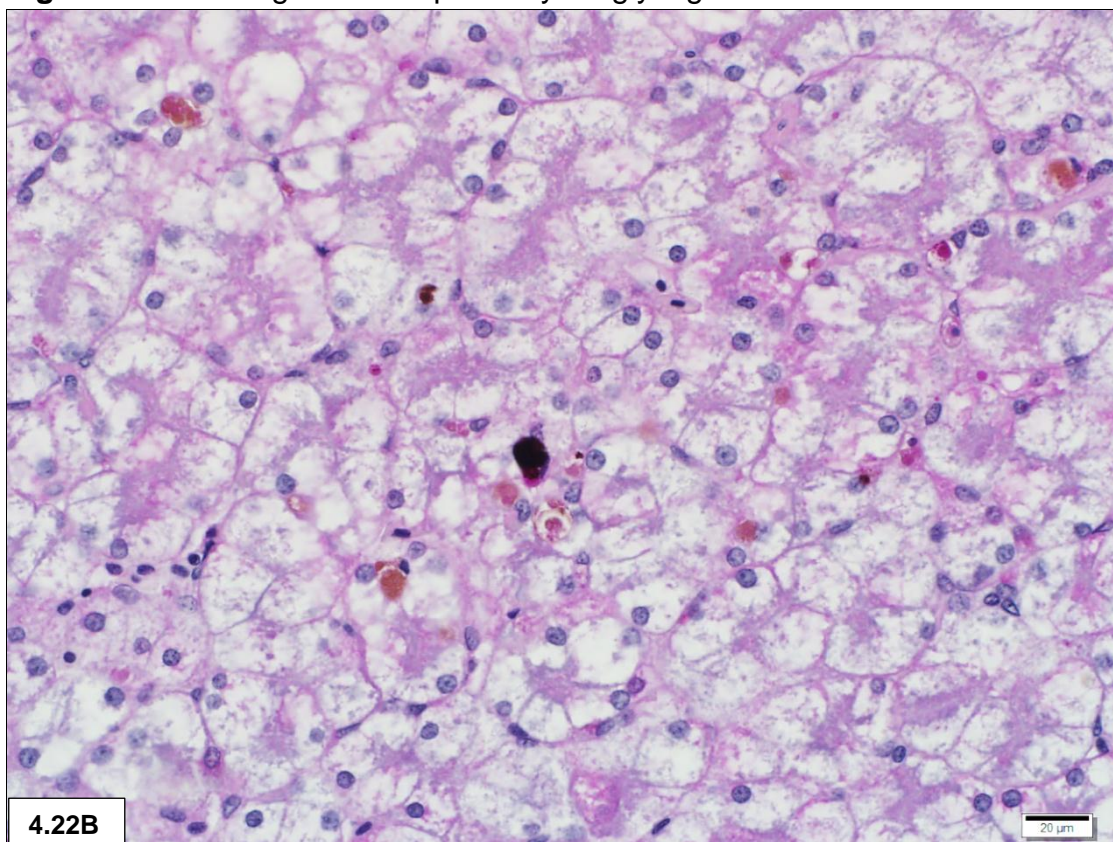**Figure 4.22 A:** Magenta PAS positivity for glycogen.

Figure 4.22 B: A similar region to that shown in Fig 4.22 A, demonstrating PAS diastase removal of glycogen.
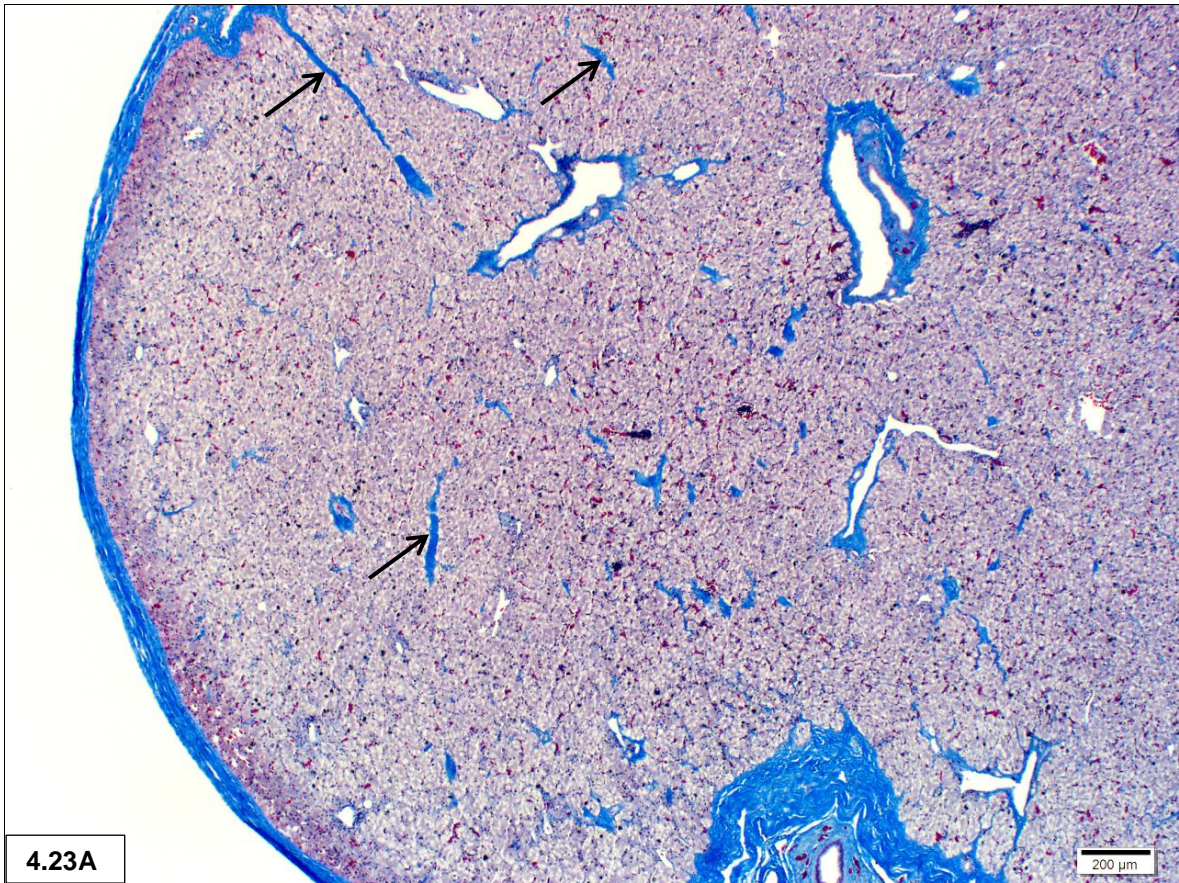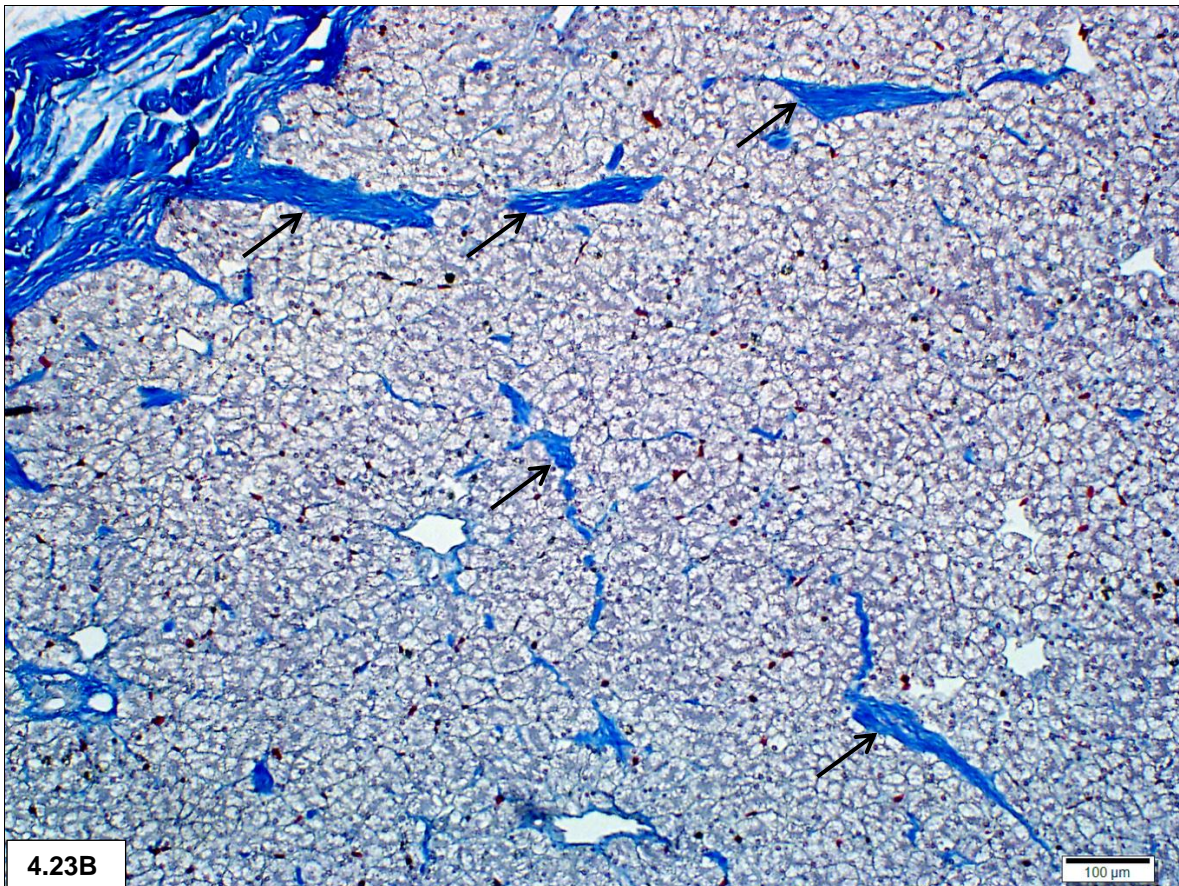
Figure 4.23 A & B: Blue collagen fibres (arrows), occasionally extending from the capsule, traversing the parenchyma haphazardly. Masson trichrome stain.

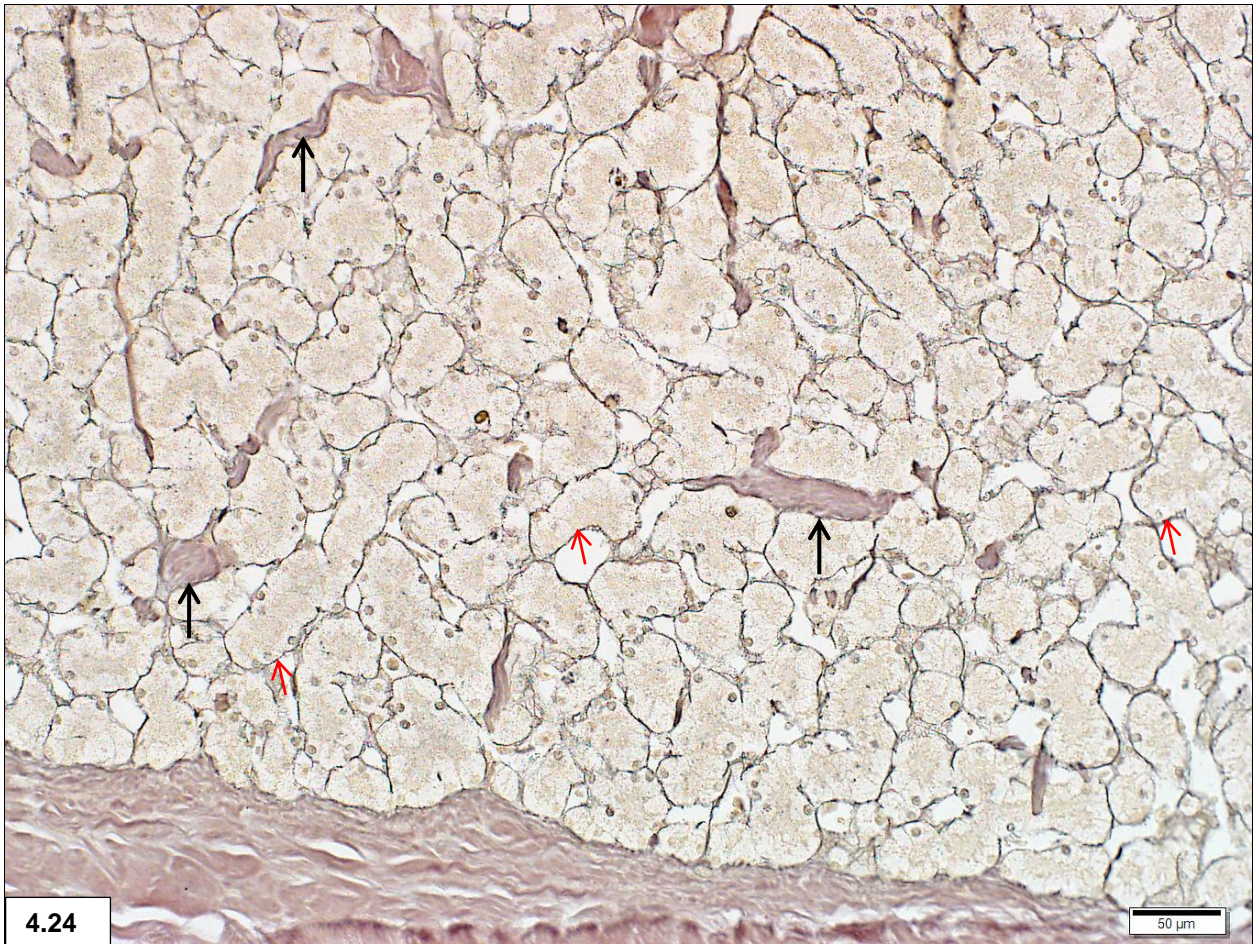**Figure 4.24:** Black reticular fibres (red arrows) surrounding the hepatocyte tubules. Gordon & Sweet's stain. Note collagen fibres (black arrows).
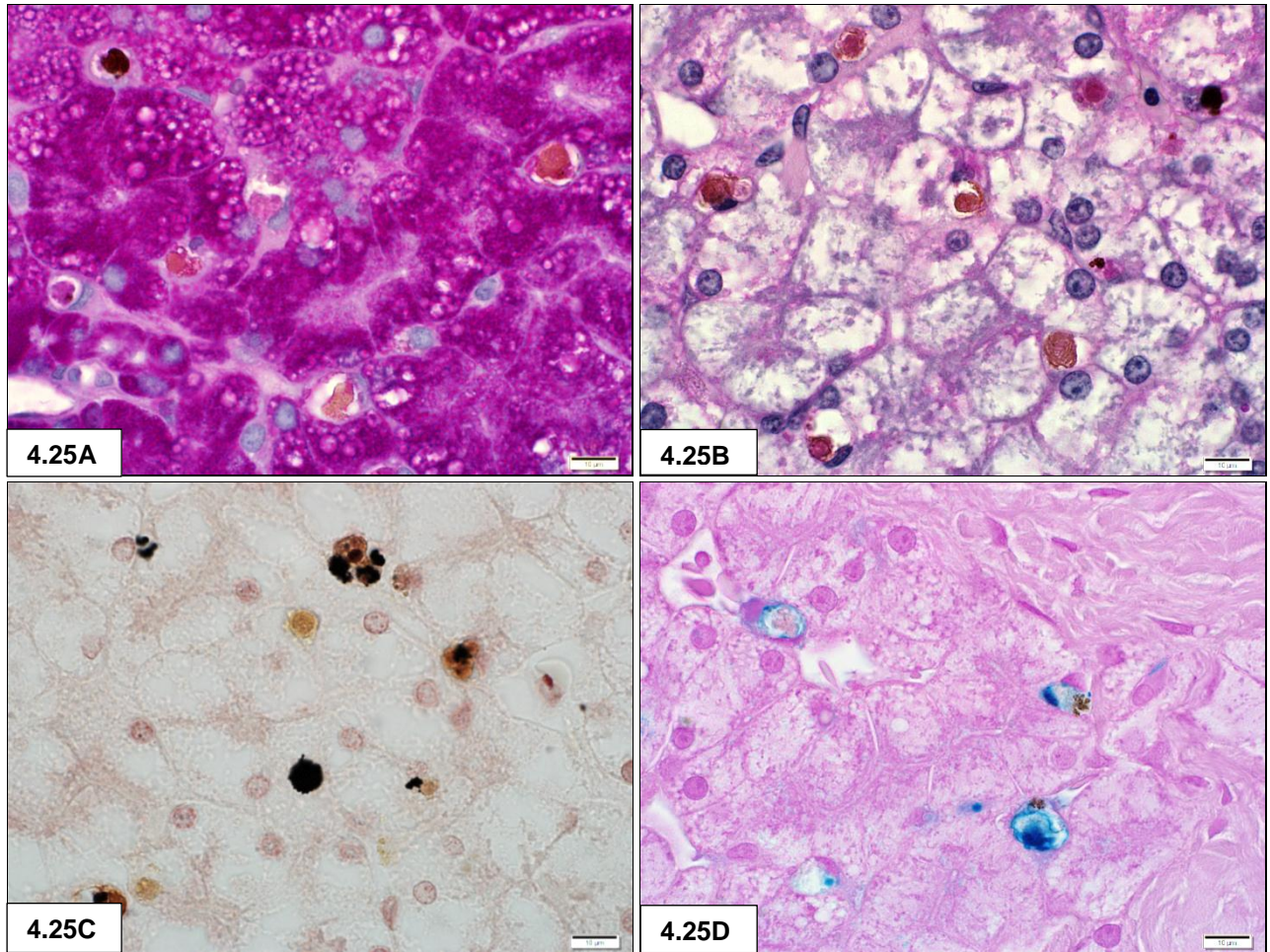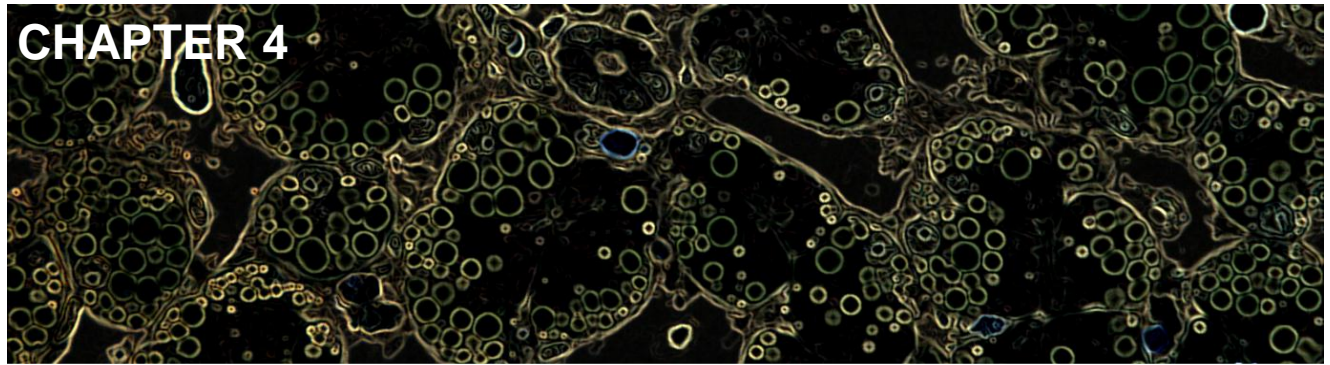
Figure 4.25: A – PAS; **B** – PAS-D; **C** – Masson-Fontana; **D –** Perls' Prussian blue

Large compound granular inclusions positive for melanin, hemosiderin and lipofuscin or ceroid. Note the diminished presence of peribiliary hemosiderin granules in **D**.

LIGHT MICROSCOPY OF THE LIVER

4.1 INTRODUCTION

The literature abounds with histological descriptions of the vertebrate liver. Hans Elias (1955) described the vertebrate liver as a muralium (system of walls) consisting of one- or two-cell-thick liver plates in which a sinusoidal network is suspended. Fried (2008) explained this muralium as a "three-dimensional lattice of interconnected plates made up of epithelial cells" tunnelled by lacunae containing sinusoids.

In 1986 Beresford and Henninger tabulated the variations in the microstructure of the liver of mammals, birds, fish and reptiles, but crocodiles were not mentioned. A brief overall view of reptilian liver histology was given by McClellan-Green *et al.* (2006) and Jacobson (2007). Schaffner (1998) wrote that the structure and cells of the reptilian liver were comparable to that of other vertebrates. Henninger (1982) and Moura *et al.* (2009) documented the light microscopy of the box turtle and the freshwater turtle respectively. Beresford (1987) briefly discussed the histology of the liver of *Caiman crocodilus* and Storch, Braunbeck and Waitkuwait (1989) included light microscopy in their ultrastructural study of the West African crocodile liver.

4.2 MATERIALS & METHODS

Liver samples were obtained from five 1-year old Nile crocodiles that were donated to the Faculty of Veterinary Science by Izintaba Crocodile Farm near Brits, North West Province, South Africa. They were euthanized by injecting sodium pentobarbital into the supra-vertebral vein. After muscular relaxation a lateral incision was made and the skin, ventral body wall and ribs were removed to expose the internal organs (Fig. 4.1).

Perfusion fixation was chosen as the method of fixation as the structural relationships in the liver are obscured by congestion when it is immersion-fixed. The portal vein to the right lobe was tied off *in situ* (Fig. 4.2), the liver removed from the body cavity and connected to a peristaltic pump (Fig. 4.3) (H.R. Flow Inducer, Watson Marlow Limited, England). The liver was perfused with a 0.5% heparin sodium (5000 IU/ml) saline solution, using the pump at 80 ml/min, to remove the blood from the sinusoids. The heparin solution was replaced with 2.5% glutaraldehyde in Millonig's buffer (pH 7.4, 0.13 M) that was pumped through the organ for approximately 20 minutes until a pale discoloration of the liver tissue indicated successful perfusion (Fig. 4.4).

With the completion of the perfusion procedure, tissue blocks were dissected from nine different areas in each of the five right liver lobes. The isthmus tissue failed to perfuse and a cross-sectional tissue block of this area was therefore immersion-fixed. All tissue samples were placed in 10% acqueous buffered formalin and fixed for a minimum of 24 hours before dehydrating through a graded ethanol series, clearing in xylene and infiltrating with paraffin wax in a Shandon Excelsior Thermo Electron Corporation tissue Processor. The samples were then embedded using a Thermolyne Histo Center 2 Embedding Unit and 3-5 micron thick sections were cut with a Reichert Jung rotary microtome.

Stains were performed to: (a) illustrate general liver architecture (haematoxylin & eosin, n=21); (b) identify glycogen (Periodic Acid-Schiff reaction & Periodic Acid-Schiff reaction with diastase treatment, both n=7), collagen (Masson Trichrome, n=14), reticular fibres (Gordon & Sweet's, n=9), iron deposits (Perls' Prussian blue reaction, n=9) and melanin (Masson Fontana, n=10) (Bancroft 2003). Toluidine blue of semi-thin resin sections was also performed (n=66).

4.3 IMAGE CAPTURING & PROCESSING

Slides of optimally perfused areas were examined by bright field & differential interference contrast illumination with an Olympus BX63 compound microscope and images were recorded with an Olympus DP72 digital camera. The Olympus CellSense software, version 1.5, was used to adjust the brightness and contrast, and a sharpening filter was applied where needed.

4.4 RESULTS

The liver consisted of parenchymal cells, i.e., hepatocytes, and diverse non-parenchymal cells, namely, endothelial cells, Kupffer cells and stellate cells. The parenchymal component occupied the largest part of the liver. The non-parenchymal cells were localized in and around the hepatic sinusoidal walls. Blood cells were occasionally found in the sinusoidal lumen and between the hepatocytes. A connective tissue stroma comprising blood and lymphatic vessels, blood cells, fibroblasts and bile ducts in a collagenous network made up the remainder of the liver. The isthmus contained liver tissue with a parenchymal and a non-parenchymal component.

4.4.1 Parenchymal organization

The principal cell in the juvenile Nile crocodile liver was the **hepatocyte**. A specific structural pattern such as the classic lobule, the portal lobule or the liver acinus was not distinguishable in the parenchyma. There was a haphazard arrangement of central veins and portal tracts surrounded by hepatocytes (Figs. 4.5 A & B, 4.9). The parenchyma was formed by anastomosing and branching cell cords consisting of two-cell-thick plates in the longitudinal sectional plane and at least 5 hepatocytes in the cross-sectional plane (Fig. 4.18 A & B). In longitudinal section long central bile channels could be discerned. The cross-sectional tubular configuration appeared gland-like with a common bile duct forming the 'lumen'. The hepatocytes appeared pyramidal in shape in cross sections and cuboidal in longitudinal section.

Hepatocytes

- Hematoxylin and eosin (H/E) staining reaction:

The cytoplasm was eosinophilic and contained blue-staining eccentric nuclei in the basal portion of the cell nearest to the sinusoids (Fig. 4.6 A & B). Distinctive pink cytoplasmic staining was present at the apical aspect of the cell abutting the bile canaliculi (peribiliary). Cytoplasmic vacuoles (Figs. 4.8 A & B) were present in the hepatocytes, most notably in the basal part of the cells, but could be present throughout the cytoplasm. The quantity of vacuoles present varied between the five livers and gave the hepatocytes a frothy

appearance. Other cytoplasmic inclusions in different shades of brown were also commonly observed (Figs. 4.6 A & B).

- Toluidine blue stain (TB) (semi-thin resin sections):

The eccentric pale-blue nuclei contained prominent dark-blue nucleoli (Fig. 4.13). The cytoplasm showed pale round inclusions of varying sizes, seemingly lipid droplets, with the rest of the cytoplasm appearing a darker blue colour (Figs. 4.8 B & 4.13).

- Periodic acid-Schiff (PAS) staining reaction:

There was a prominent magenta-staining cytoplasmic positivity indicating the presence of carbodydrates (Fig. 4.10).

- Periodic acid-Schiff staining reaction with diastase digestion (PAS-D):

The elimination of the magenta positivity by diastase digestion revealed that the hepatocytes contained an abundance of the carbohydrate glycogen (Fig. 4.11).

- Perls' Prussian blue reaction:

A fine blue granular positivity for hemosiderin was found in the peribiliary hepatocyte cytoplasm (Fig. 4.12).

- Masson-Fontana staining method:

Melanin granules were present, but it was difficult to discern whether the granules were present in the hepatocytes (Fig. 4.15).

4.4.2 Non-parenchymal organization

The sinusoids in the juvenile Nile crocodile liver were asymmetrical. Depending on the plane of sectioning endothelial cells, Kupffer cells and stellate cells were seen in and around the irregular sinusoids with hematoxylin and eosin staining. Small numbers of blood cells also appeared in this area.

The **Endothelial cells** were flat cells that lined the sinusoids (Fig. 4.13).

Kupffer cells (Fig. 4.13) were large pleomorphic cells that appeared to be lining the sinusoids or protruding into the sinusoidal lumen. Large yellow to brown granular inclusions (H/E - Figs. 4.6 A & B) were positive for melanin with the Masson-Fontana method (Figs. 4.15 & 4.16 C) and positive for hemosiderin with the Perls' Prussian blue method (Figs. 4.14 & 4.16 D) The granules consequently contained both melanin and hemosiderin - there was an additional light-pink staining component revealed in certain granules with the periodic-acid Schiff and the PAS-D reaction (Fig. 4.16 A & B).

Stellate cells (Fig. 4.21B) were difficult to identify in light microscopy sections, but occupied a subendothelial position.

Occasional **blood cells** (Fig. 4.13) were present in the sinusoidal lumen. Prominent bright-pink cytoplasmic granules with hematoxylin and eosin staining showed some of these cells to be eosinophils (Fig. 4.6 A) that in certain instances were also found between the hepatocytes.

4.4.3 Connective tissue stroma

The liver was enveloped by a **connective tissue capsule** (Glisson's capsule) (Fig. 4.9) ranging in thickness between 40 μm and 60 μm. It comprised an outer single layer of mesothelial cells covering a layer of prominent pink-staining fibres that sometimes extended from the capsule into the parenchyma between the hepatocytes. These fibres, present in all five livers, were of varying width and length and traversed the parenchyma in a haphazard manner. The fibres stained a vibrant blue with the Masson trichrome stain indicating the presence of **collagen** (Fig. 4.17 A - D). The capsule was in direct contact with the parenchymal tubular structures.

The parenchymal cellular arrangement was interrupted by **blood vessels, lymphatic vessels** and **bile ducts**, enclosed by a connective tissue network which also showed blue positivity for collagen using the Masson's stain (Fig. 4.17 A). Randomly distributed **portal triads** (Figs. 4.7 A & B; 4.8 A & B) consisting of an artery, a vein and a bile duct, surrounded by a blue collagenous meshwork (Figs. 4.8 B & 4.17 A), were seen. Lymphatic vessels (Fig. 4.8 A) sometimes accompanied the triads. The bile ducts were lined by simple cuboidal epithelium. Several cells, probably **fibroblasts, plasma cells** and **lymphocytes** were present in the surrounding fibrous sheath in some areas. Black-staining **reticular fibres**

(Gordon & Sweet's; Fig. 4.18 A & B) formed a delicate framework around hepatocyte groups, sinusoids and portal areas. Distinctive pink borders, partially surrounding some of the hepatocyte tubules, were seen with the PAS-D reaction, indicating the presence of a basal lamina (Fig. 4.16 B).

4.4.4 Isthmus

The **isthmus** (Fig. 4.19) consisted of liver tissue comprising parenchymal and non-parenchymal cells enclosed by Glisson's capsule. Collagen fibres, occasionally extending from the capsule, traversed the parenchyma haphazardly (Fig.4.23 A & B). Portal triads (Fig. 4.20) enmeshed in collagen (Fig. 4.21 A) and central veins were evident, although no lobulation was seen. The hepatocytes exhibited a clear cytoplasm (Fig. 4.20) in areas and the tubular nature of the hepatocyte cords could be discerned despite the tissue being immersion-fixed. PAS and PAS-D staining reactions revealed the hepatocyte cytoplasm to be filled with glycogen (Figs. 4.22 A & B). The immersion fixation procedure made the recognition of the sinusoids, endothelial cells, stellate cells and blood cells (excluding red blood cells) difficult in H/E preparations, but Toluidine blue resin sections revealed these structures adequately (Fig. 4.21 B). Kupffer cells were identified by means of large granular inclusions that were again melanin, hemosiderin and PAS-D positive (Fig. 4.25 A-D). There was a diminished presence of peribiliary hemosiderin granules (Fig. 4.25 D). A fine network of black reticular fibres (Fig. 4.24) surrounded the groups of hepatocytes and clearly showed their tubular nature.

4.5 DISCUSSION

4.5.1 Parenchymal organization

The present study concurs with several authors that the classic lobular pattern seen in the livers of mammals does not apply to reptiles in general (Henninger 1982; Goldblatt *et al.* 1987; Schaffner 1998; McClellan-Green *et al.* 2006) or to the West African crocodile and the broad-nosed caiman (Storch *et al.* 1989; Starck *et al.* 2007). Hepatocyte tubules (McClellan-Green *et al.* 2006; Jacobson 2007) or plates (Richardson *et al.* 2002) may be organized radially around central veins or around portal veins (Henninger 1982). Parenchymal lobulation may be completely absent in some reptiles (McClellan-Green *et al.* 2006) as in the case of the juvenile Nile crocodile. 'Discrete hepatic lobules' were found by Richardson *et al.*

(2002) in the Saltwater and Australian freshwater crocodiles and Kassab *et al.* (2009) described classic hepatic lobules in the Desert tortoise.

Beresford & Henninger (1986) reviewed the various microscopical differences in the livers of mammals, birds, fish, reptiles & amphibians - crocodiles were however excluded. The authors' criteria for perceived parenchymal tubules, namely separate round cross-sectional profiles of pyramidal cells with central lumina, have been described in the four non-mammalian vertebrate classes. This interpretation is shared by the current findings of a tubular parenchymal structure in the juvenile Nile crocodile and was also described in *Caiman latirostris* (Starck *et al.* 2007) and in the freshwater turtle by Moura *et al.* (2009). The branching and anastomosing of hepatocyte tubules found in the juvenile Nile crocodile, as well as the two-cell-thick tubules, were also described in the crocodilian *Osteoleamus* by Storch *et al.* (1989) and in some reptiles (Elias and Bengelsdorf 1952, Schaffner 1998). The findings of Goldblatt *et al.* (1987) in the Newt liver and in *Phrynops geoffroanus* (Moura *et al.* 2009) that the hepatocyte chords were two to five cells thick corresponds to the current observations of the tubules in longitudinal and cross-sectional profile.

A limiting plate consisting of a single layer of hepatocytes beneath Glisson's capsule and also encircling the portal tracts is present in the human liver (Elias 1955, Fried 2008, www.pathologyoutlines.com). This continuous single cell layer was absent in the Nile crocodile where the parenchymal structures abutted the capsule and portal tracts directly.

The location of hepatocyte nuclei differs among the reptiles. Central nuclei were found in both the Newt (Goldblatt *et al.* 1987) and the freshwater turtle (Moura *et al.* 2009). Nuclei were described as being 'near to the vascular pole' in the West African crocodile (Storch *et al.* 1989) and basal nuclei were found by Henninger (1982) in the box turtle. The latter matches the eccentric nuclei seen in the juvenile Nile crocodile.

Henninger (1982) found hemosiderin positive granules in the apical hepatocytes of the Box turtle. Some of the pink (H/E) cytoplasmic granules seen peribiliary in the hepatocytes stained positive for hemosiderin (Perl's Prussian blue reaction) whereas the remaining pink granules may represent normal cytoplasmic organelles, for example mitochondria. The large brownish inclusions that seemed to be part of the parenchyma may be credited to the presence of bile pigments in hepatocytes (Kumar & Kiernan 2010). Electron microscopy (Chapter 5) will shed more light on these two observations.

The five livers in the present study contained varying quantities of vacuoles that in H/E preparations imparted a frothy look to the hepatocytes. The toluidine blue stain showed distinctive pale-coloured round vacuoles of differing sizes, mostly in the basal region, indicating lipid droplets. Starck *et al.* (2007) found lipid droplets in the apical part of the hepatocytes in the caiman. At the light microscopical level (H/E) vacuolation may be ascribed to the presence of water, glycogen, lipid or other material (Divers & Cooper 2000). Moura *et al.* (2009) attributed the vacuolated appearance of the hepatocytes in the freshwater turtle to an abundance of glycogen. Storch *et al.* (1989) described basal glycogen and the presence of lipid in glycogen areas. Ultrastructural examination (see Chapter 5) resolves this uncertainty.

4.5.2 Non-parenchymal organization

Elias and Bengelsdorf (1952) proposed that narrow, cylindrical **sinusoids** be called tubulosinusoidal and wide, irregularly shaped sinusoids be called sacculosinusoidal. They found the livers of lizards and tortoises to be of the sacculosinusoidal type and that of young alligators to be intermediate between the two sinusoidal types. The sinusoids of the broad-nosed caiman were described as 'very narrow' by Starck *et al.* (2007). The sinusoids in the present study were also of the intermediary type.

Some authors differentiate between **Kupffer cells** and melanomacrophages and some call these cells 'pigment cells' or 'specialized Kupffer cells' when containing melanin granules (Storch *et al.* 1989; Schaffner 1998; McClellan-Green *et al.* 2006; Jacobson 2007). Barni *et al.* (1999) deemed the pigment cells to derive from Kupffer cells. The Kupffer cells in this study were located in different areas and not only bound to the sinusoidal wall – it is difficult to type these cells as Kupffer cells or melanomacrophages at the light microscopical level and this matter will be considered in Chapter 5. Pigment cell clusters or collections of specialized Kupffer cells have been noted in other reptiles (Henninger 1982; Henninger & Beresford 1990; McClellan-Green *et al.* 2006; Jacobson 2007), but cell collections were not seen in the juvenile Nile crocodile liver. Instead, numerous but discretely scattered pigmented Kupffer cells were observed. Pigment cells were rare in the juvenile West African crocodile (Storch *et al.* 1989) and in some other reptile species (Hack & Helmy 1964; McClellan-Green *et al.* 2006). The hepatocytes of the lizard *Sceloporus* also contained pigment in addition to the pigment found in the Kupffer cells (Ells 1954). Moura (2009) did not mention Kupffer cells in the liver of the Freshwater turtle, but commented on the

presence of many melanomacrophages in the parenchyma. Perhaps the cells seen containing the identical yellow-brownish granules as Kupffer cells, and that were part of the hepatocyte groups in the Nile crocodile, are in fact melanomacrophages.

The large yellow-brownish cytoplasmic inclusions seen in the Nile crocodile Kupffer cells were positive for both **melanin** and **hemosiderin**, a feature also described by Jacobson (2007) in other reptiles, and also contained a third element. Hemosiderin is usually seen in cells responsible for the breakdown of effete red blood cells and consists, among others, of ferritin and glycoproteins (Kumar & Kiernan 2010). Glycoproteins are PAS positive and may account for the third pink element in the large yellow-brown granules. Other possible contenders for the third pink component may be either **ceroid** or **lipofuscin** as both these pigments are PAS positive (www.pathologyoutlines.com, Schaffner 1998). According to these two references ceroid pigment represents degraded cellular debris and lipofuscin denotes the accumulation of indigestible material mixed with lipid droplets. Kumar & Kiernan (2010) however describe ceroid as a type of lipofuscin. Ultrastructural features (see Chapter 5) distinguished between the two pigments.

4.5.3 Connective tissue stroma

The livers of the Saltwater and Australian freshwater crocodiles were covered by a 'thick fibrous capsule' and showed 'relatively little interstitial connective tissue' (Richardson *et al*. 2002). The connective tissue layers separating neighbouring liver lobules in some mammals were not evident in reptiles (Jacobson 2007). The juvenile Nile crocodile liver revealed prominent collagenous fibres of varying sizes criss-crossing the liver parenchyma from Glisson's capsule to the portal areas. Beresford (1987) found connective tissue only in the liver capsule, portal tracts and large hepatic venules of the juvenile *Caiman crocodilus,* but a further study (Beresford 1993) found thin collagenous trabeculae in the parenchyma in three out of four Caiman livers examined. The liver of *Alligator mississippiensis* showed intermediate trabeculae of collagen linking the connective tissue of the liver capsule and portal tracts. Beresford (1993) hypothesized that the function of the collagen trabeculae in the alligator liver was to withstand thrashing of the body when subduing prey. Goldblatt *et al.* (1987) found connective tissue to be sparse in the Newt liver.

Schaffner (1998) desribed the portal tracts of reptiles to be randomly organized and Moura *et al.* (2009) noted an abundant connective tissue support for the portal tracts in the

Freshwater turtle. This is in agreement with the findings in the juvenile Nile crocodile. Beresford (1987) described the larger bile ducts of the Caiman to have a thick collagenous and cellular wall and speculated that this feature may have a supporting function.

The liver architecture in the present study was characterised by a delicate network of black reticular fibers (Gordon & Sweet's stain) around the hepatocytic tubules, sinusoids and portal areas. This was also found to be true of the Freshwater turtle (Moura *et al.* 2009). Kassab *et al.* (2009) described 'a fine meshwork of reticular fibres around the sinusoids and within the perisinusoidal spaces' of the Desert tortoise liver. Many studies do not mention the staining of reticular fibres.

Henninger (1982) and Storch *et al.* (1989) both noticed distinct PAS-positive boundaries, indicating the presence of basal lamina, around the hepatocyte tubules of the box turtle and the West African crocodile respectively. These boundaries, although incomplete and not present around all tubules, were demonstrated by the PAS-D reaction in the Nile crocodile. (See Chapter 5).

4.5.4 Isthmus

The light microscopical findings supported the macroscopical assumption (Chapter 3) that the flattened isthmus consisted of liver tissue and consequently contained parenchymal and non-parenchymal components. Marycz & Rogowska (2007) and Kassab (2009) described the isthmus of tortoises as consisting of connective tissue. Some authors mention the isthmus (Mushonga & Horowitz 1996), or dorsal bridge (Huchzermeyer 2003), or 'middle constricted portion' (Chiasson 1962), but do not elaborate further on its composition. Other authors do not refer to the existence of an isthmus in reptiles (Schaffner 1998, McClellan-Green *et al.* 2006).

The clear cytoplasm of the hepatocytes in this region may be due to the leaching of glycogen & lipid during histological processing. The light microscopical results of the isthmus indicate that this narrow tissue bridge is an extension of the two liver lobes with the same functional capabilities. Perhaps the existence of an isthmus can be ascribed to a developmental adaptation for the incorporation of other organs in the body cavity.

4.6 REFERENCES

BANCROFT, J.D. 2003. *Theory and Practice of Histological Techniques*. New York, Churchill Livingstone.

BARNI, S., BERTONI, V., CROCE, A.C., BOTTIROLLI, G., BERNINI, F. & GERZELI, G. 1999. Increase in liver pigmentation during natural hibernation in some amphibians. *Journal of Anatomy,* 195: 19-25.

BERESFORD, W.A. 1987. Some light microscopic histology of the liver in *Caiman crocodilus. The Anatomical Record,* 218: 16A.

BERESFORD, W.A. 1993. Fibrous trabeculae in the liver of alligator (*Alligator mississipiensis). Annals of Anatomy,* 175: 357-359.

BERESFORD, W.A. & HENNINGER, J.M. 1986. A tabular comparative histology of the liver. *Archives Histology Japan,* 49: 267-281.

CHIASSON, R.B. 1962. Digestive system, in *Laboratory anatomy of the alligator.* USA: WM.C. Brown, pp. 36-37.

DIVERS, S.J. & COOPER, J.E. 2000. Reptile hepatic lipidosis. *Seminars in Avian and Exotic Pet Medicine,* 9: 153-164.

ELIAS, H. & BENGELSDORF, H. 1952. The structure of the liver of vertebrates. *Acta Anatomica,* 15: 297-337.

ELIAS, H. 1955. Liver morphology. *Biological Reviews,* 30: 263-310.

ELLS, H.A. 1954. The gross and microscopic anatomy of the liver and gall bladder of the lizard, *Sceloporus occidentalis biseriatus* (Hallowell). *The Anatomical Record,*119: 213-229.

FRIED, G.H. 2008. Liver, in *AccessScience.* © McGraw-Hill Companies.

http://www.accessscience.com

GOLDBLATT, P.J., HAMPTON, J.A., DIDIO, L.N., SKEEL, K.A. & KLAUNIG, J.E. 1987. Morphologic and histochemical analysis of the Newt (*Notophthalmus viridescens*) liver. *The Anatomical Record,* 217: 328-338.

HACK, M.H. & HELMY, F.M. 1964. A comparative chemical study of the liver of various vertebrates. *Acta Histochemistry,* 19: 316-328.

HENNINGER, J.M. 1982. Histology of the liver in the box turtle. *The Anatomical Record,* 202: 79A.

HENNINGER, J.M. & BERESFORD, W.A. 1990. Is it coincidence that iron and melanin coexist in hepatic and other melanomacrophages? *Histology and Histopathology*, 5: 457-459.

HUCHZERMEYER, F.W. 2003. Crocodiles and alligators, in *Crocodiles: biology, husbandry and diseases,* edited by F.W. Huchzermeyer. Cambridge: CABI Publishing, 1:1-52.

JACOBSON, E.R. 2007. Overview of reptile biology, anatomy, and histology, in *Infectious diseases and pathology of reptiles,* edited by E.R. Jacobson. CRC Press, Taylor & Francis Group, 6000 Broken Sound Parkway NW, Suite 300, Boca Raton, FL 33487-2742, pp.1-130.

KASSAB, A., SHOUSHA, S. & FARGANI, A. 2009. Morphology of blood cells, liver and spleen of the Desert Tortoise (*Testudo graeca*). *The Open Anatomy Journal,* 1*:* 1-10.

KUMAR, G.L. & KIERNAN, J.A. 2010. *Education guide: Special stains and H & E.* Dako North America, California. www.dako.com.

MARYCZ K., ROGOWSKA K. 2007. The liver morphology and topography of Horsfield's (*Testudo horsfieldi*) and Hermann's (*T. Hermanni*) terrestrial tortoises. *Electronic Journal of Polish Agricultural Universities,* 10: 1-9.

MCCLELLAN-GREEN, P., CELANDER, M. & OBERDÖRSTER, E. 2006. Hepatic, renal and adrenal toxicology, in *Toxicology of reptiles,* edited by S.C. Gardner & E. Oberdörster. CRC Press, Taylor & Francis Group, 6000 Broken Sound Parkway NW, Suite 300, Boca Raton, FL 33487-2742, pp.123-148.

MOURA, L.R., SANTOS, A.L.Q., BELLETI, M.E., VIEIRA, L.G., ORPINELLI, S.R.T. & DE SIMONE, S.B.S. 2009. Morphological aspects of the liver of the freshwater turtle *Phrynops geoffroanus* Schweigger, 1812 (Testudines, Chelidae). *Brazilian Journal of Morphological Science,* 26: 129-134.

MUSHONGA, B. & HOROWITZ, A. 1996. Serous cavities of the Nile crocodile (*Crocodylus niloticus). Journal of Zoo and Wildlife Medicine,* 27: 170-179.

RICHARDSON, K.C., WEBB, G.J.W. & MANOLIS, S.C. 2002. Digestive system, in C*rocodiles: inside out,* edited by K.C. Richardson. Australia: Surrey Beatty & Sons PTY LIMITED, pp. 89-94.

SCHAFFNER, F. 1998. The hepatic system, in *Biology of reptilia: volume 19, Morphology G: Visceral organs,* edited by C. Gans & A.B. Gaunt. Society for the Study of Amphibians and Reptiles, Missouri, pp. 485-531.

STARCK, M.J., CRUZ-NETO, A.P. & ABE, A.S. 2007. Physiological and morphological responses to feeding in broad-nosed caiman (*Caiman latirostris*). *The Journal of Experimental Biology,* 210: 2033-2045.

STORCH, V., BRAUNBECK, T. & WAITKUWAIT, W.E. 1989. The liver of the West African crocodile *Osteolaemus tetraspis.* An ultrastructural study. *Submicroscopical Cytology and Pathology,* 21: 317-327.

WWW Site reference:

www.pathologyoutlines.com
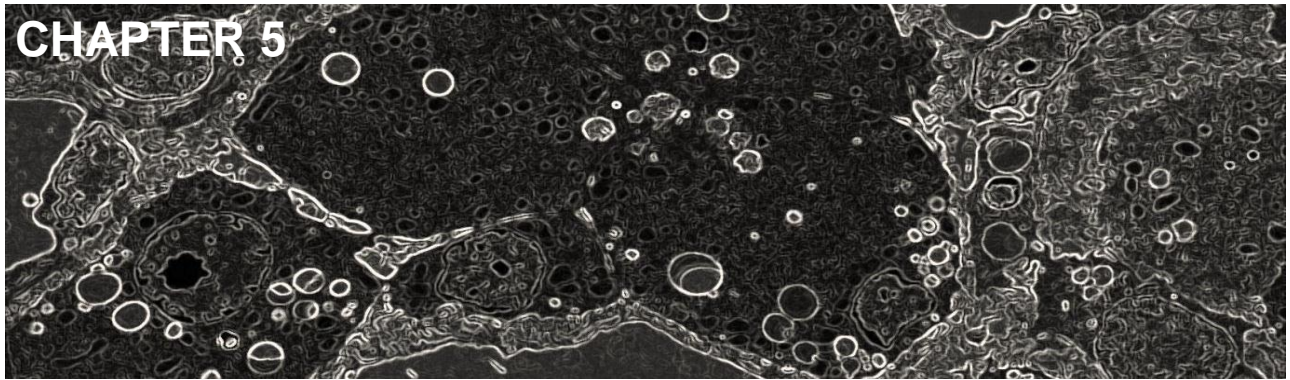
TRANSMISSION ELECTRON MICROSCOPY OF THE LIVER

5.1 INTRODUCTION

In addition to textbooks, for example, Ross *et al.* (2003), that discuss the electron microscopy of the human liver, its ultrastructure is also dealt with in great depth by Phillips *et al.* (1987) as well as by Goldblatt & Gunning in a brief review in 1984. The fine structure of the liver of other mammalian species is covered extensively in the literature (Wisse & Knook 1977; De Leeuw *et al.* 1990; McCuskey & McCuskey 1990; Van Bezooijen 1990; Baratta *et al.* 2009). Some publications compare the electron microscopical aspects of liver cells of various species, including reptiles (Beresford & Henninger 1986; Kalashnikova 1996; Schaffner 1998). The liver of the Nile crocodile was not specifically investigated by these authors. Goldblatt *et al.* (1987) and Henninger (1982) gave short descriptions of the ultrastructure of the newt liver and the box turtle respectively. The West African crocodile *Osteolaemus tetraspis* liver was explored ultrastructurally by Storch *et al.* in 1989. There is an obvious paucity of literature dealing with the ultrastructure of the crocodilian liver and the present study will therefore rely on the descriptions in other vertebrates for evaluation.

5.2 MATERIALS AND METHODS

After removal of the liver from the body cavity the portal vein was connected to a perfusion apparatus (Chapter 4, Fig. 4.3) and perfused with a 0.5% heparin sodium (5000 IU/ml) saline solution, using the peristaltic pump at 80 ml/min, to remove the blood from the sinusoids. The heparin solution was replaced with 2.5% glutaraldehyde in Millonig's buffer (pH 7.4, 0.13 M) and perfused for approximately 20 minutes until a pale discoloration of the liver tissue indicated successful perfusion (Chapter 4, Fig. 4.4).

Small samples taken in parallel to the histology tissue blocks (namely 9 areas/liver lobe, 5 right liver lobes) were diced into 1mm^3 tissue blocks and immersion-fixed in 2.5% glutaraldehyde in Millonig's phosphate buffer (pH 7.2) for at least 24 hours. The tissue blocks were then rinsed in Millonig's buffer, post-fixed in 1% osmium tetroxide in the same buffer for a minimum of one hour, rinsed again and dehydrated through a series of graded ethanols before infiltrating with propylene oxide and epoxy resin (TAAB 812 resin, TAAB Laboratories, England) (Bozzola & Russell 1992). The isthmus tissue failed to perfuse in areas and a cross-sectional tissue block (n=5) of this area was therefore also immersion-fixed in 10% acqueous buffered formalin and fixed for a minimum of 24 hours before dissecting into smaller blocks and processing into epoxy resin.

Toluidine blue stained (Hayat 2000) 0.35 micron semi-thin resin sections (n=66) were assessed light microscopically for the selection of optimally perfused areas (sinusoids not disrupted or collapsed) for ultrastructural examination. Ultra-thin (50-90 nm) sections (Reichert-Jung Ultramicrotome) were collected onto copper grids (n=132) and stained with Reynold's lead citrate and an acqueous saturated solution of uranyl acetate (Hayat 2000).

5.3 IMAGE CAPTURING & PROCESSING

The ultrastructure of the resident liver cells with their organelles, bile canaliculi, sinusoidal spaces and connective tissue in 80 grids were examined with a Philips CM 10 transmission electron microscope (FEI, Eindhoven, Netherlands) operated at 80 kV. A Megaview III side-mounted digital camera was used to capture the images and iTEM software (Olympus Soft Imaging System GMBH) to adjust the brightness and contrast.

5.4 RESULTS

The ultrastructural findings in the liver of the juvenile Nile crocodile reflected the light microscopy results (Chapter 4): a parenchyma with hepatocytes, and non-parenchymal cells, namely endothelial, Kupffer and stellate cells, with a connective stromal component, were present. Blood cells, for example, pit cells, lymphocytes, plasma cells, eosinophils and thrombocytes were seen. The isthmus contained the same components as the liver tissue proper.

5.4.1 Parenchyma

Hepatocytes

Hepatocytes were arranged in the form of tubular cell cords. In transverse section the cords were composed of approximately five hepatocytes arranged around a bile canaliculus (Fig. 5.1) while in longitudinal section they appeared as a two-cell-thick plate between which the bile canaliculus was sometimes observed. The four individual cell sides of a hepatocyte as seen in both the transverse and longitudinal sections were in contact basally with a sinusoidal wall, laterally with two adjacent hepatocytes and apically with a bile canaliculus. The hepatocyte surface facing the sinusoid was lined by microvilli that presented in the space of Disse - the hepatocytes were therefore not in direct contact with the sinusoidal wall. The cross-sectional tubular cell arrangement showed hepatocytes converging to form a central bile canaliculus (Fig. 5.1). In this instance the hepatocyte side facing the sinusoid was dome-shaped. Pinocytotic vesicles between the microvilli were apparent (Fig. 5.2). The lateral cell membranes of the hepatocytes, a distance away from the canaliculi, sometimes exhibited occasional desmosomes (Fig. 5.4) and microvilli. The basal lamina surrounding groups of hepatocytes, as demonstrated with the PAS-D reaction (Chapter 4), was absent ultrastructurally. A basal lamina was however found lining the hepatocytes on the side directly adjacent to Glisson's capsule (Fig. 5.3).

Nucleus – Generally one, round, eccentrically placed nucleus was present close to the sinusoidal lumen (Fig. 5.1). Occasional bi-nucleated cells were found (Fig. 5.6). Heterochromatin masses were displayed throughout the nucleus as well as forming a definite rim along the nuclear envelope. The nucleus was enclosed by a typical double membraned nuclear envelope. Prominent nucleoli (Fig. 5.5), mostly one per nucleus, were seen. The nucleoli were large with no limiting membrane and were mostly positioned off-centre in the nuclei. They had rough edges and some displayed a combination of electron-dense and lightly contrasted material occasionally surrounding an open space. No nuclear inclusions were noted.

Endoplasmic Reticulum – The granular endoplasmic reticulum (GER) presented as matching membrane pairs dotted with ribosomes and was present between the other cytoplasmic constituents. GER membranes also appeared in parallel with the lateral plasma membranes and often surrounded mitochondria (Fig. 5.7). Nude membraned

vesicles (i.e. without ribosomes) representing smooth endoplasmic reticulum (SER) were also found in the cytoplasm.

<u>Mitochondria</u> – Several mitochondria surrounded by a double membrane, with the inner membrane forming the cristae, were seen in the hepatocytes. The mitochondrial matrix contained electron-dense granules (Figs. 5.7 & 5.8). There was a polar orientation of the mitochondria in some hepatocytes with most of the mitochondria converging towards the bile canaliculi.

<u>Peroxisomes</u> – A few scattered, spherical, single-membrane-bound peroxisomes with amorphous contents of medium electron density were seen (Fig. 5.8). These organelles were indistinct and smaller than mitochondria and a nucleoid or marginal plate could not be identified.

<u>Lysosomes</u> – Lysosomes limited by a single membrane were present in the cytoplasm, mostly at the peribiliary pole of the hepatocytes. The lysosomes contained hemosiderin granules (Fig. 5.9) and slit-like spaces indicating the presence of cholesterol esters (Fig. 5.10).

<u>Golgi </u>– The accepted description of this organelle as parallel, curved, flattened saccules of cisternae with bulbous ends applied to the Golgi apparatus (Fig. 5.14). This structure was frequently found in the pericanalicular cytoplasm.

<u>Cytoskeleton</u> – Microtubules and microfilaments (Fig. 5.14) were seen in the cytoplasm.

<u>Glycogen</u> – Monoparticulate glycogen particles (beta or single glycogen particles) and glycogen rosettes (alpha or clusters of electron dense monoparticulate glycogen particles) (Fig. 5.8) were abundant throughout the cytosol except in areas where lipid droplets and lysosomes dominated.

<u>Lipid </u>– Variable numbers of lipid droplets that varied in size (Fig. 5.1) were present and were concentrated at the sinusoidal pole in some hepatocytes. The lipid droplets were virtually electron-lucent and not surrounded by a membrane.

<u>Centrioles </u>– These structures were seen at the pericanalicular pole in a few hepatocytes (Fig. 5.13).

<u>Pigments</u> - Loose lying cytoplasmic melanin granules were occasionally seen (Fig. 5.11). Prominent membranous concretions with morphological features typical of bile pigment were also noticed (Fig. 5.12).

<u>Other inclusions</u> - Cytoplasmic electron opaque slit-like areas (Fig. 5.10), indicating cholesterol esters, were found near the bile canaliculi.

Due to their position in relation to the hepatocytes the **bile canaliculi** will be discussed under this heading. In transverse section they appeared as small spaces forming a 'lumen' lined by hepatocyte plasma membranes displaying scanty microvilli protruding into the space (Fig. 5.13). Longitudinal sections of cords of hepatocytes showed elongated bile canaliculi (Fig. 5.15). Junctional complexes between neighbouring hepatocytes sealed off the canalicular spaces (Fig. 5.14).

5.4.2 Non-parenchymal Component

The angular **sinusoids** (Figs. 5.16 & 5.17) found between groups of hepatocytes were lined by endothelial cells. Kupffer cells could sometimes be found lining the spaces and stellate cells were resident in the subendothelial tissue. A few blood cells also occupied the sinusoidal lumen. No basal lamina was seen around the sinusoids, but the space of Disse (Fig. 5.18) containing the basal microvilli of the hepatocytes was present between the endothelial cells and groups of hepatocytes. Normal collagen fibrils and long-spacing collagen fibrils were noted in the space of Disse (Figs. 5.20 & 5.21).

Endothelial cells

Lining the sinusoids were flat endothelial cells with thin nuclei and long cytoplasmic extensions (Figs. 5.16 & 5.17). Very active endothelial cells were more bulky in appearance. This lining was sometimes interrupted by Kupffer cell cytoplasmic protrusions or Kupffer cells forming part of the lining (Figs. 5.17 & 5.31). Fenestrated cytoplasmic extensions and gaps between neighbouring endothelial cells were seen (Fig. 5.18). Overlapping cell extensions with tight junctions were noticed in a few instances (Fig. 5.19). The endothelial cell nuclei sometimes nestled in the recess between neighbouring hepatocyte groups (Fig. 5.22) and nucleoli were present. The endothelial cell cytoplasm was packed with pinocytotic vesicles that included bristle-coated pinocytotic vesicles. The

formation of invaginations of the cell membrane that close and break off to form pinocytotic vesicles in the cytoplasm were evident (Fig. 5.23). Many prominent lysosomes with electron-dense contents (Figs. 5.20 & 5.21), a few mitochondria and inconspicuous strands of GER were also observed in the cytoplasm.

Kupffer cells

The Kupffer cells were large pleomorphic pigmented cells that formed part of the sinusoidal lining (Fig. 5.17 & 5.31), but also protruded into the sinusoidal lumen (Figs. 5.24 & 5.25), sometimes spanning the lumen (Fig. 5.36). They often inserted between hepatocyte groups forming bridges between adjacent sinusoids or were located in the space of Disse (Fig. 5.26 & 5.27) and were also frequently noted as part of the hepatocyte cell cords (Figs. 5.28 & 5.29). The Kupffer cells themselves did not form groups, but were seen as isolated cells in the areas mentioned. Their surfaces were irregular due to the presence of filipodia and lamellapodia. No junctions were present between Kupffer and endothelial cells, but close contact and penetration through fenestrae were seen in some instances (Figs. 5.25 & 5.30). Kupffer cells were also seen interacting with pit cells (Fig. 5.62) and were found close to some hepatic stellate cells in Disse's space (Fig. 5.27). Kupffer cell nuclei were irregular, conforming to the very large phagosomes and inclusions by having indentations and being pushed to an eccentric position in the cytoplasm (Figs. 5.28 & 5.29).

Clusters of melanin granules admixed with an electron-dense fine granular component (hemosiderin) and other electron-lucent fragments (ceroid) were found in large phagosomes (Figs. 5.32 & 5.33). Melanin granules were also present in the sinusoidal luminal Kupffer cells (Fig. 5.31). Typical lipofuscin granules consisting of an electron-dense component mixed with lipid were absent from these compound inclusions. Engulfment of apoptotic or dying white blood cells, red blood cells, thrombocytes and cellular debris was evident (Figs. 5.34, 5.35 & 5.36).

Conspicuous cytoplasmic organelles that consisted of elongated, parallel tubular structures (Fig. 5.26) bound by a single membrane and containing electron-dense filamentous or crystalline material (depending on the sectioning plane) were seen (Fig. 5.39 to Fig. 5.42). For the purpose of the present study this structure will be called 'tubulosomes'. There was a clear zone visible between the filamentous or crystalline

interiors and the limiting membranes. The tubulosomes were usually grouped together displaying longitudinal, transverse or oblique profiles, but were also sometimes separated into smaller groups around phagosomes (Fig. 5.37). They were occasionally found close to mitochondria where they seemed to originate from the mitochondria (Fig. 5.38). In cross sections of the tubulosomes the contents displayed circular, angular and divided contours (Figs. 5.39, 5.40, 5.41 & 5.42). The width of the tubulosomes varied from 77 nm to 192 nm with the longest one being observed measuring 6.5 μm. A few appeared curved. The tubulosomes were also present in the pigmented cells forming part of the hepatocyte groups.

Scanty cytoplasmic lipid droplets (Fig. 5.25) were observed and mitochondria (some with dilated cristae), Golgi, GER, SER and microtubules were also present throughout the cytoplasm.

Stellate cells

Stellate cells with long cytoplasmic extensions were seen lying in the space of Disse (Figs. 5.43 & 5.44). They were in close contact with endothelial cells, Kupffer cells and hepatocytes, sometimes touching the endothelial cells (Fig. 5.46). Usually one or two prominent, non-membrane bound lipid droplets were present that often indented the nucleus giving it an angular shape (Figs. 5.45 & 5.46). Cytoplasmic filaments, microtubules, coated and pinocytotic vesicles were observed (Figs. 5.47 & 5.48). Pairs of centrioles were often noted with some forming ciliary basal bodies (Fig. 5.49). The cytoplasm also contained a few small mitochondria, insignificant GER, Golgi, glycogen and sparse mulltivesicular bodies (Fig. 5.47). A cytoplasmic structure with the periodicity of long-spacing collagen (Fig. 5.48), similar to that found in Disse's space, was seen. Collagen fibrils and long-spacing collagen fibrils were also found in close association with the cytoplasm.

Other cells, also with subendothelial extensions and occupying the same position as stellate cells, exhibited myofibroblastic features (Figs. 5.50 & 5.51). They contained filaments forming subplasmalemmal densities (Figs. 5.54 & 5.55) and a few cells also displayed dilated granular endoplasmic reticulum (Fig. 5.56). Pinocytotic vesicles and microtubules were evident (Figs. 5.54 & 5.55). No lipid droplets were seen in these cells.

Stellate cells and myofibroblastic cells were often found occupying the same recess (Fig. 5.51) with the latter also touching the endothelial and Kupffer cells (Figs. 5.52 & 5.53).

Blood cells

<u>Pit cells</u>

A few cells known as pit cells, resembling a larger version of lymphocytes in shape and the presence of pseudopodia, were seen in the sinusoids (Fig. 5.57). They contained many small membrane-bound electron dense granules (Figs. 5.57 & 5.58) of approximately the same size (0.11-0.18 µm) and electron-density. They also exhibited an indented eccentric nucleus (Fig. 5.57) and a few larger membrane-bound clear vesicles (>0.2 µm) (Fig. 5.60) that sometimes contained electron-dense material (Fig. 5.58). Cytoplasmic collections of intermediate filaments (Fig. 5.59), as well as mitochondria, Golgi, a few multivesicular bodies (Fig. 5.60), single endocytotic vesicles and lipid droplets (Fig. 5.60) were present. They were often located in close contact with endothelial and Kupffer cells (Figs. 5.61 & 5.62).

<u>Other blood cells</u>

Typical plasma cells, thrombocytes, lymphocytes and eosinophils (Figs. 5.63, 5.64 & 5.65) were present in the sinusoidal spaces.

<u>Intercalated cells</u>

A few cells (Figs. 5.66 & 5.67), resembling lymphocytes, with an electron-lucent cytoplasm and sparse organelles (mainly mitochondria) were seen in the space of Disse and occasionally between hepatocytes.

5.4.3 Connective Tissue Stroma

Glisson's capsule consisted of an outer mesothelial lining supported by a thick collagenous layer that contained fibroblasts (Fig. 5.68). Prominent **fibrous trabeculae** (Fig. 5.69) were unmistakable between the hepatocyte groups, as was a collagenous framework around the portal triads containing fibroblasts. The black reticular fibres, demonstrated by light microscopy (Gordon & Sweets' stain, Chapter 4), appeared in the

space of Disse as sparse threads with a wider periodicity (Figs. 5.70 & 5.71) than normal collagen fibrils.

<u>Nerves</u>

Intrahepatic **nerves** were rare (Figs. 5.72 & 5.73) and consisted of unmyelinated axons enclosed in a basal lamina. Neurosecretory granules, mitochondria, lysosomes and microtubules were observed.

<u>Portal tract</u>

The portal triad consisted of branches of a **portal vein**, **hepatic artery** and **bile duct** (Figs. 5.74 & 5.75). **Lymphatic** vessels sometimes accompanied the triads. The structure of the blood and lymphatic vessels were generic. Cuboidal biliary cells with basal nuclei lined the bile ducts that were surrounded by a continuous basal lamina (Figs. 5.76 & 5.78). Apart from the usual cytoplasmic organelles, prominent intermediate filaments (Fig. 5.80) and interdigitations between the lateral membranes (Fig. 5.78) were noted. Concretions of bile pigment were demonstrated in certain biliary cells (Fig. 5.79). Apical surfaces presented with junctional complexes between neighbouring cells and projected microvilli and cilia into the ductal lumen (Fig. 5.77). Macrophages, lymphocytes, plasma cells and fibroblasts resided in the supporting collagenous framework. Collections of lymphocytes were occasionally seen in the portal areas (Figs. 5.81 & 5.82).

5.4.4 Isthmus

The ultrastructural make-up of the isthmus revealed the same elements found in the liver tissue proper. Despite the difficulty to discern the different components in areas due to incomplete perfusion fixation, the tubular nature of the hepatocyte groups interspersed by sinusoidal spaces could still be recognised (Fig. 5.83). The fine structure of the hepatocytes, endothelial cells, Kupffer cells, stellate cells, myofibroblastic blood cells, portal triads and collagenous trabeculae (Fig. 5.84 to Fig. 5.94) were identical to that found in the right liver lobes. Stellate cells seemed to be fewer in number and pit cells were not recognised. The isthmus deviated from the norm by the presence of hepatocytic cellular material being present in the sinusoidal spaces (Figs. 5.89, 5.91 & 5.92).

5.5 DISCUSSION

5.5.1 Parenchymal component

Hepatocytes

Descriptions of reptilian hepatocytes in the literature agree with the current findings in the juvenile Nile crocodile liver of large, polygonal cells arranged in either two-cell-thick plates (longitudinal section) or gland-like tubules (cross section) that also branched and anastomosed (Goldblatt *et al.*1987; Storch *et al.* 1989, Schaffner 1998; Starck *et al.* 2007).

Hepatocyte nuclei are round to oval (some are pleomorphic) in the liver of humans and in some reptilians (Phillips *et al.* 1987; Schaffner 1998; www.pathologyoutlines.com) as opposed to the uniformly round nuclear shape seen in this study. Nuclear features of the Nile crocodile hepatocytes, such as the marginal rim of heterochromatin with chromatin masses distributed throughout the nucleus and the presence of a double nuclear membrane, agrees with the findings in other reptiles (Storch *et al.* 1989; Schaffner 1998).

The morphology of the nucleolus in this study concurs with Schaffner's (1998) finding in reptiles that the nucleoli consist of electron-dense material mixed with pale areas. Two types of nucleoli, namely, open and compact nucleoli are described by Ghadially (1988) and the morphology of the nucleoli in the current study appears to fall between these two descriptions.

The Nile crocodile hepatocytes displayed scanty lateral microvillous projections. Lateral surfaces of hepatocytes in humans did not have microvilli (Phillips *et al.* 1987), but Fried (2008) found adjacent hepatocytes to be linked by 'projections' in vertebrates. Schaffner (1998) commented on lateral cell membrane 'peg & groove arrangements' in reptiles, while Phillips *et al.* (1987) found no microvilli on the lateral surfaces in the vertebrates they studied.

The peribiliary pink staining structures seen in the hepatocytes with the light microscope (Chapter 4) were confirmed ultrastructurally as mitochondria and hemosiderin granules and the large brown inclusions as bile pigment.

The combined presence of lipid droplets and glycogen accounted for the frothy appearance of the hepatocytes in histological preparations. Prominent lipid droplets of

varying sizes and quantities were present in the Nile crocodile hepatocytes. Extensive lipid accumulation is pathologic in mammalian livers, but fatty infiltration in crocodiles should not always be regarded as abnormal (Divers & Cooper 2000; Starck *et al.* 2007). Frequent feeding and underexercise during captivity, as well as other causes, for example, toxins (Schaffner 1998; Divers & Cooper 2000), contribute to lipid accumulation.

Peroxisomes in vertebrates commonly contain a nucleoid or crystalline inclusions or a marginal plate (Phillips *et al.* 1987; Schaffner 1998; Fried 2008). The peroxisomes in the present study had an amorphous interior of medium electron-density with no inclusions, comparable to the findings in the West African crocodile (Storch *et al.* 1989).

Bile canaliculi only existed at the apical borders between groups of hepatocytes in this study, in contrast to their location between the lateral membranes of hepatocytes in mammals. This observation concurs with the findings of a central shared canalicular lumen in the hepatocyte tubules of reptiles, including crocodilians, and testudines (Storch *et al.* 1989; Schaffner 1998; Moura *et al.* 2009).

The PAS-positive (Chapter 4) boundaries indicating the presence of a basal lamina around the groups of hepatocytes in the current study was not confirmed by electron microscopy. Storch *et al.* (1989) hypothesised that the PAS positive 'basal lamina' in the West African crocodile was due to the presence of collagen fibrils in the space of Disse. Perhaps the long-spacing collagen fibrils found in this location in the Nile crocodile liver accounts for the PAS positivity seen. Tanuma (1987) and Goldblatt *et al.* (1987) mentioned a basal lamina covering the basal surfaces of the hepatocytes in the turtle and newt respectively.

5.5.2 Non-parenchymal component

Sinusoids

The current study established that the angular sinusoids were lined by fenestrated endothelial cells with Kupffer cells sometimes forming part of this lining. Elias (1955) was of the opinion that the sinusoids of vertebrates were lined by potential phagocytes that do not span the lumen. Basement membranes were absent around sinusoids (De Leeuw *et al.* 1990; Fried 2008) as was supported by the findings of this study. Ghoddusi & Kelly (2004) reported that in chickens the endothelial cells were supported by a basement

membrane and Wisse *et al.* (1996) found fragments of subendothelial basal lamina-like material in rats.

Endothelial cells

Liver endothelial cells have a variety of functions including a filtration function allowing the two-way diffusion of substances and a pronounced endocytic capability (Kmieć 2001). This is also reflected in the current study by their ultrastructural morphology illustrating the presence of cytoplasmic fenestrations as well as numerous pinocytotic vesicles and prominent lysosomes. A basement membrane supporting the endothelial cells of the sinusoids is absent in most vertebrates, as in the juvenile Nile crocodile. This differs from the findings of Ghoddusi & Kelly (2004) that the chicken liver endothelium is supported by a basement membrane. Storch *et al.* (1989) described the endothelial cell processes of the West African crocodile as forming up to three layers, although they conceded that stellate cell projections may have been involved – this may also be ascribed to the tissue sectioning plane. The sinusoidal endothelium of the Nile crocodile liver exhibited only a single layer of endothelial cell processes.

Kupffer cells

The literature states that Kupffer cells are macrophages that form part of the reticuloendothelial system and reside in liver sinusoids (www.pathologyoutlines.com). They play a pivotal role in host defence by eliminating toxins and foreign substances (McCuskey & McCuskey 1990; Naito *et al.* 2004) and also remove effete and apoptotic red and white blood cells (Dini *et al.* 2002). They degrade hemoglobin to form hemosiderin (Kumar & Kiernan 2010) and bilirubin (www.pathologyoutlines.com).

Several publications (Junqueira *et al.* 1975; Wisse & Knook 1977; Phillips *et al.* 1987; Wisse et al 1996; Schaffner 1998; Ross *et al.* 2003; Ghoddusi & Kelly 2004) describe the position of Kupffer cells as being inside the sinusoidal lumen, part of the sinusoidal lining, embedded in the endothelial lining, situated as intraluminal macrophages or as fixed cells. Elias (1955) mentioned that the sinusoids were lined by potential phagocytes that never bridge the lumen. The Kupffer cells in the juvenile Nile crocodile liver did not reflect these findings as they were found in several positions and not only in the sinusoidal spaces. They can therefore be considered as highly mobile and not fixed cells.

The large phagosomes seen in the present study contained ceroid in addition to other pigments (Chapter 4, Light microscopy). Typical lipofuscin granules were not observed with the electron microscope which may be due to the age of the Nile crocodiles used, as it is an age related pigment (Yin 1996). Yin (1996) also stated that ceroid consisted of degraded cellular material and accumulated rapidly in secondary lysosomes throughout life and Kumar & Kiernan (2010) described ceroid as a type of lipofuscin – the present study therefore concludes that the PAS and PAS-D pink positivity (Chapter 4) found in the compound granules of the Kupffer cells was due to the presence of ceroid and not lipofuscin.

Two other pigments, namely, melanin and hemosiderin co-existed in the Kupffer cells in the present study. It has been established that the Kupffer cells of reptiles and amphibians synthesize melanin (Henninger & Beresford 1990; Kalashnikova 1992; Corsaro *et al.* 2000; Sichel *et al.* 2002). Iron (hemosiderin from breakdown of hemoglobin) catalyzes the formation of free radicals and the melanin traps these superoxide radicals (Beresford 1987; Sichel 2002; McClellan *et al.* 2006). The hypothesis of Henninger & Beresford (1990) that the production of melanin is a defence mechanism in response to possibly harmful iron may be an acceptable explanation for their co-existence in the Kupffer cells of the juvenile Nile crocodile as well.

Corsaro *et al.* (2000) described two types of Kupffer cells in amphibian livers – a small type with almost no melanin granules and a larger type that synthesizes melanin and is filled with melanin granules - the authors thought this to be a developmental stage of the Kupffer cells. The small type of Kupffer cell was not seen in the current study with only relatively large Kupffer cells containing numerous melanin granules being present in the different locations.

Lipid droplets were present in the Kupffer cells in this study, as well as in Kupffer cells of the lizard (Taira & Mutoh 1981), but McCuskey & McCuskey (1990) found no lipid in their study of mammals.

Several of the mentioned publications refer to vermiform processes formed by the Kupffer cell cytoplasm, but none were found in the Kupffer cells of the Nile crocodile liver.

No comparable structures to the conspicuous tubular cytoplasmic organelles ('tubulosomes') with filamentous/crystalline interiors found in the Kupffer cells of the juvenile Nile crocodile could be traced in the literature. Storch *et al.* 1989 mentioned the presence of small membrane-bound vesicles of unknown origin in the West African crocodile Kupffer cell – however, no images were published to illustrate them. Boler (1969) described the ultrastructure of cytosomes in canine Kupffer cells, but these were larger than the tubulosomes, spherical in form and contained tubular structures. The proposed hypotheses are that these organelles are specialised lysosomes dedicated to the breakdown of phagosome contents or are perhaps involved in melanin synthesis or may be responsible for cell mobility. A combination of these functions is also plausible. Mitochondria are often closely associated with other organelles (Ghadially 1988) that require adenosine triphosphate (Lehninger 1965, in Ghadially 1988) for energy transfer, which may explain the close relationship between the tubulosomes and the mitochondria in this study.

Schaffner (1998) mentioned a second pigmented macrophage in a perisinusoidal location in reptiles and Jacobson (2007) called them melanomacrophages. The present study found the same ultrastructural features, including the tubular structures, in the 'pigmented' cells in all the mentioned locations, i.e. in the sinusoids, perisinusoidal and as part of the groups of hepatocytes, and therefore deducts that these cells are all Kupffer cells.

Stellate cells

The hepatic stellate cells were previously also known as Ito cells, fat-storing cells, lipocytes, vitamin A-rich cells, perisinusoidal cells and interstitial cells (Flisiak 1997; Kmieć 2001; Sato *et al.* 2003; Senoo *et al.* 2010). Wisse *et al.* (1996), Dudas *et al.* (2009) and Sato *et al.* (2003) refer to them as the pericytes of liver sinusoids. According to the literature these cells exist in either the quiescent state as the storage cell of vitamin A, or are activated to become myofibroblast-like cells during liver injury in which case they lose their vitamin A component (Schaffner 1998; Kmieć 2001; Sato *et al.* 2003; Dudas *et al.* 2009; Senoo *et al.* 2010). They also play a role in the contractability of the sinusoids and produce extracellular matrix components (Sato *et al.* 2003).

The stellate cells in the present study have the same general ultrastructural features and location as those mentioned in the cited literature above. However, these cells differ in

some respects from published accounts in the literature. Cytoplasmic projections of stellate cells in the livers of two lizard species were found in the sinusoidal spaces (De Brito Gitirana 1988). No stellate cell processes were seen protruding into the spaces in the current study. The cells were however in close apposition to the endothelial cell cytoplasm, as was also noted by Sato *et al.* (2003), sometimes touching the endothelial cells.

De Brito Gitirana (1988) and Senoo *et al.* (2010) mention a well-developed GER – only a few GER strands were noticed in this study. Taira & Mutoh (1981) also found prominent GER in the lizard and the snake, but not in the turtle that they investigated.

Lipid droplets were sparse in the stellate cells studied in the lizard with most of the cells being devoid of lipid inclusions (De Brito Gitirana 1988) – almost all the stellate cells in the Nile crocodile liver exhibited lipid droplets with only a few cells not containing them. Storch *et al.* (1989) identified numerous lipid droplets in stellate cells of the West African crocodile. In contrast, only one or two, and at the most four large droplets, were seen in the Nile crocodile. Beresford & Henninger (1986) concluded that variable numbers and sizes of lipid droplets are present in the different reptile species. Wake (1974, in Geerts *et al.* 1990) distinguishes between two types of lipid droplets found in rat stellate cells, namely, membrane bound Type I and non-membrane bound Type II – only the latter was present in this study.

Wisse & Knook (1977) found the single cilium of the rat stellate cell projecting into the sinusoidal lumen – the current study showed that this structure was only present in the space of Disse. Tobe *et al.* (1985) established a '9+0' microtubular arrangement in the ciliary ultrastructure of the single cilium in human hepatic stellate cells and concluded that these cilia were immotile which would conform with the sensory or chemoreceptor function ascribed to single cilia in other locations (Ross *et al.* 2003).

Senoo *et al.* (2010) in a review article of hepatic stellate cells regarded multivesicular bodies as essential 'for the development of vitamin A containing lipid droplets'. Storch *et al.* (1989) consistently found multivesicular bodies in the stellate cells of the West African crocodile – this organelle was infrequently observed in the present study.

Most of the cited literature agrees that hepatic stellate cells store vitamin A and transform into fibroblasts or myofibroblastic cells under certain circumstances and are responsible for

the upkeep of the collagenous and reticular network around the sinusoids. Tanuma (1987) did not elude to this in his electron microscopy study of the turtle sinusoidal wall – he however described the existence of smooth muscle cells, in addition to stellate cells, as another subset of perisinusoidal cells. The present study showed cells with the combined features of smooth muscle cells and fibroblasts (Ghadially 1988) occupying the same position as stellate cells, sometimes accompanying the stellate cells. The fact that both cell types are present simultaneously in the same location leads to the conclusion that these may in fact be two separate cell populations, with the myofibroblastic cell regulating sinusoidal blood flow and being responsible for maintaining the extracellular matrix. Another scenario would be that these two cells are present in the same location due to separate stages of differentiation from stellate into myofibroblastic cell occurring in the same area.

Pit cells

Pit cells, also known as liver-specific natural killer cells (Luo *et al.* 2000; Kmieć 2001), were first described in 1976 (Wisse *et al.*1976, in Luo *et al.* 2000 & Nakatani *et al.* 2004). The name derives from the spherical dense cytoplasmic granules that are comparable to grape seeds ('pit' means seed). Phillips *et al.* (1987) described them as a variant of circulating lymphocytes.

Their function as natural killer cells was revealed by Kaneda *et al.* (1983, in Luo *et al.* 2000 & Nakatani *et al.* 2004). Pit cells are cytotoxic and destroy target cells by inducing necrosis and /or apoptosis (Luo *et al.* 2000) and are ideally located in the sinusoids as the first line of defence in the liver. Pit cell functions are apparently controlled by Kupffer cells Vanderkerken *et al.* (1995, in Wisse *et al.* 1996).

The ultrastructure of the pit cells described in this study is analogous to those in the literature. However, the larger vesicles with electron-dense contents differ from the rod-cored vesicles described by Bouwens *et al.* (1987), Nakatani *et al.* (2004) and Luo *et al.* (2000), in that they appear to be larger and do not have the distinctive internal rod bridging the diameter of the vesicle. Wisse *et al.* (1996) stated that pit cells lack pinocytotic activity, but single pinocytotic vesicles were demonstrated in this study.

Intercalated cells

Ghoddusi & Kelly (2004) described cells in the chicken liver that were mostly devoid of organelles and appeared between hepatocytes and in the space of Disse and called them intercalated cells. The authors eluded to the possibility that this cell may be the avian counterpart of the pit cell – the cells however lacked the electron-dense membrane-bound granules. Purton (1976, in Ghoddusi & Kelly 2004) referred to these immature mesenchymal cells as extrasinusoidal macrophages. The equivalent cell was described in the West African crocodile as free phagocytes (Storch *et al.* 1989). No evidence of phagocytosis was found in the intercalated cells of the present study – perhaps they are lymphocytes or the tissue equivalent of pit cells that have possibly degranulated.

5.5.3 Connective tissue stroma

A basal lamina was absent around hepatocyte groups in this study despite the PAS-D positive reaction for basal lamina demonstrated in figure 4.16 B (Chapter 4). However, the collagen fibres in the same figure also stained a pink colour - perhaps the pink borders partially surrounding some of the hepatocyte tubules, were the reticular fibres (collagen type III) ultrastructurally illustrated to be present. The long-spacing collagen fibres seen in the space of Disse are most probably reticular fibres.

The fine structural features found in the portal tracts of the current study correlates with that described in mammals and reptiles (Phillips *et al.*1987; Schaffner 1998). The presence of accumulations of lymphoid cells in the portal tracts of Nile crocodile liver were however not referred to by these authors. Kanesada (1956a, in Beresford & Henninger 1986) mentioned the presence of lymphoid tissue in the tortoise liver. Lymphocytes are immunocompetent cells that are distributed in connective tissue for immunological surveillance (Ross *et al.* 2003) and this may account for their occurrence in this region. The presence of a few lymphocytes and fibroblasts were mentioned by Goldbaltt & Gunning (1984), but they also noted that other inflammatory cells were generally absent - plasma cells are antibody-producing cells and were a regular occurrence in the portal tracts in this study. Perhaps the presence of lymphoid tissue in the portal tract area of the liver of farmed juvenile Nile crocodiles is part of the normal defensive system against antigens in the young crocodile – livers of farmed adult crocodiles, as well as those of wild

crocodiles, need to be examined for the presence of lymphoid tissue in the portal tract region to determine whether this is a unique feature of the livers of juvenile Nile crocodiles.

5.5.4 Isthmus

The ultrastructural results reflected the histology findings that the isthmus consisted of the full complement of liver tissue. However, the isthmus deviated in respect of the presence of hepatocytic cellular material in the sinusoidal spaces. A possible reason may be the failure of the isthmus to perfuse properly and the cellular material therefore not being washed out of the sinusoids. Kalashnikova (1996) terms this shedding of hepatocyte cytoplasmic fragments into the sinusoids of avian, reptilian and mammalian livers 'clasmatosis', the purpose being either the elimination of redundant cellular waste, or to provide the body with essential substances.

5.5 REFERENCES

BARATTA, J.L., NGO, A., LOPEZ, B., KASABWALLA, N., LONGMUIR, K.L. & ROBERTSON, R.T. 2009. Cellular organization of normal mouse liver: a histological, quantitative immunocytochemical, and fine structural analysis. *Histochemistry Cellular Biology,* 131: 713-726.

BERESFORD, W.A. 1987. Some light microscopic histology of the liver in *Caiman crocodilus. The Anatomical Record,* 218: 16A.

BERESFORD, W.A. & HENNINGER, J.M. 1986. A tabular comparative histology of the liver. *Archivum Histologicum Japonicum,* 49: 267-281.

BOLER, R.K. 1969. Fine structure of canine Kupffer cells and their microtubule-containing cytosomes. *The Anatomical Record,* 164: 483-496.

BOUWENS, L., REMELS, L., BEAKELAND, M., VAN BOSSUYT, H. & WISSE, E. 1987. Large granular lymphocytes or "Pit cells" from rat liver: isolation, ultrastructural characterization and natural killer activity. *European Journal of Immunology,* 17: 37-42.

BOZZOLA, J.J. & RUSSELL, L.D. 1992. *Electron microscopy: principles and techniques for biologists.* Jones and Bartlett Publishers, Massachusets.

CORSARO, C., SCALIA, M., LEOTTA, N., MONDIO, F. & SICHEL, G. 2000. Characterisation of Kupffer cells in some Amphibia. *Journal of Anatomy,* 196: 249-261.

DE LEEUW, A.M., BROUWER, A. & KNOOK, D.L. 1990. Sinusoidal endothelial cells of the liver: fine structure and function in relation to age. *Journal of Electron Microscopy Technique,* 14: 218-236.

DE BRITO GITIRANA, L. 1988. The fine structure of the fat-storing cell (Ito cell) in the liver of some reptiles. *Zeitschrift Mikroskopish- Anatomische Forschung,* 102: 143-149.

DINI, L., PAGLIARA, P. & CARLA, E.C. 2002. Phagocytosis of apoptotic cells by liver: a morphological study. *Microscopy Research and Technique,* 57: 530–540.

DIVERS, S.J. & COOPER, J.E. 2000. Reptile Hepatic Lipidosis. *Seminars in Avian and Exotic Pet Medicine,* 9: 153-164.

DUDAS, J., MANSUROGLU, T., BATUSIC, D. & RAMADORI, G. 2009. Thy-1 is expressed in myofibroblasts but not found in hepatic stellate cells following liver injury. *Histochemistry and Cell Biology,* 131:115–127.

ELIAS, H. 1955. Liver morphology. *Biological Reviews,* 30: 263-310.

FLISIAK, R. 1997. Role of Ito cells in the liver function. *Polish Journal of Pathology,* 48: 139-145.

FRIED, G.H. 2008. Liver, in *AccessScience.* © McGraw-Hill Companies. http://www.accessscience.com

GEERTS, A., BOUWENS, L. & WISSE, E. 1990. Ultrastructure and function of hepatic fat-storing and pit cells. *Journal of Electron Microscopy Technique,* 14: 247-256.

GHADIALLY, F.N. 1988. *Ultrastructural pathology of the cell and matrix.* Butterworths, London.

GHODDUSI, M. & KELLY, W.R. 2004. Ultrastructure of *in situ* perfusion-fixed avian liver, with special reference to structure of the sinusoids. *Microscopy Research and Technique,* 65:101–111.

GOLDBLATT, P.J. & GUNNING, W.T. 1984. Ultrastructure of the liver and biliary tract in health and disease. *Annals of Clinical and Laboratory Science,* 14: 159-167.

GOLDBLATT, P.J., HAMPTON, J.A., DIDIO, L.N., SKEEL, K.A. & KLAUNIG, J.E. 1987. Morphologic and histochemical analysis of the Newt (*Notophthalmus viridescens*) liver. *The Anatomical Record,* 217: 328-338.

HAYAT, M.A. 2000. *Principles and techniques of electron microscopy: biological applications.* Cambridge University Press, Cambridge, UK.

HENNINGER, J.M. 1982. Histology of the liver in the box turtle. *The Anatomical Record,* 202: 79A.

HENNINGER, J.M. & BERESFORD, W. A. 1990. Is it coincidence that iron and melanin coexist in hepatic and other melanomacrophages? *Histology and Histopathology,* 5: 457-459.

JACOBSON, E.R. 2007. Overview of reptile biology, anatomy, and histology, in *Infectious diseases and pathology of reptiles,* edited by E.R. Jacobson. CRC Press, Taylor & Francis Group, 6000 Broken Sound Parkway NW, Suite 300, Boca Raton, FL 33487-2742, pp.1-130.

JUNQUEIRA, L.C., CARNEIRO, J & CONTOPOULUS, A.N. 1975. *Basic histology.* Lange Medical Publications, Canada.

KALASHNIKOVA, M.M. 1992. Erythrophagocytosis and pigmented cells of the amphibian liver. *Byulleten' Éksperimental'noi Biologii i Meditsiny,* 113: 82-84.

KALASHNIKOVA, M.M. 1996. Liver cells in a comparative morphological series of animals: ultrastructural features and their significance. *Bulletin of Experimental Biology and Medicine,* 121: 543-548.

KMIEĆ , Z. 2001. Cooperation of liver cells in health and disease. *Advanced Anatomy, Embryology and Cellular Biology,* 161: 1-151.

KUMAR, G.L. & KIERNAN, J.A. 2010. *Education guide: Special stains and H & E.* Dako North America, California. www.dako.com.

LUO, D.Z., VERMIJLEN, D., AHISHALI, B., TRIANTIS, V., PLAKOUTSI, G., BRAET, F., VANDERKERKEN, K. & WISSE, E. 2000. On the cell biology of pit cells, the liver-specific NK cells. *World Journal of Gastroenterology,* 6: 1-11.

MCCLELLAN-GREEN, P., CELANDER, M. & OBERDÖRSTER, E. 2006. Hepatic, renal and adrenal toxicology, in *Toxicology of reptiles,* edited by S.C. Gardner & E. Oberdörster. CRC Press, Taylor & Francis Group, 6000 Broken Sound Parkway NW, Suite 300, Boca Raton, FL 33487-2742, pp.123-148.

MCCUSKEY, R.S. & MCCUSKEY, P.A. 1990. Fine structure and function of Kupffer cells. *Journal of Electron Microscopy Technique,* 14: 237-246.

NAITO, M., HASEGAWA, G., EBE, Y. & YAMAMOTO, T. 2004. Differentiation and function of Kupffer cells. *Medical Electron Microscopy,* 37:16–28.

NAKATANI, K., KANEDA, K., SEKI, S. & NAKAJIMA, Y. 2004. Pit cells as liver-associated natural killer cells: morphology and function. *Medical Electron Microscopy,* 37: 29–36.

PHILLIPS, M.J., POUCELL, S., PATTERSON, J & VALENCIA, P. 1987. *The liver: an atlas and text of ultrastructural pathology.* Raven Press, New York.

ROSS, M.H., KAYE, G.I. & PAWLINA, W. 2003. *Histology: a text and atlas.* Lippincott Williams & Wilkens, USA.

SATO, M. SUZUKI, S. & SENOO, H. 2003. Hepatic stellate cells: unique characteristics in cell biology and phenotype. *Cell Structure and Function,* 28: 105-112.

SCHAFFNER, F. 1998. The hepatic system, in *Biology of reptilia: volume 19, Morphology G: Visceral organs,* edited by C. Gans & A.B. Gaunt. Society for the Study of Amphibians and Reptiles, Missouri, pp. 485-531.

SENOO, H., YOSHIKAWA, K., MORII, M., MIURA, M., IMAI, K. & MEZAKI, Y. 2010. Hepatic stellate cell (vitamin A-storing cell) and its relative – past, present and future. *Cell Biology International,* 34: 1247–1272.

SICHEL, G., SCALIA, M. & CORSARO, C. 2002. Amphibia Kupffer cells. *Microscopy Research and Technique,* 57:477–490.

STARCK, M.J., CRUZ-NETO, A.P. & ABE, A.S. 2007. Physiological and morphological responses to feeding in broad-nosed caiman (*Caiman latirostris*). *The Journal of Experimental Biology,* 210: 2033-2045.

STORCH, V., BRAUNBECK, T. & WAITKUWAIT, W.E. 1989. The liver of the West African crocodile *Osteolaemus tetraspis.* An ultrastructural study. *Submicroscopical Cytology and Pathology,* 21: 317-327.

TAIRA, K. & MUTOH, H. 1981. Comparative ultrastructural study of the Ito cells in the liver of some reptiles. *Archivum Histologicum Japonicum,* 44: 373-384.

TANUMA, Y. 1987. Electron microscopic study on the hepatic sinusoidal wall of the soft-shelled turtle (*Amyda japonica*) with special remarks on the smooth muscle cells. *Archivum Histologicum Japonicum,* 50: 251-272.

TOBE, K., TSUCHIYA, T., ITOSHIMA, T., NAGASHIMA, H. & KOBAYASHI, T. 1985. Electron microscopy of fat-storing cells in liver diseases with special reference to cilia and cytoplasmic cholesterol crystals. *Archivum Histologicum Japonicum,* 48: 435-441.

VAN BEZOOIJEN, C.F A. 1990. Morphology, ultrastructure and function of hepatocytes during liver drug metabolism. *Journal of Electron Microscopy Technique,* 14: 152-174.

WISSE, E. & KNOOK, D.L. 1977. *Kupffer cells and other liver sinusoidal cells.* Elsevier, Amsterdam, Netherlands.

WISSE, E., BRAET, F., LUO, D., DE ZANGER, R., JANS, D., CRABBÉ, E. & VERMOESEN, A. 1996. Structure and function of sinusoidal lining cells in the liver. *Toxicologic Pathology,* 24: 100-111.

YIN, D. 1996. Biochemical basis of lipofuscin, ceroid, and age pigment-like fluorophores. *Free Radical Biology and Medicine,* 21: 871-888.

WWW Site reference:

www.pathologyoutlines.com
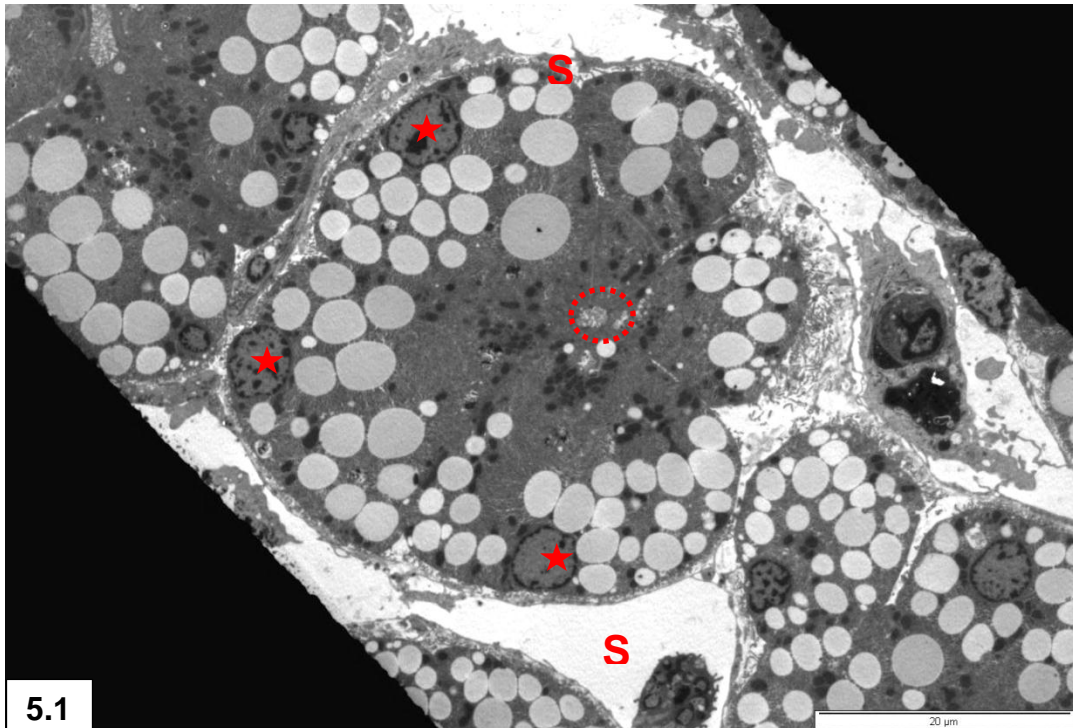
Figure 5.1: Cross-sectional cord of hepatocytes converging to form a central bile canaliculis (dashed circle). The cell membranes of each hepatocyte are in contact basally with a sinusoidal wall, laterally with adjacent hepatocytes and apically with a bile canaliculus. Note eccentric basal nuclei (stars) and the dome-shaped basal surface of the hepatocytes facing the sinusoids (**S**). Lipid droplets are evident.
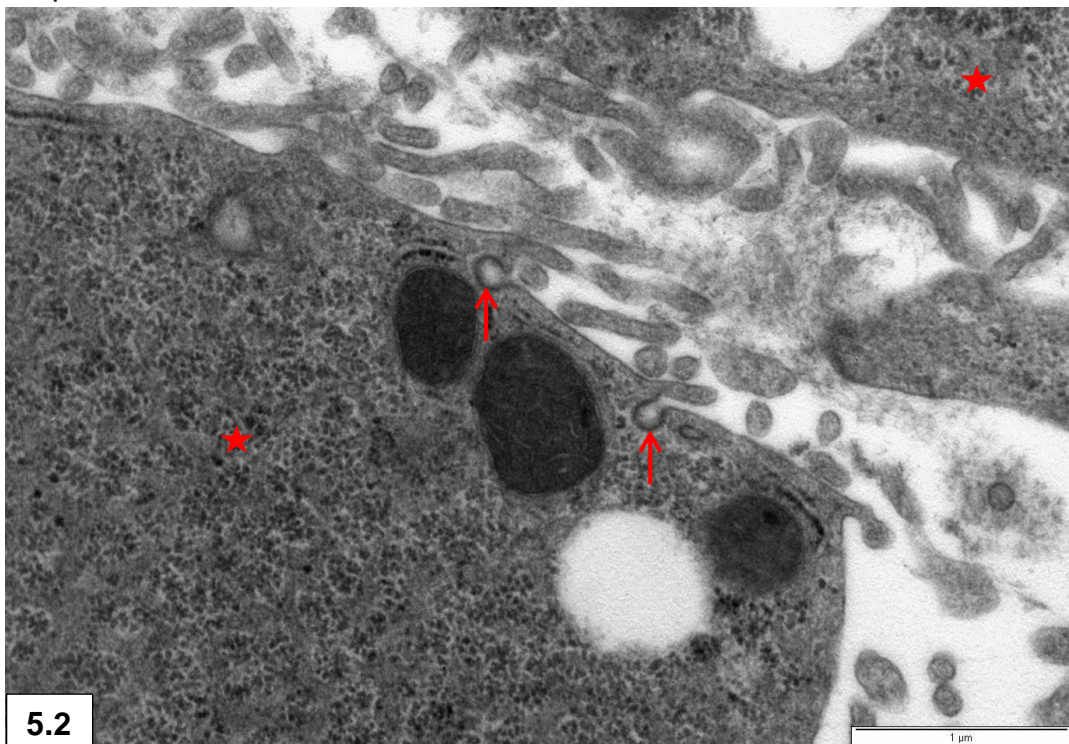
Figure 5.2: Pinocytotic vesicles (arrows) between microvilli of a hepatocyte. Note association of hepatocytes (stars) in two groups of hepatocytes.
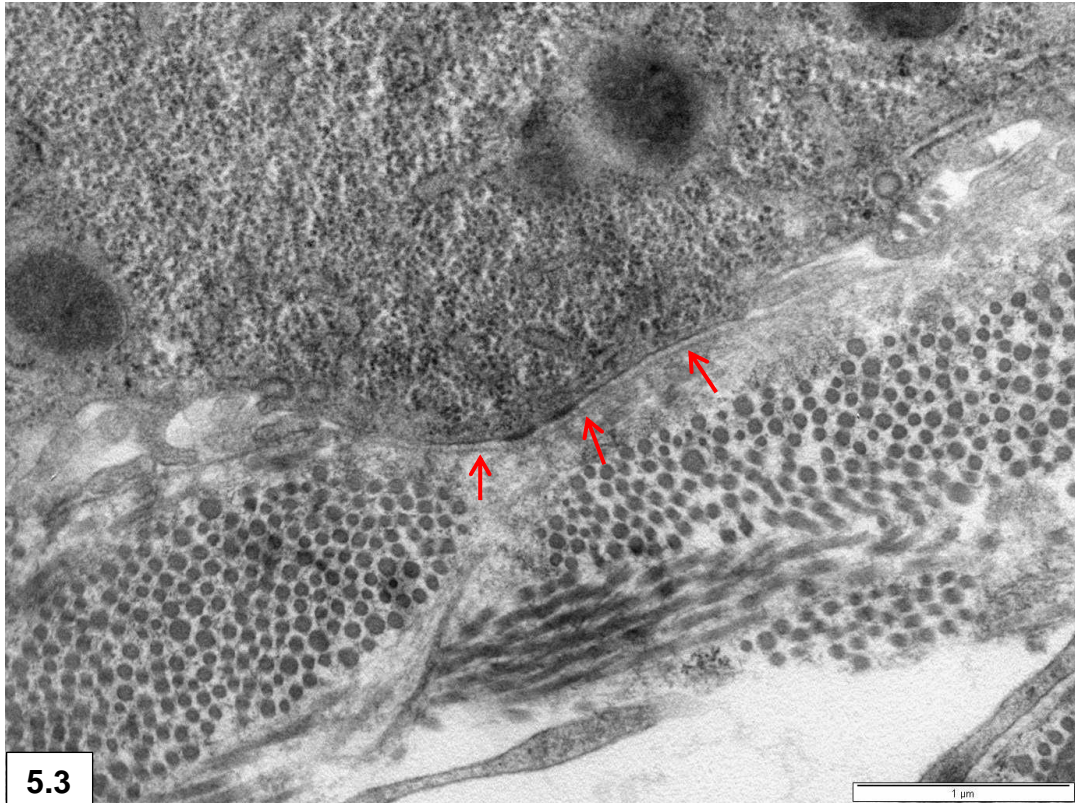
Figure 5.3: Basal lamina (arrows) lining the surface of the hepatocyte directly adjacent to Glisson's capsule.
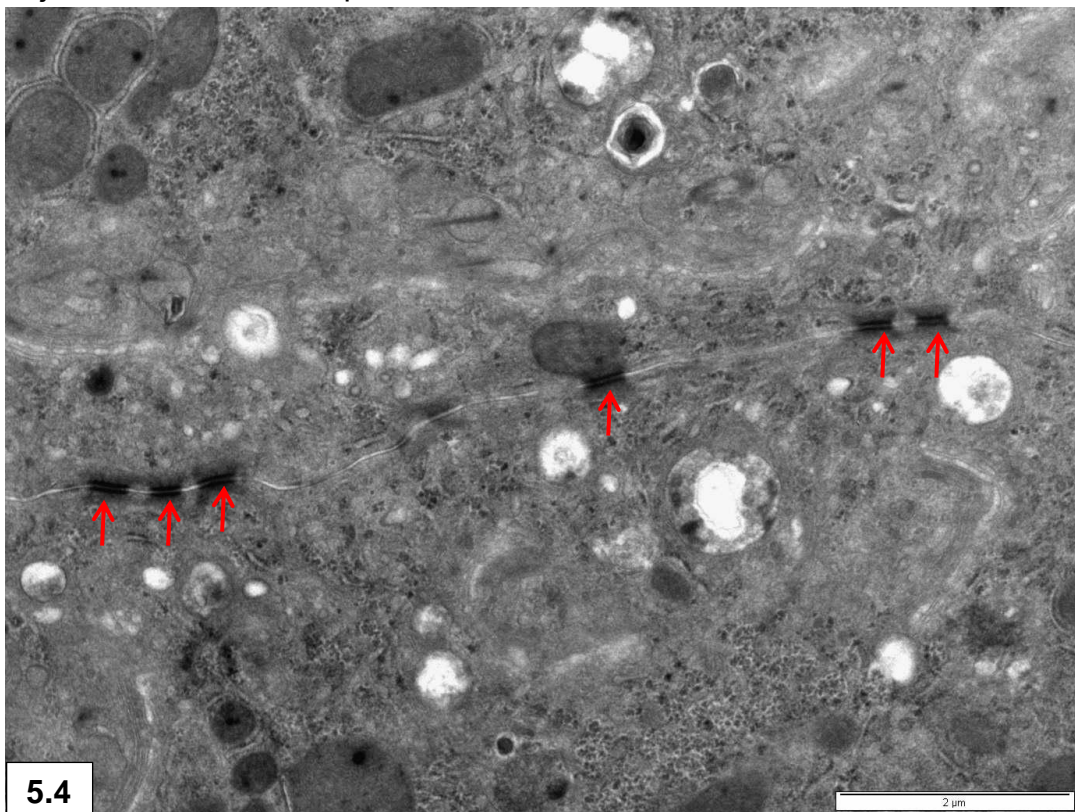
Figure 5.4: The lateral surface of two adjoining hepatocytes demonstrating desmosomes (arrows). Note the close apposition of the apposed cell membranes in this region.
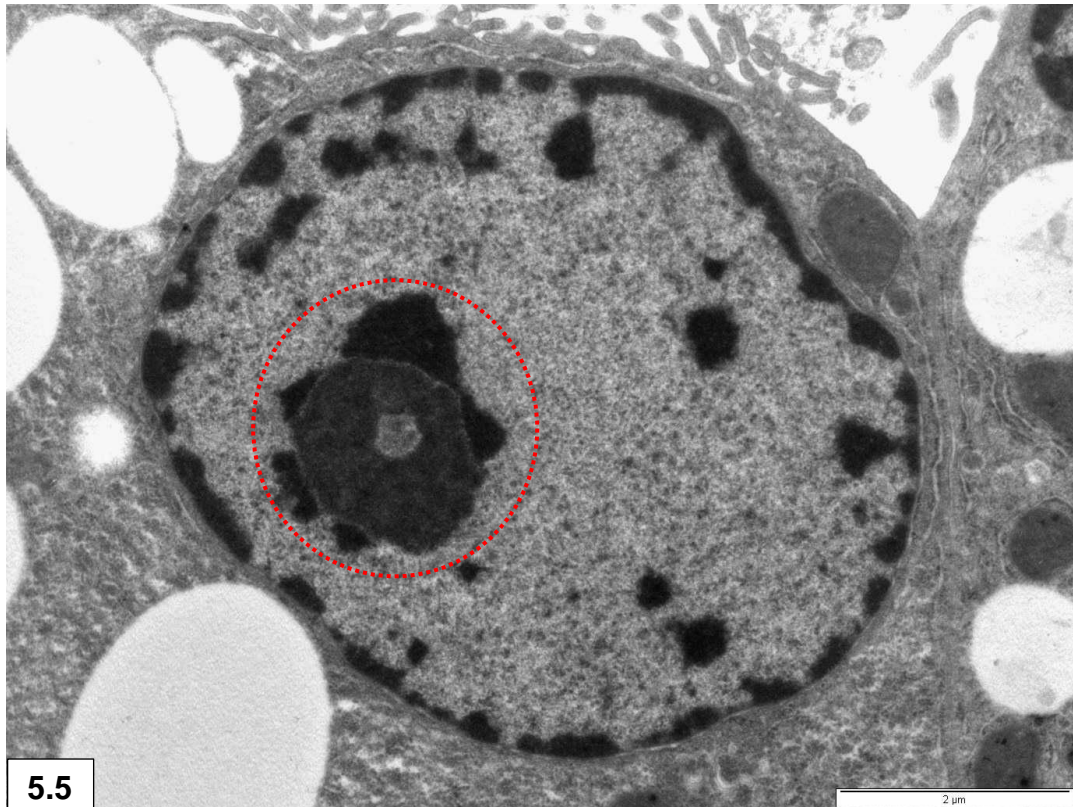
Figure 5.5: Prominent nucleolus (dashed circle) surrounding an open space containing nuclear matrix. Note heterochromatin masses throughout the nucleus, and forming a definite rim along the nuclear membrane.
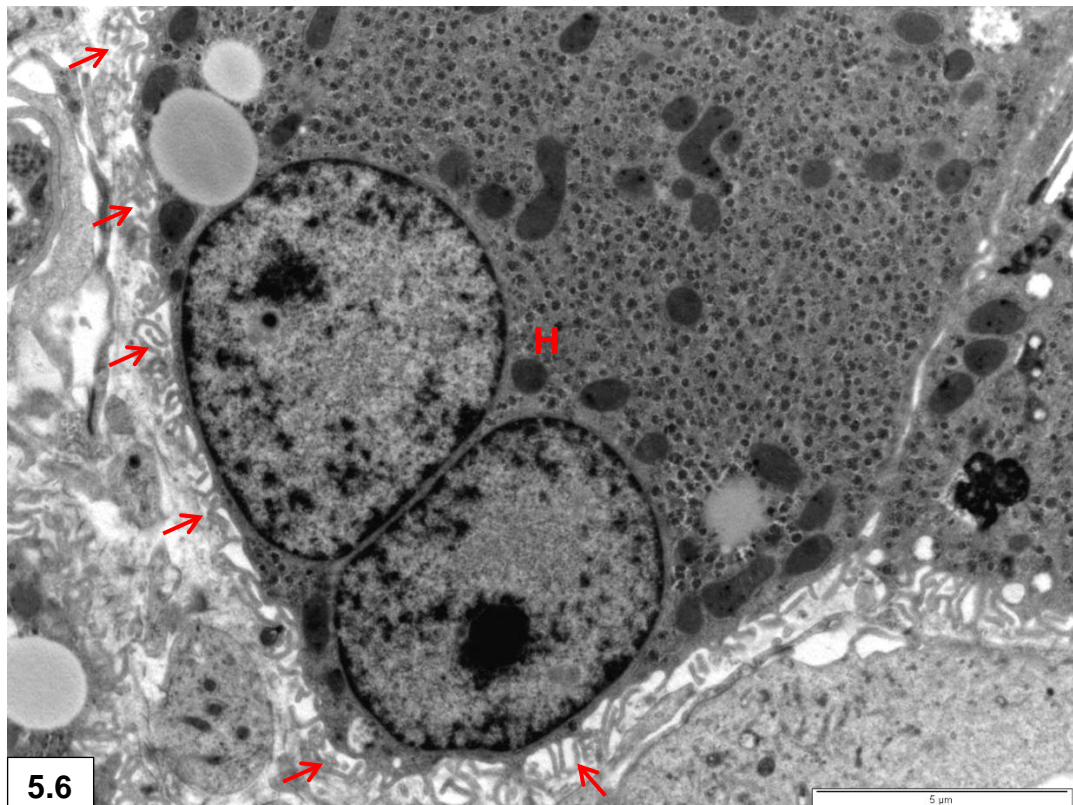
Figure 5.6: Bi-nucleated hepatocyte (**H**). Note the microvilli at the surface of the hepatocyte protruding into the space of Disse (arrows).
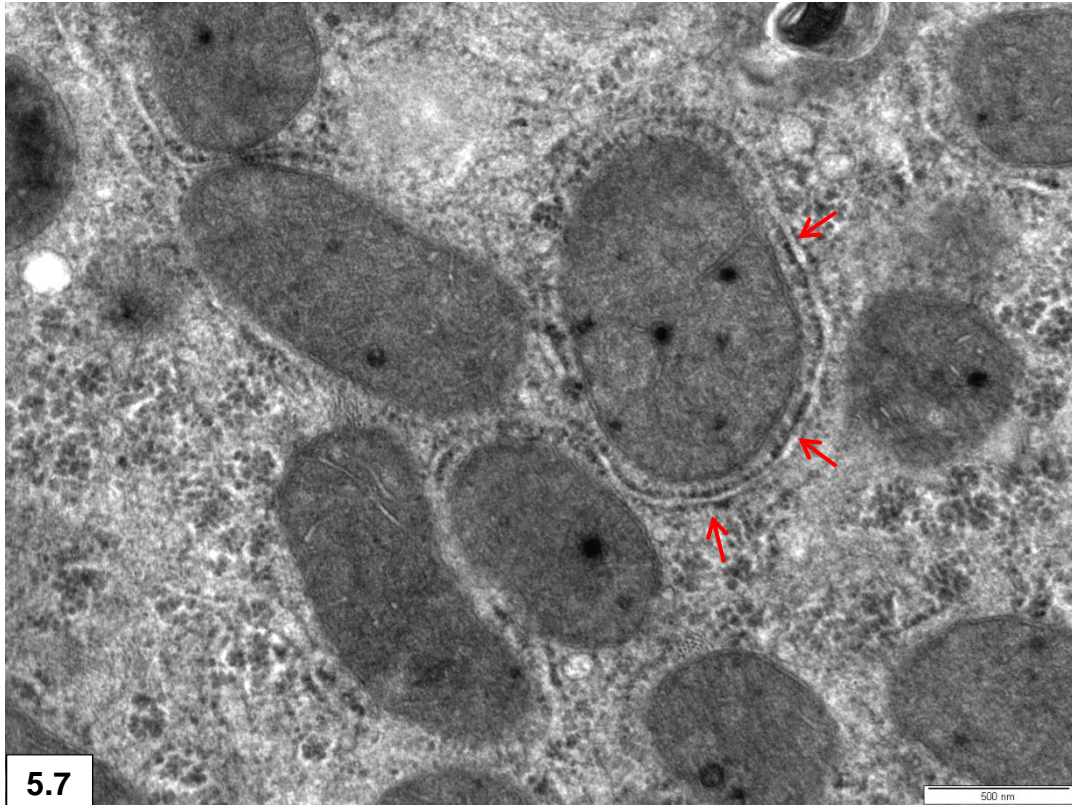
Figure 5.7: GER (arrows) often surrounded mitochondria. Note mitochondrial matrix granules and cristae.
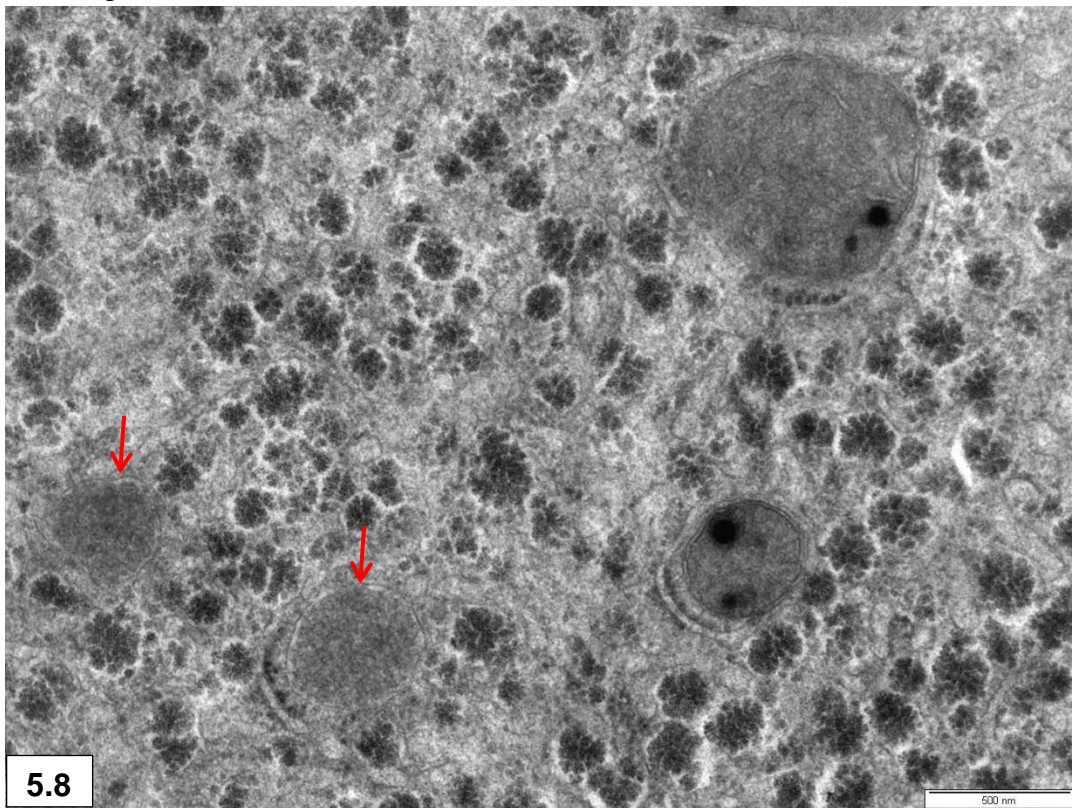
Figure 5.8: Single-membrane-bound peroxisomes (arrows) with amorphous contents of medium electron density. Note glycogen rosettes, mitochondrial matrix granules and cristae.
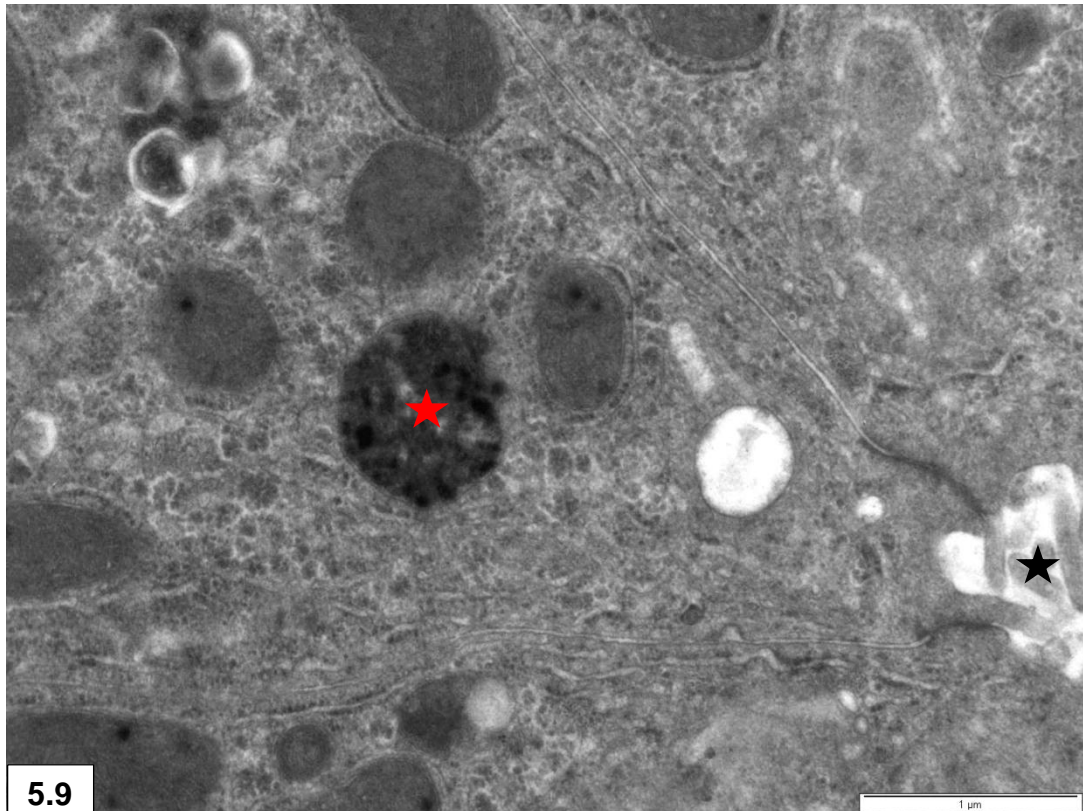
Figure 5.9: A lysosome filled with hemosiderin granules (red star) present at the apical tip of a hepatocyte. Note the bile canaliculus (black star).
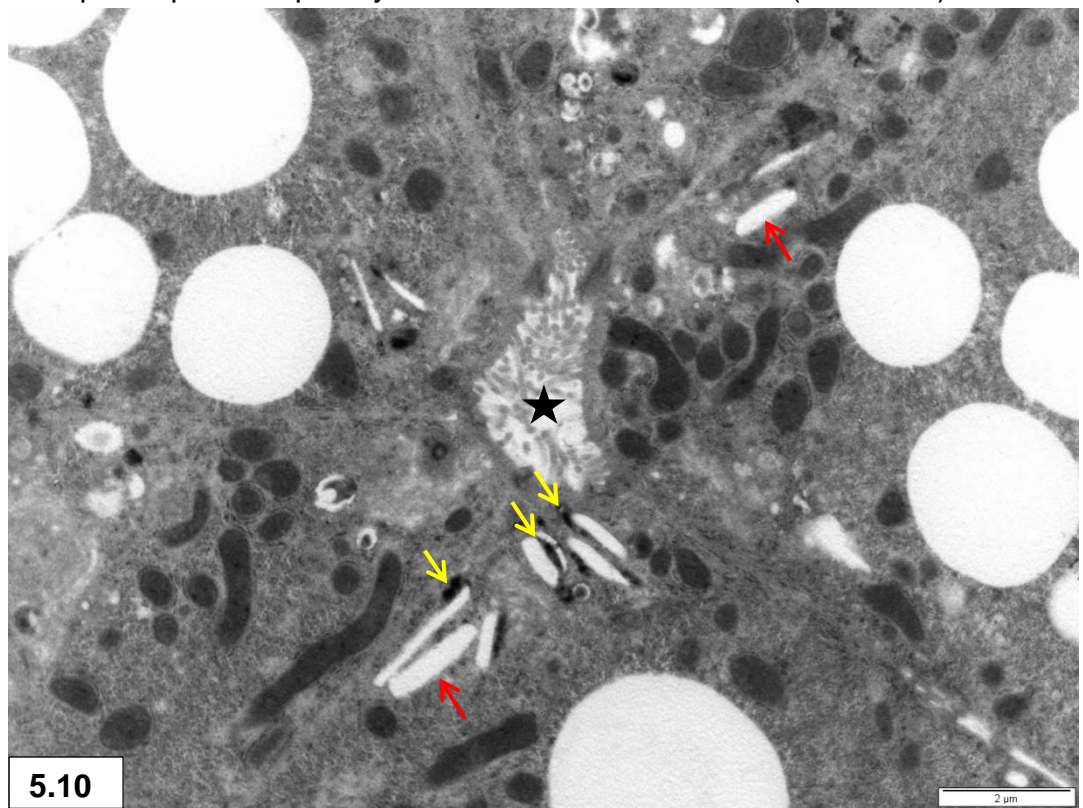
Figure 5.10: Cholesterol slits (red arrows) and slit-like spaces associated with lysosomes (yellow arrows) in the apical region of hepatocytes. Note bile canaliculus (star).
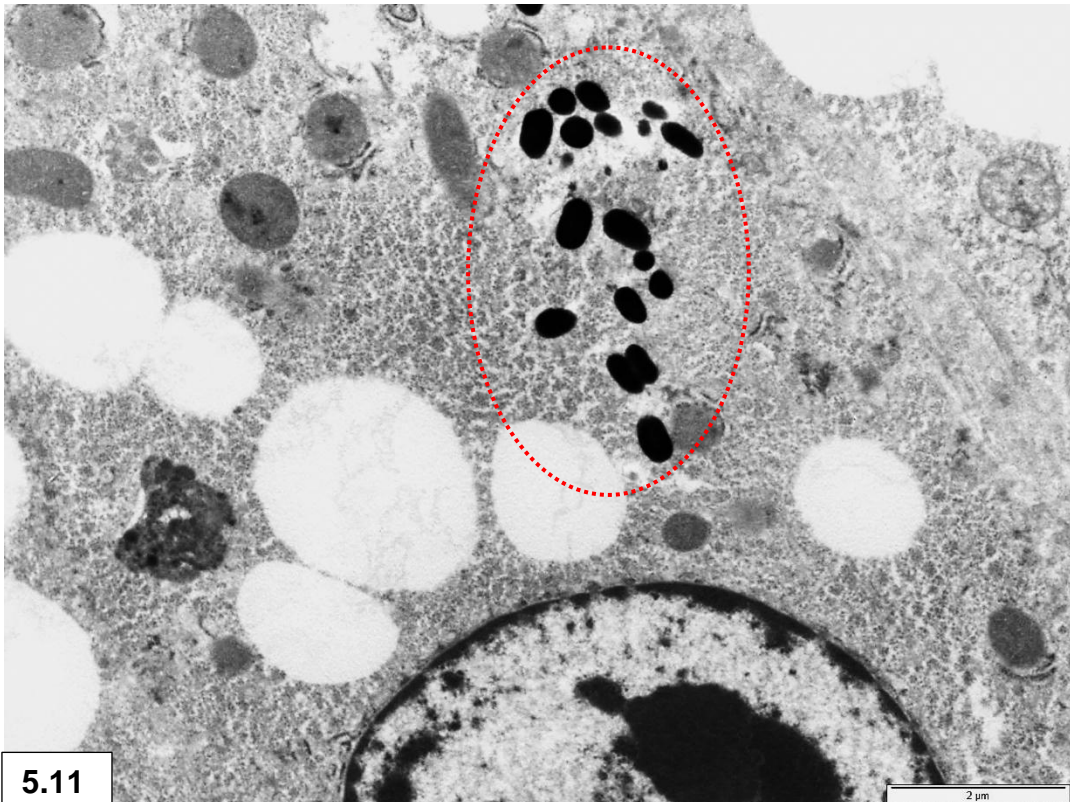
Figure 5.11: Loose lying cytoplasmic melanin granules (encircled) in hepatocyte.
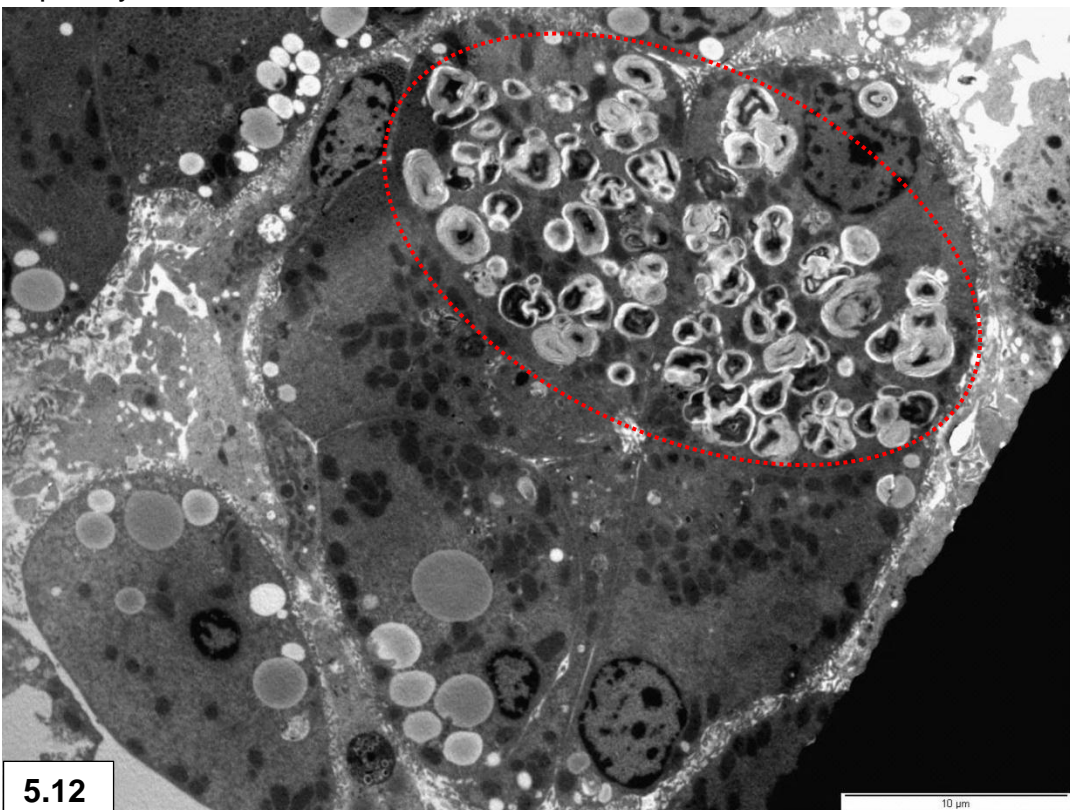
Figure 5.12: Prominent membranous concretions of bile pigment (circle) present in group of hepatocytes.
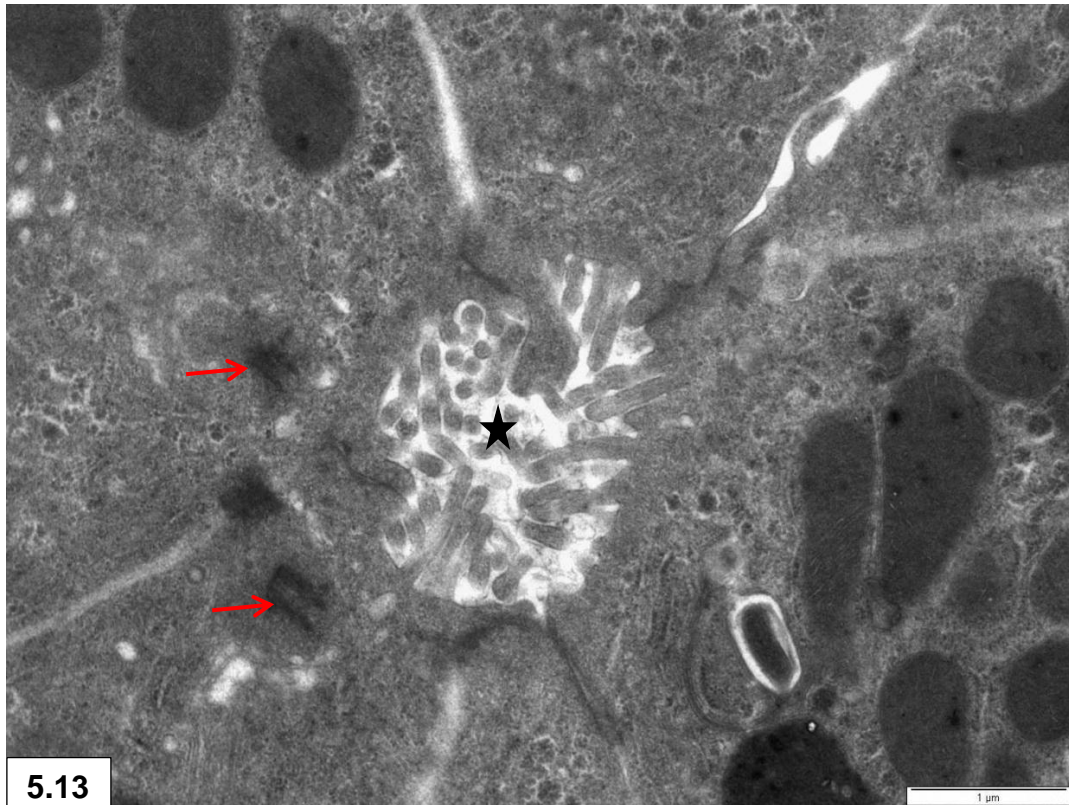
Figure 5.13: Bile canaliculus (star) lined by microvilli. Note centrioles (red arrows).
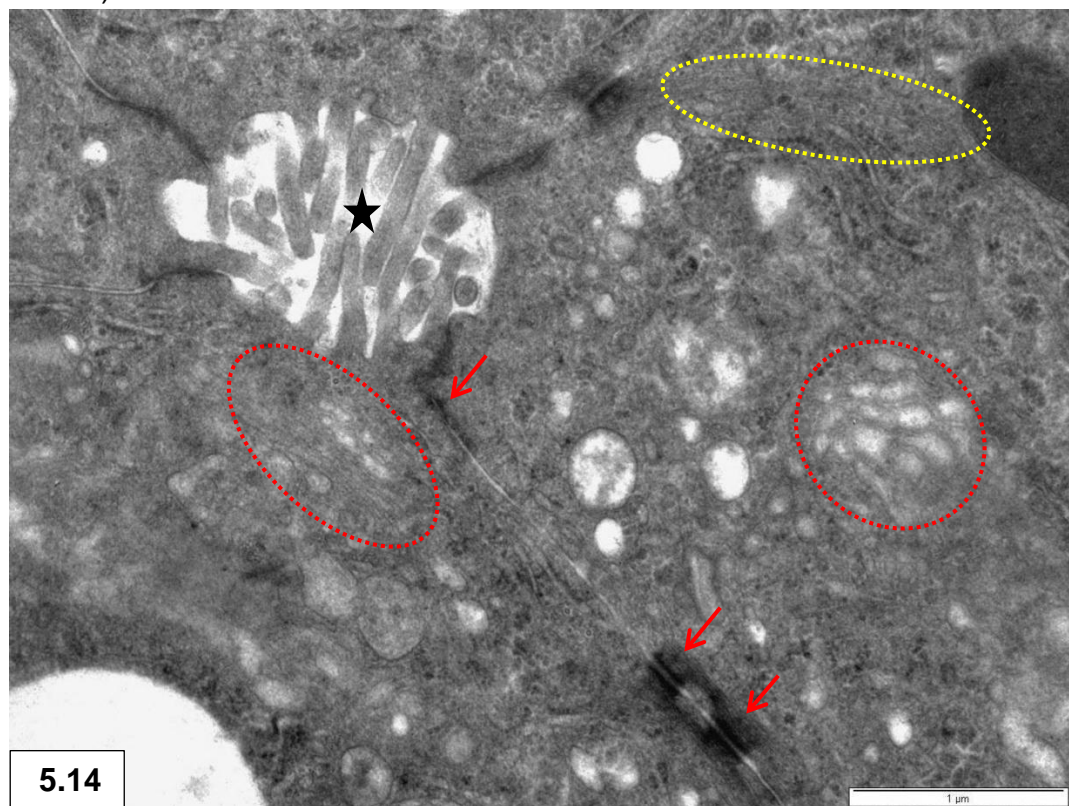
Figure 5.14: Junctional complexes (arrows) between the lateral cell membranes sealing a bile canaliculus (star). Note Golgi (red circles) and microfilaments (yellow circle).
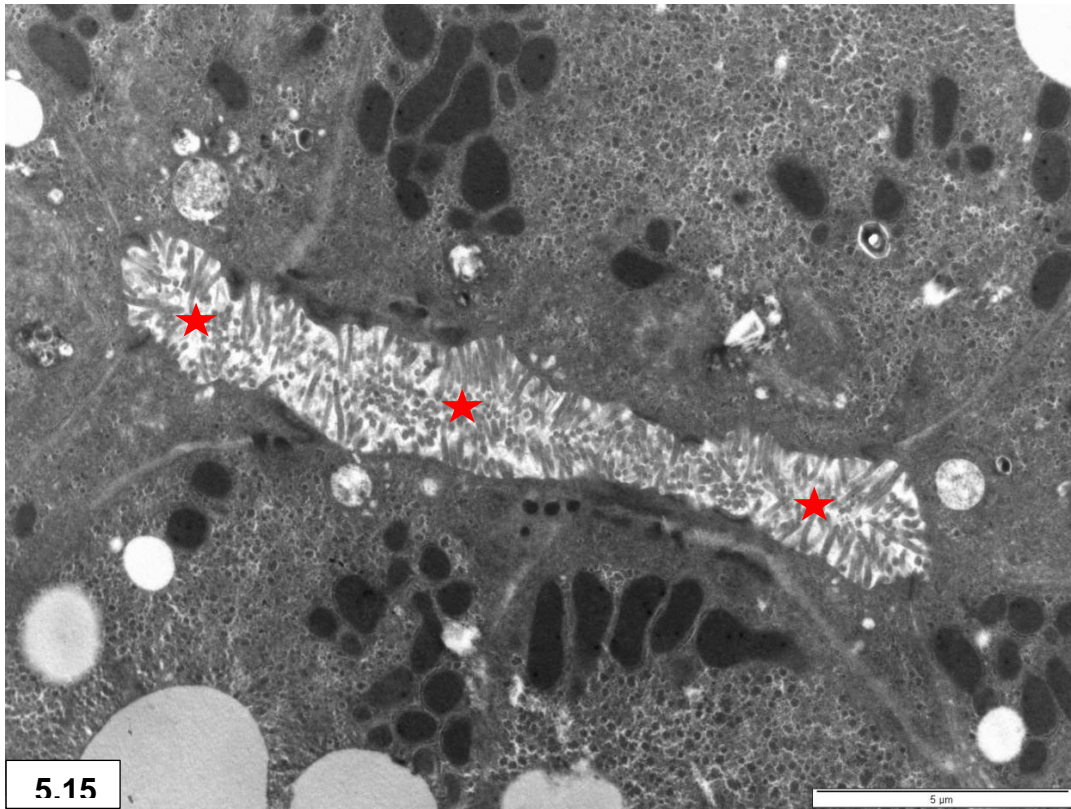
Figure 5.15: A longitudinal section of a cord of heptocytes with an elongated bile canaliculus (stars).
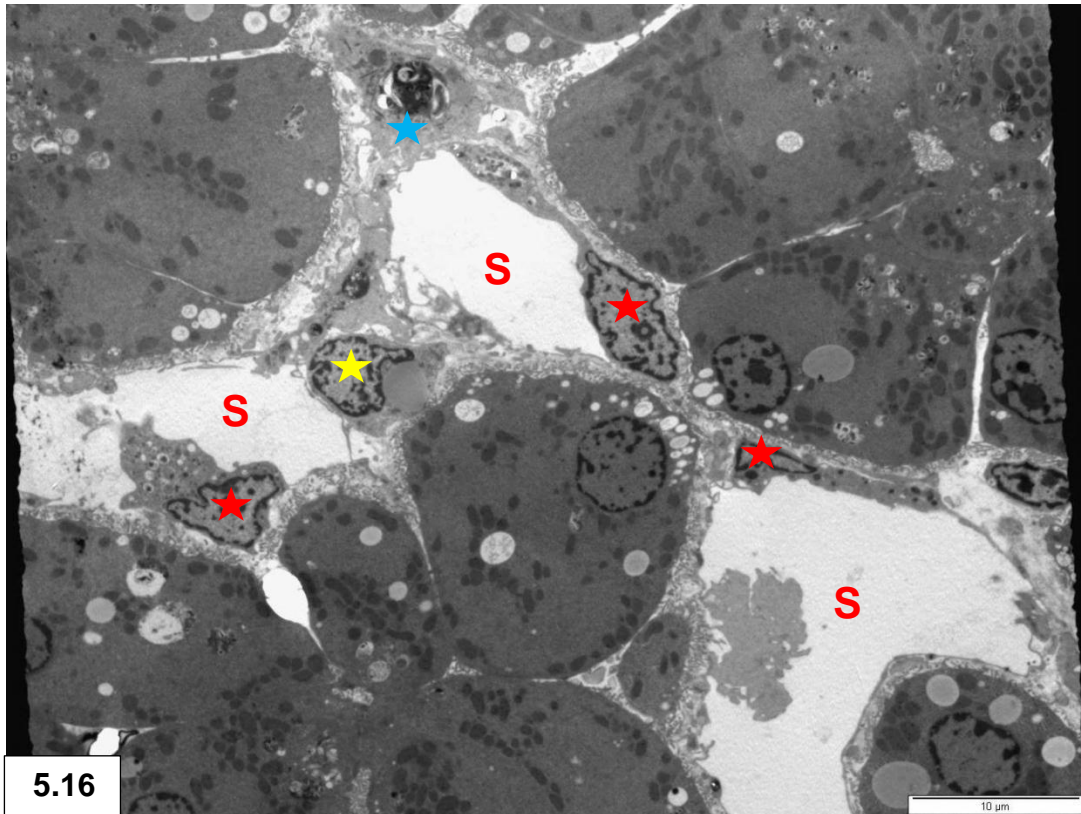
Figure 5.16: Flat and bulky endothelial cells (red stars) lining angular sinusoids (**S**) between adjacent groups of hepatocytes. Stellate cell (yellow star), Kupffer cell (blue star).
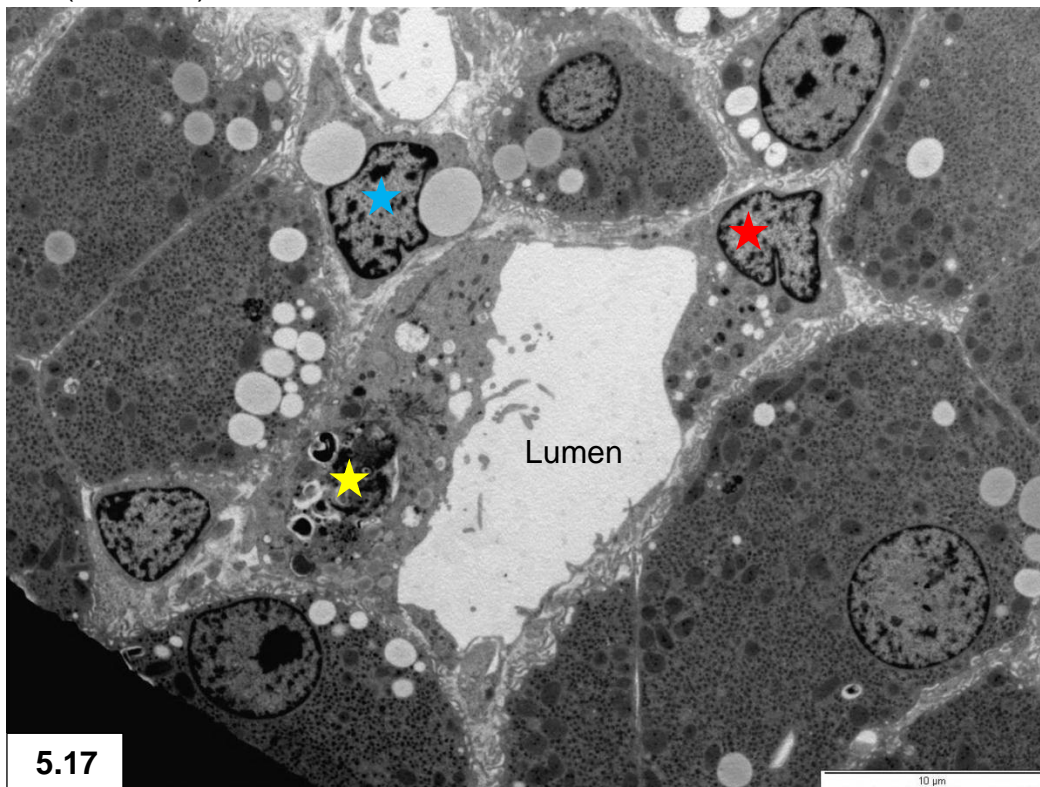
Figure 5.17: Endothelial cell (red star) with long extensions. A Kupffer cell (yellow star) forms part of the sinusoidal lining. Note stellate cell (blue star) containing lipid droplets in the space of Disse.
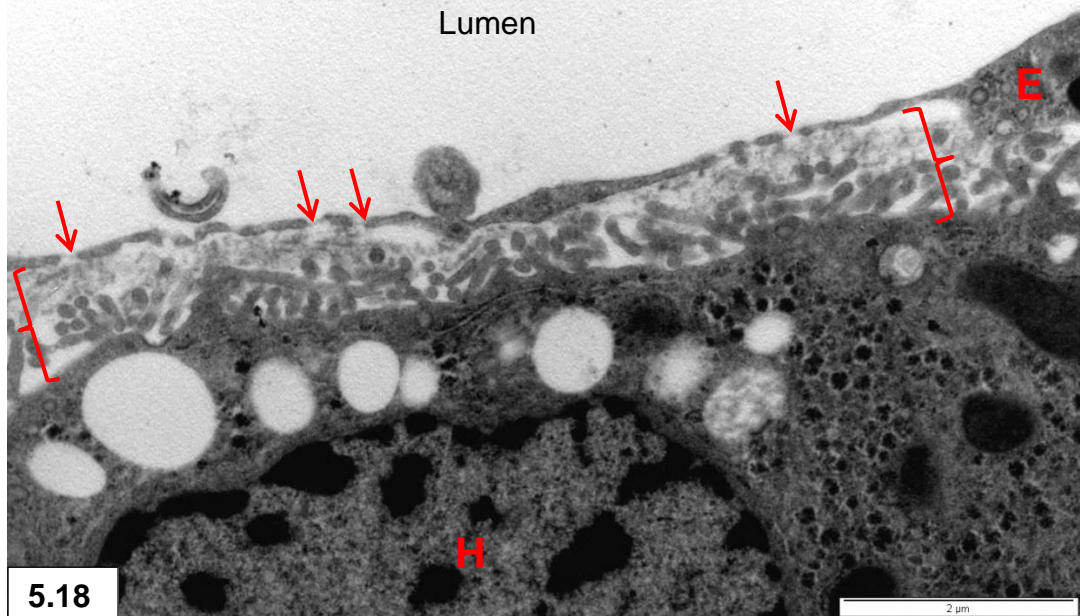
Figure 5.18: Fenestrated cytoplasmic extensions (arrows) of endothelial cell (**E**). Space of Disse (brackets) filled with surface microvilli of hepatocyte (**H**).

Figure 5.19: Overlapping endothelial cell extensions with tight junctions (dashed circle). Stellate cell (**S**) with coated pit (arrow).
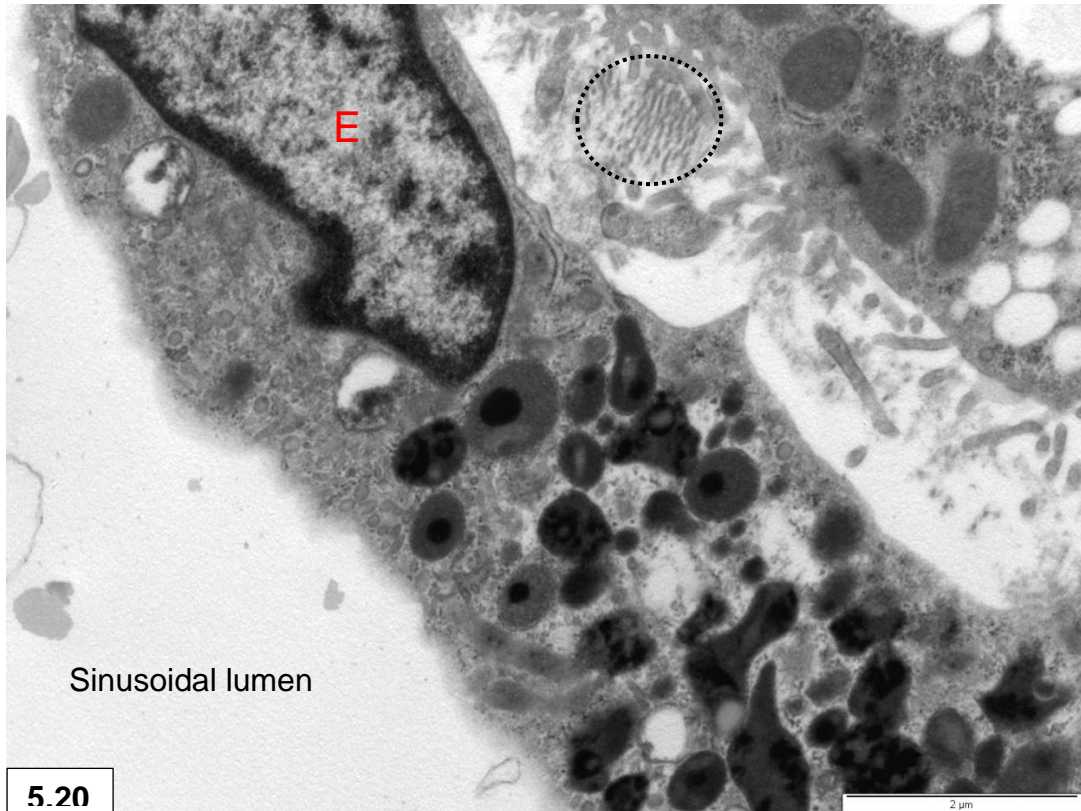
Figure 5.20 & 5.21: Prominent lysosomes with electron-dense contents in endothelial cells (**E**) lining sinusoids. Note collagen fibrils (black circle) and long-spacing collagen fibrils (red circle) in the space of Disse.
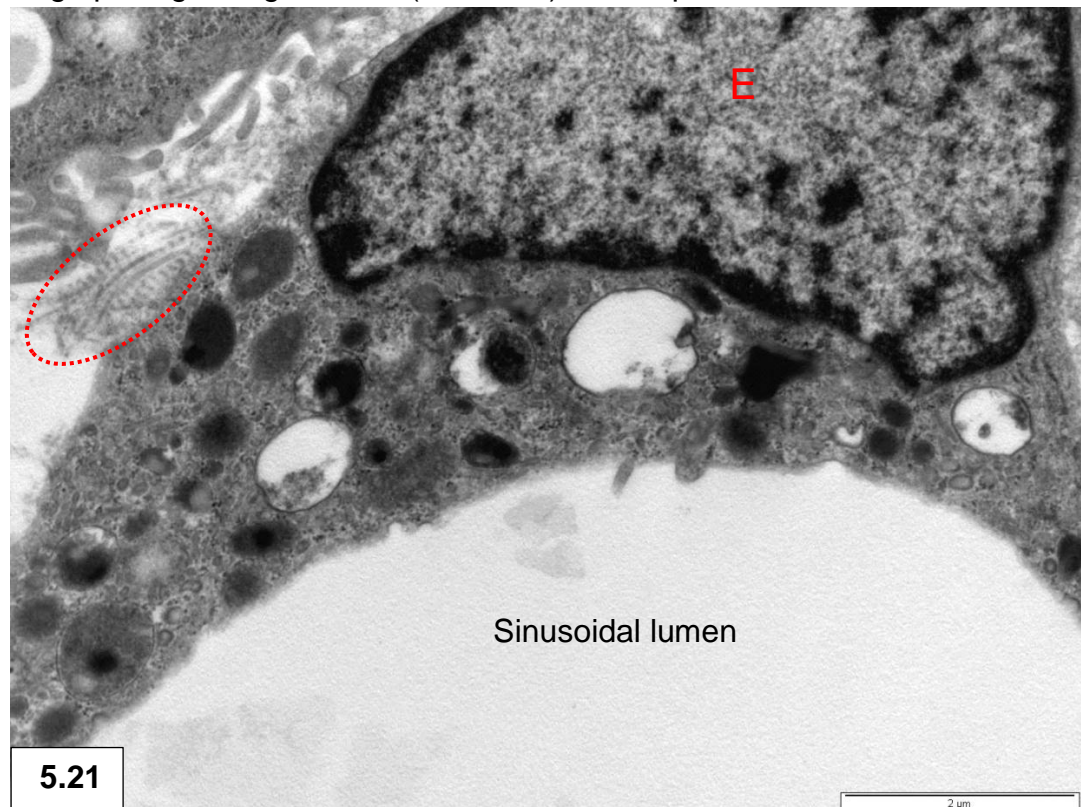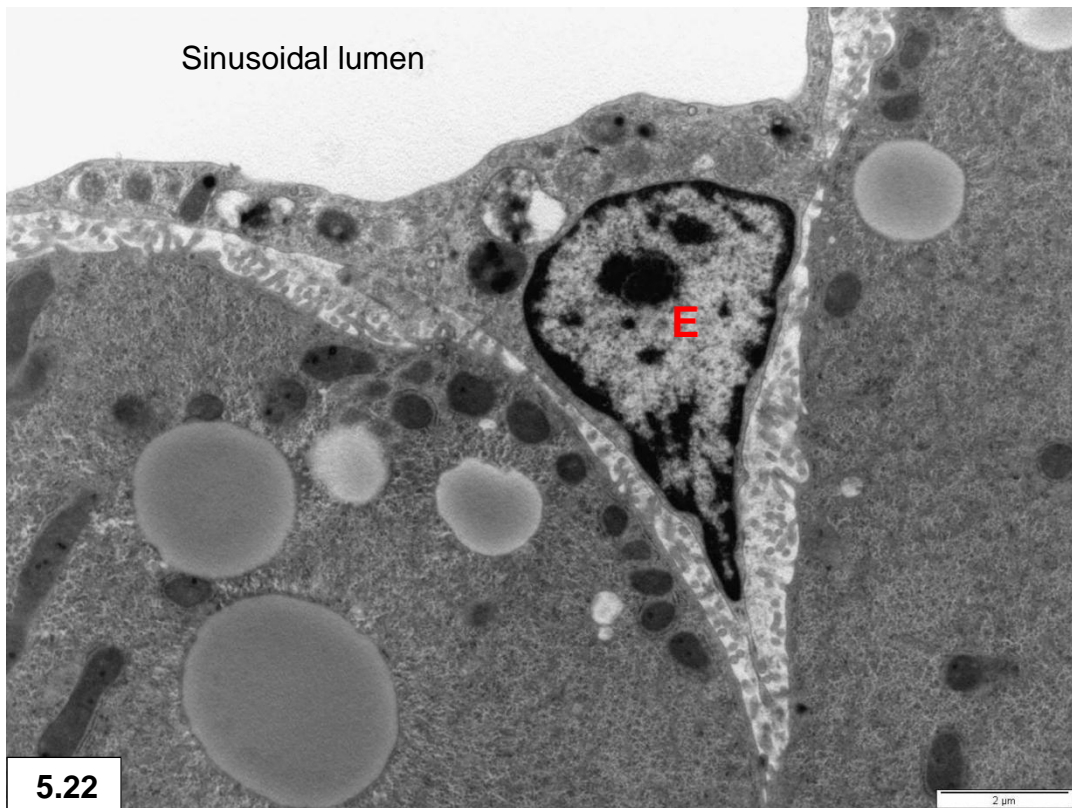
Figure 5.22: Endothelial cell nucleus (**E**) in the recess between neighbouring groups of hepatocytes.
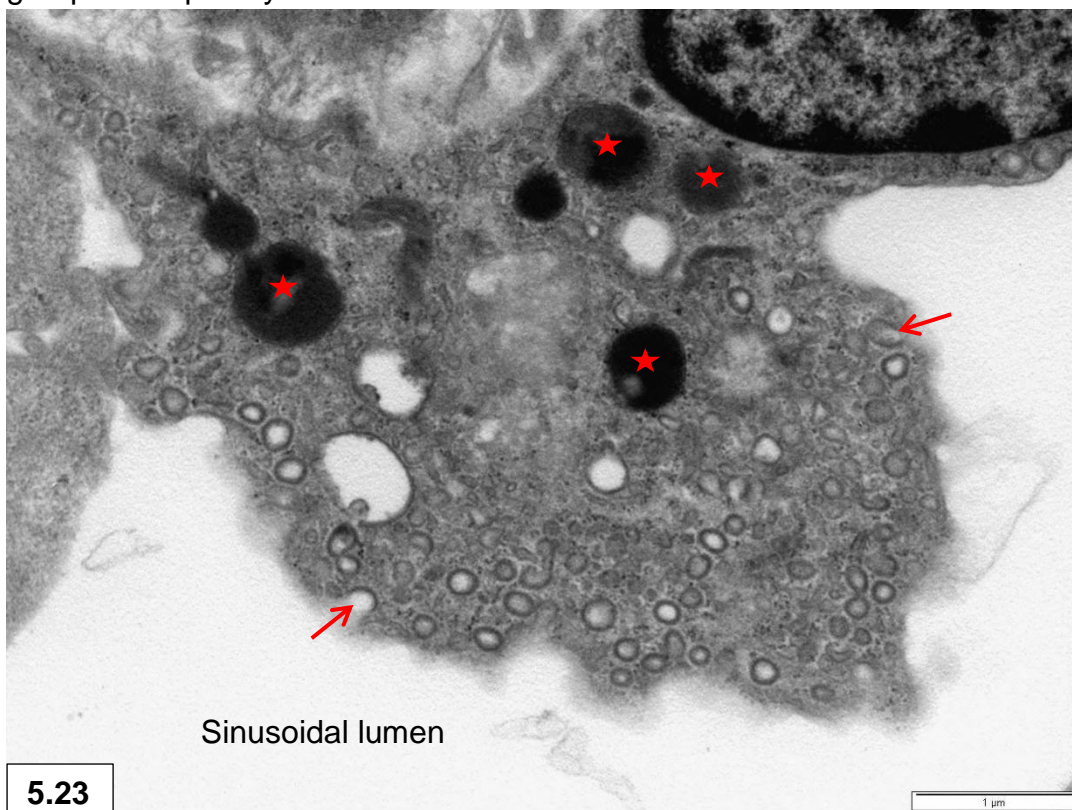
Figure 5.23: Endothelial cell cytoplasm packed with pinocytotic vesicles in different stages of formation. Invagination of the cell membrane (arrows) to form pinocytotic vesicles. Note electron-dense lysosomes (stars).
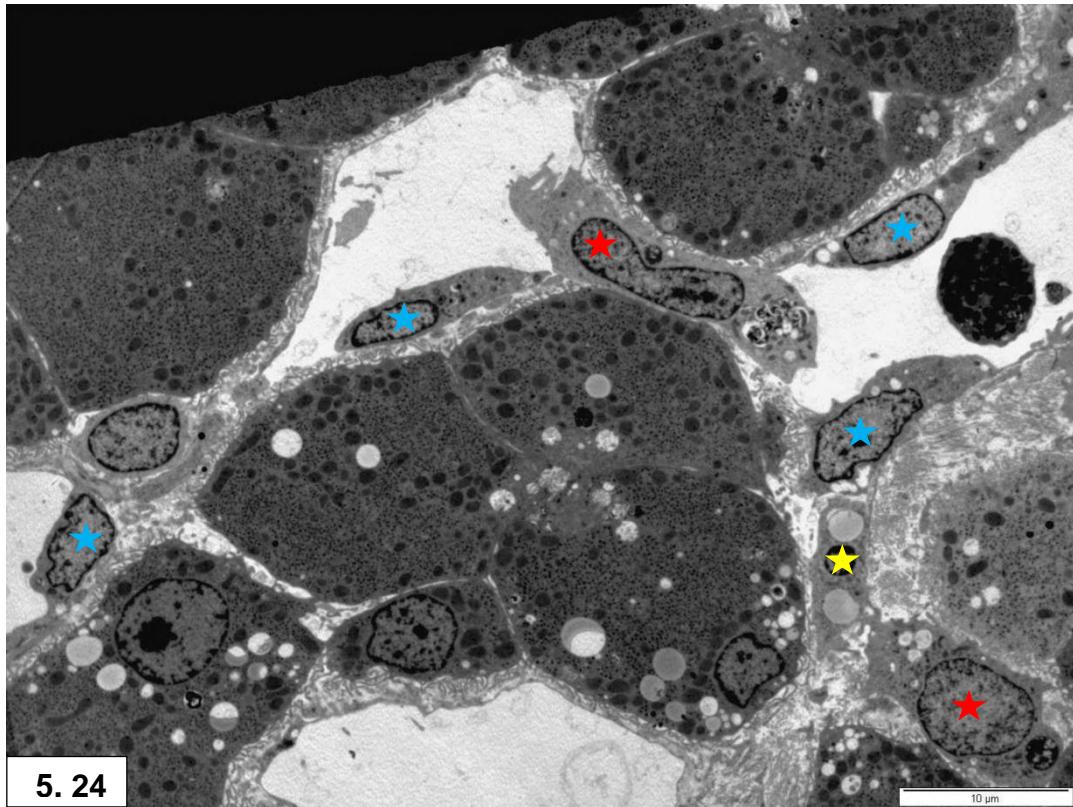
Figure 5.24: Large pleomorphic pigmented Kupffer cell (red star) protruding into the sinusoidal lumen and connecting adjacent sinusoids. Endothelial cell (blue stars), stellate cell (yellow star).
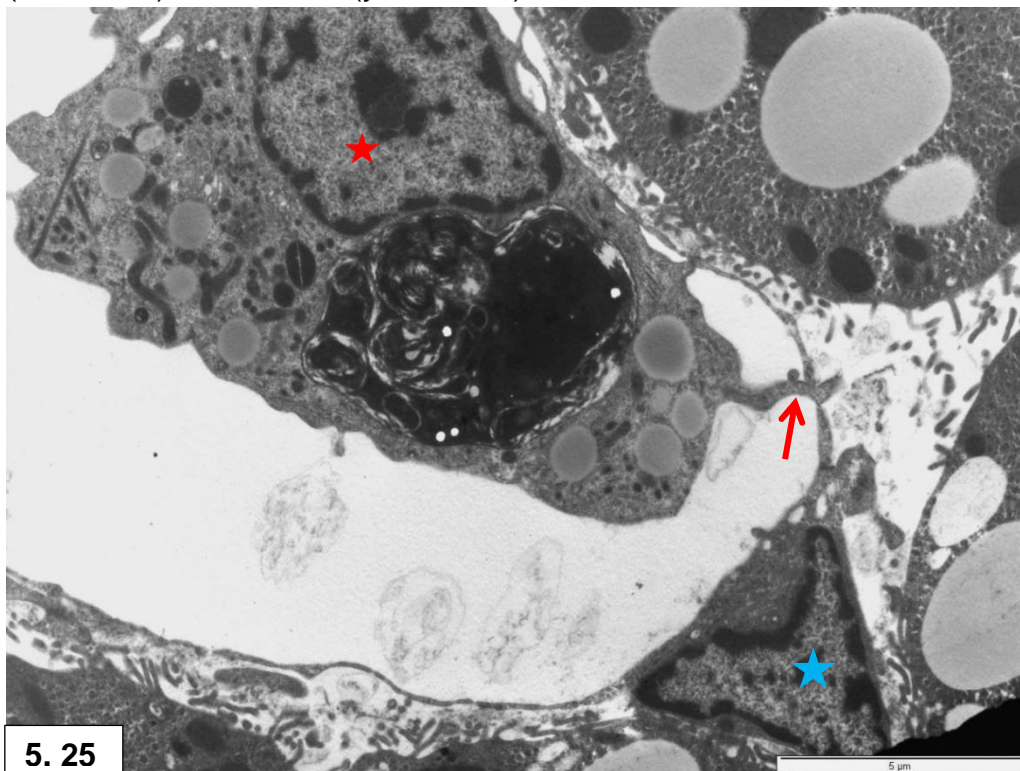
Figure 5.25: Filopodium (arrow) of Kupffer cell (red star) penetrating through endothelium fenestrae. Note cytoplasmic lipid droplets and large phagosome in Kupffer cell. Endothelial cell (blue stars).
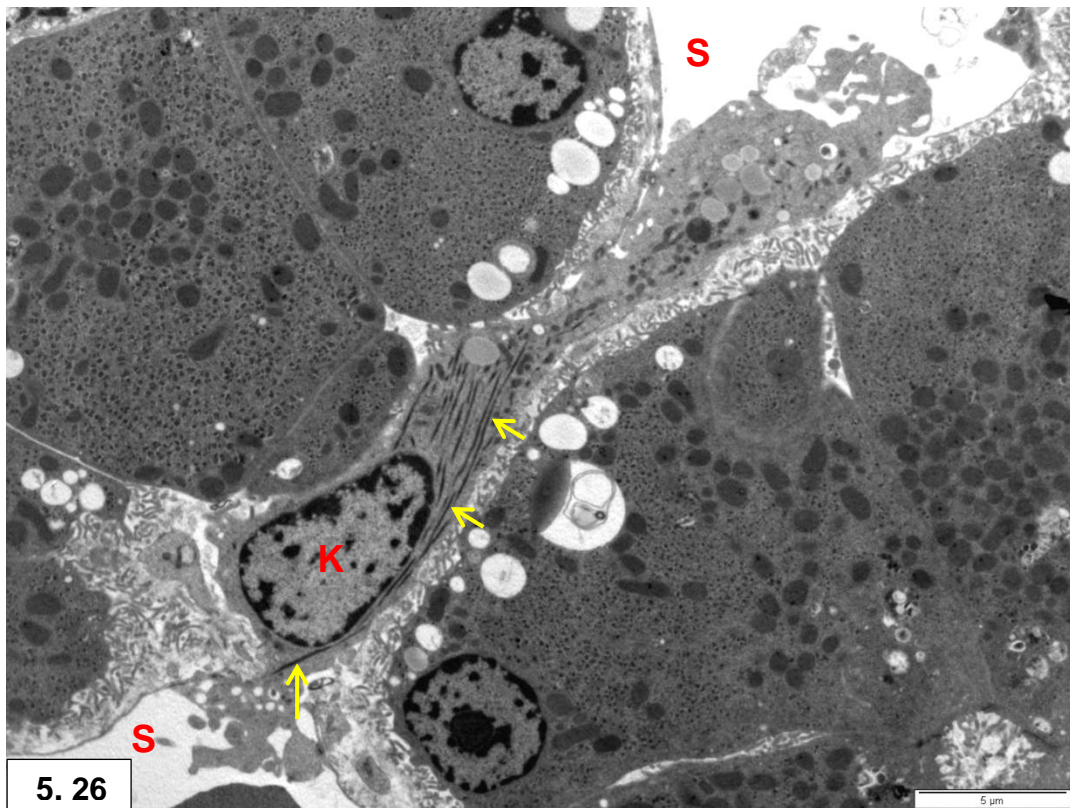
Figure 5.26: Kupffer cell (**K**) insertion between groups of hepatocytes forming a bridge between adjacent sinusoids (**S**). Note longitudinal tubulosome profiles (arrows).
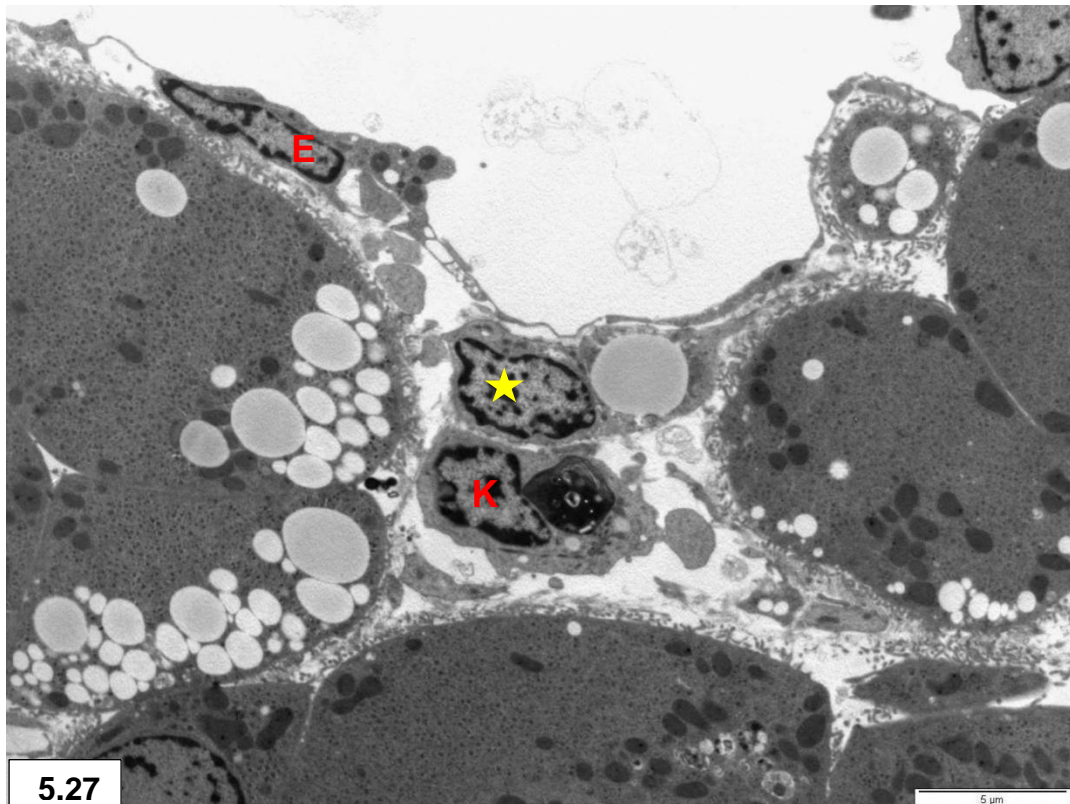
Figure 5.27: Kupffer cell (**K**) located in the space of Disse. Note stellate cell (star) containing a lipid droplet and endothelial cell (**E**) lining a sinusoid.
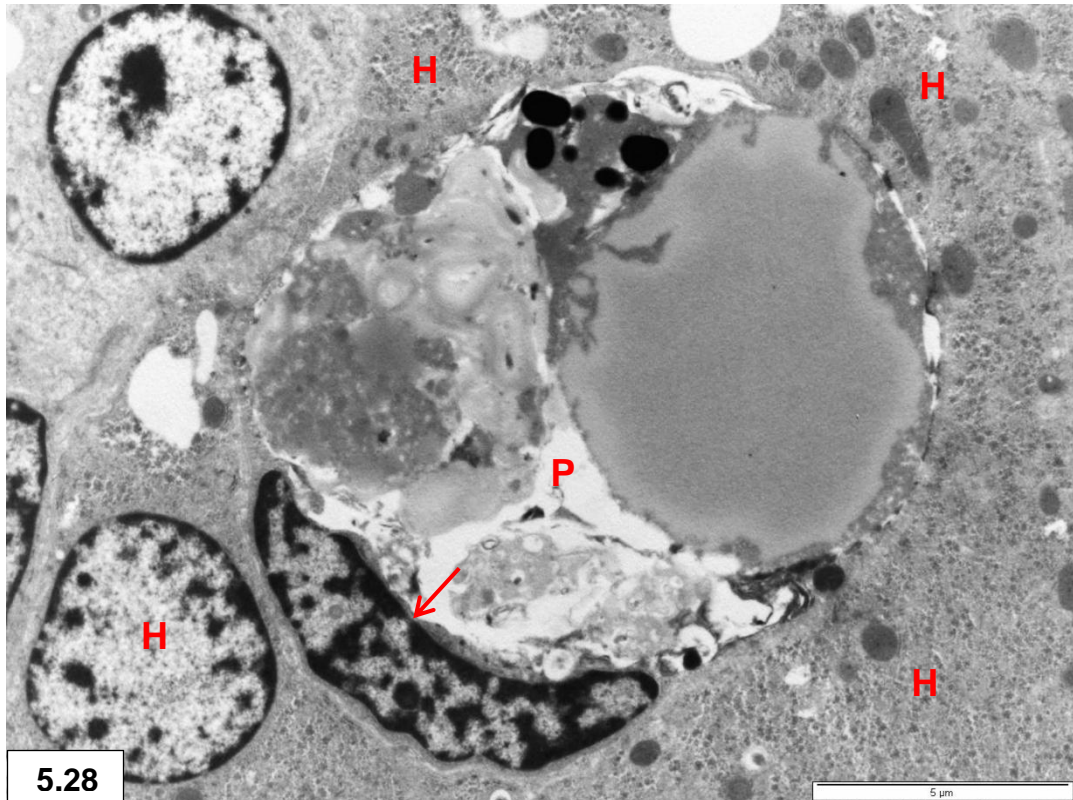
Figure 5.28 & 5.29: Pigmented cells (**P**) forming part of the hepatocyte (**H**) cell cords. Eccentric displacement of nuclei (arrows) by large inclusions containing melanin granules and other constituents. Note stellate cell (star) containing a lipid droplet.
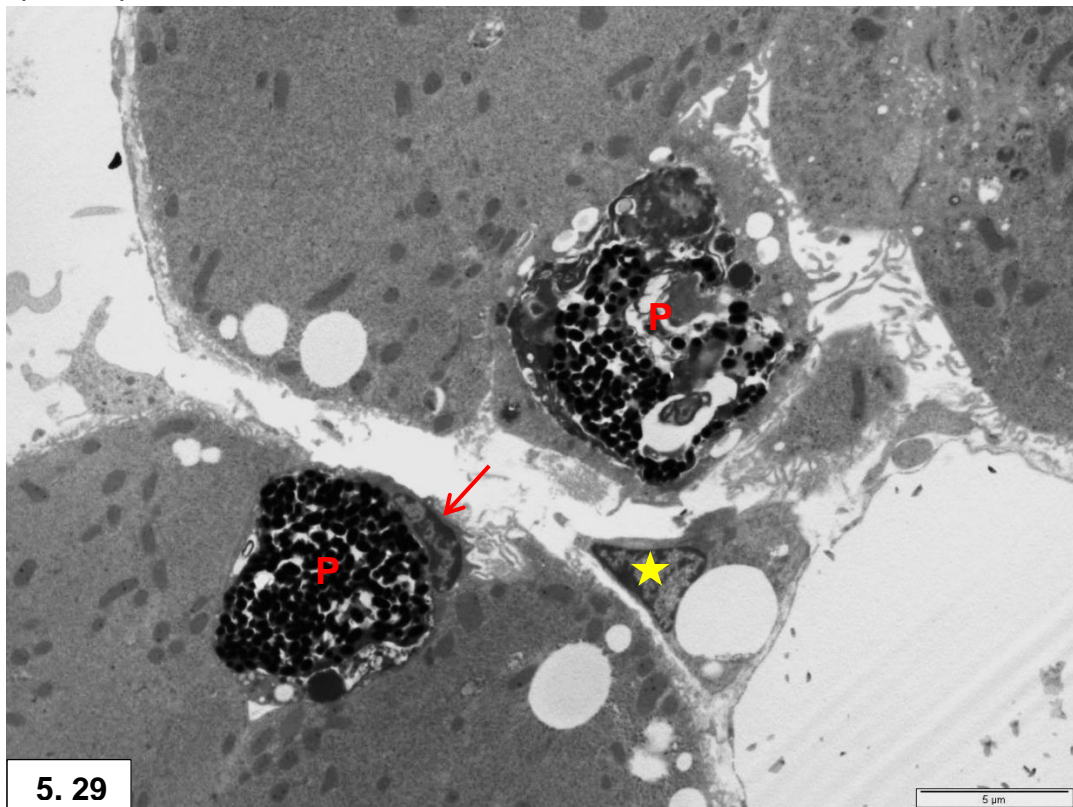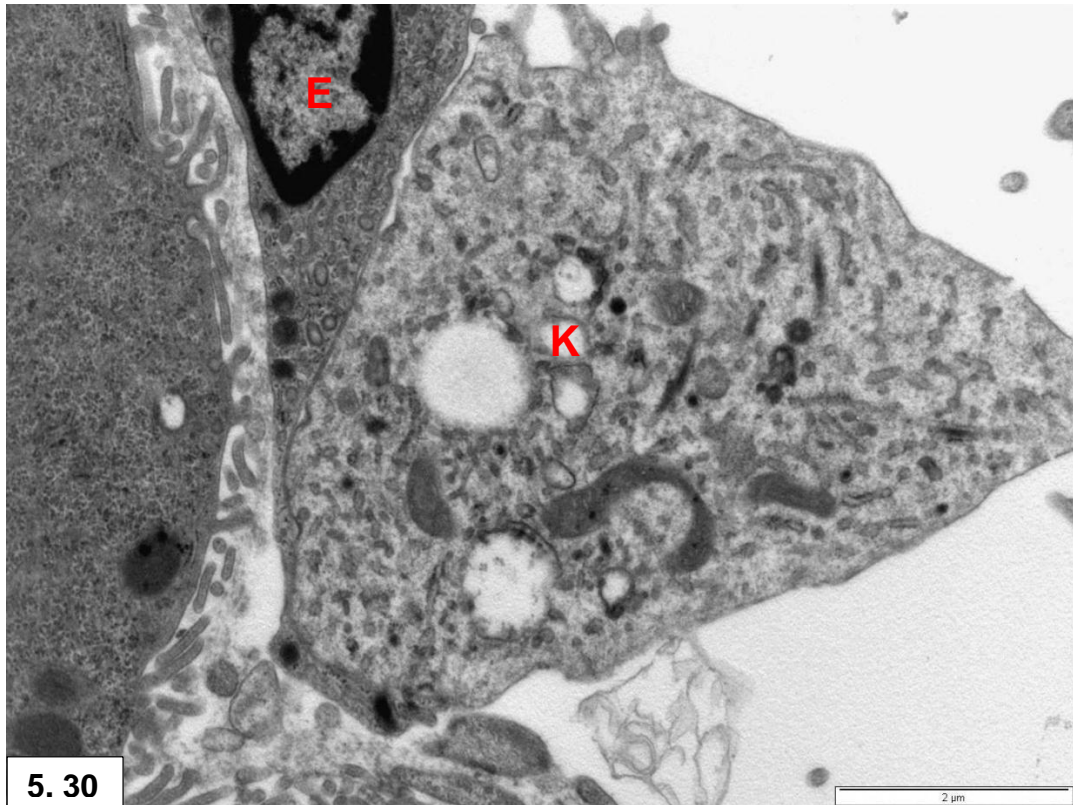
Figure 5.30: Close contact between Kupffer (**K**) and endothelial cell (**E**).
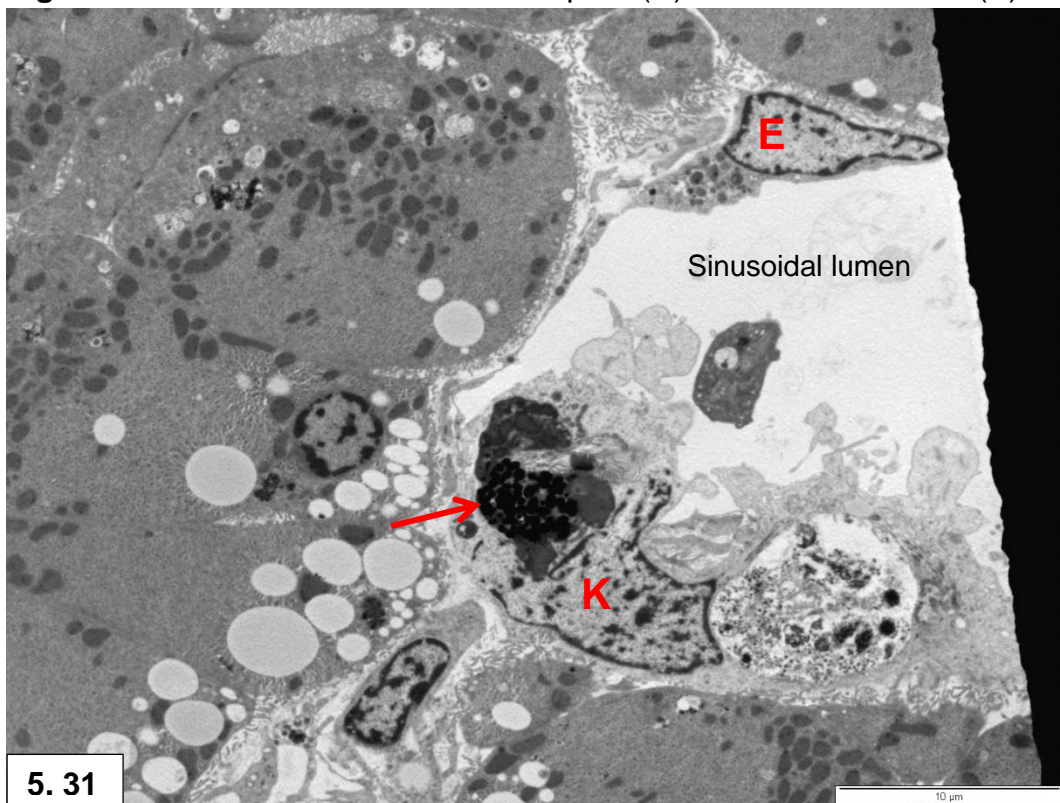
Figure 5.31: Melanin granules (arrow) present in luminal Kupffer cell (**K**) forming part of the sinusoidal lining. Endothelial cell (**E**).
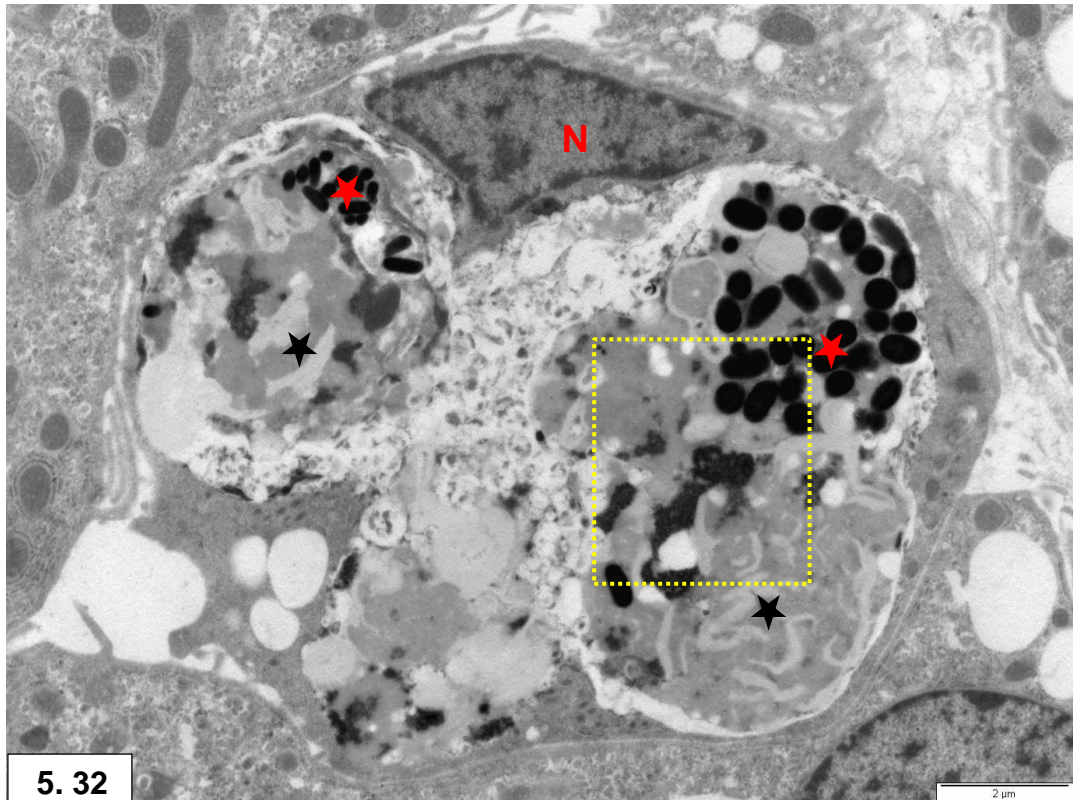
Figure 5.32: Pigmented cell containing melanin granules (red stars) mixed with electron-lucent fragments (ceroid) (black stars). Note eccentric displacement of nucleus (**N**).
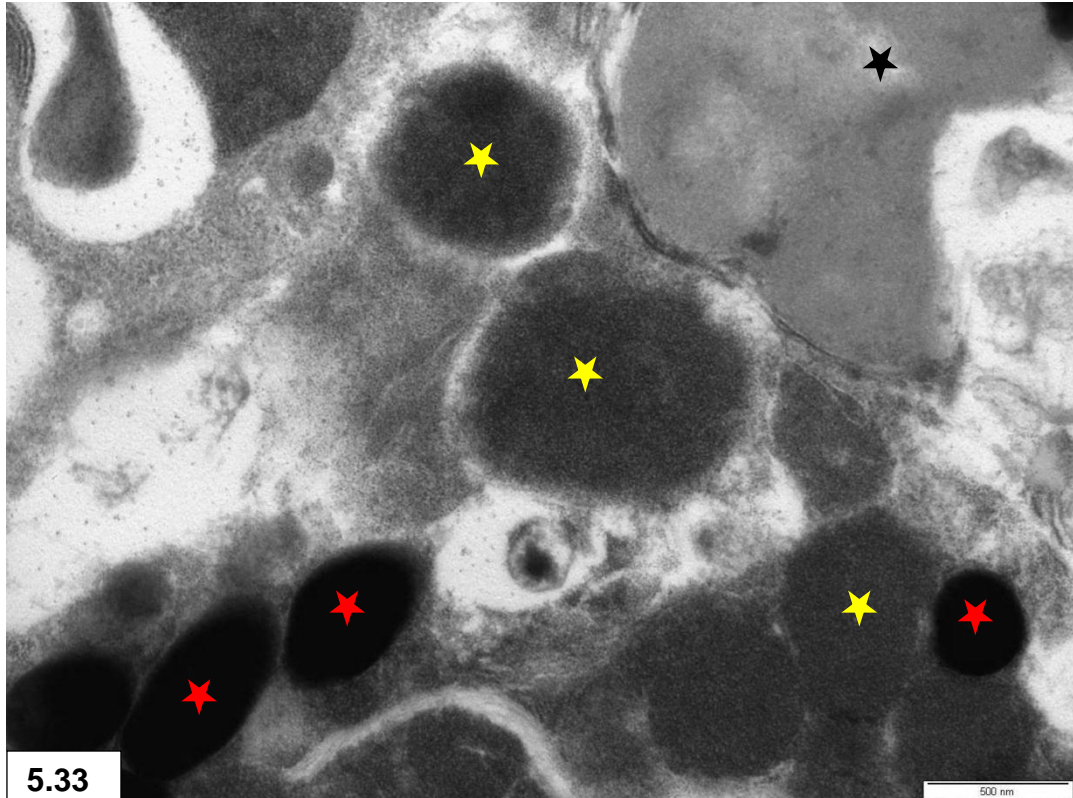
Figure 5.33: Higher magnification of a similar area to that blocked in Fig. 5.32. Note melanin granules (red stars), fine granular hemosiderin component (yellow stars) and ceroid (black stars).
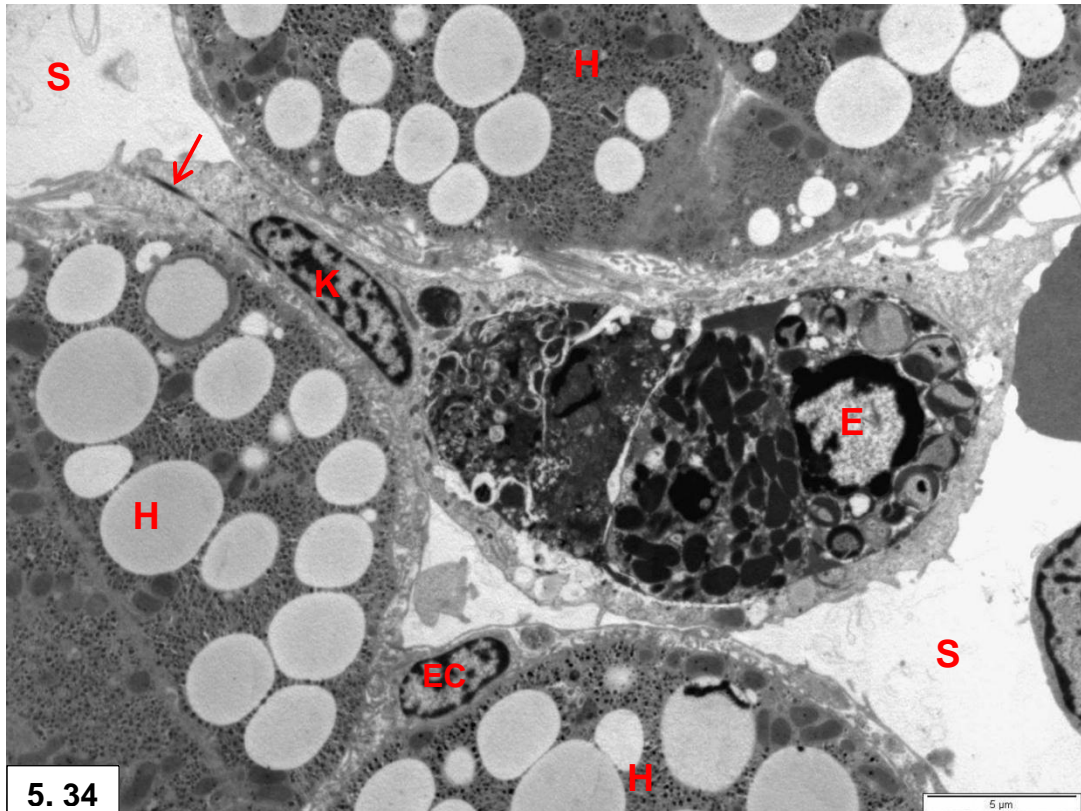
Figure 5.34: Engulfment of eosinophil (**E**) by Kupffer cell (**K**). Note Kupffer cell insertion between adjacent sinusoids (**S**) and cytoplasmic tubulosomes (arrow). Hepatocytes (**H**), endothelial cell (**EC**).
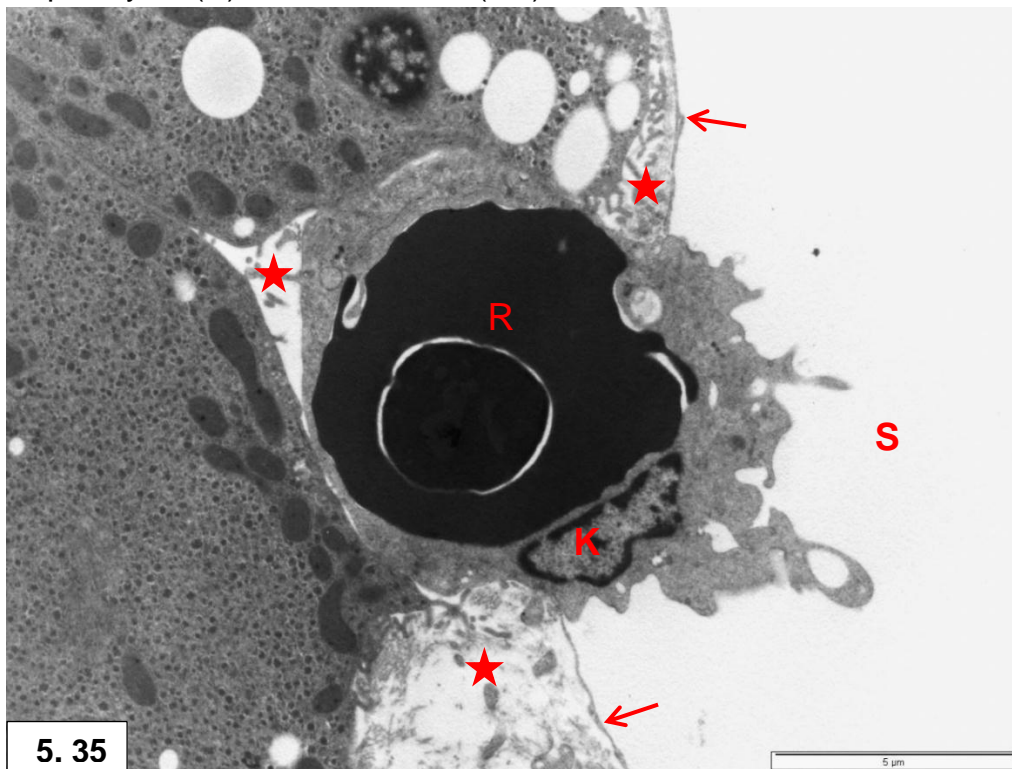
Figure 5.35: Engulfment of red blood cell (**R**) by Kupffer cell (**K**) that extends from the space of Disse (stars) through the endothelium (arrows) into the lumen of a sinusoid (**S**).
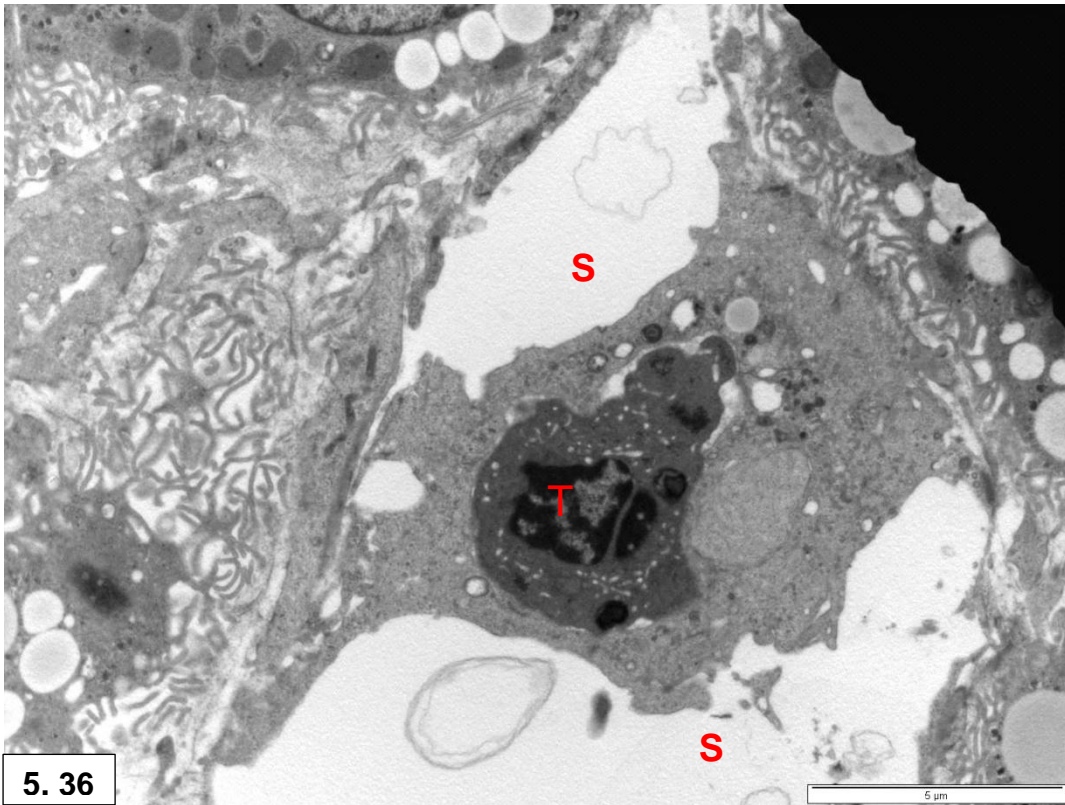
Figure 5.36: Kupffer cell bridging a sinusoidal lumen (**S**) and engulfing a thrombocyte (**T**).
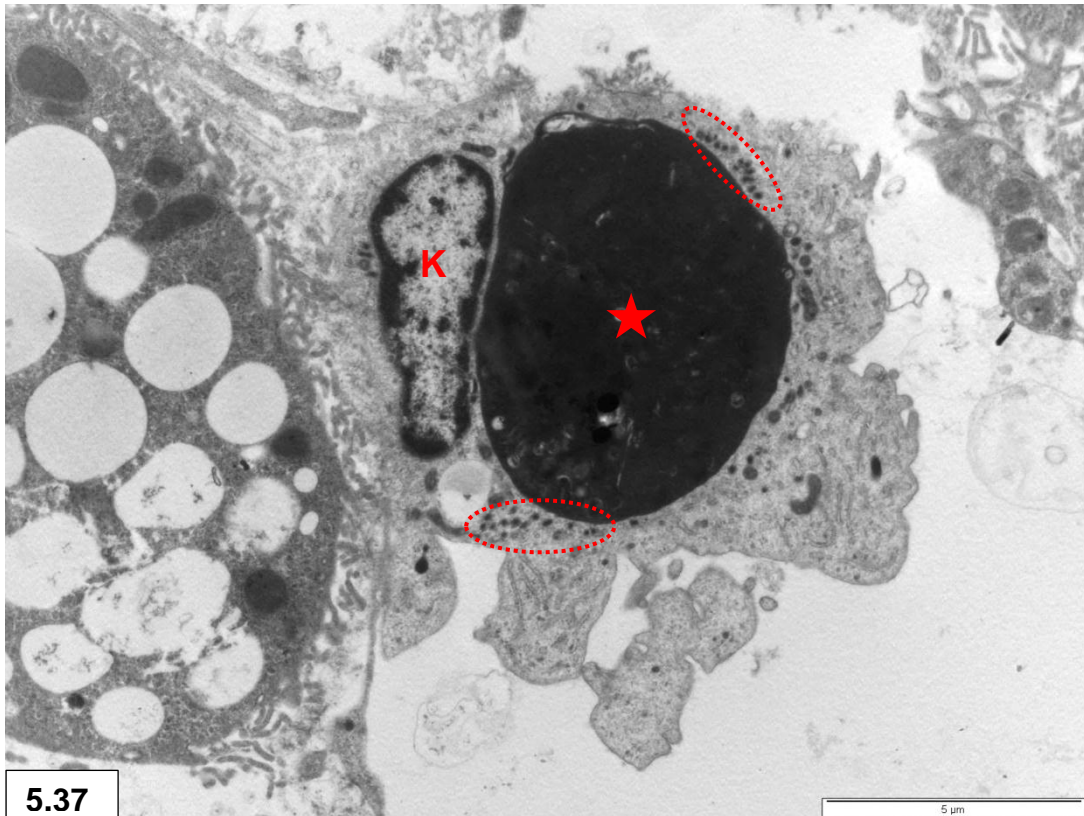
Figure 5.37: Tubulosomes (dashed circles) in Kupffer cell (**K**) separated into smaller groups around a phagosome (star).

Figure 5.38: Close contact between elongated tubulosomes (arrows) and mitochondria (stars) in Kupffer cell.
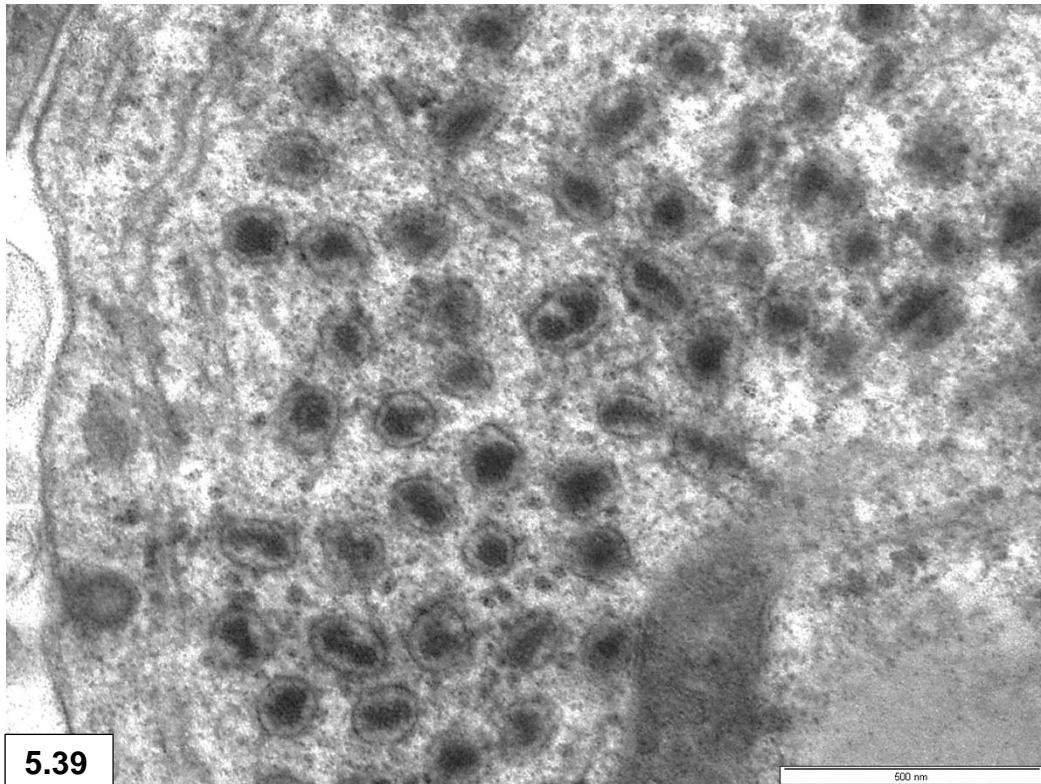
Figure 5.39: Variable cross-sectional interior profiles of tubulosomes: circular and angular contours are apparent. Note single outer membrane.
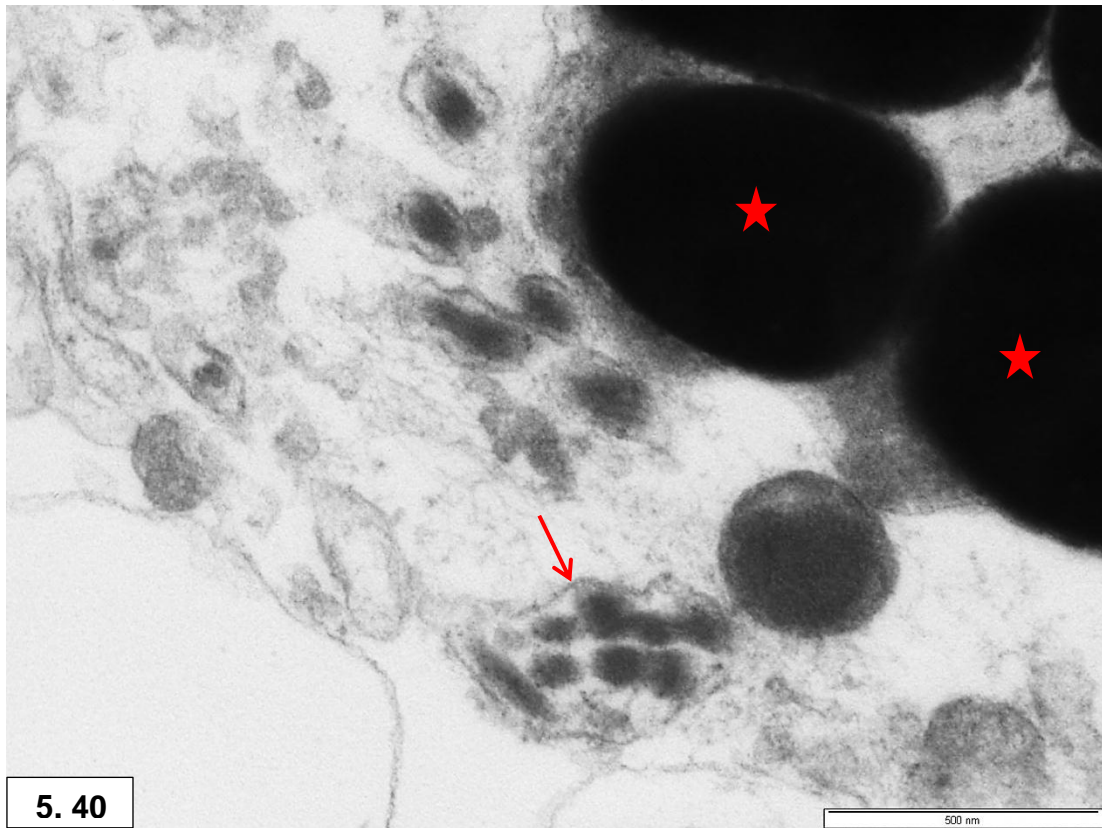
Figure 5.40: Tubulosome (arrow) illustrating divided interior profiles. Melanin granules (stars).
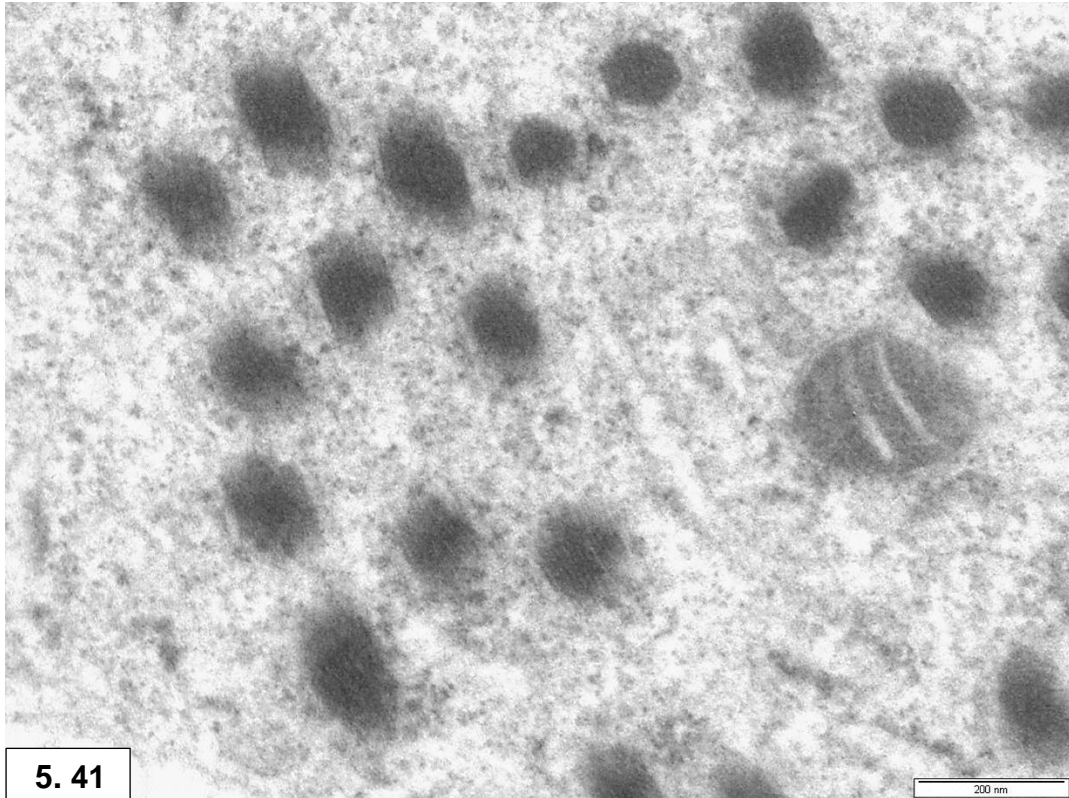
Figure 5.41: Electron-dense filamentous material in tubulosomes.
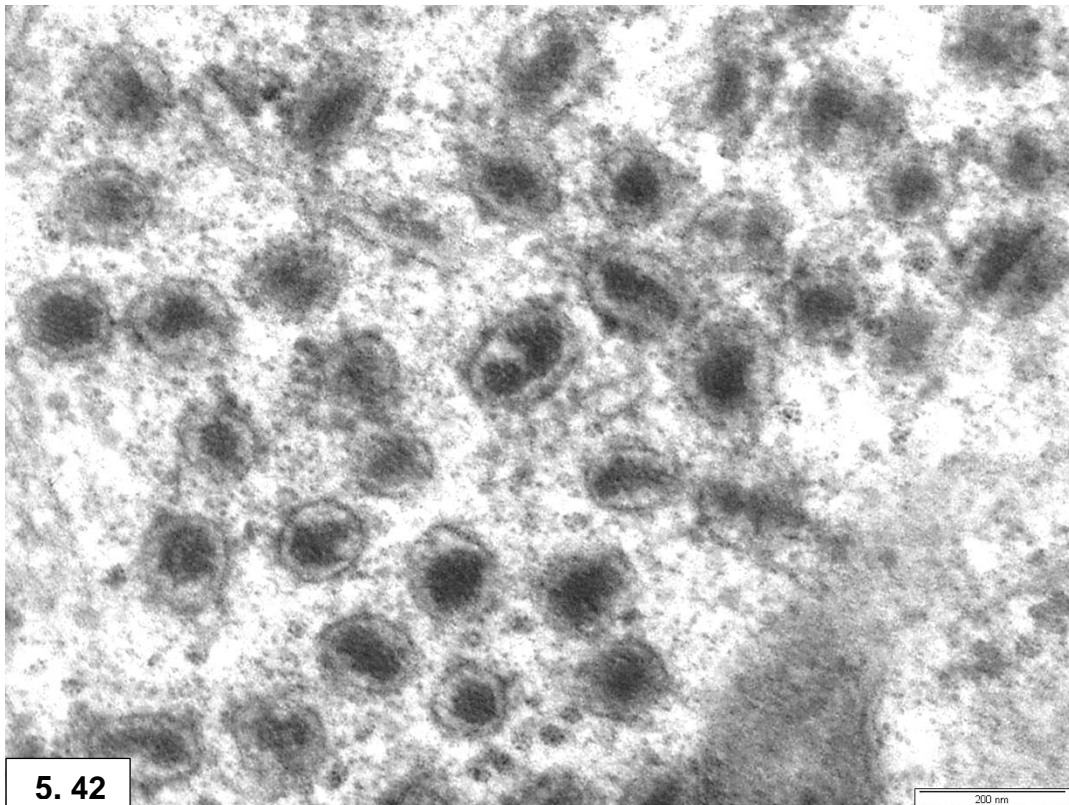
Figure 5.42: Electron-dense crystalline material in tubulosomes.
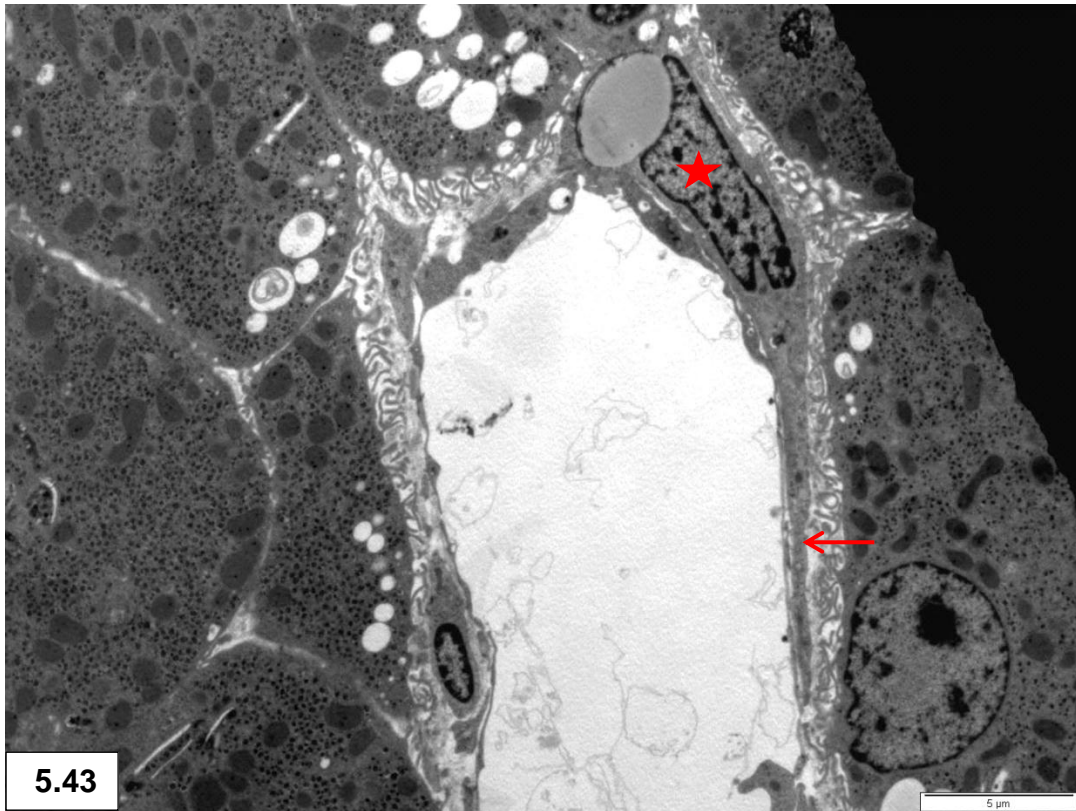
Figure 5.43 & 5.44: Stellate cells (stars) in the space of Disse. Note long cytoplasmic extension (arrow) in close contact with endothelial cell and prominent lipid droplet in the cytoplasm.
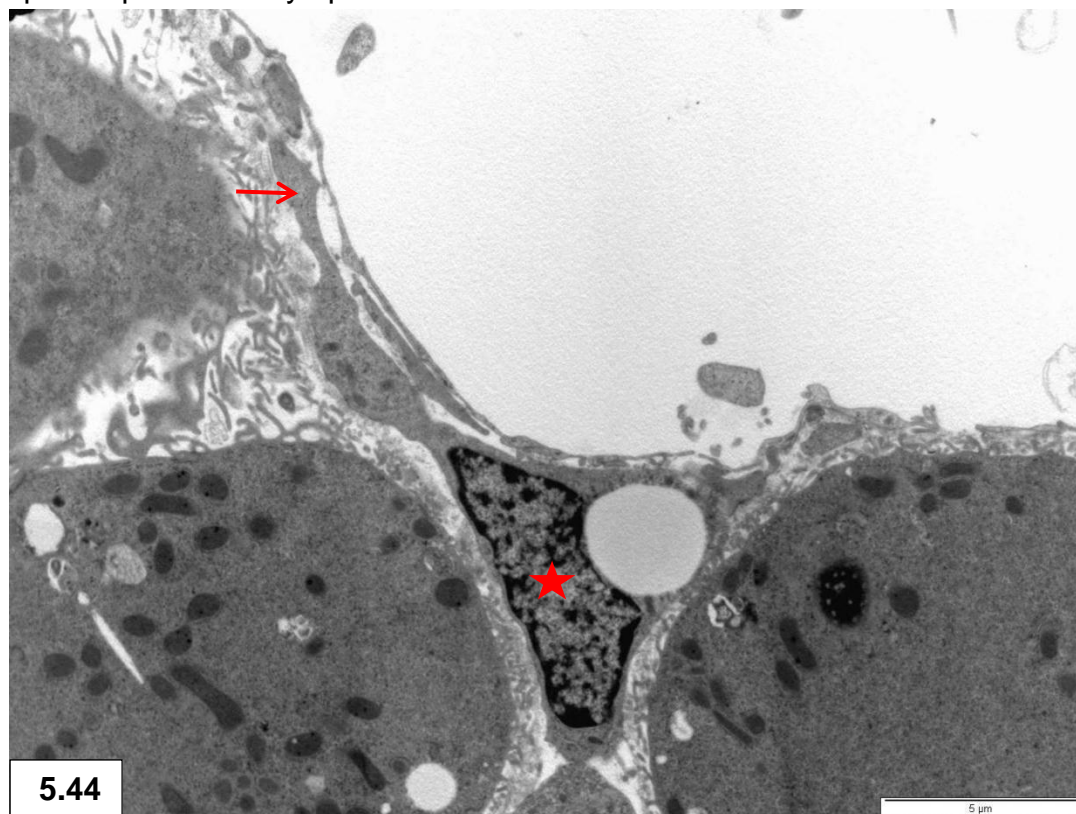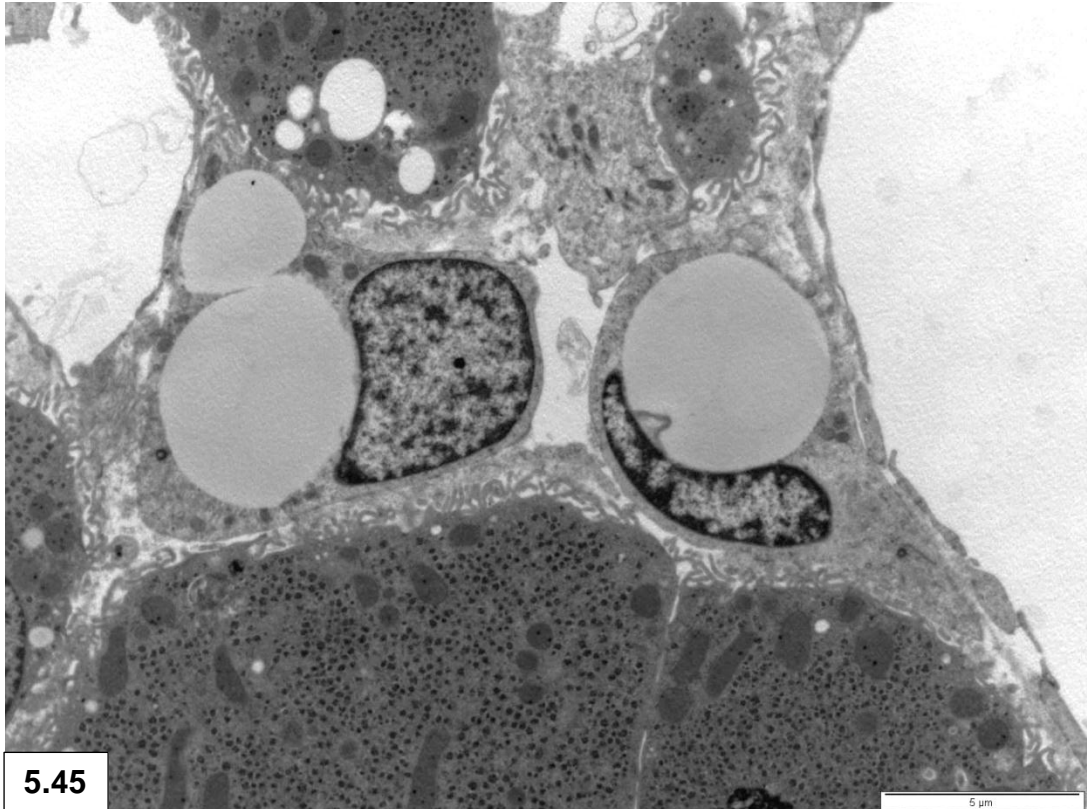
Figure 5.45 & 5.46: Prominent, non-membrane bound lipid droplets in stellate cells indenting the nucleus giving it an angular shape. Note close contact with endothelial cell (**E**).
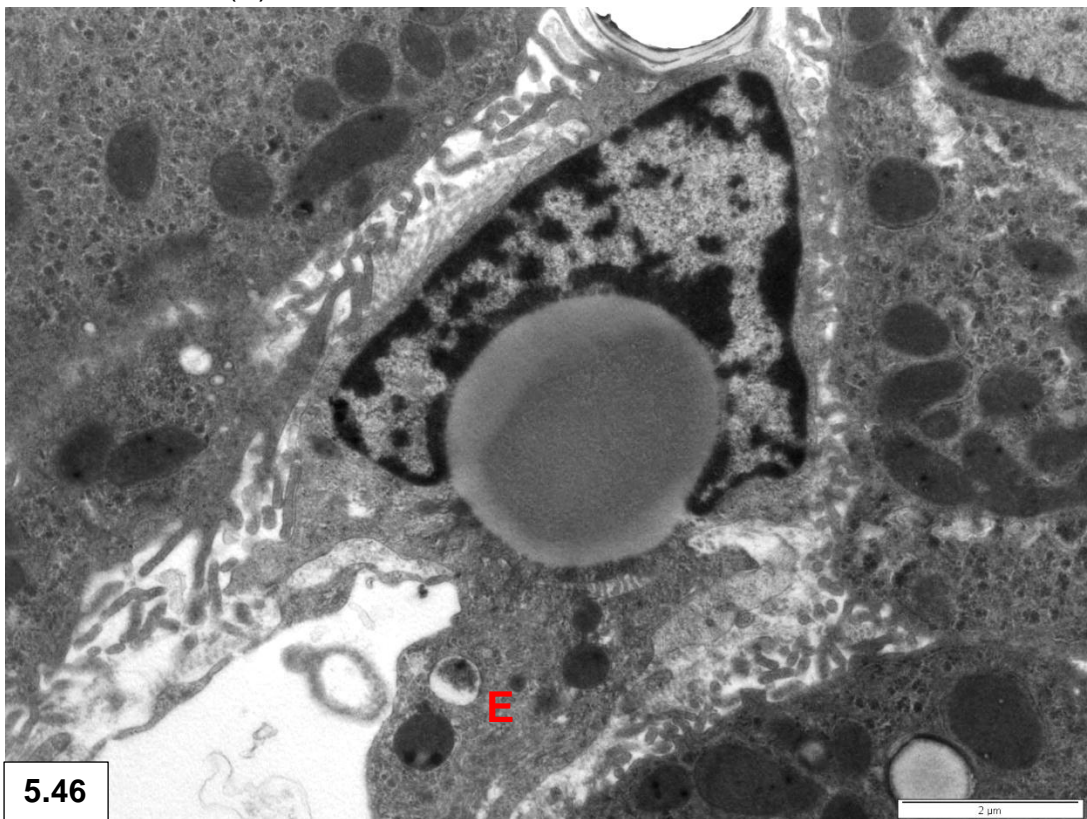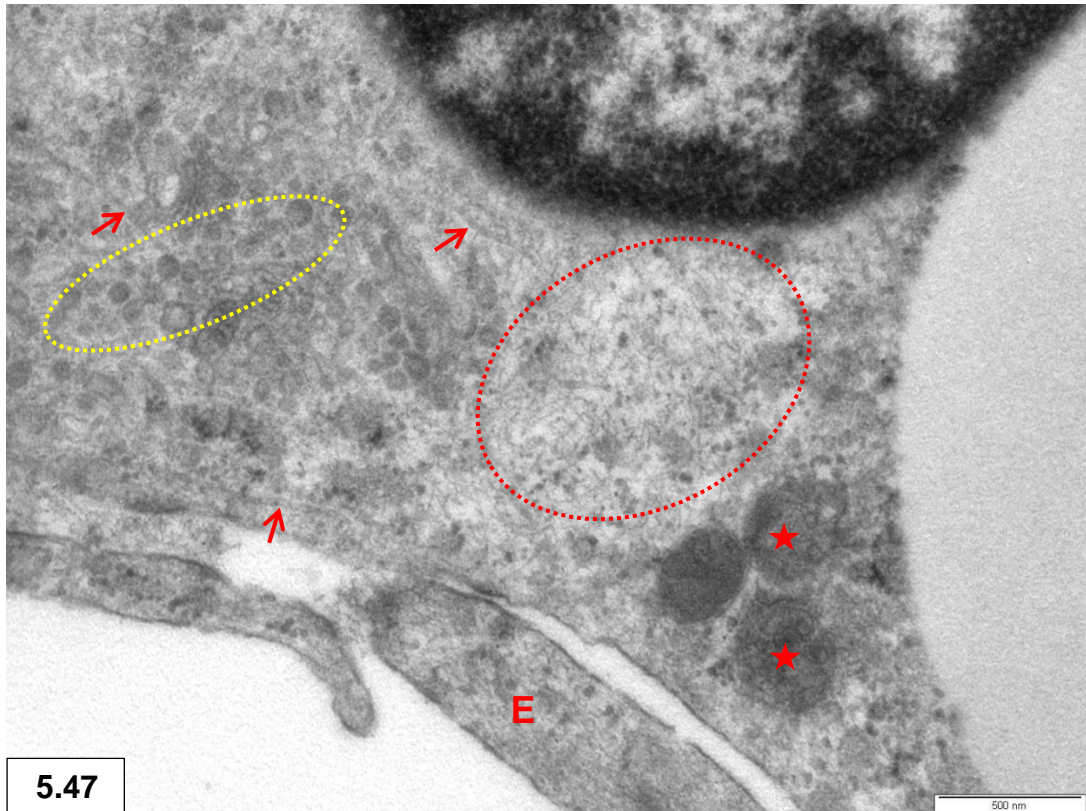
Figure 5.47 & 5.48: Cytoplasmic filaments (red dashed circle), microtubules (red arrows) and multivesicular bodies (stars) in stellate cells. Cytoplasmic structure with the periodicity of long-spacing collagen (yellow arrow). Note coated (black arrow) and pinocytotic vesicles (yellow dashed circle), and centriole (blue arrow). Endothelial extensions (**E**).
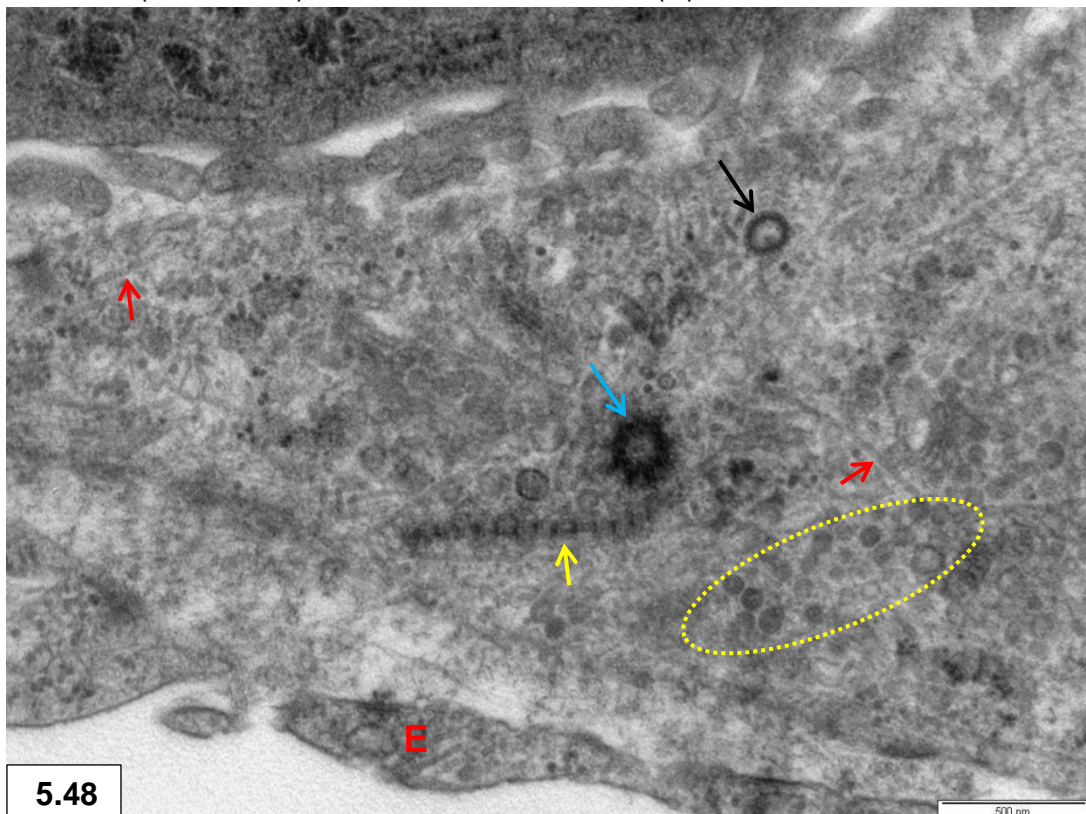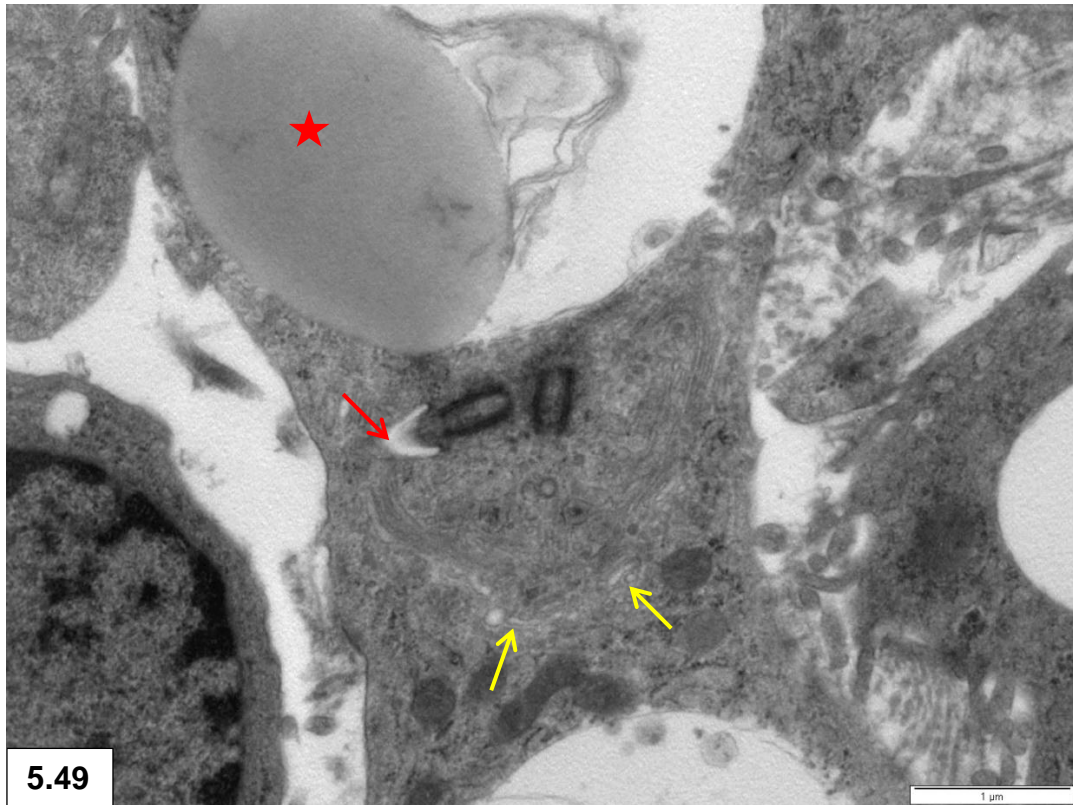
Figure 5.49: Centriole pair forming a ciliary basal body in a stellate cell. Note the intracytoplasmic ciliary canal (red arrow), Golgi (yellow arrows) and lipid droplet (star).

Figure 5.50: Myofibroblastic cell (**M**) with subendothelial extensions in the space of Disse. Endothelial cell (arrows).
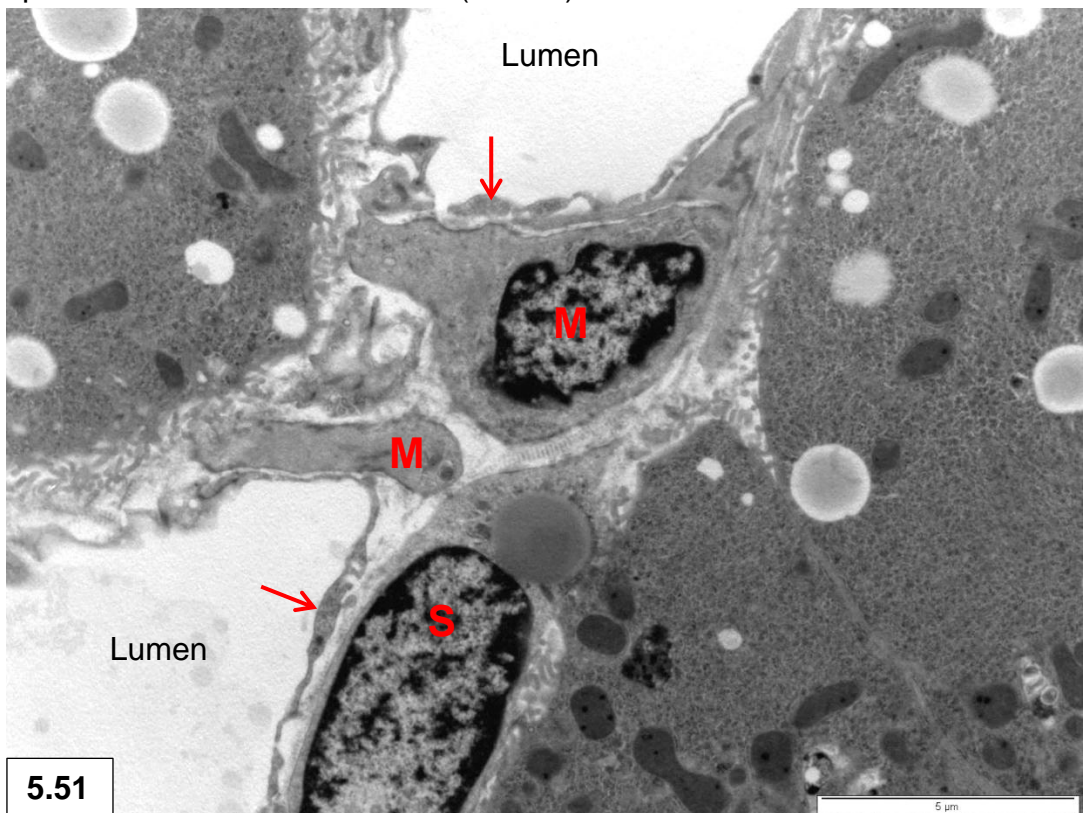
Figure 5.51 : Myofibroblastic cells (**M**) and stellate cell (**S**) containing a lipid droplet occupying the same area in the space of Disse. Endothelial cells (arrows).
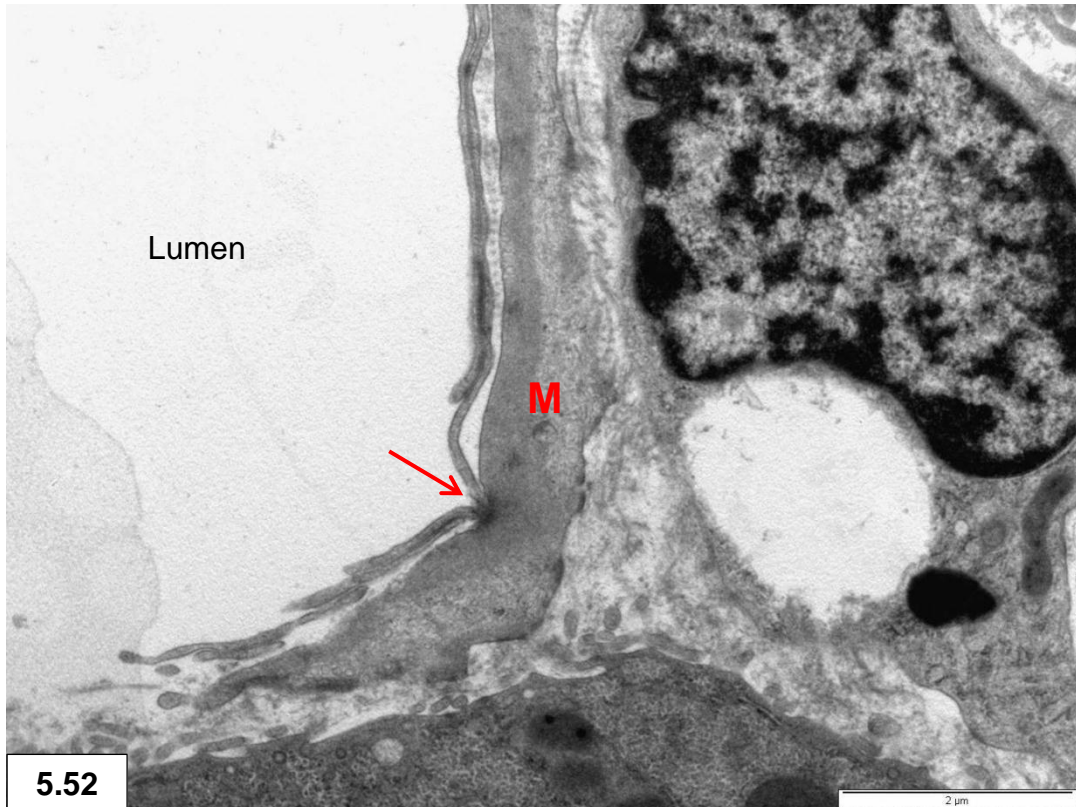
Figure 5.52: Myofibroblastic cell extension (**M**) touching an endothelial cell (arrow).
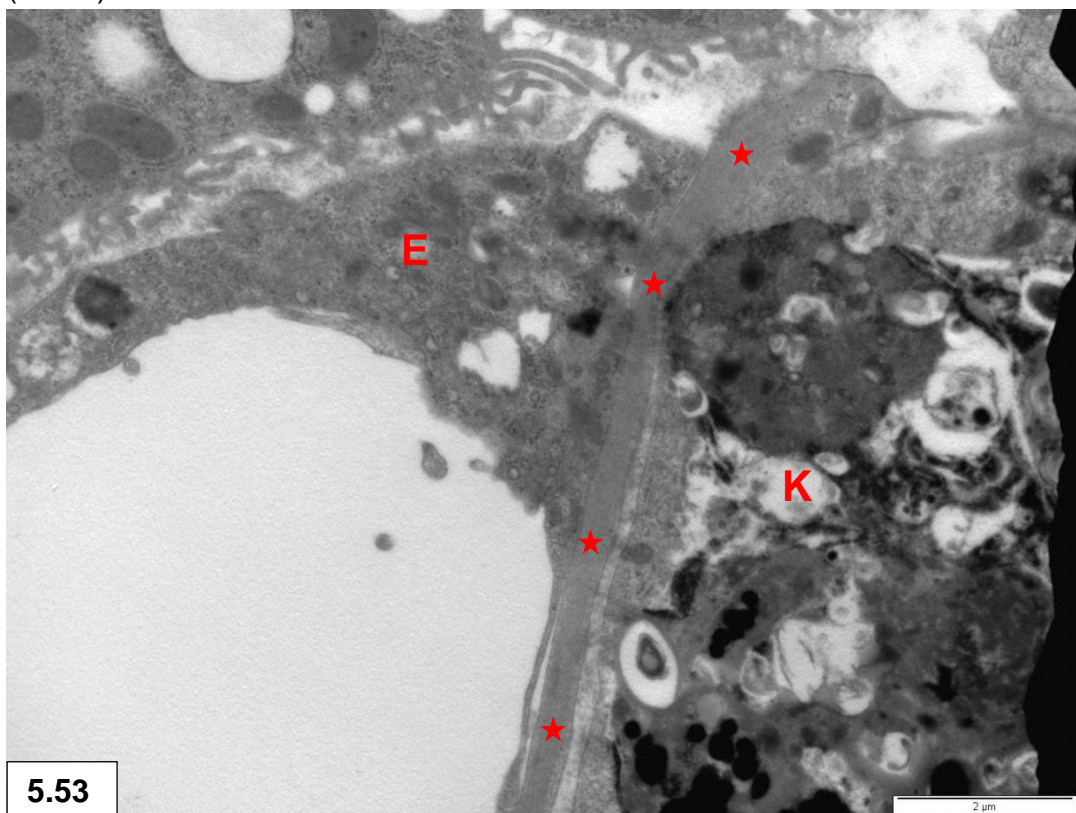
Figure 5.53: Cytoplasmic extension (stars) of a myofibroblastic cell in close contact with an endothelial (E) and a Kupffer cell (K).
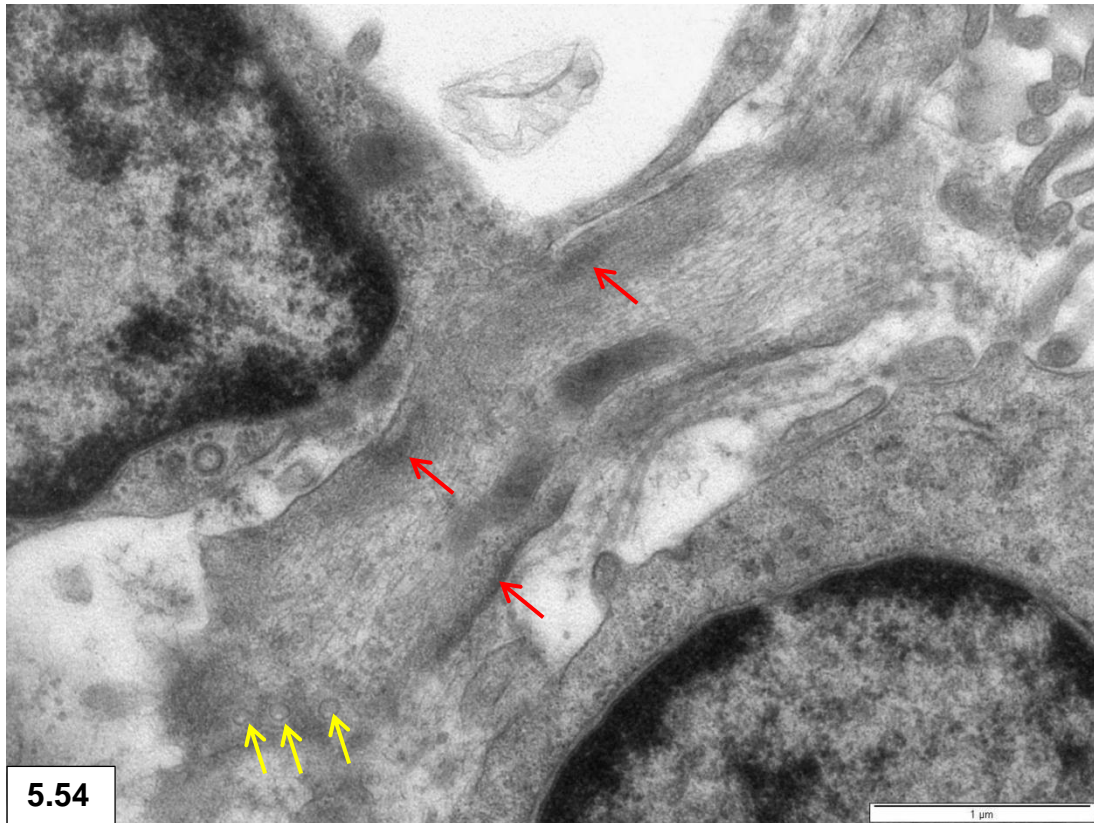
Figure 5.54 & 5.55: Filaments forming subplasmalemmal densities (red arrows) in a myofibroblastic cell. Pinocytotic vesicles (yellow arrows).
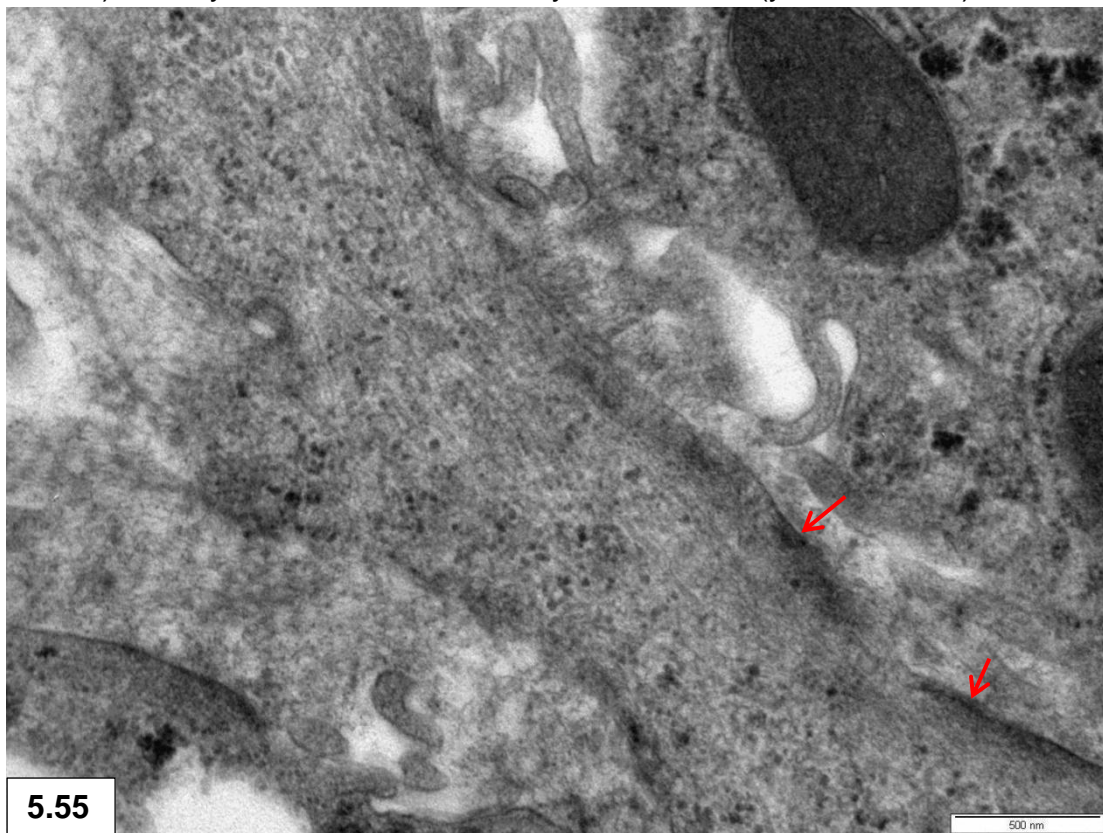
Figure 5.55: Myofibroblastic cell cytoplasm containing numerous longitudinally disposed microtubules. Note subplasmalemmal densities (red arrows).
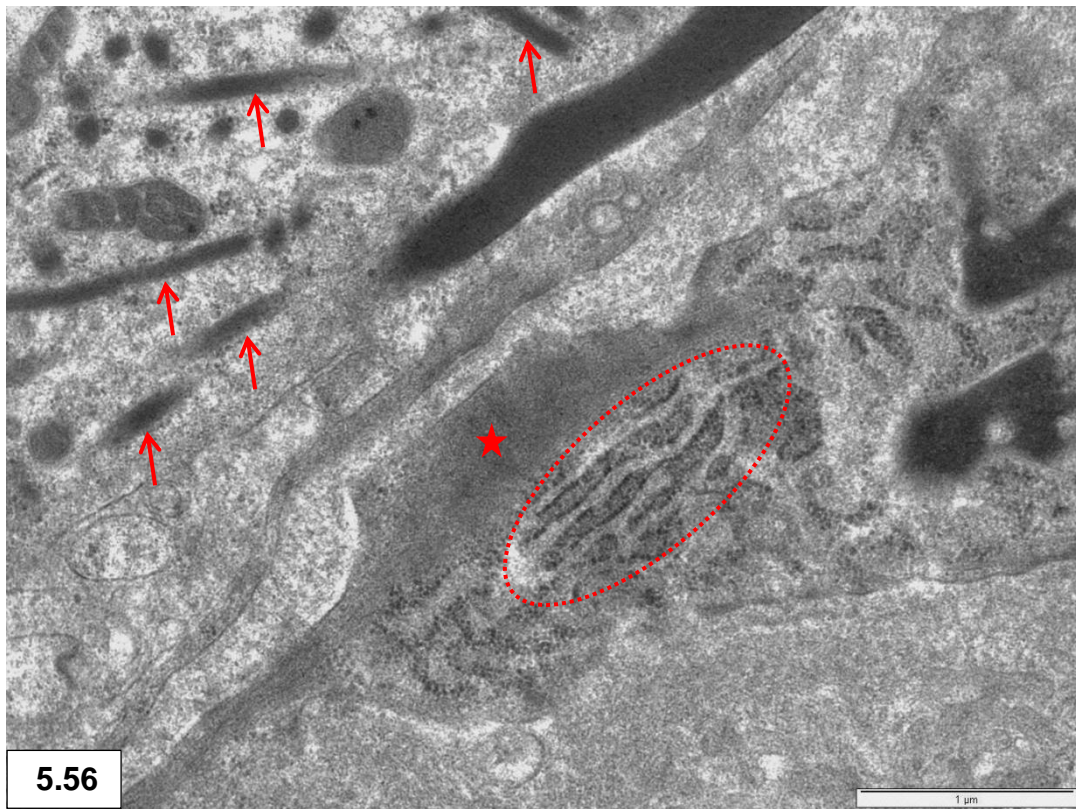
Figure 5.56: Dilated GER (dashed circle) and fine filaments (star) in a myofibroblastic cell. Note tubulosomes (arrows) in a neighbouring Kupffer cell.
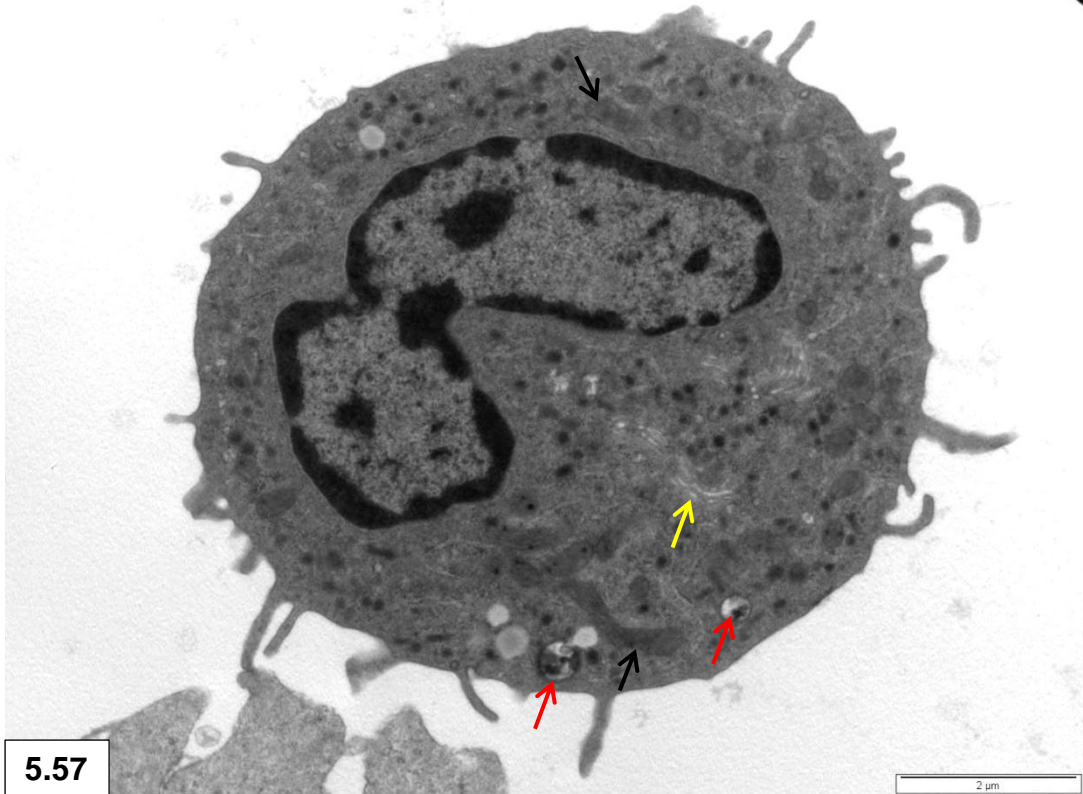
Figure 5.57 & 5.58: Pit cells with pseudopodia and indented eccentric nucleus present in a sinusoid. Note the many small membrane-bound electron dense granules and larger membrane-bound clear vesicles with electron-dense contents (red arrows). Golgi (yellow arrows), mitochondria (black arrows).
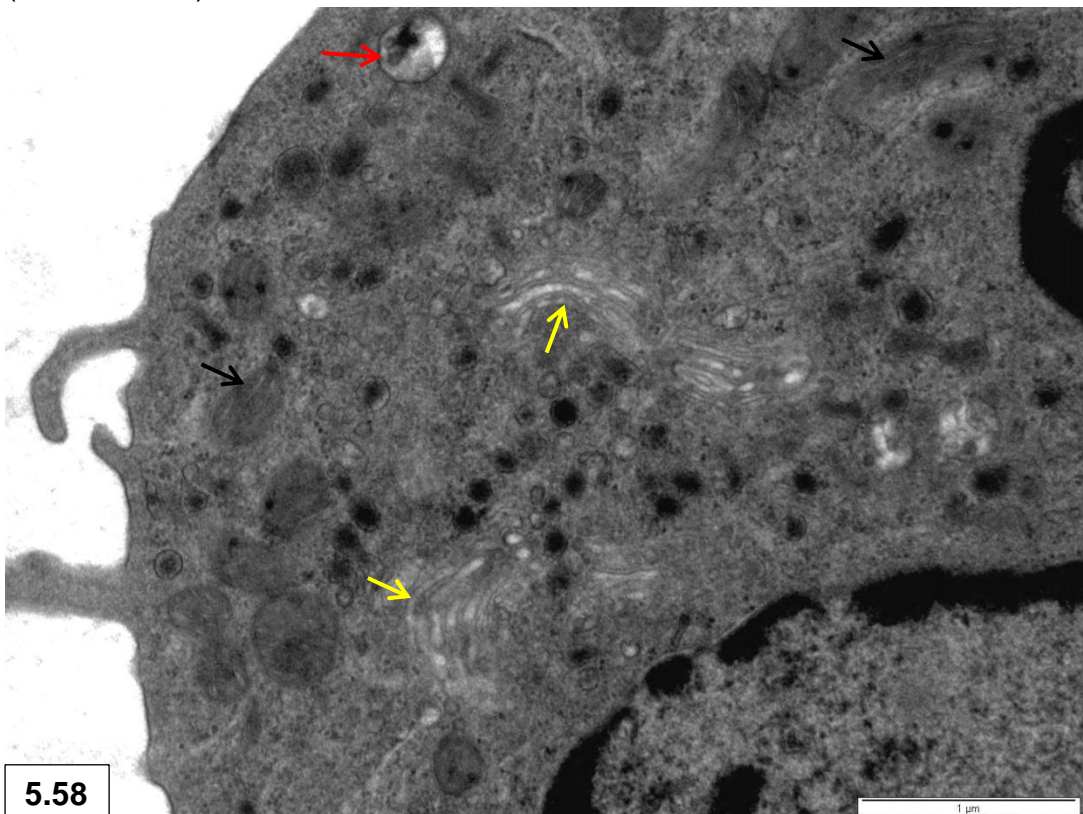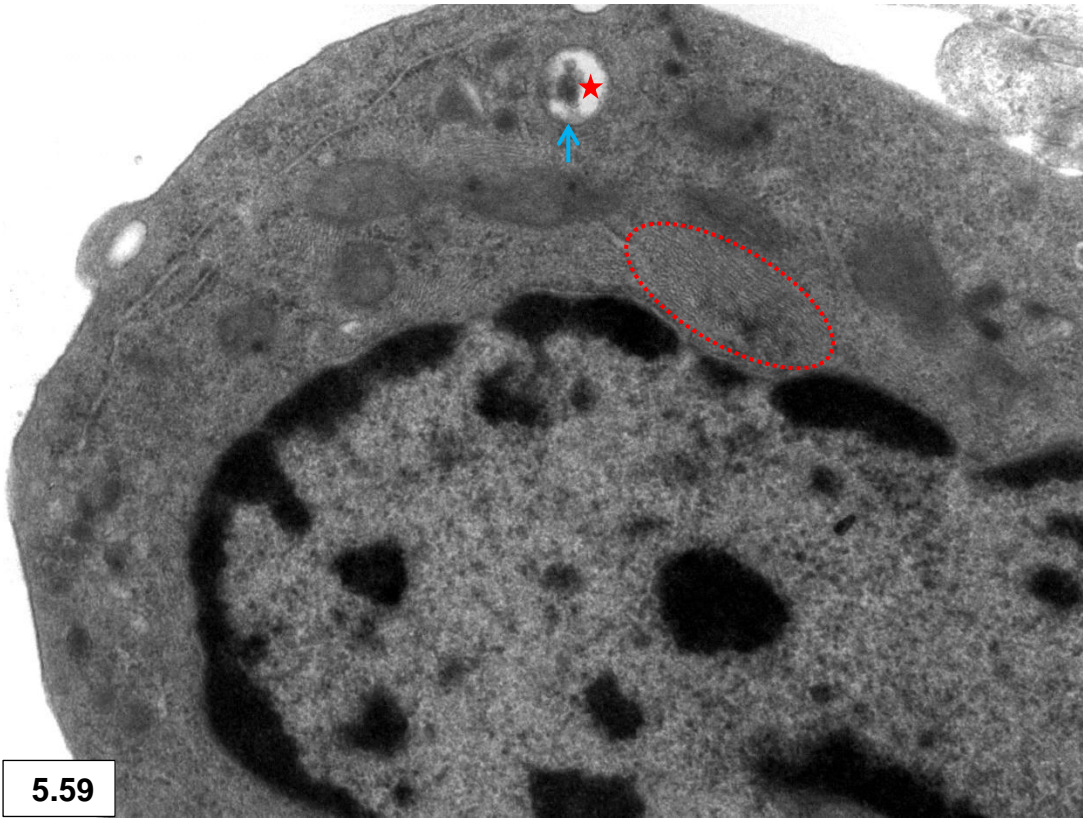
5.59

Figure 5.59 & 5.60 : Intermediate filaments (dashed circle) in pit cells. Note large membrane-bound clear vesicles (blue arrows), some with electron-dense contents (red star). Multivesicular bodies (red arrows), endocytotic vesicles (yellow arrows), lipid droplet (yellow star) and Golgi (black arrow).

5.60

112
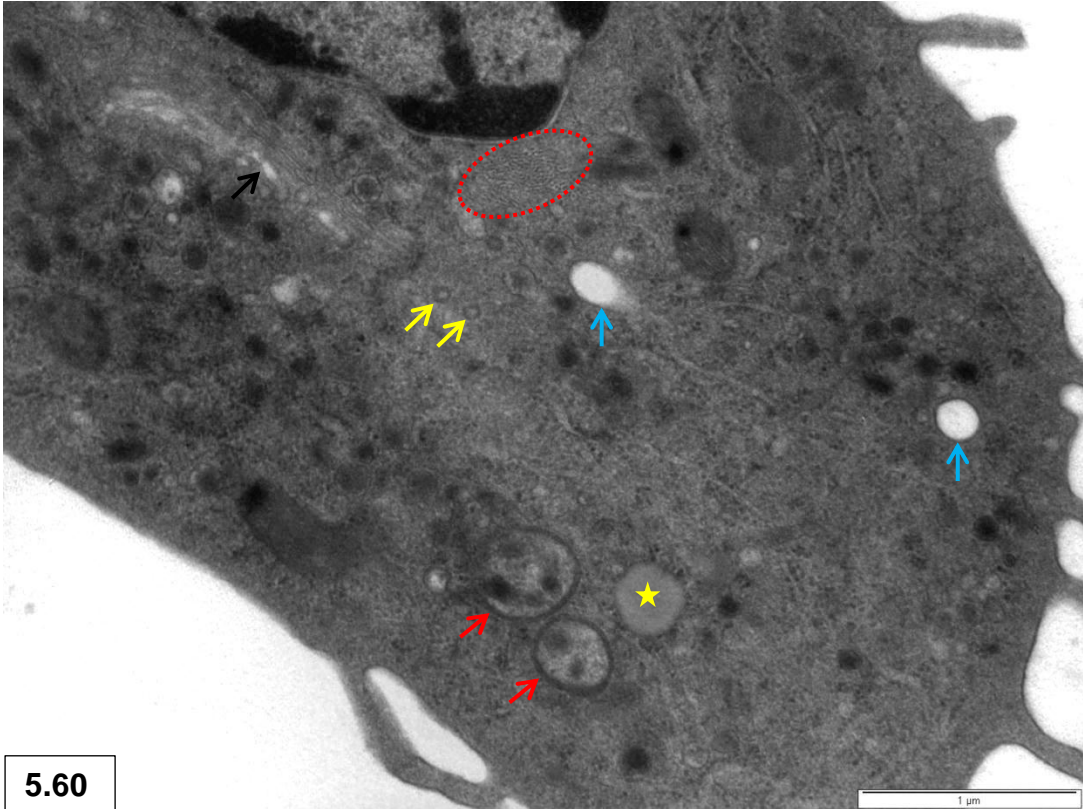
5.61

Figure 5.61 & 5.62: Contact of pit cells (**P**), containing small membrane-bound granules, with an endothelial cell (**E**) and the lamellapodia of a Kupffer cell (**K**).
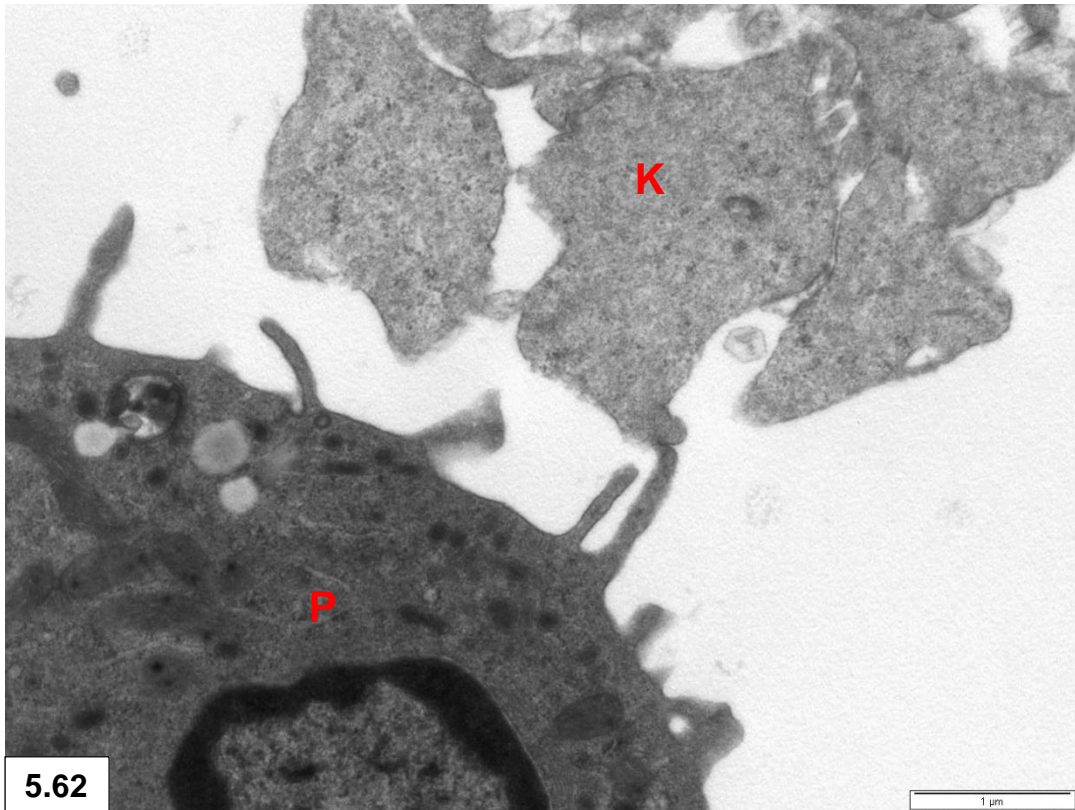
5.62
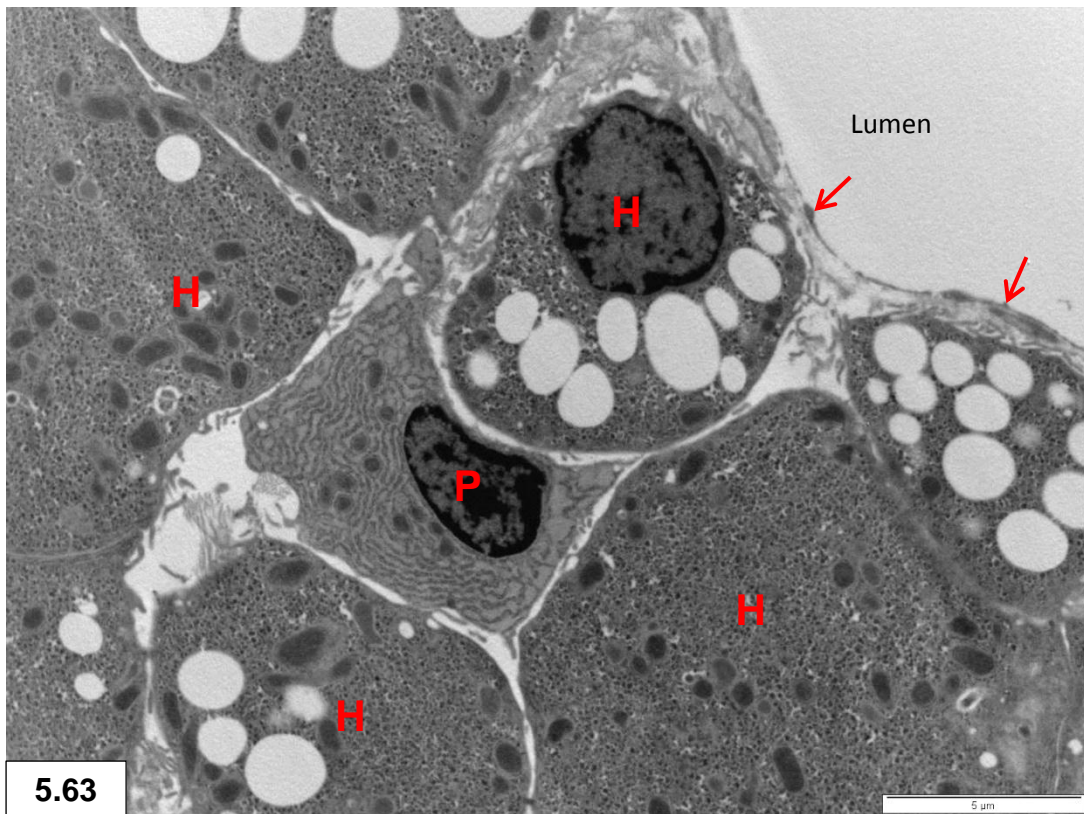
Figure 5.63: Plasma cell (**P**) present among hepatocytes (**H**). Endothelial cell (arrows).

Figure 5.64: Two thrombocytes (**T**) present in a sinusoidal lumen. Note Kupffer cell (**K**) containing tubulosomes and lipid droplets. Endothelial cell (**E**), hepatocytes (**H**), myofibroblastic cell extension (star).
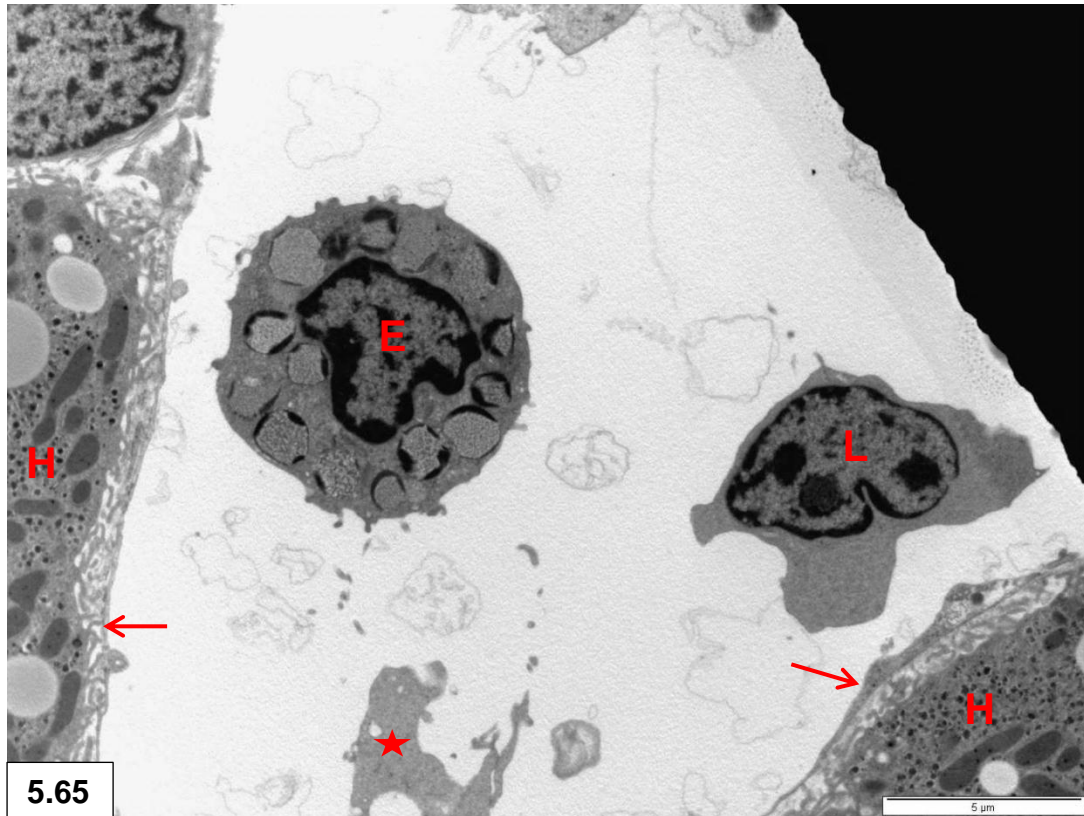
Figure 5.65: Eosinophil (**E**) & lymphocyte (**L**) present in a sinusoidal lumen. Note hepatocytes (**H**), endothelial cell extensions (arrows) and Kupffer cell lamellipodium (star).
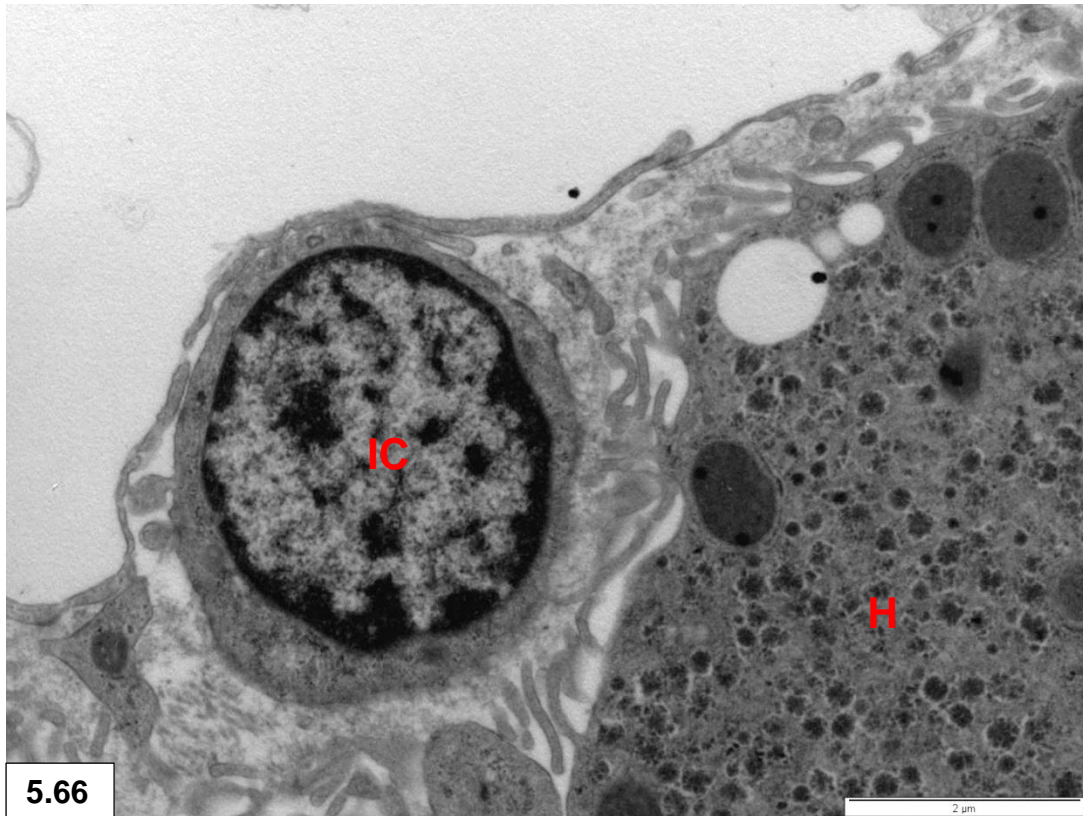
Figure 5.66 & 5.67: Intercalated cells (**IC**) with sparse organelles present in the space of Disse and in a group of hepatocytes.
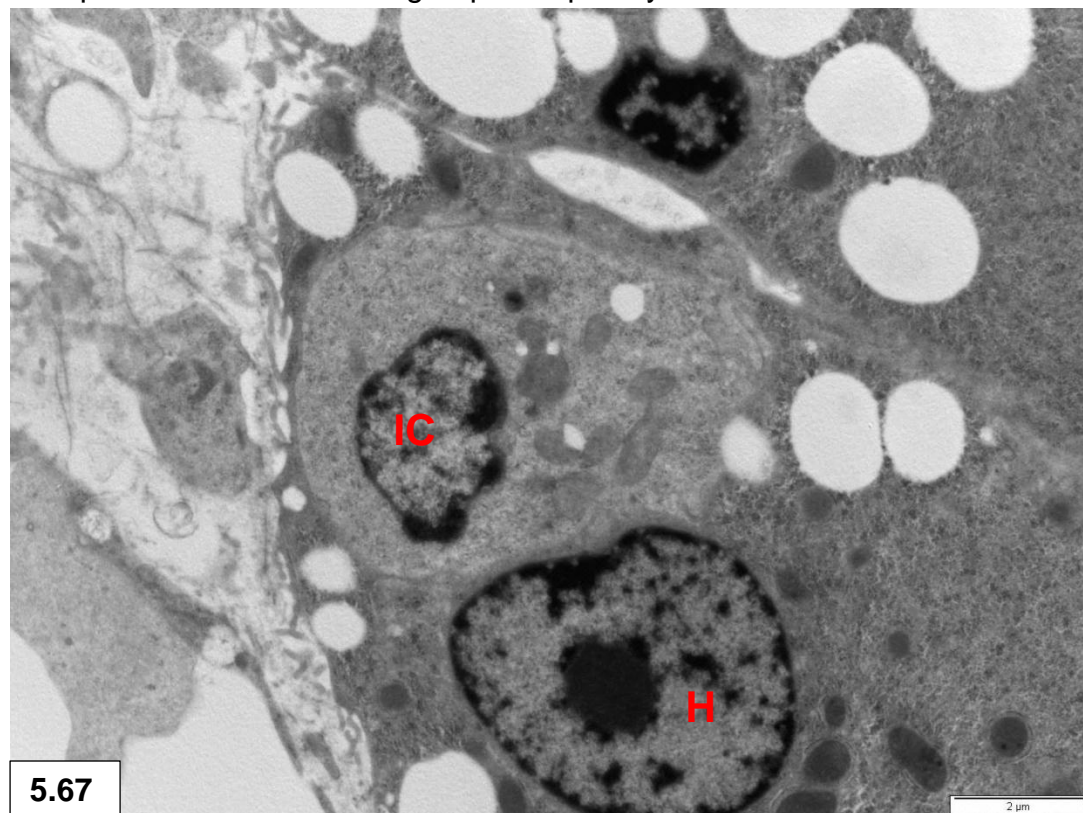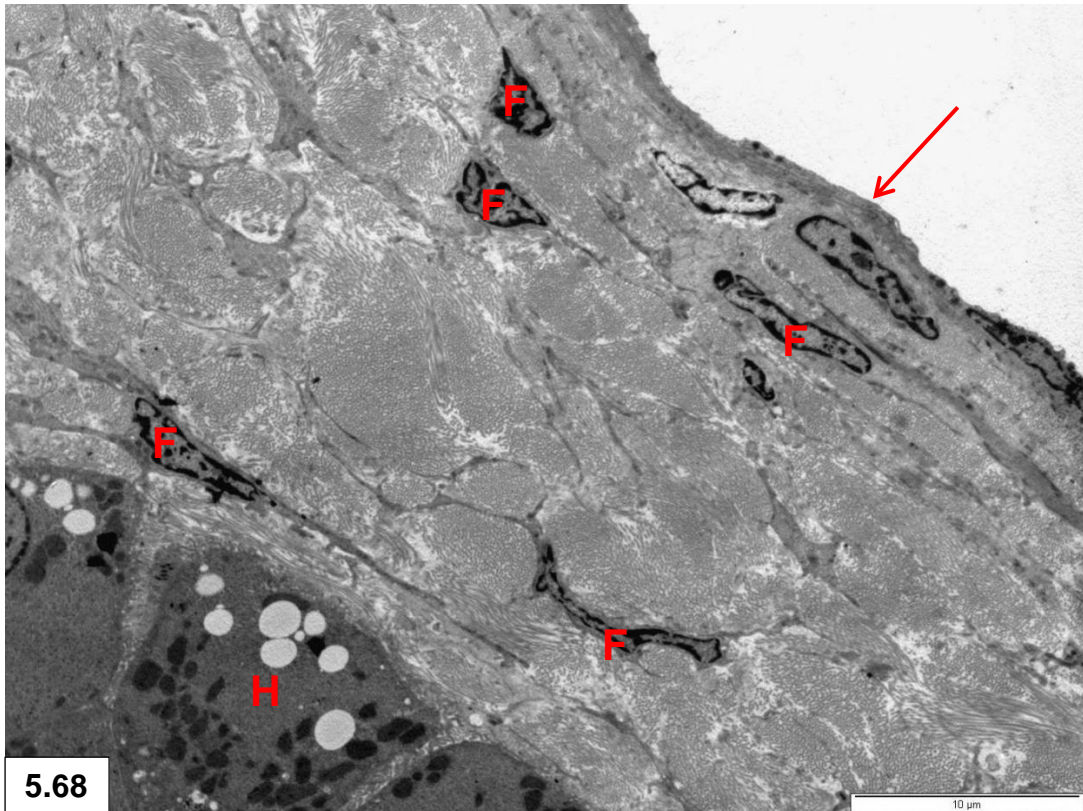
Figure 5.68: Glisson's capsule consisting of mesothelial cells (arrow) and a collagen layer containing fibroblasts (**F**). Hepatocytes (**H**).
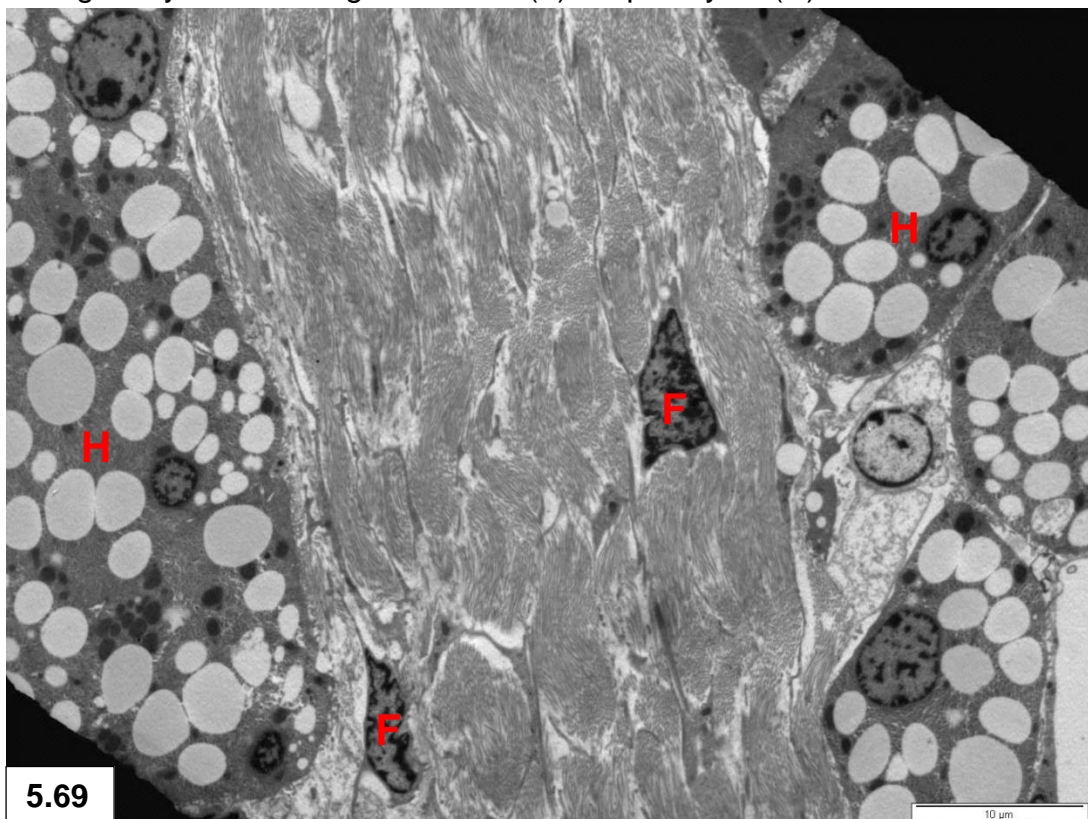
Figure 5.69: Fibrous trabecula between groups of hepatocytes.
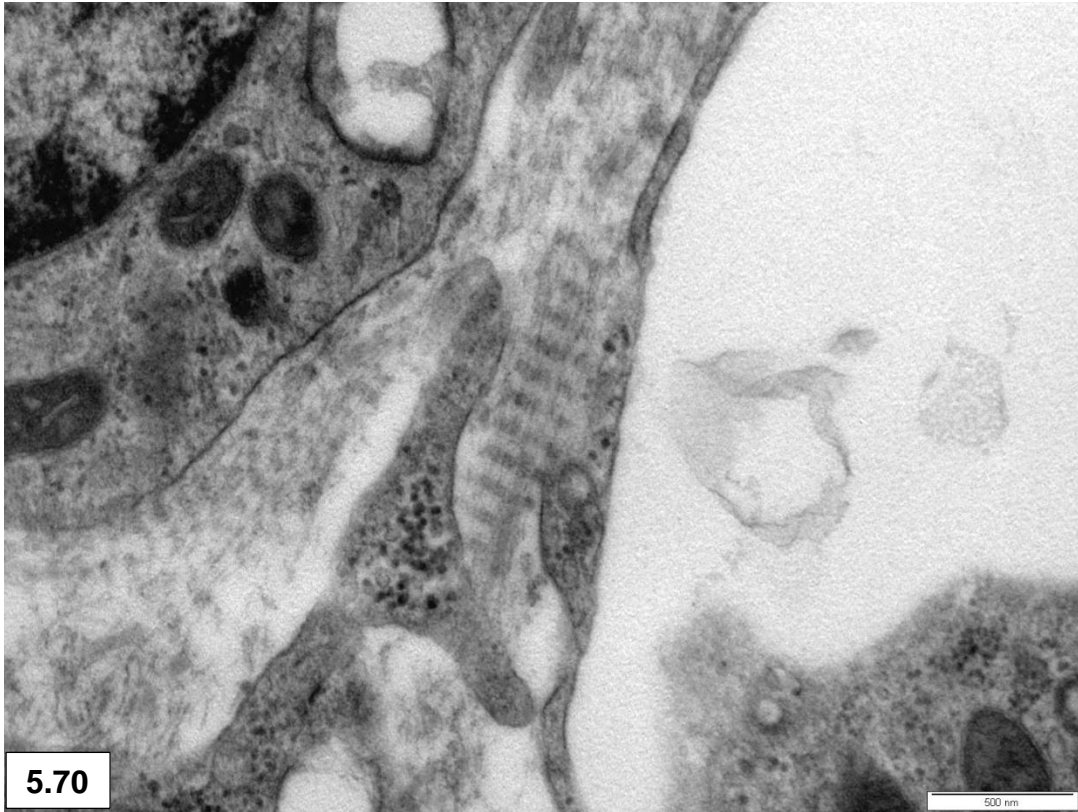
Figure 5.70 & 5.71: Long-spacing collagen fibrils in the space of Disse.
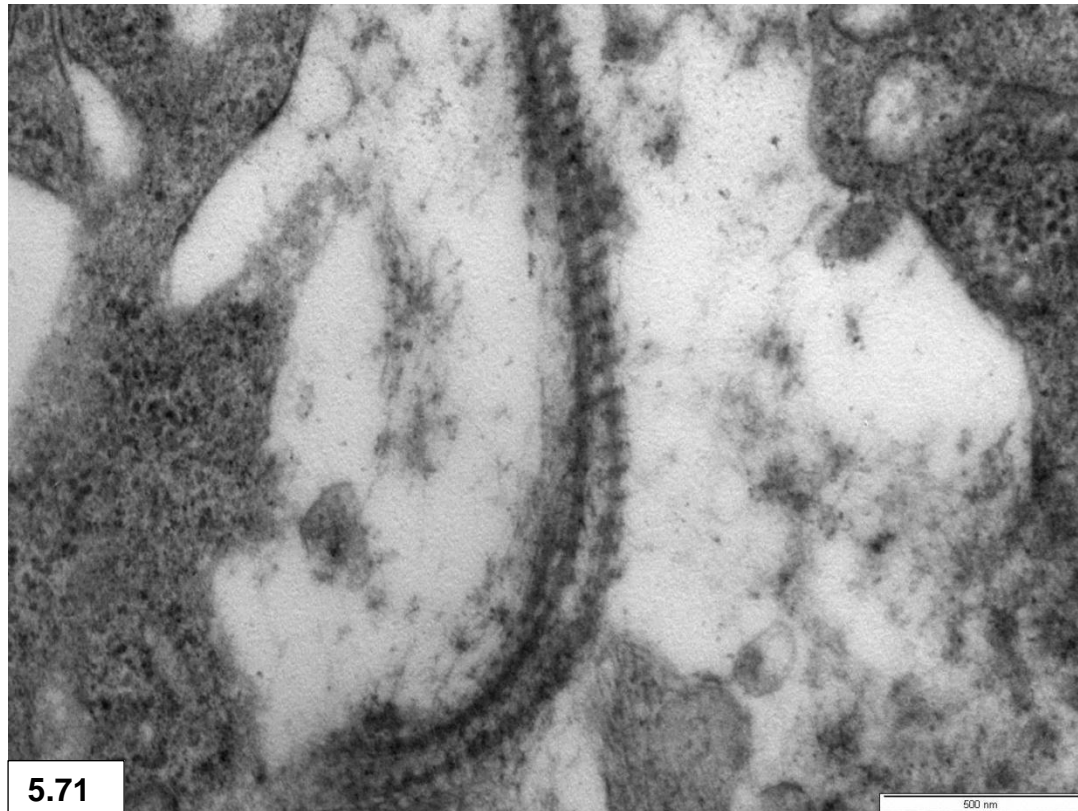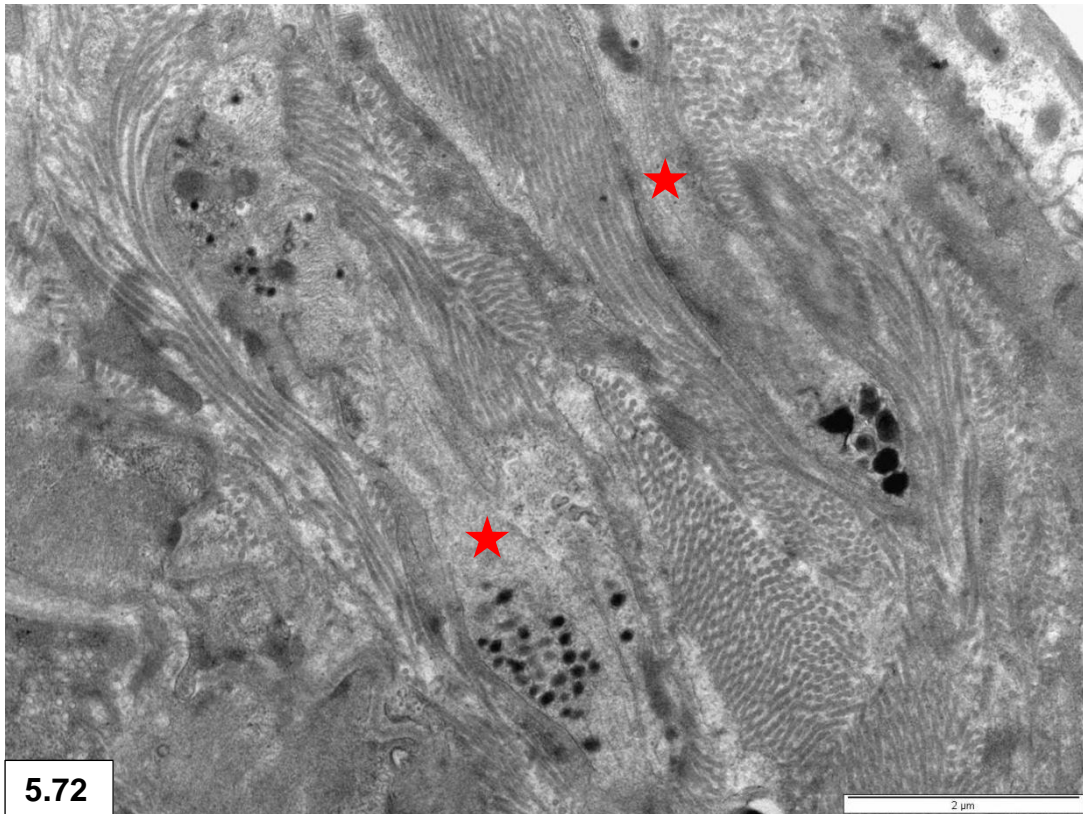
Figure 5.72 & 5.73: Intrahepatic non-myelinated nerves (stars). Note neurosecretory granules, microtubules, mitochondria, intermediate filaments and lysosomes.
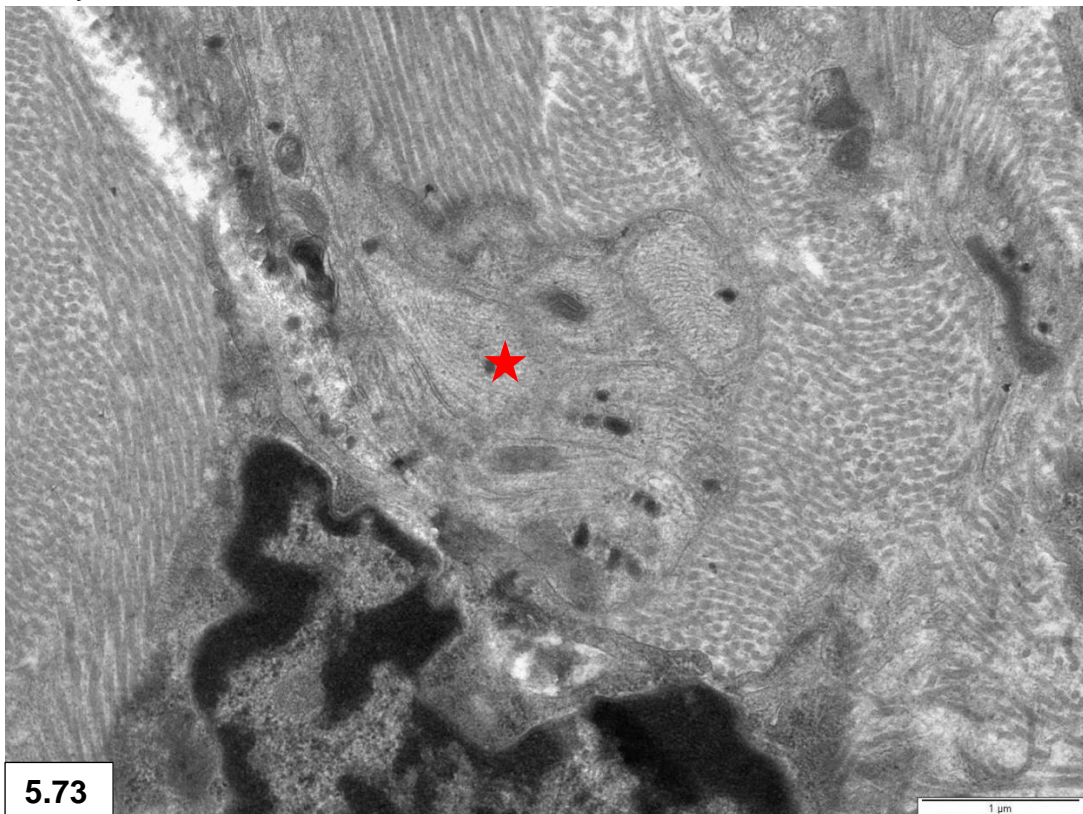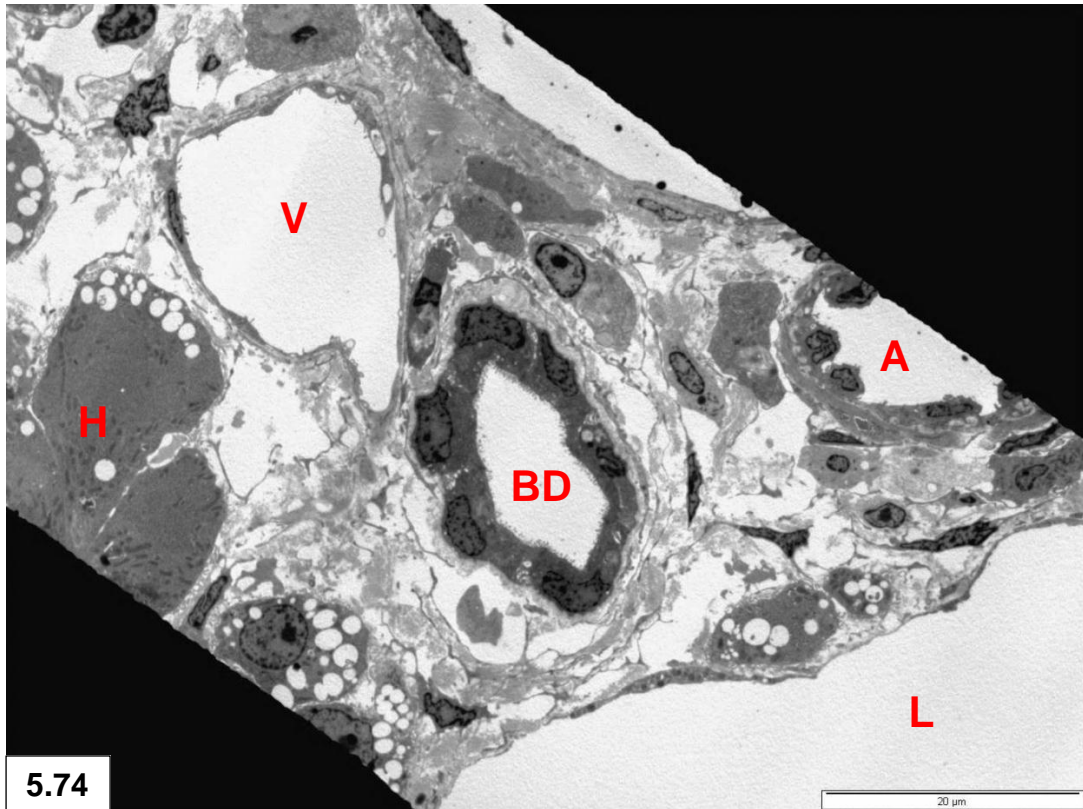
Figure 5.74 & 5.75: Portal tracts consisting of a portal vein (**V**), hepatic artery (**A**) and bile duct (**BD**). Lymphatic vessel (**L**), hepatocytes (**H**). Note collagen fibrils, fibroblasts, lymphocytes and plasma cells in the surrounding stroma.
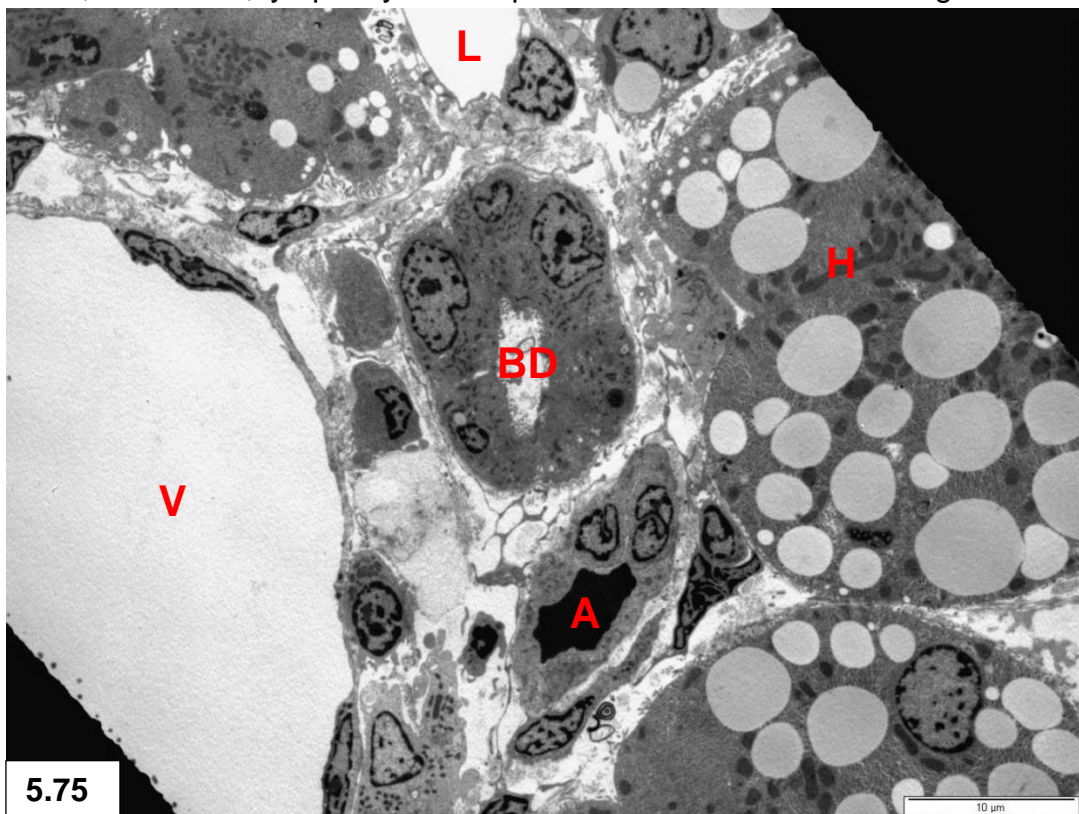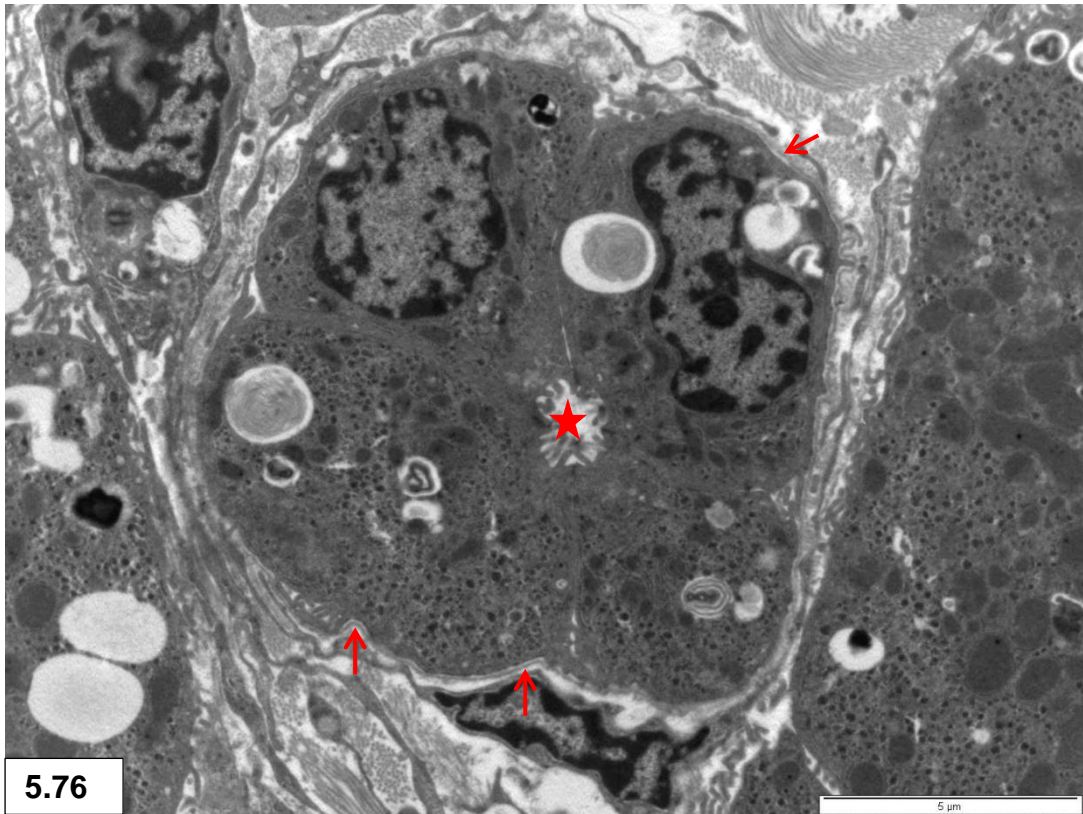
Figure 5.76: Bile duct surrounded by a basal lamina (arrows). Ductal lumen (star).
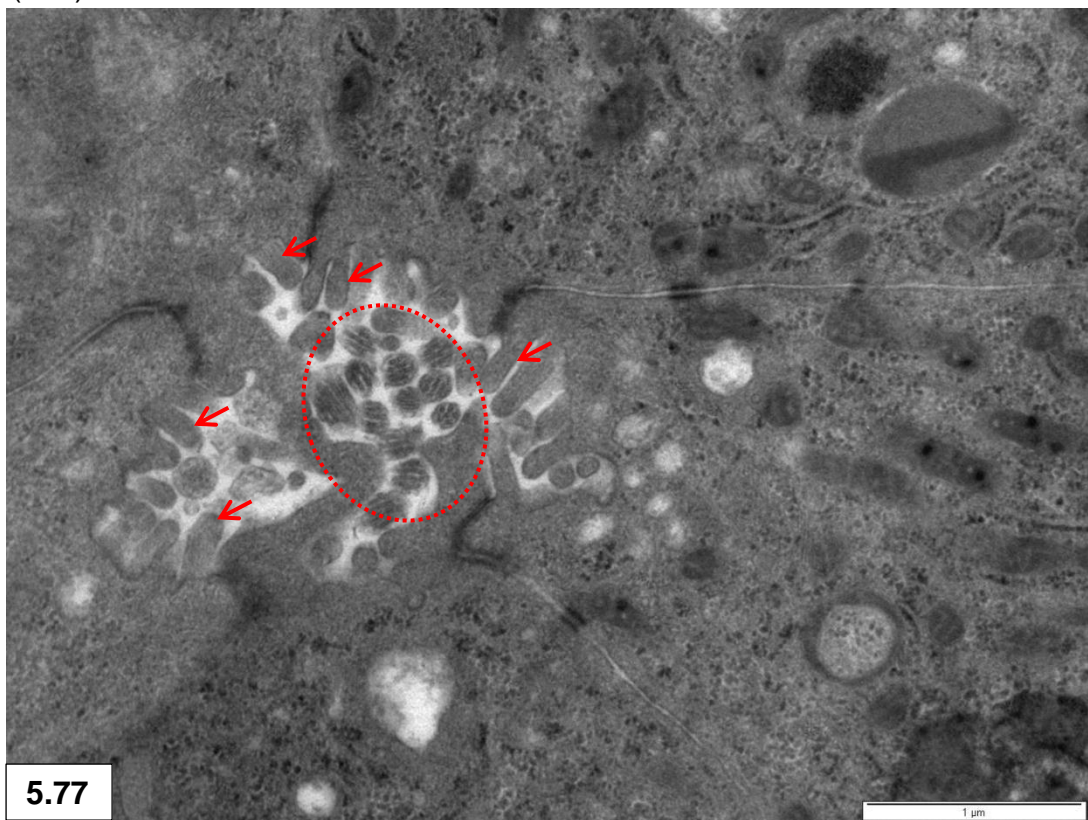
Figure 5.77: Higher magnification of the apical cell surfaces with junctional complexes of a bile duct. Note microvilli (arrows) and cilia (dashed circle) containing microtubules in the ductal lumen.

Figure 5.78: Interdigitations (dashed circles) between the lateral membranes of a bile duct. Note basal lamina (arrows).
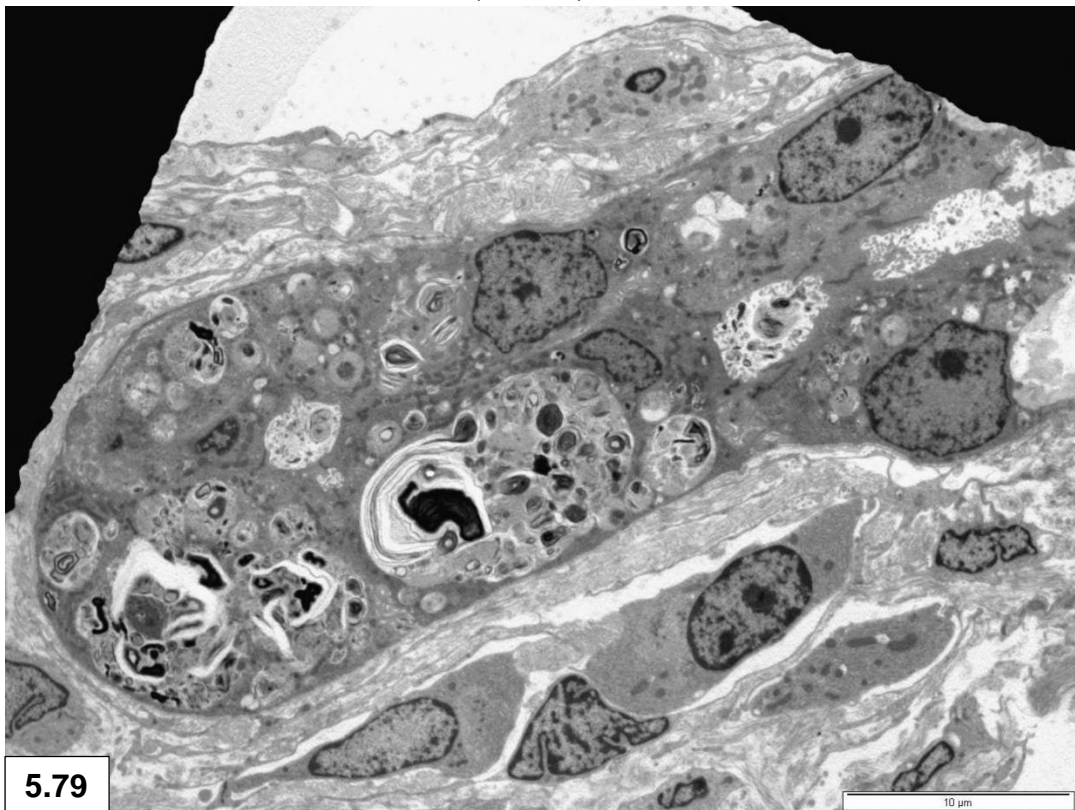
Figure 5.79: Concretions of bile pigment present in biliary cells.
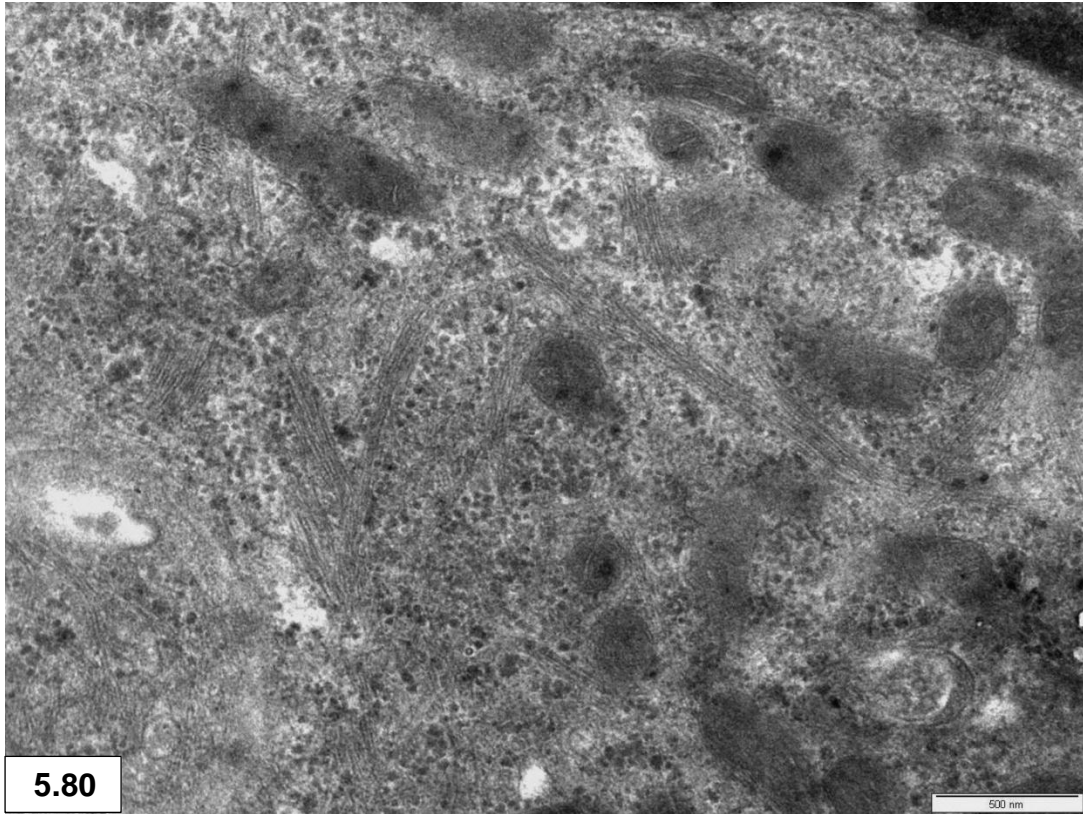
Figure 5.80: Prominent bundles of intermediate filaments in biliary cells.
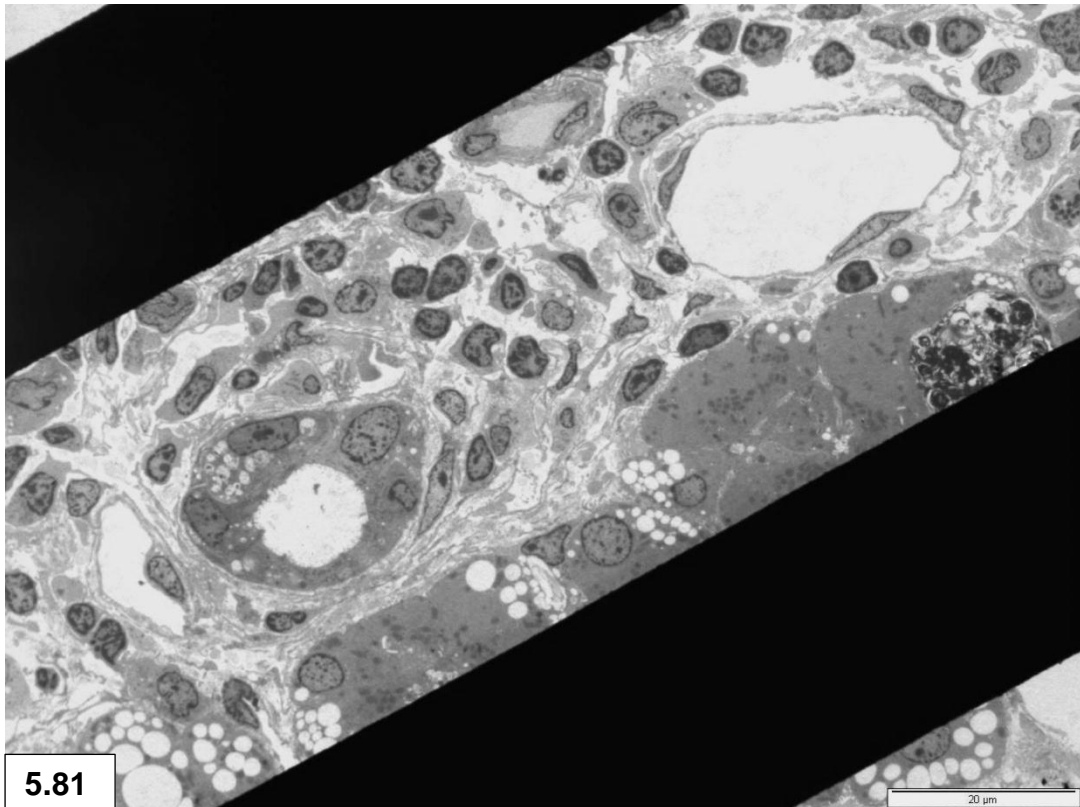
Figure 5.81 & 5.82: Collections of lymphocytes were occasionally seen in the portal areas.
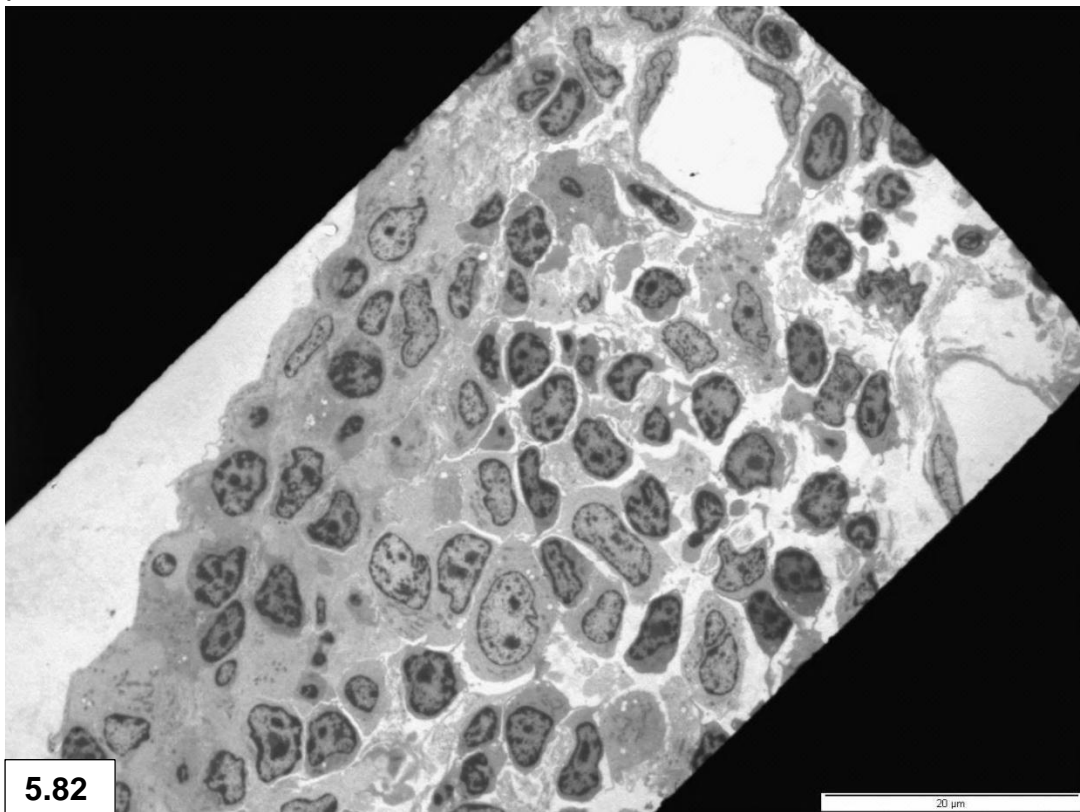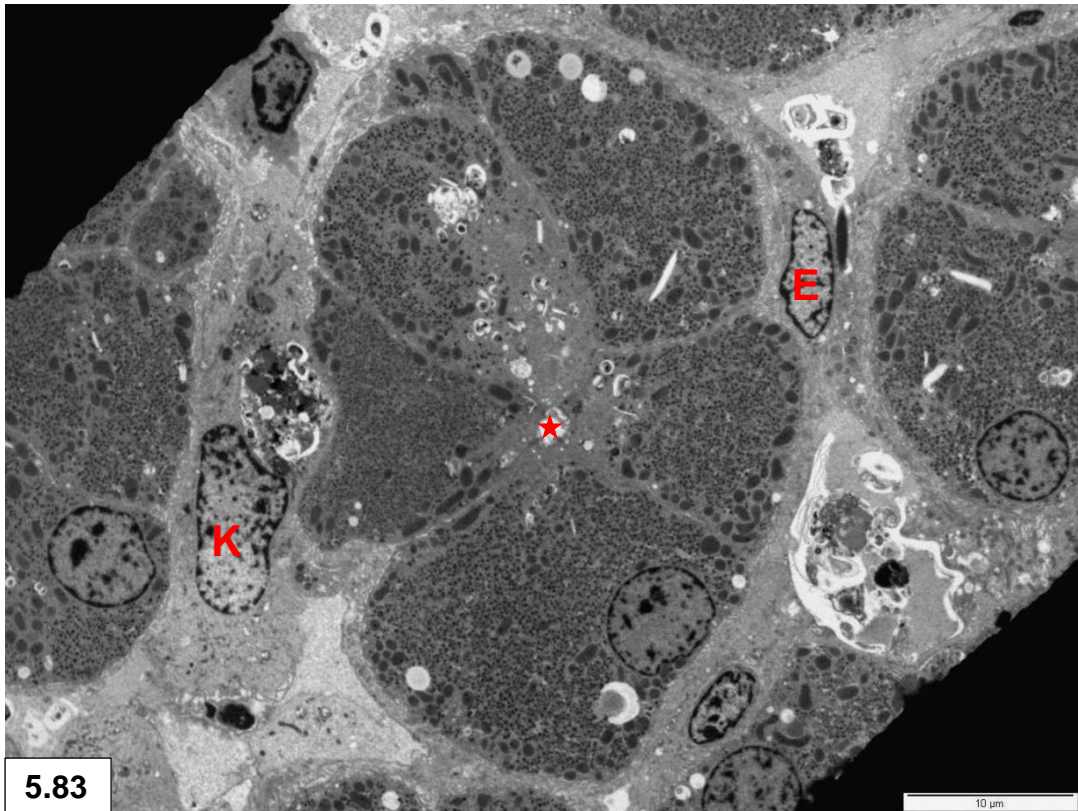
Figure 5.83: Isthmus – A group of hepatocytes with a central bile canaliculus (star) surrounded by a Kupffer cell (**K**) and an endothelial cell (**E**).
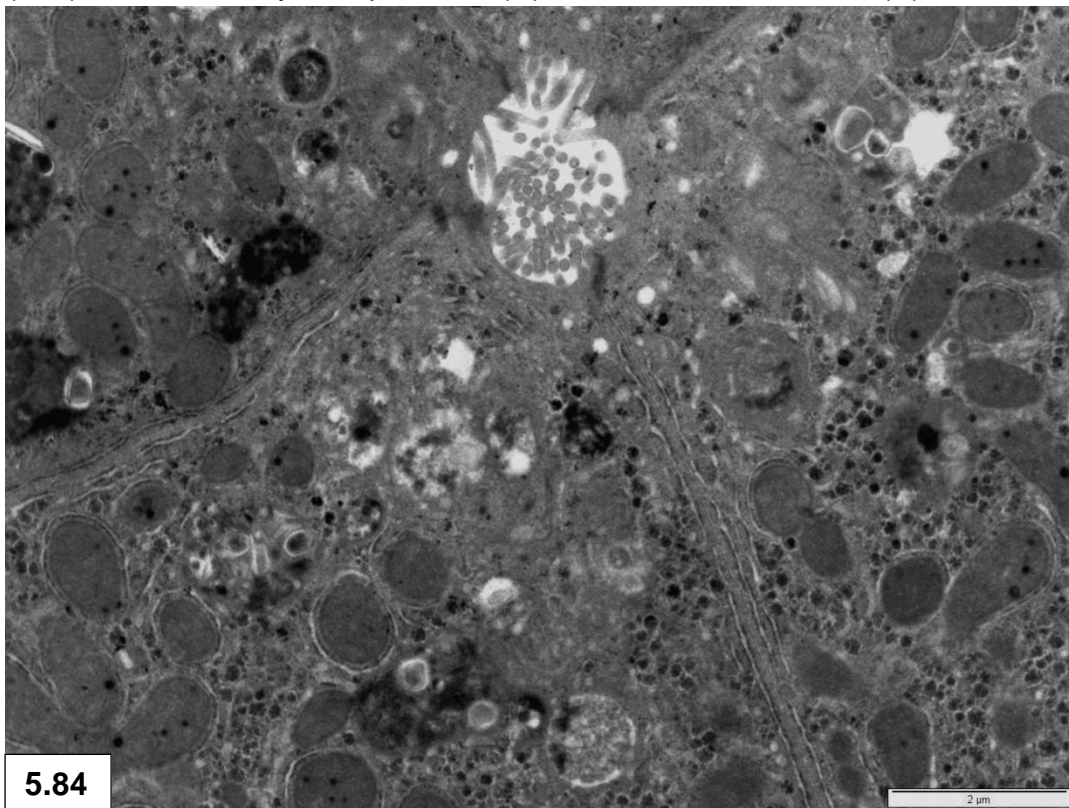
Figure 5.84: Isthmus - Bile canaliculus forming the lumen of the tubular hepatocyte cords.
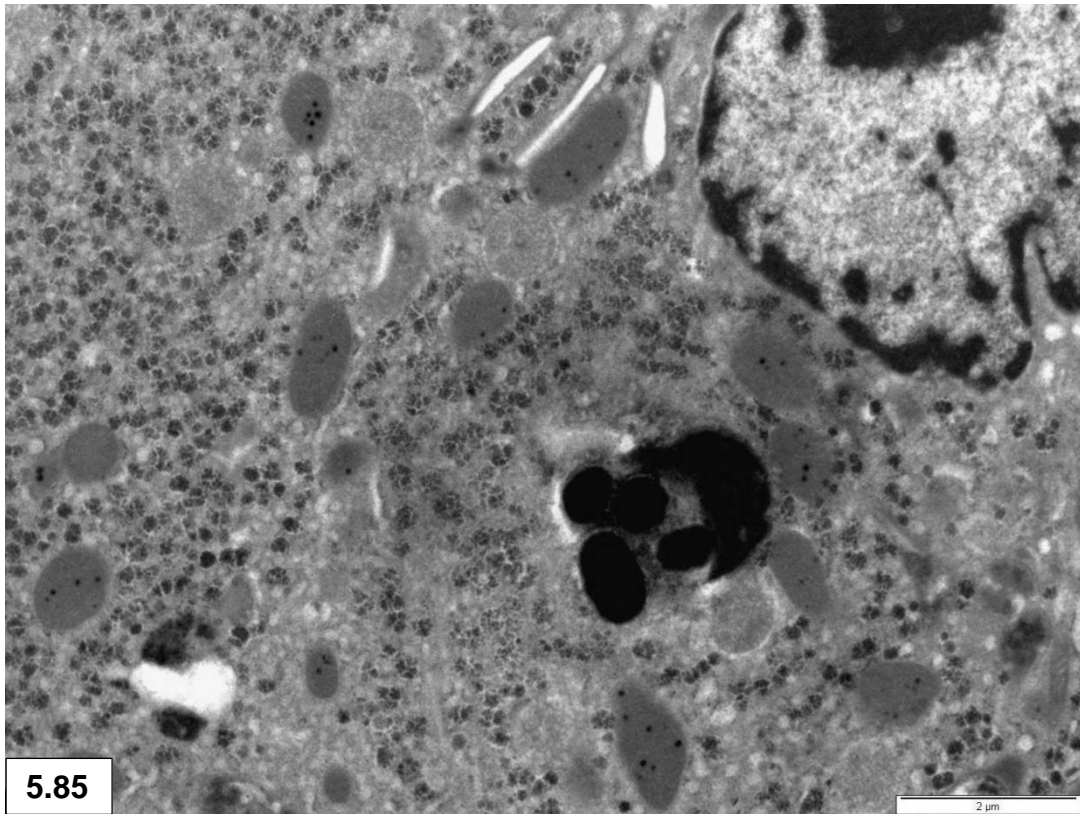
Figure 5.85: Melanin granules in a hepatocyte of the isthmus.
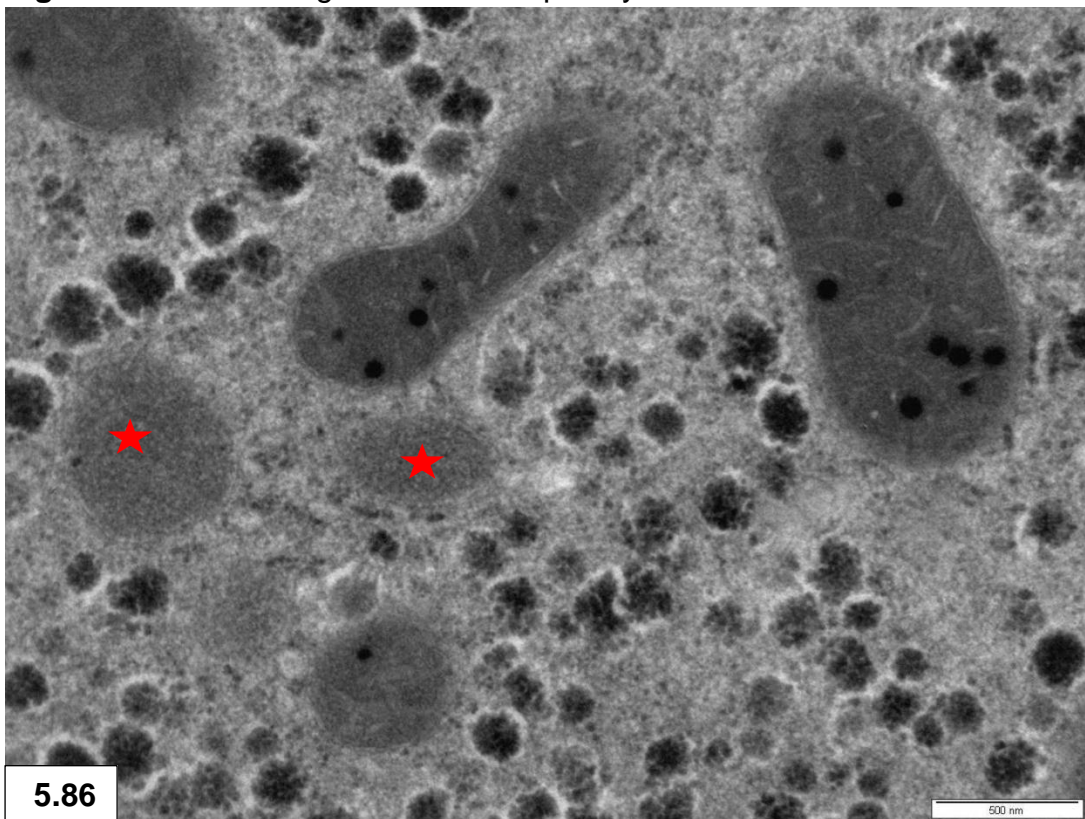
Figure 5.86: Peroxisomes in hepatocyte (stars) of the isthmus. Mitochondria with matrix granules and glycogen rosettes are also present.
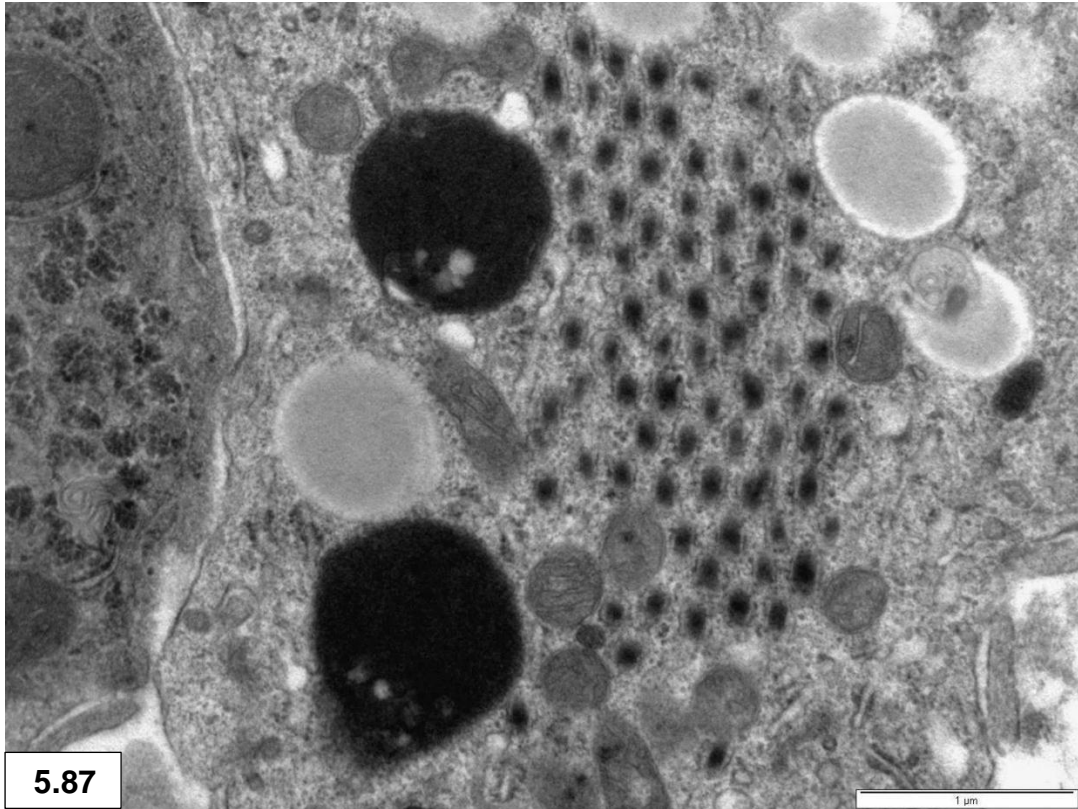
Figure 5.87: A group of tubulosomes in transverse profile in a Kupffer cell of the isthmus.
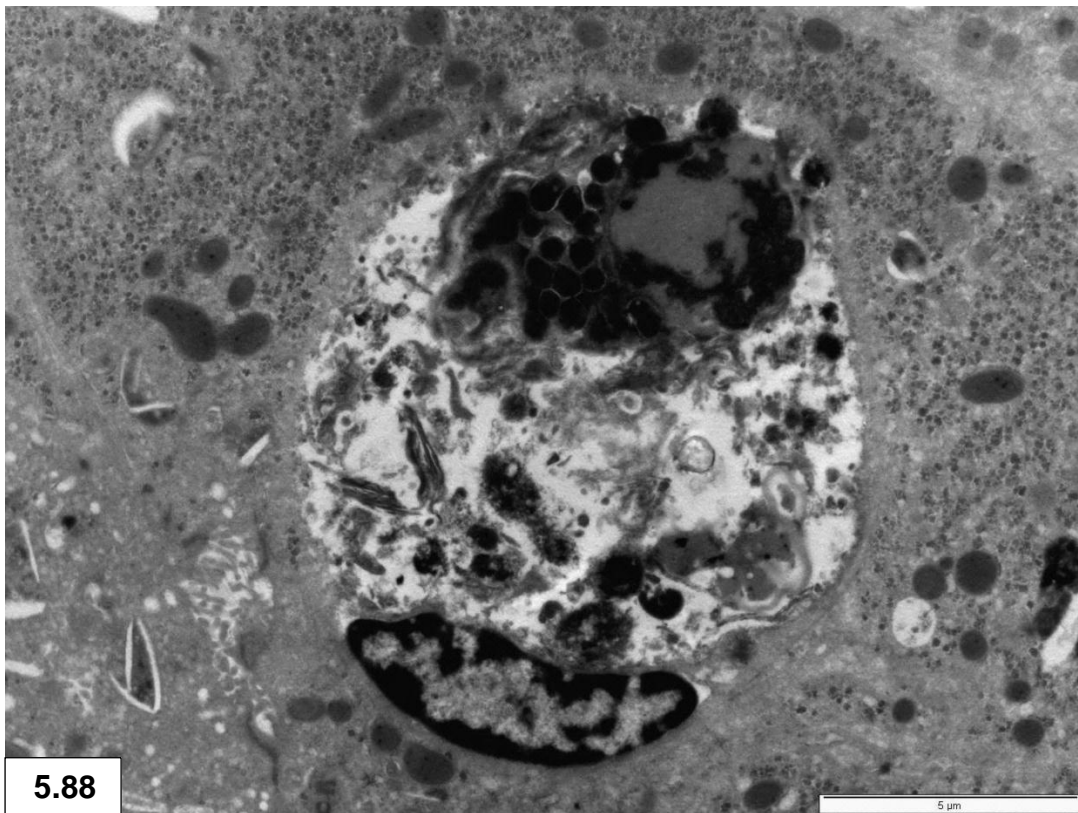
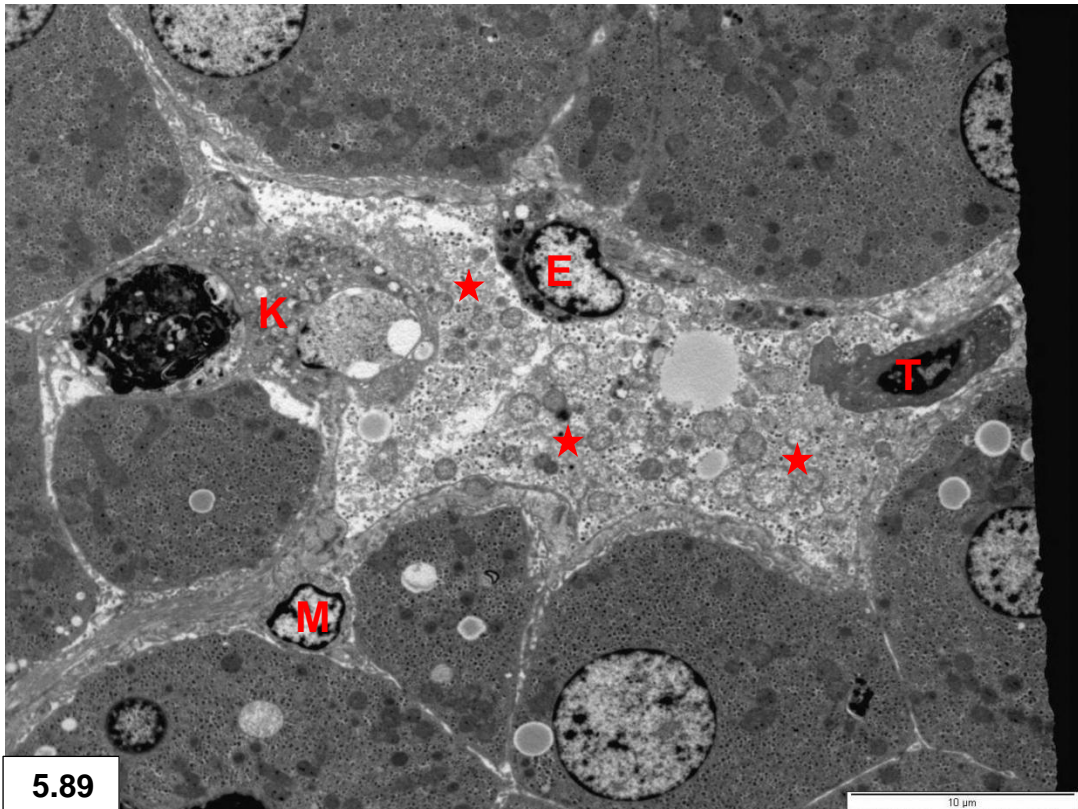**Figure 5.88:** A pigmented cell present in a group of hepatocytes of the isthmus.

Figure 5.89: Isthmus - sinusoid with a thrombocyte (**T**), Kupffer cell (**K**) and endothelial cell (**E**). Note cellular debris (stars) in lumen. Myofibroblastic cell (**M**).
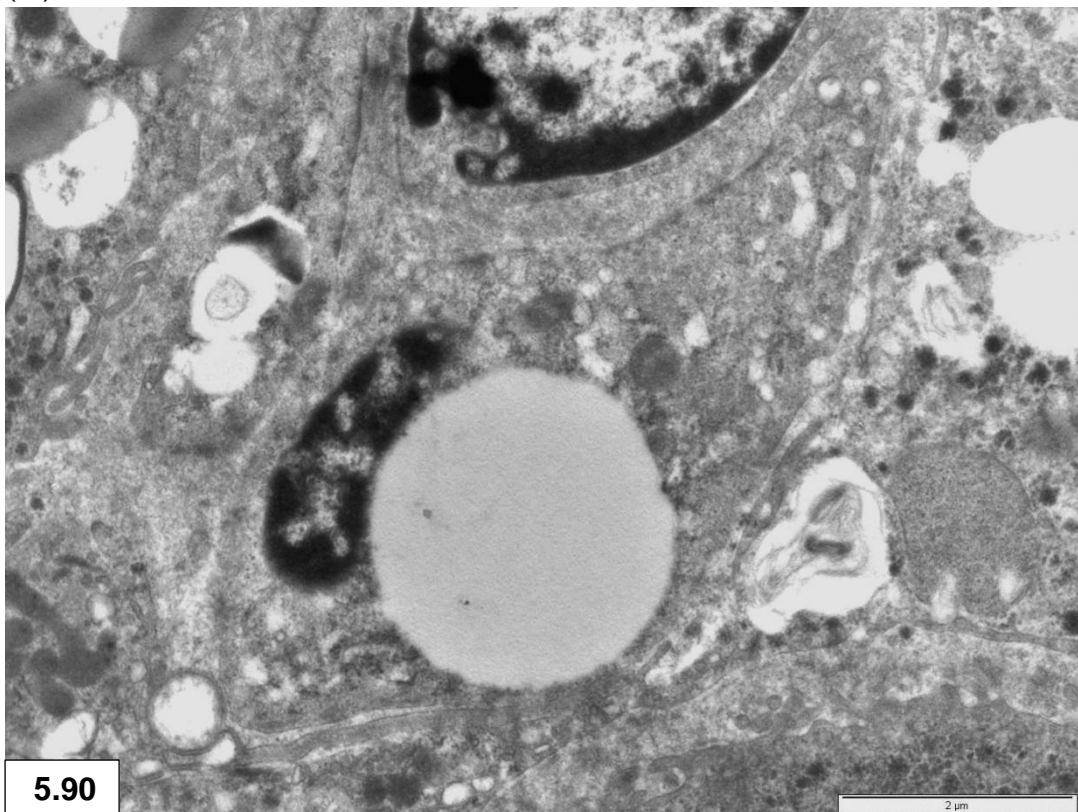

Figure 5.90: Isthmus - stellate cell containing a lipid droplet.
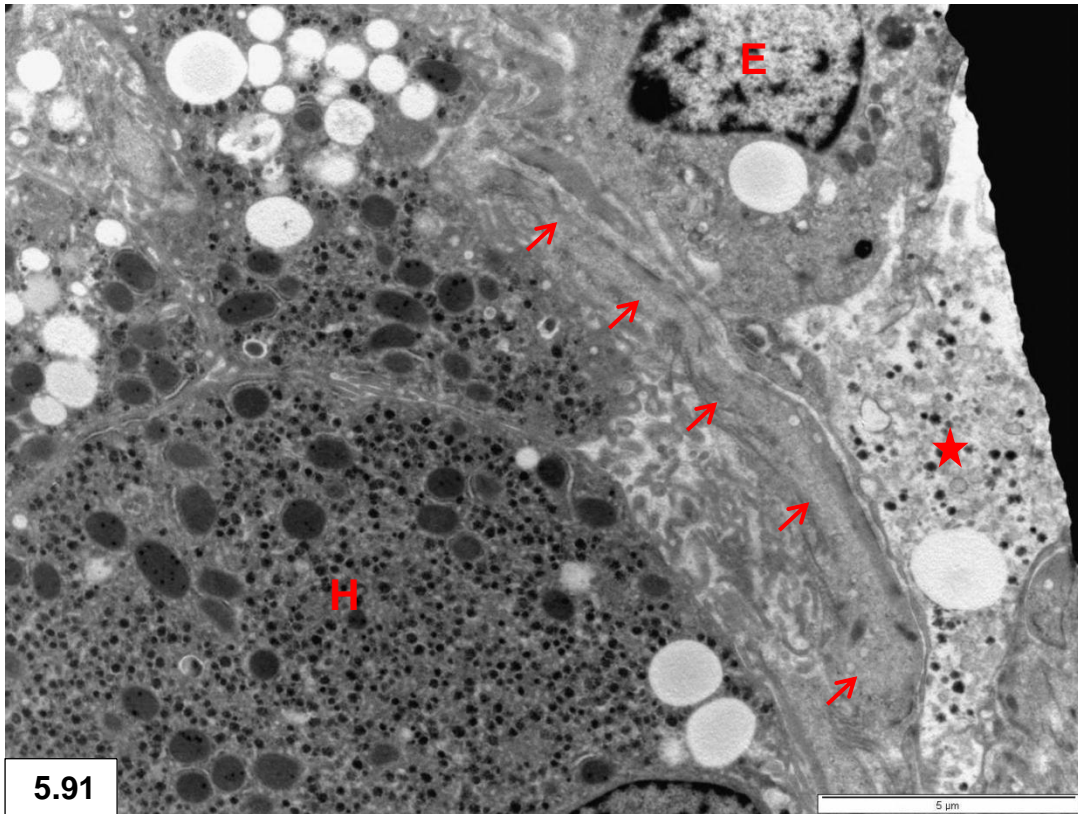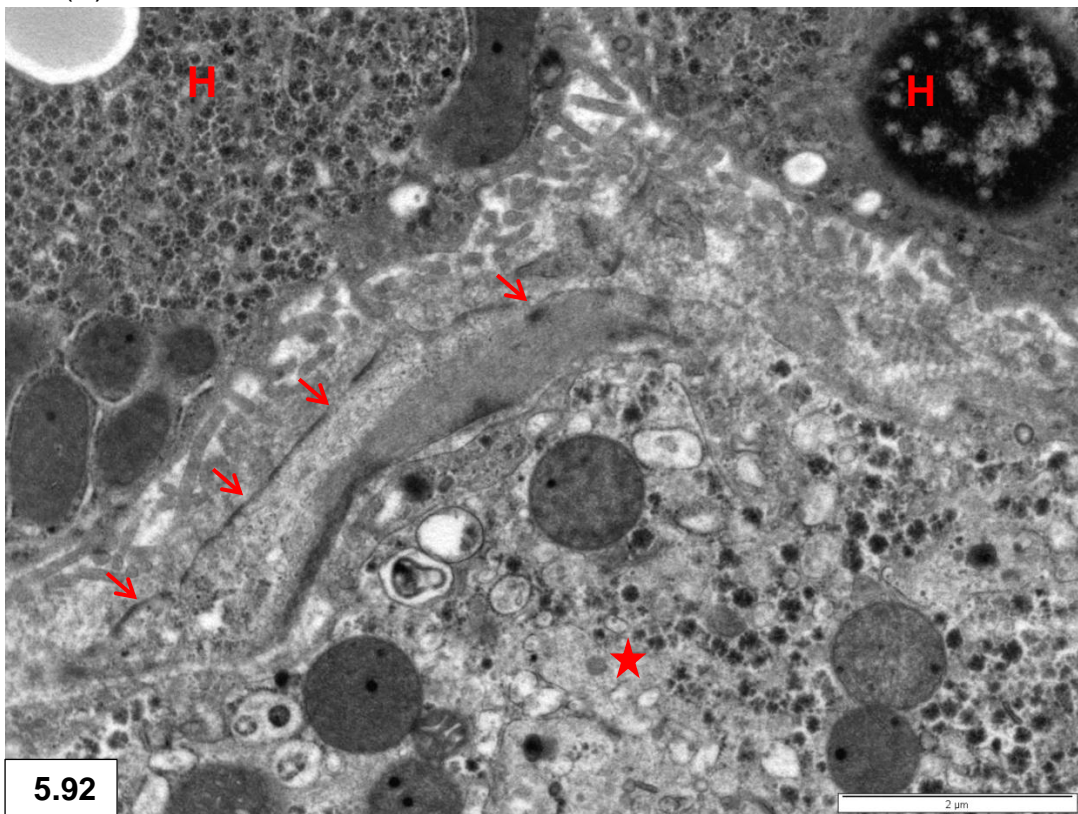
Figure 5.91 & 5.92 : Myofibroblastic cytoplasmic extension (arrows) in the space of Disse. Note cellular debris in lumen (star). Hepatocyte (**H**), endothelial cell (**E**).
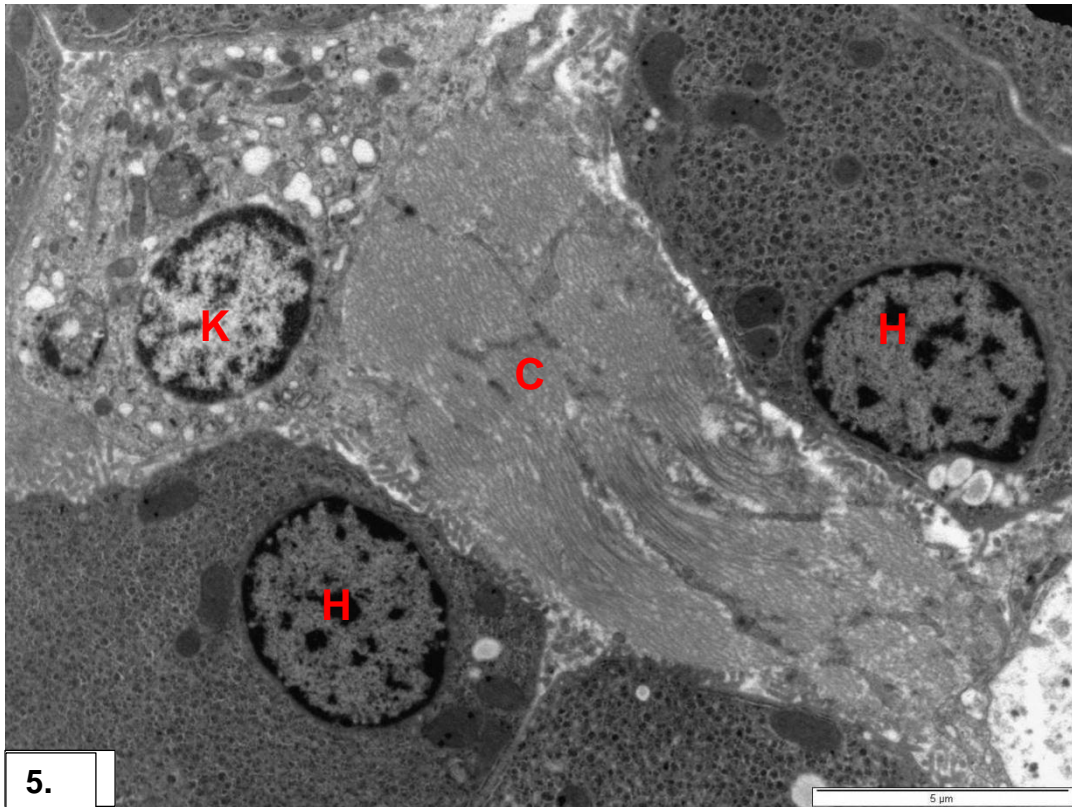
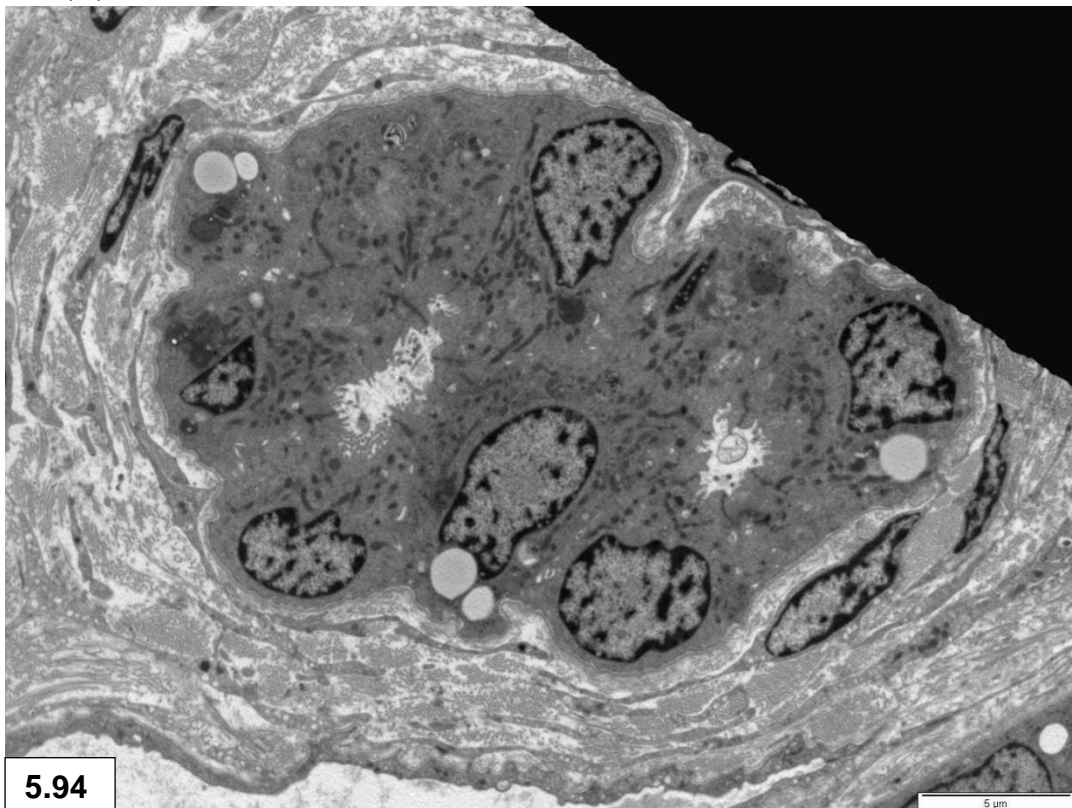**Figure 5.93:** Isthmus - collagen trabecula (**C**)between hepatocytes (**H**). Kupffer cell (**K**).

Figure 5.94: Bile duct surrounded by collagenous stroma in the isthmus.
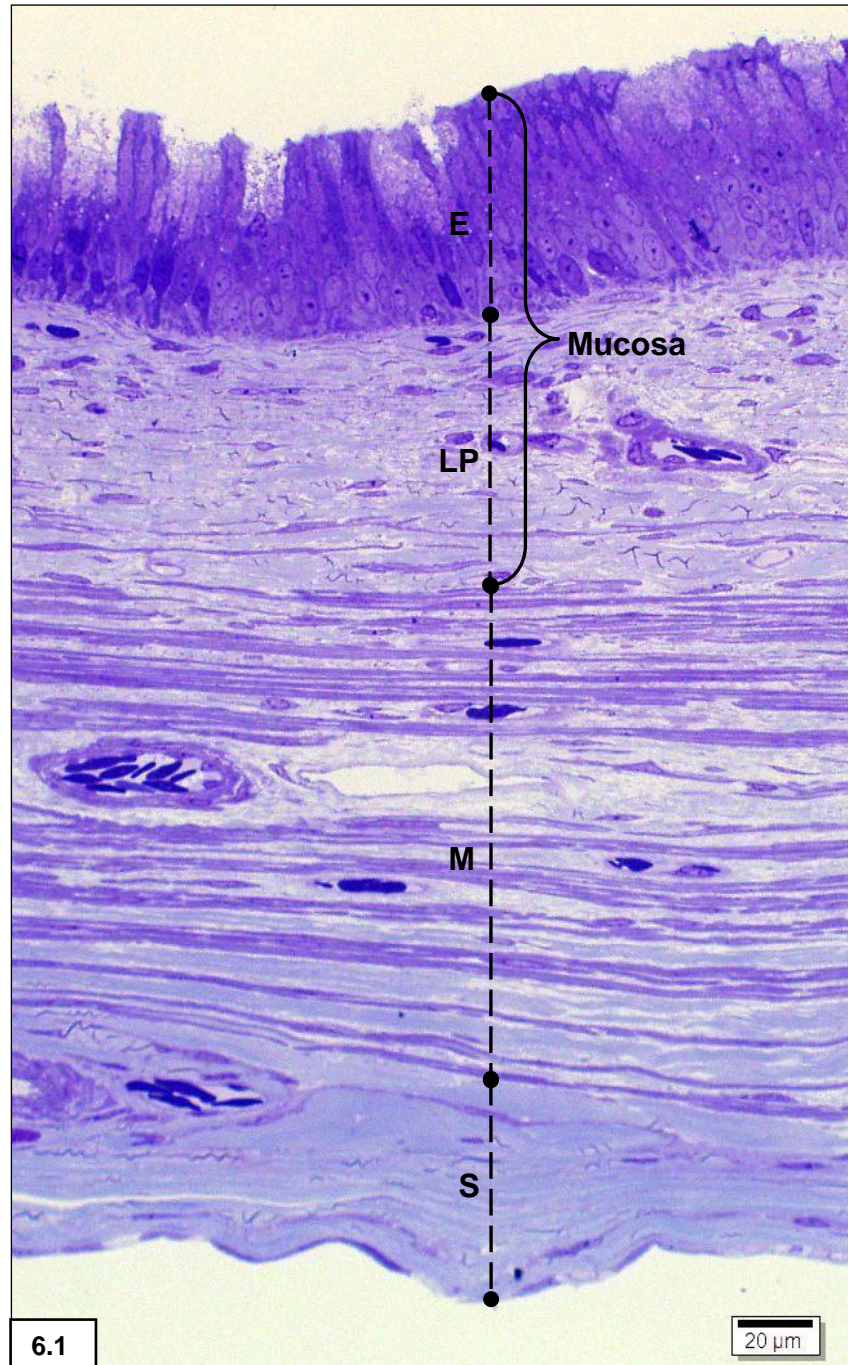
Figure 6.1: Toluidine blue (TB) resin section illustrating the full-thickness of the gallbladder wall: pseudostratified columnarv epithelium (**E**), *lamina propria* (**LP**)*, muscularis externa* (**M**) and serosa including the subserosa (**S**).
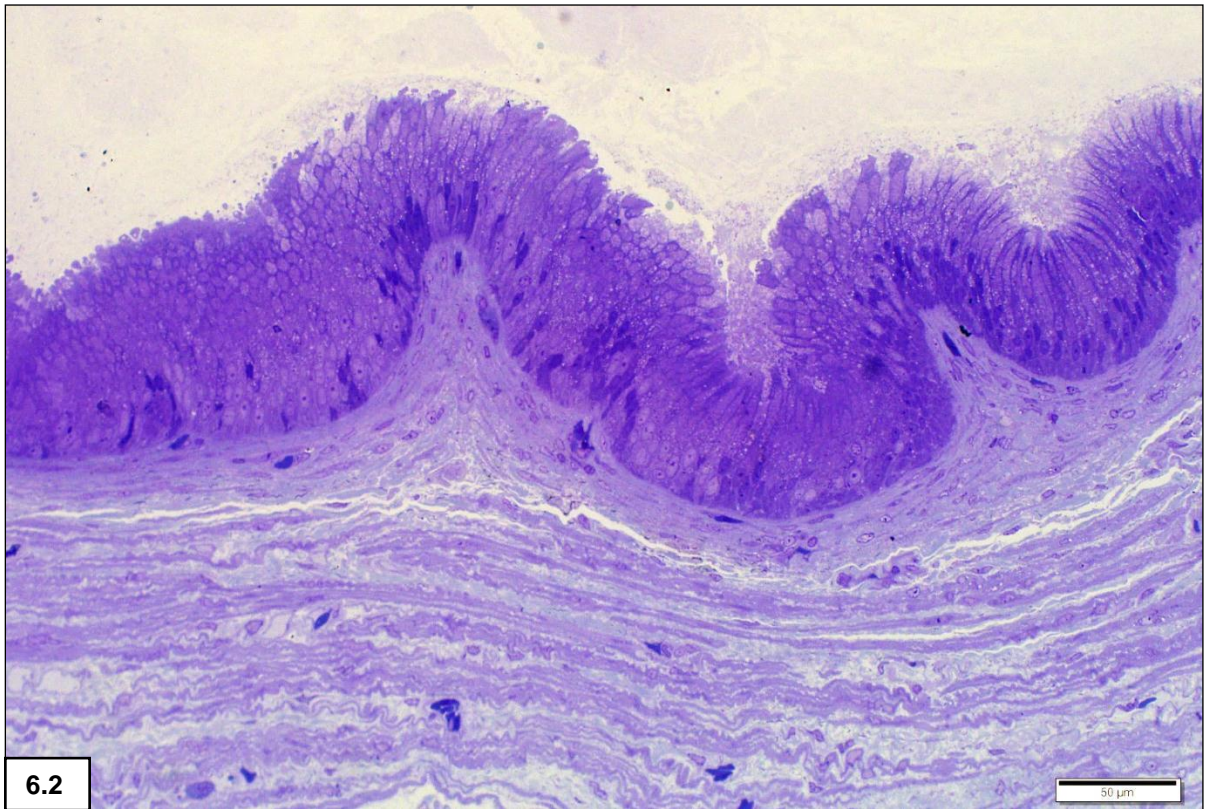
Figure 6.2: Pseudostratified columnar epithelium of the gallbladder mucosa showing irregular shallow folding. TB.
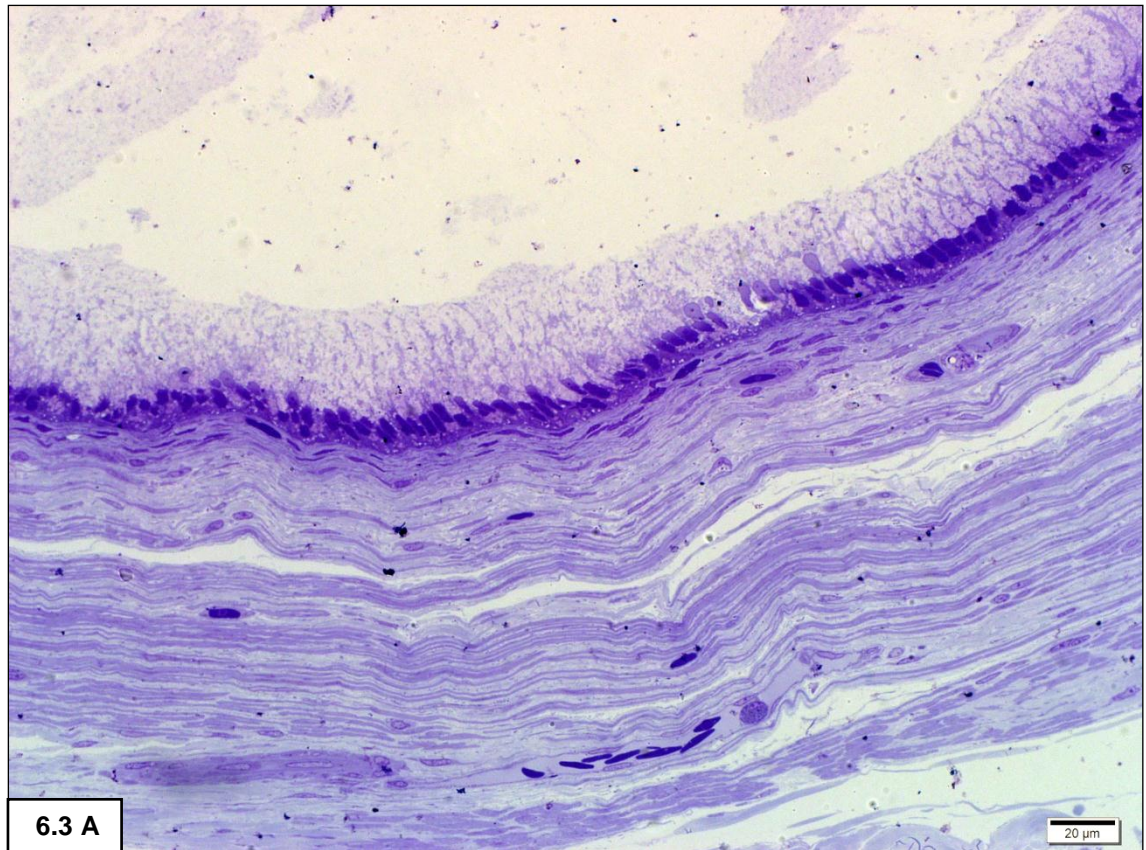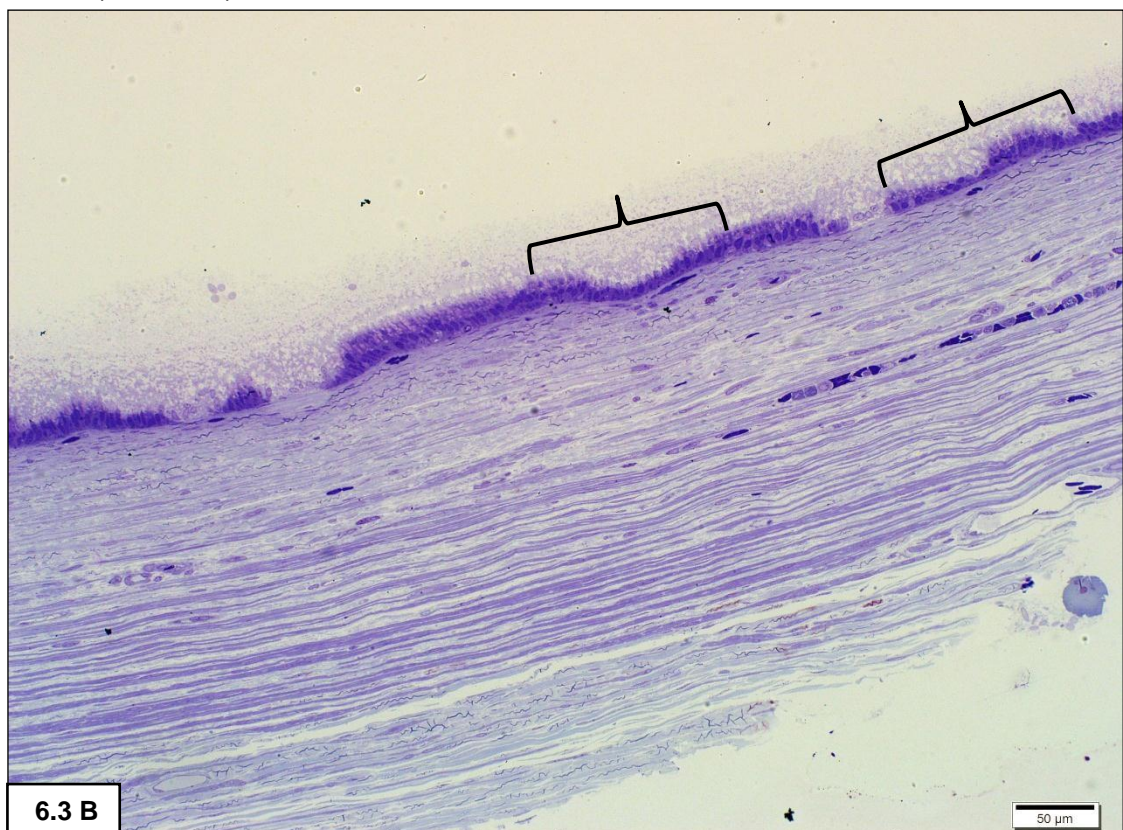
Figure 6.3 A: Putative simple columnar epithelium. TB.
B: Apparent merging of simple into pseudostratified columnar epithelium in two areas (brackets).TB.
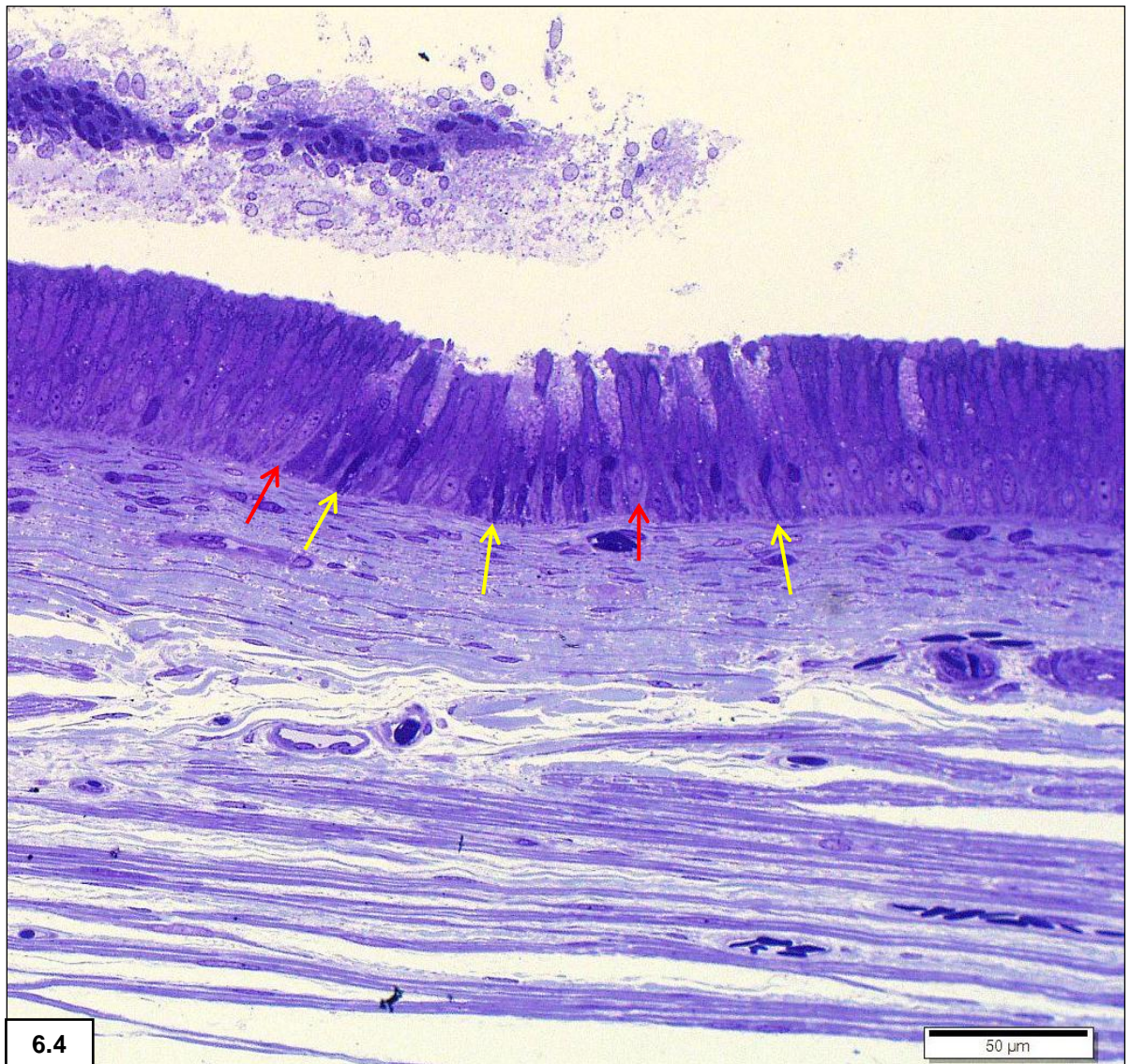
Figure 6.4: Pseudostratified columnar epithelium showing dark (yellow arrows) and light cells (red arrows). Note cellular debris in lumen. TB.

Figure 6.5: Slender goblet cells showing a PAS-positive staining reaction for carbohydrates in the apical and basal epithelial cytoplasm.

Figure 6.6: PAS staining reaction with diastase treatment illustrating the removal of glycogen in the basal regions with mucus positivity remaining in the apical portions. Note the pink-staining basement membrane (white arrows), vacuole (black arrow) and epithelial lymphocytes (arrowheads).

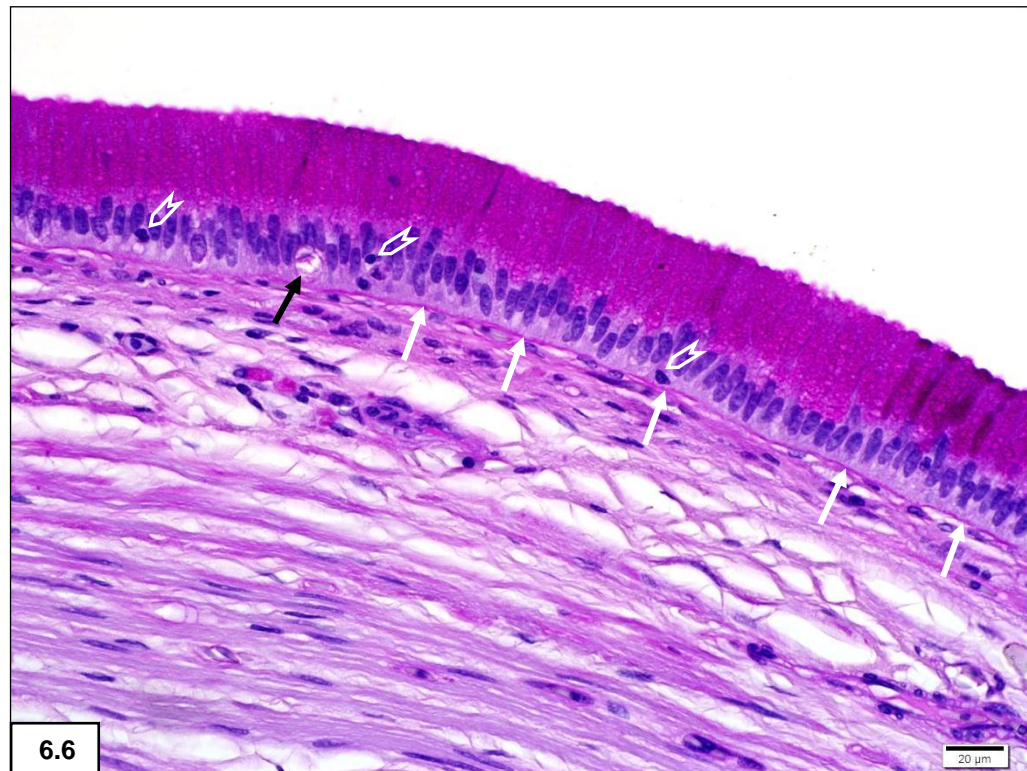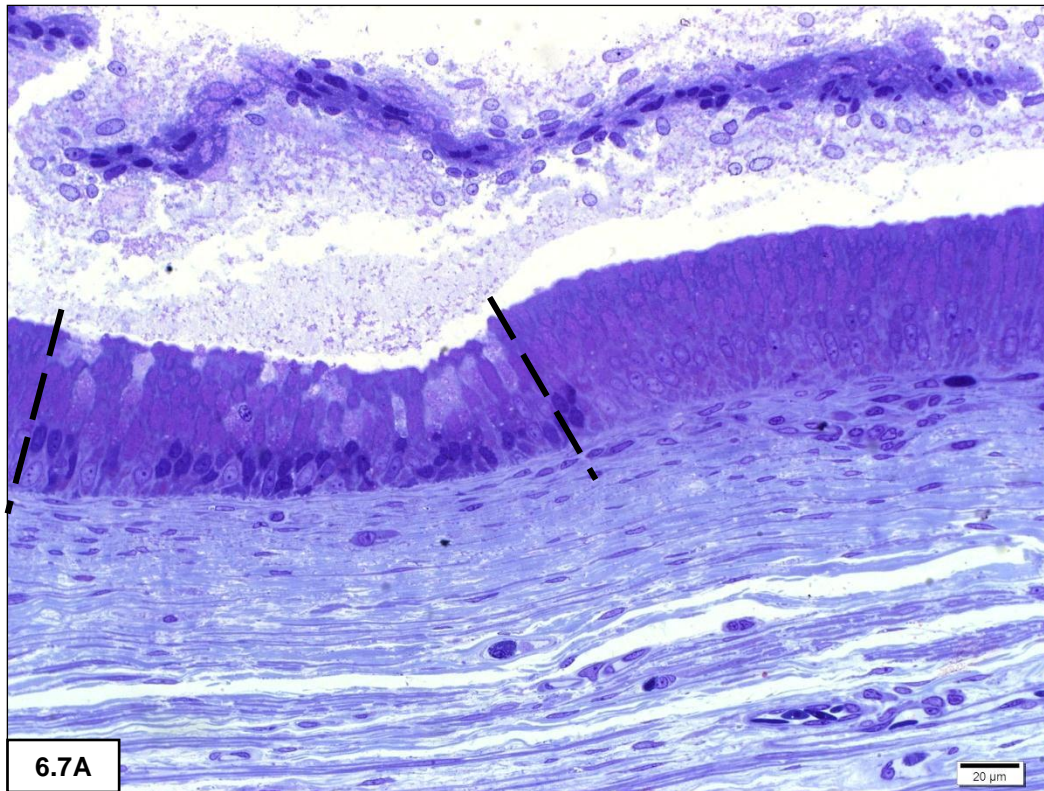**Figure 6.7A:** Epithelium in initial secretory phase or recovery phase (between dashed lines) adjacent to "resting" epithelium. Note the increase in dark cells in this area. Cellular debris and mucous remnants are evident in the lumen. TB
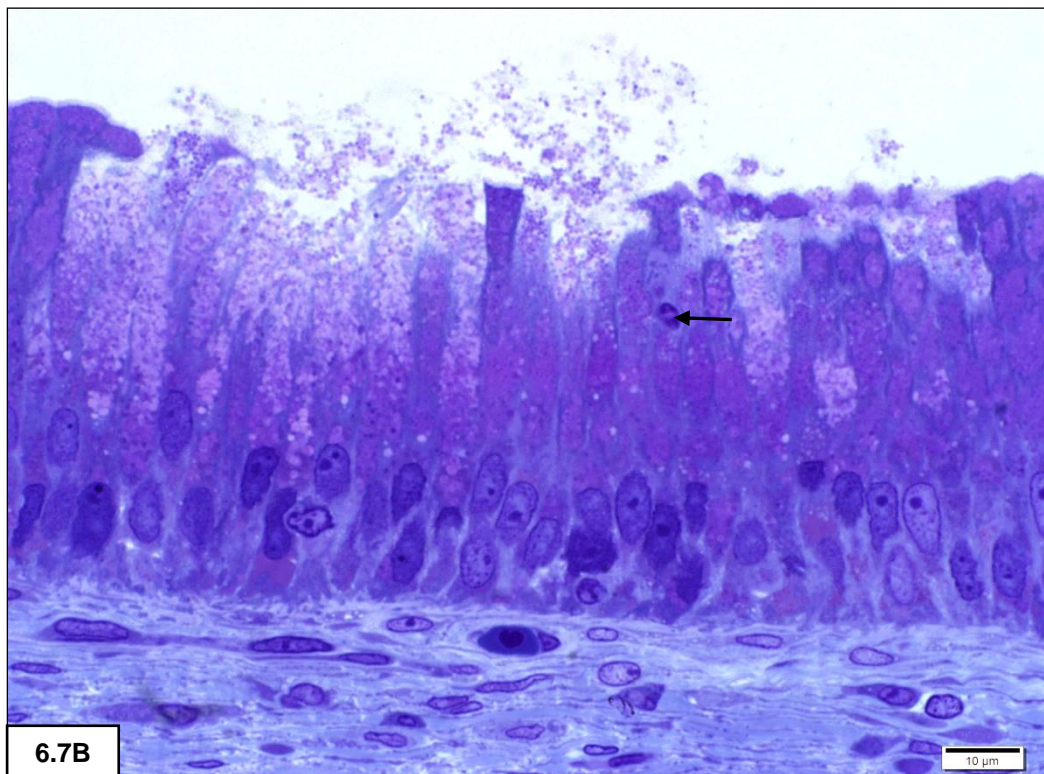
Figure 6.7B: Exocytosis of secretory granules from the epithelium. Note the pink cytoplasmic metachromasia indicating the presence of mucus and glycogen and a lymphocyte (arrow) traversing the epithelium. TB

148
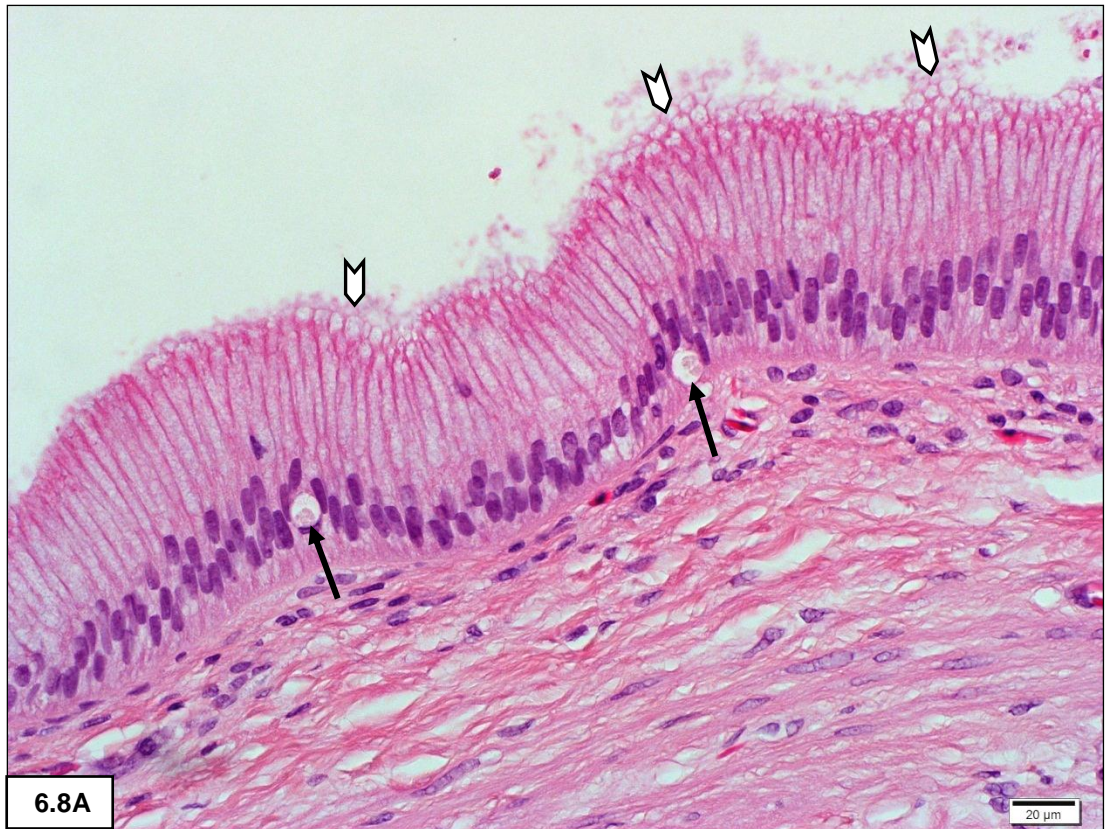
Figure 6.8: A - Vacuoles (black arrows) and apical bulging (white arrows) in the pseudostratified epithelium. H/E. **B -** Apical bulging (white arrows). TB.
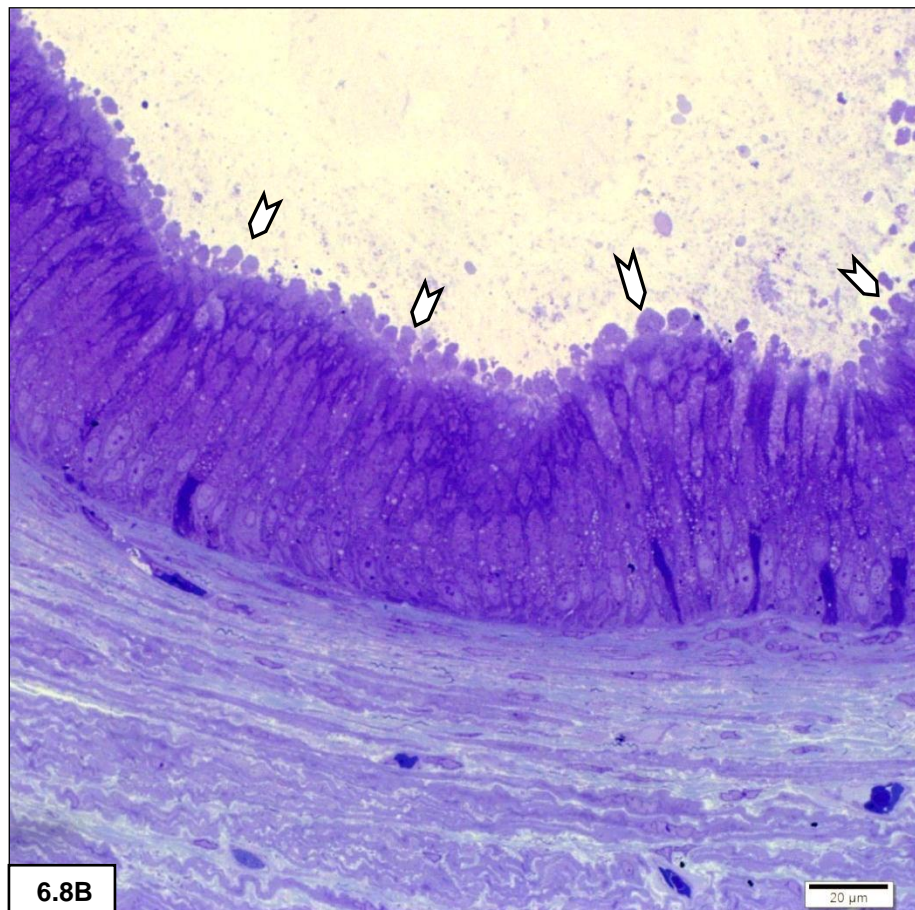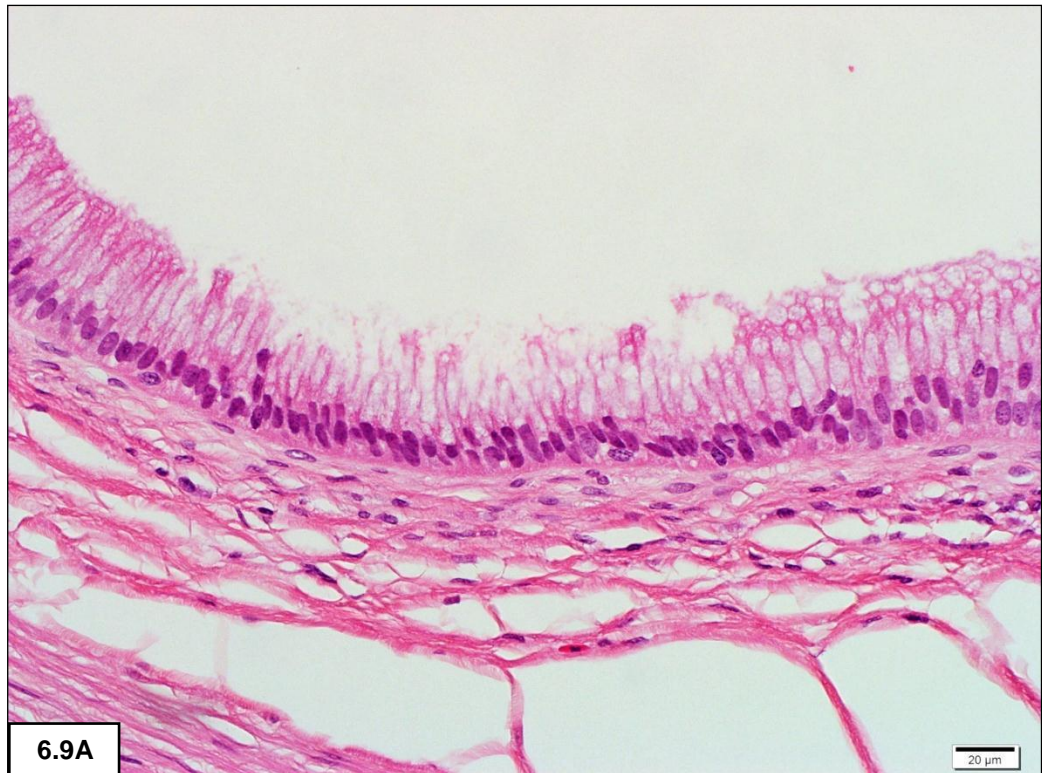
Figure 6.9A: Loss of apical portions of epithelial cells. H/E.
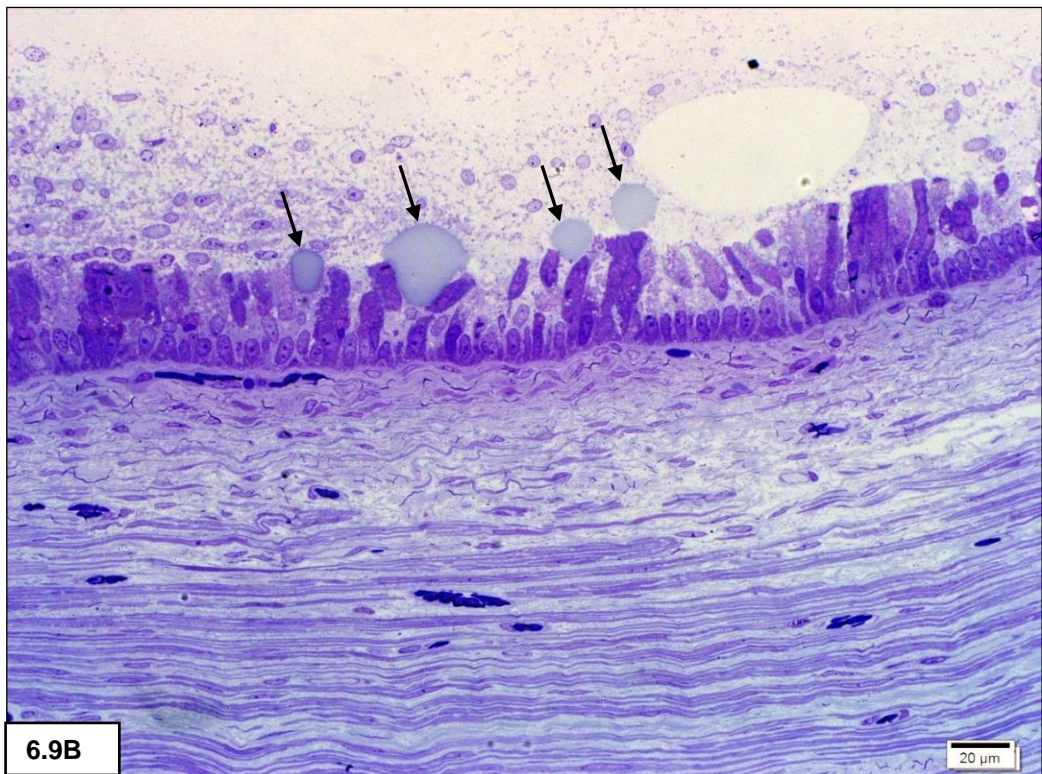
Figure 6.9B: Large lipid-like globules (arrows) attached to or near epithelial cells. Loss of cellular material from the epithelium is evidenced by the presence of cellular remnants and secretory product in the lumen. The basal nuclei are intact. The parallel arrangement of smooth muscle cells in the muscularis layer is prominent in the lower part of the image. TB.
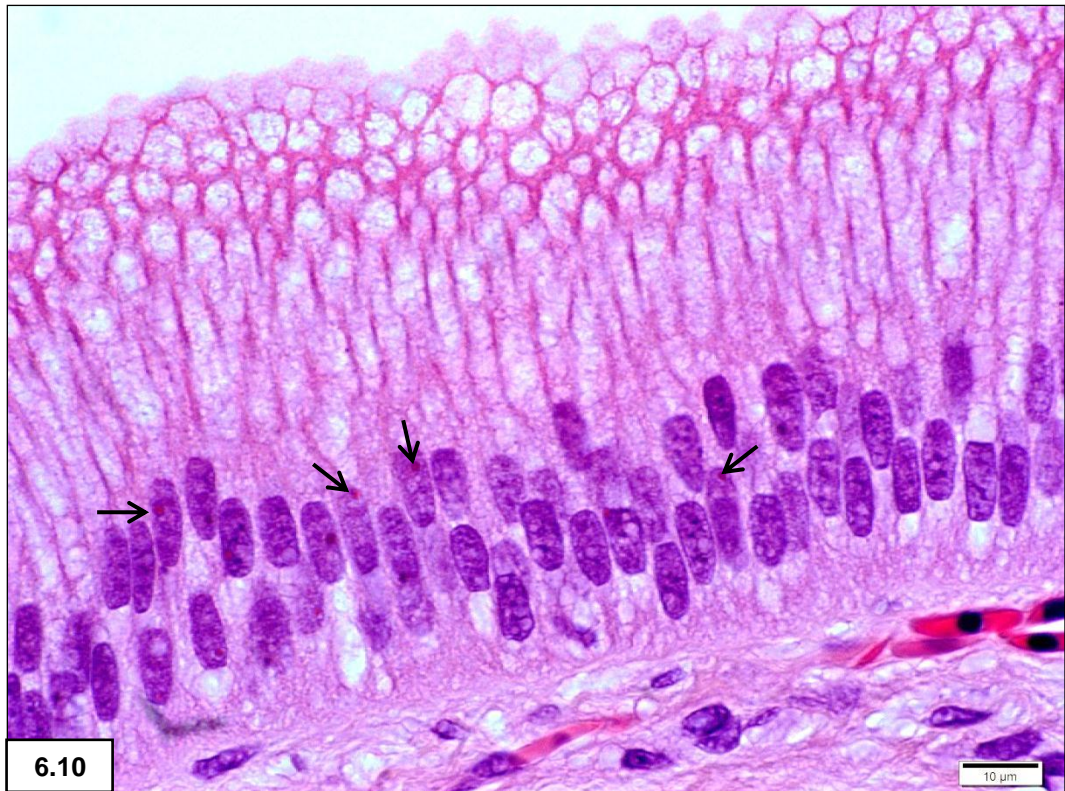
Figure 6.10: Prominent red nucleoli (arrows) in epithelial nuclei. Note different levels of nuclei typical of pseudostrtified columnar epithelium. H/E.
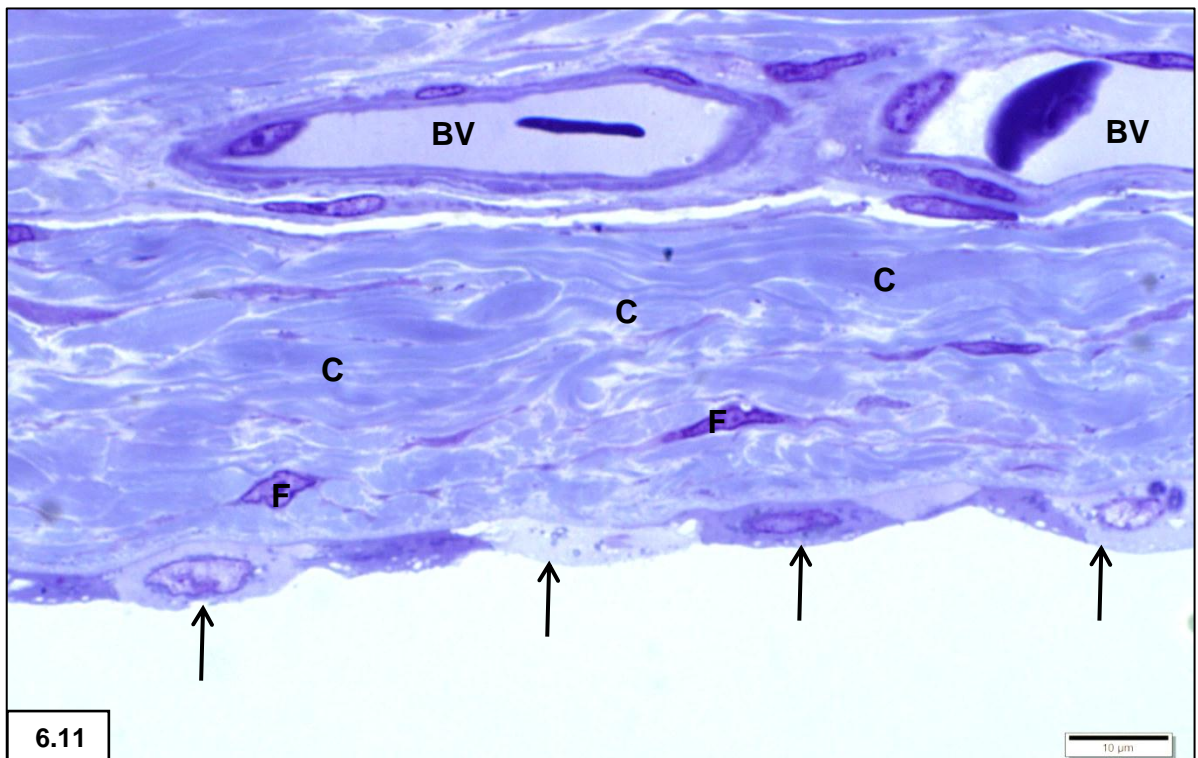
Figure 6.11: Serosa: External single layer mesothelium (arrows) covering the gallbladder with underlying subserosa consisting of supporting connective tissue, namely, collagen (**C**), fibroblasts (**F**) and blood vessels (**BV**). Note dark and light mesothelial cells. TB.

151

TRANSMISSION ELECTRON MICROSCOPY: PSEUDOSTRATIFIED EPITHELIUM
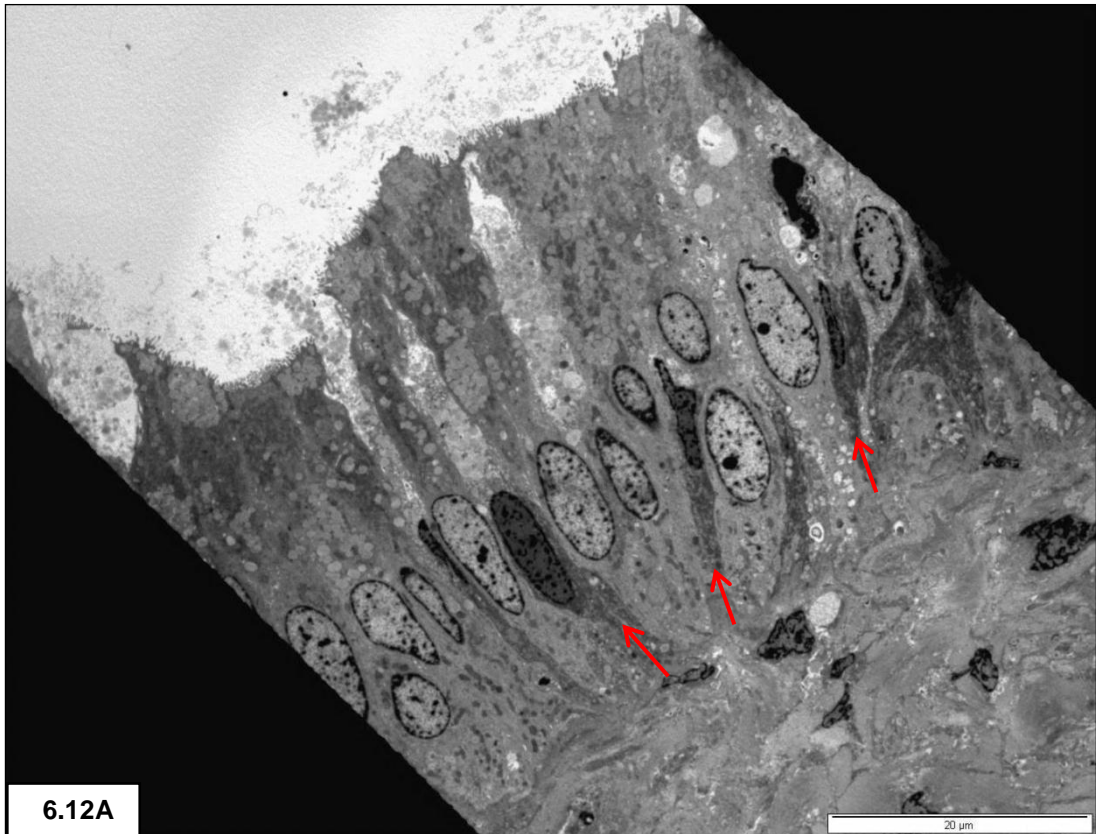
6.12A

Figure 6.12 A & B: Pseudostratified columnar epithelium with slender dark cells (red arrows) interposed between light cells. Note lymphocyte (yellow arrow) in **B**.

6.12B
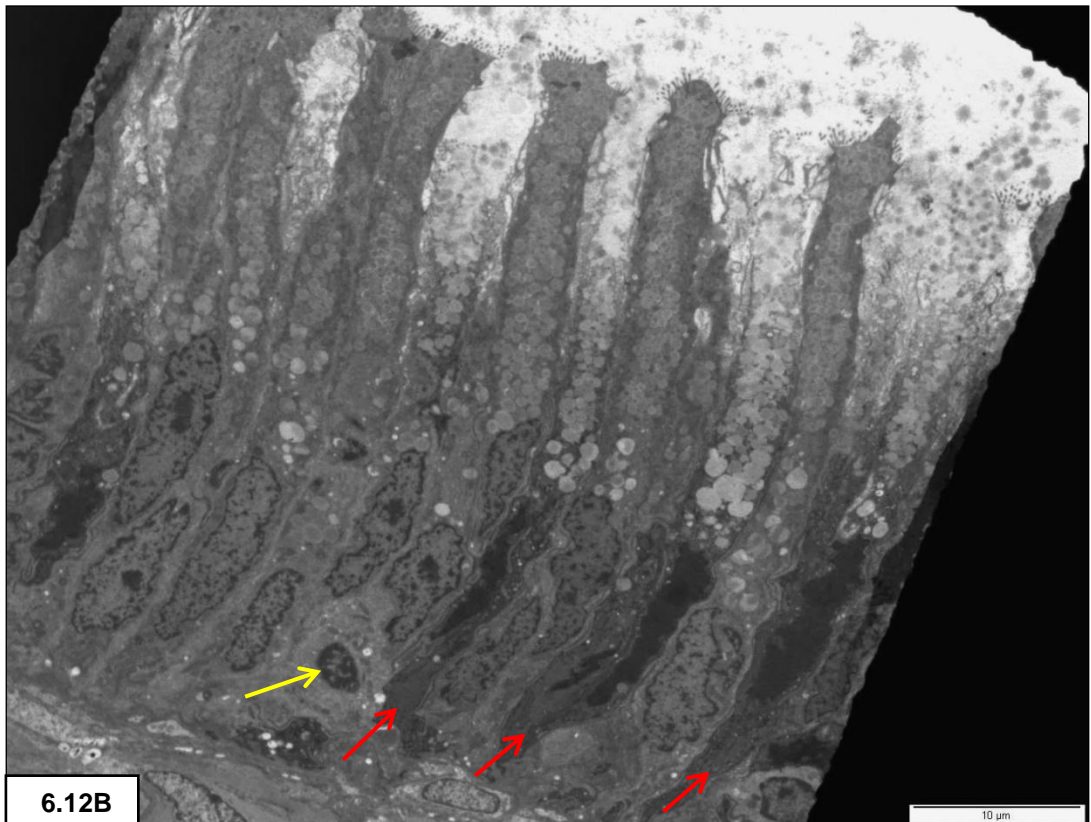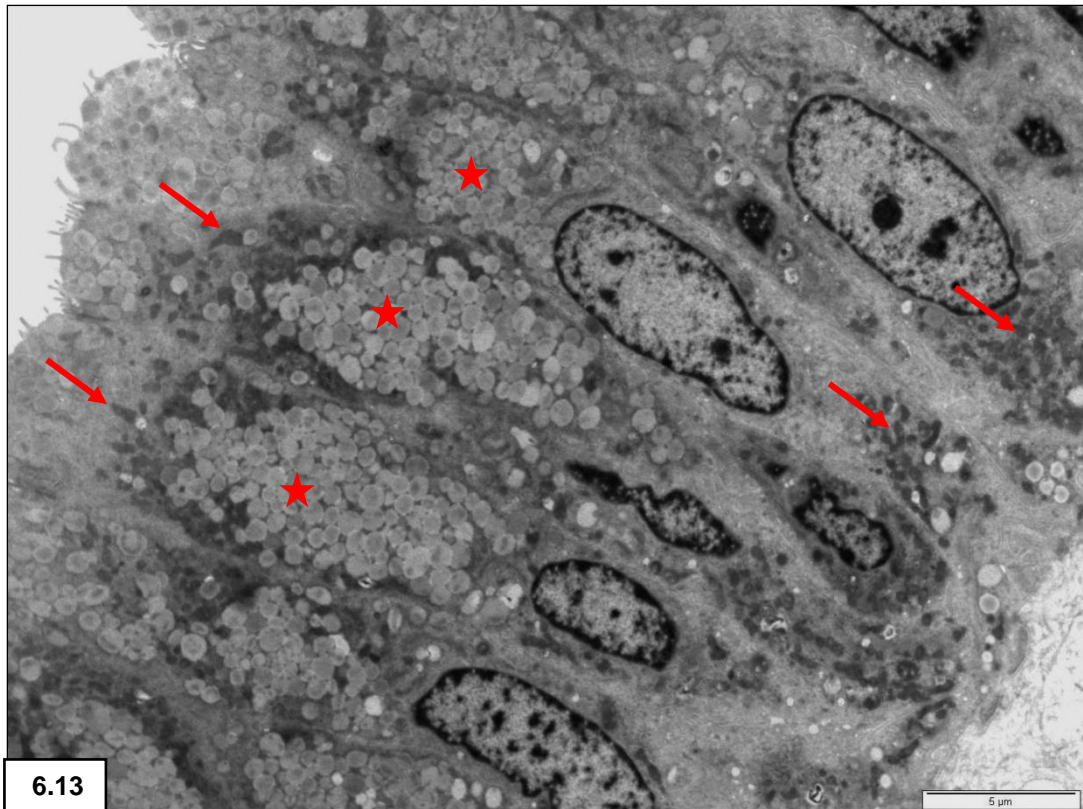
Figure 6.13: Slender goblet cells packed with secretory granules (stars). Note concentrations of basal & apical mitochondria (arrows) and oval-shaped nuclei.
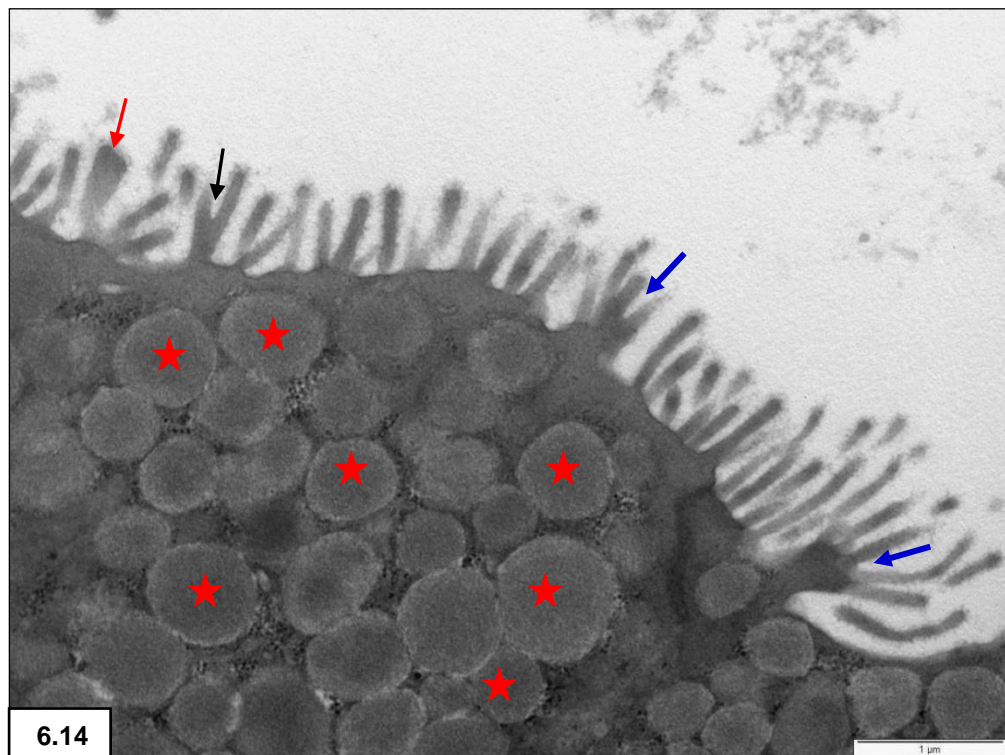
Figure 6.14: Staghorn (black arrow), branching (blue arrows) and club-shaped (red arrow) microvilli on apices. Note glycocalyx covering the villi. Spherical secretory granules of medium electron density (stars).
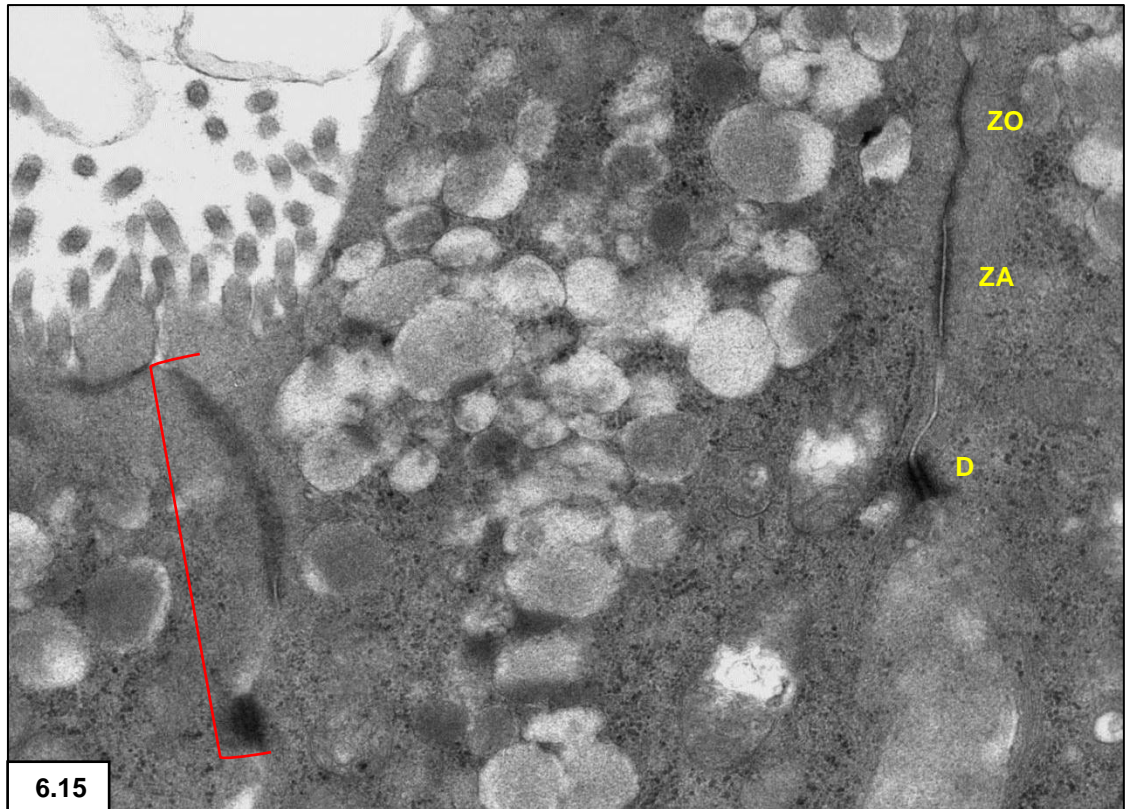
Figure 6.15: Apical junctional complex composed of a zonula occludens (ZO), zonula adherens (ZA) and desmosome (D). A second junctional complex (bracket) is sectioned obliquely.
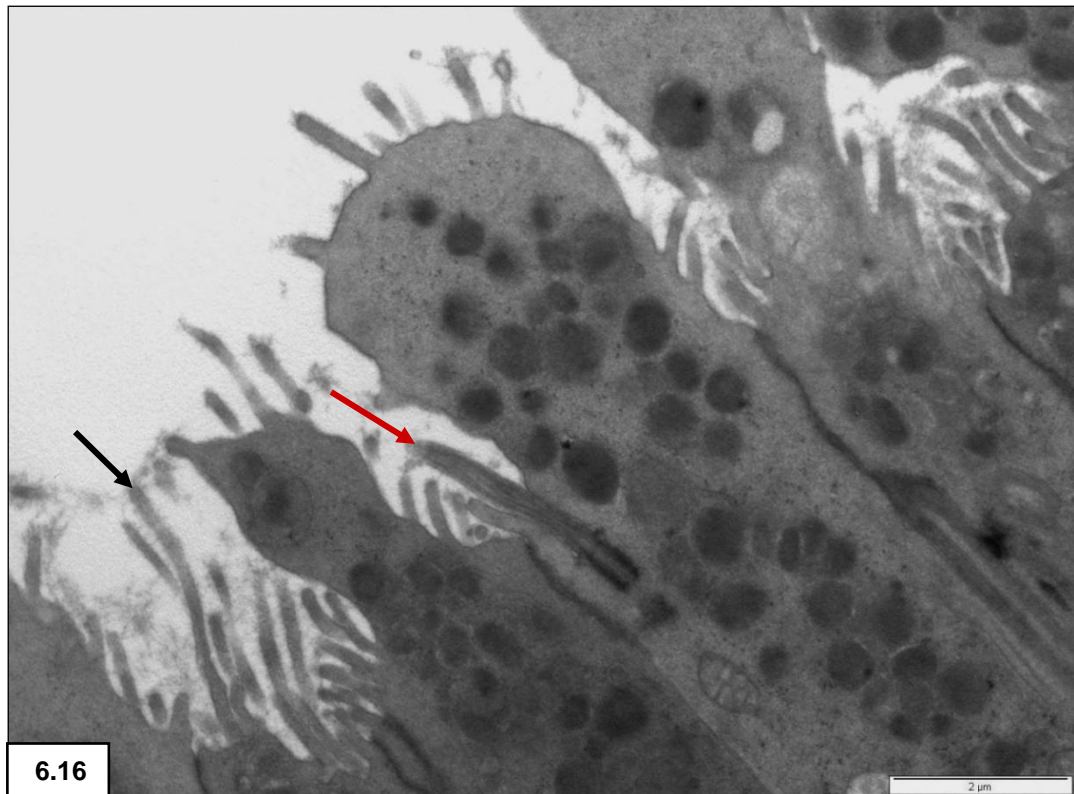
Figure 6.16: A cilium protruding from the cell apex (red arrow). Note bulging apices and a single long microvillus (black arrow).
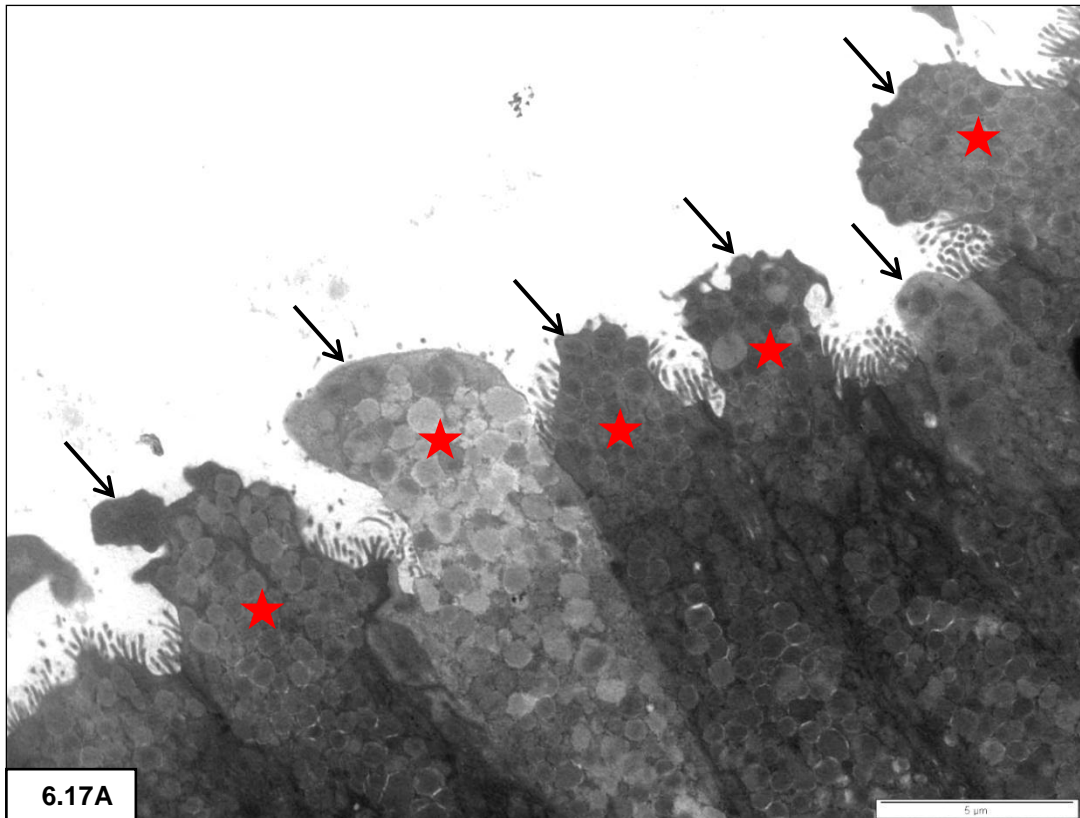
Figure 6.17: A & B: Collections of secretory granules (stars) in the subapical space and apical bulging with decrease or loss of microvilli (black arrows). **B:** Note junctional complexes (red arrows) and the fusion of granules forming vacuoles (blue arrow).
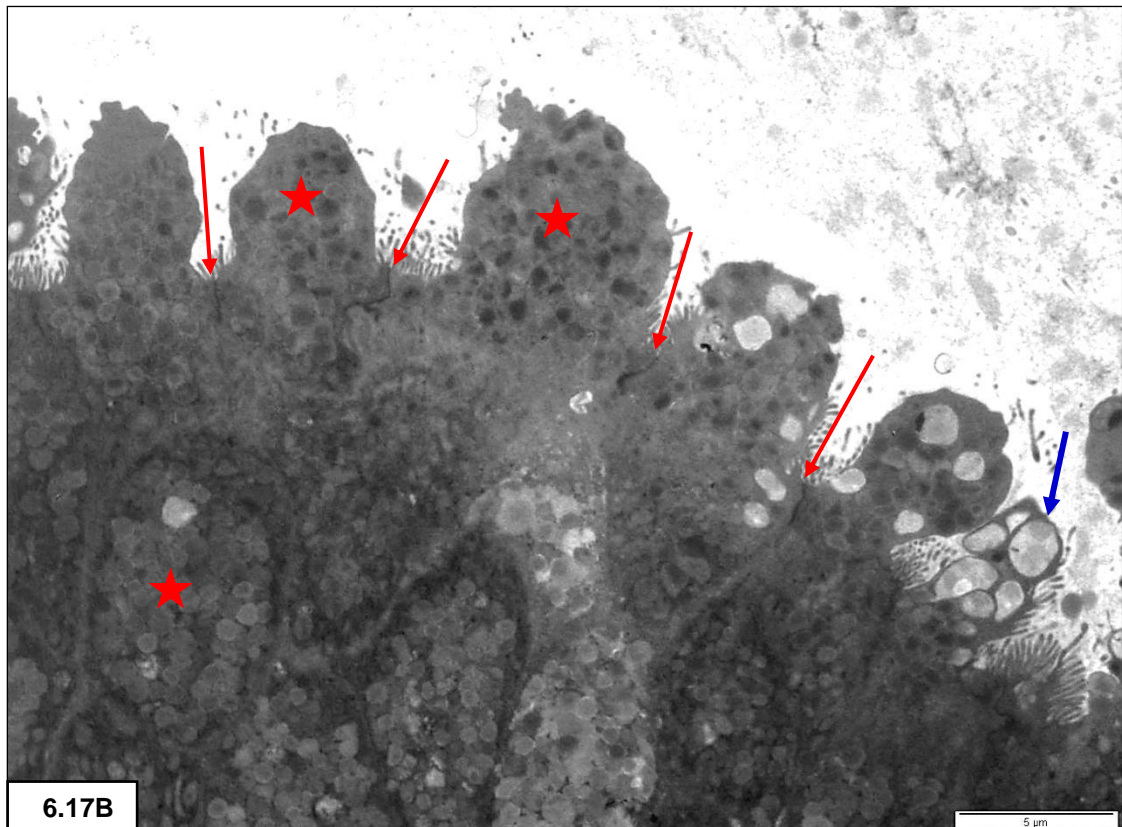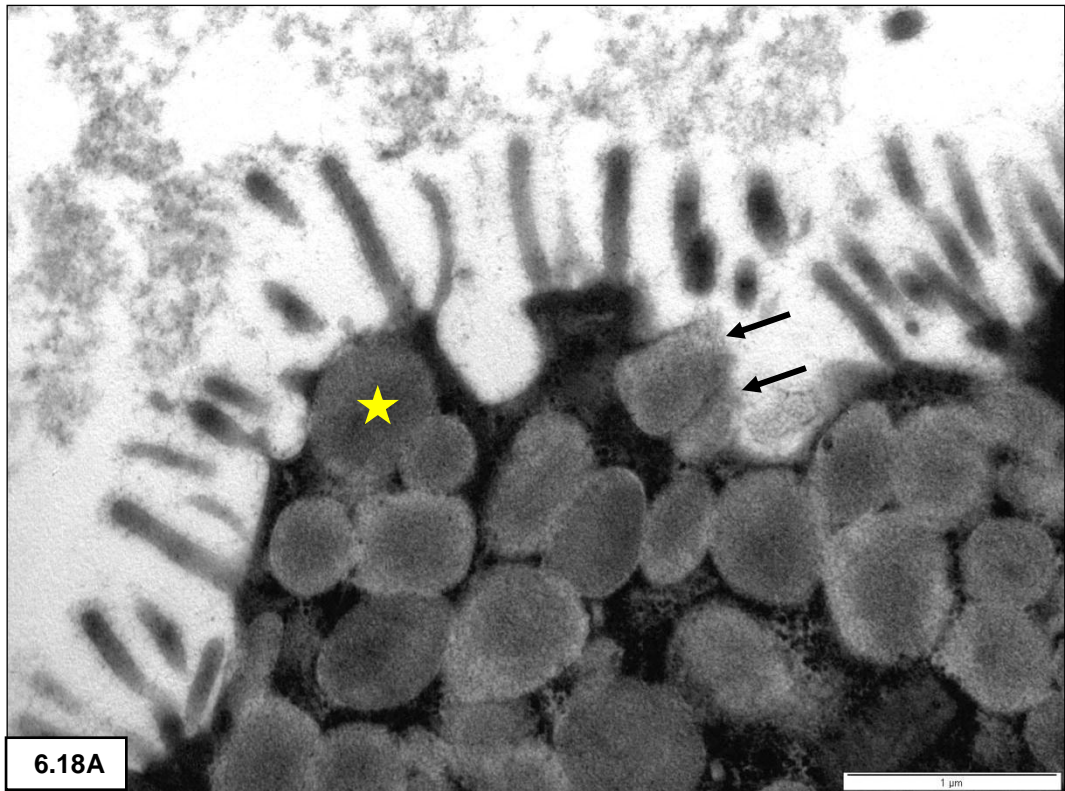
Figure 6.18: A: Exocytosis of secretory granules (black arrows). Note granule at the point of merging with the cell membrane (star).
B: Goblet cell at the point of extruding secretory granules (red arrow).Note junctional complex (bracket).
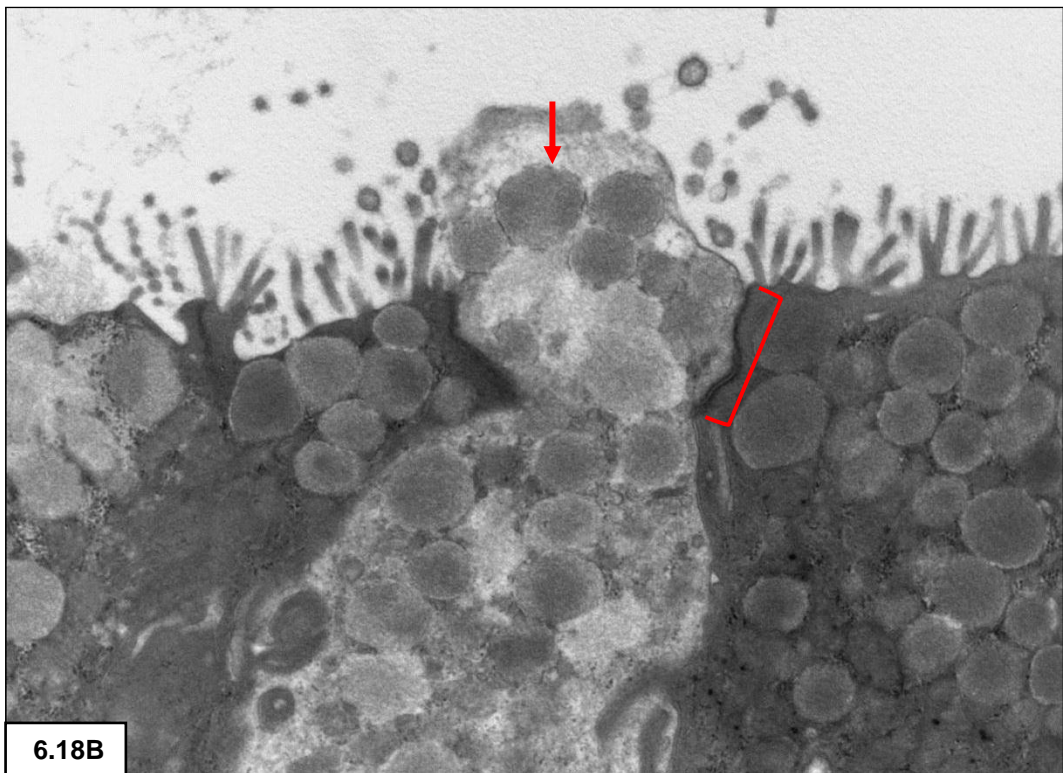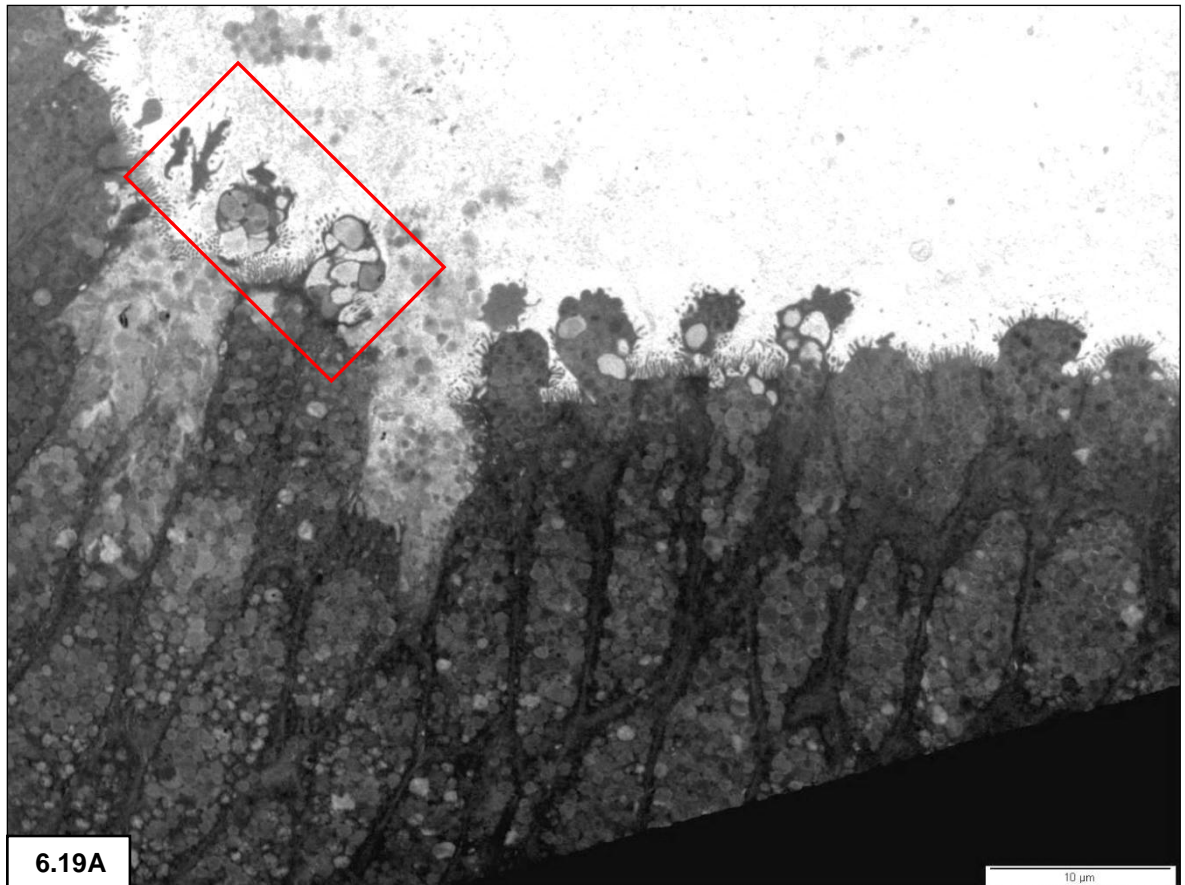
6.19A

Figure 6.19: A: Different stages of apical bulging.
B: Blocked area in A - Pinching off of apical cell cytoplasm.

6.19B
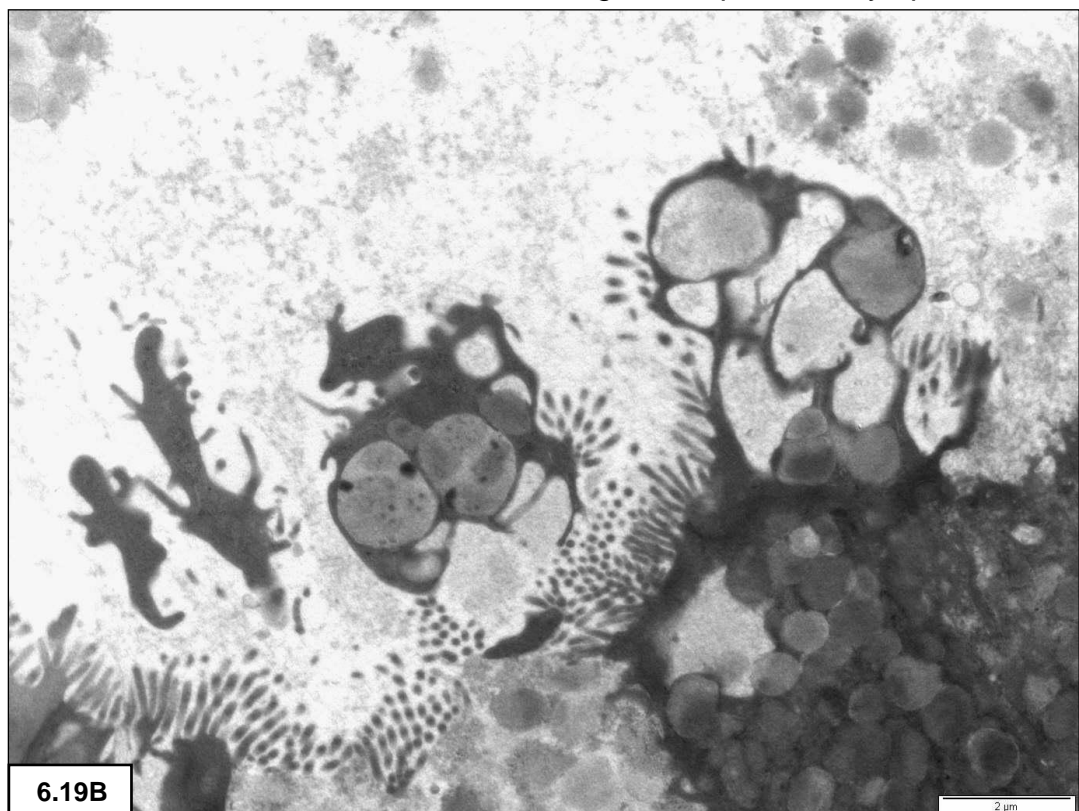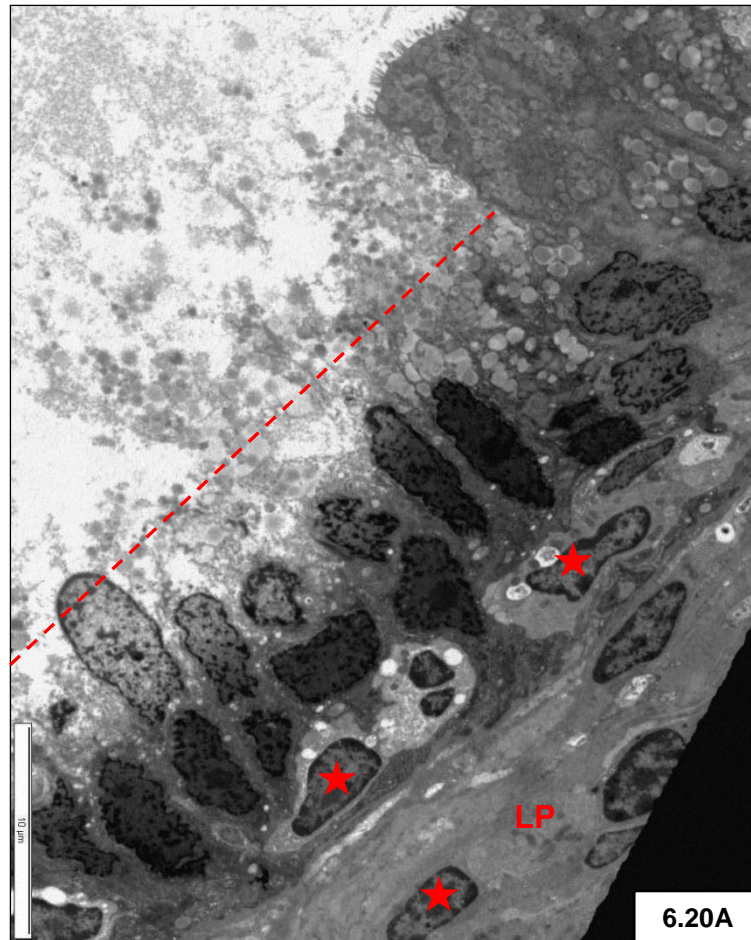
Figure 6.20: A & B: Loss of cell apices (dashed line in **A**) with an increase of dark cells with corrugated nuclei. Note lymphocytes (stars) positioned at the base of the epithelium and in the lamina propria (LP) just beneath the basal lamina.
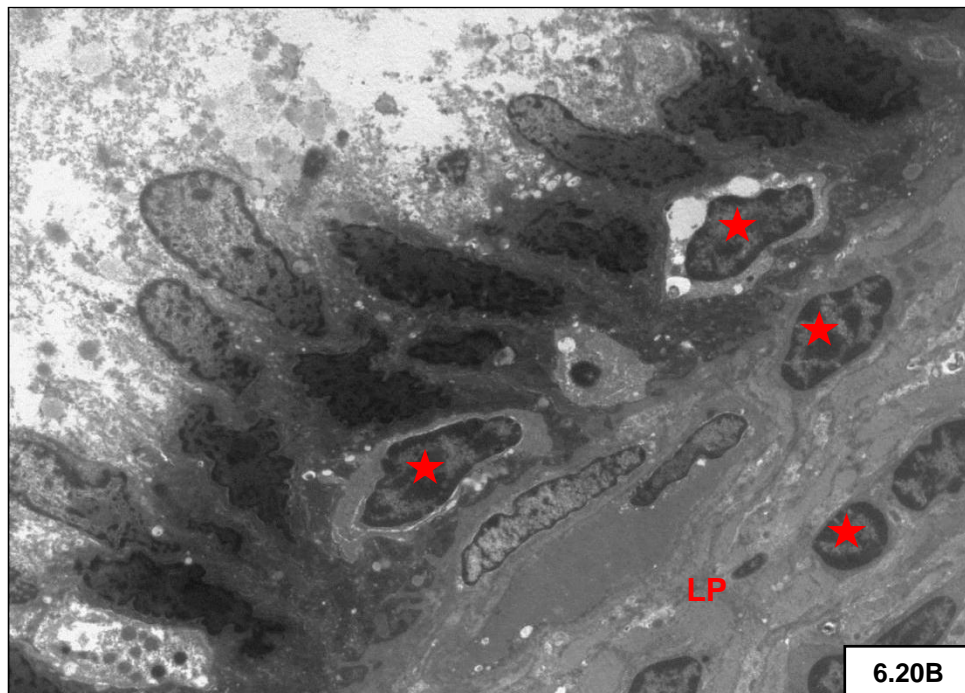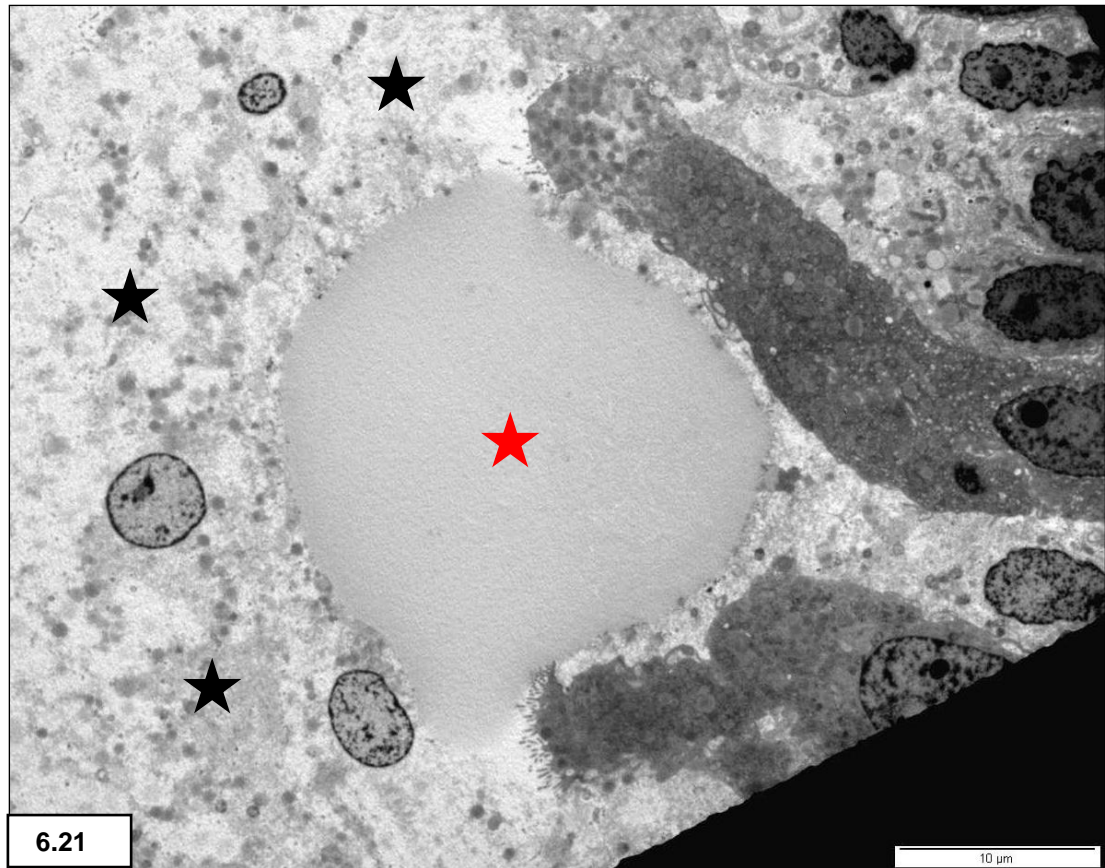
Figure 6.21: Lipid-like globule (red star) closely associated with the surface epithelium. Note cell debris in the lumen (black stars).
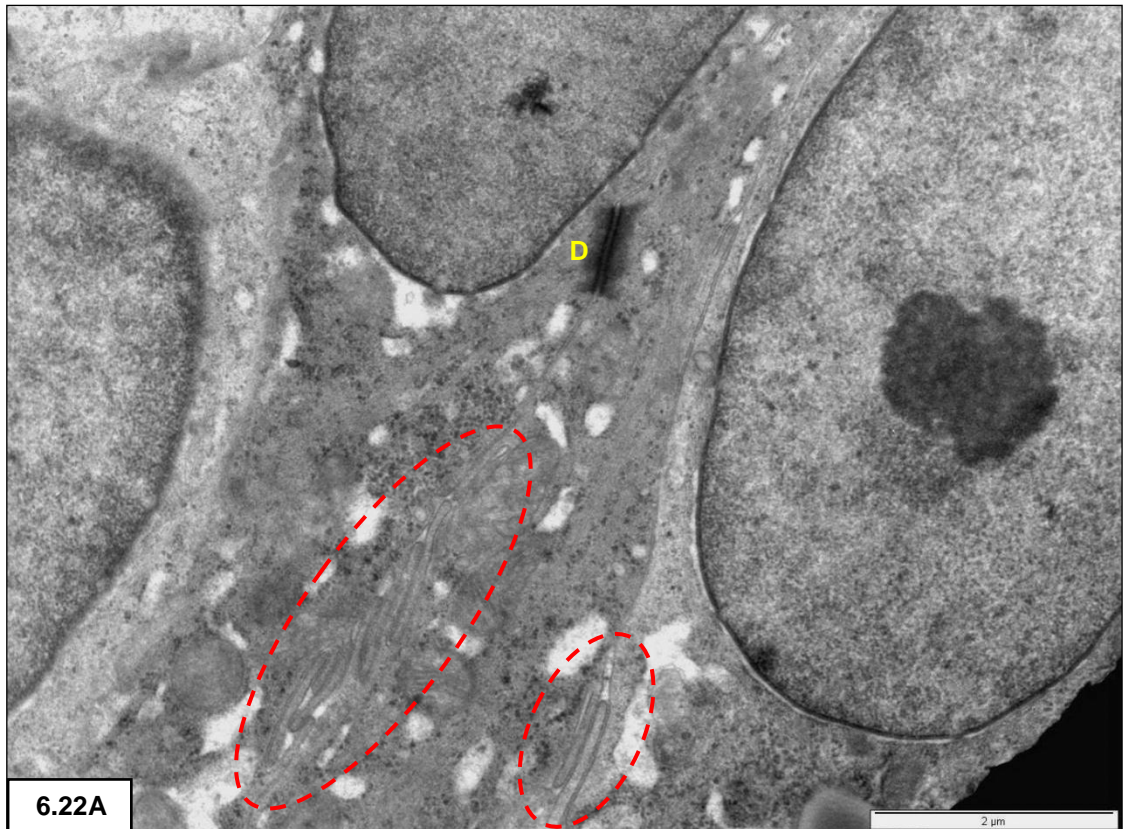
Figure 6.22: A - Desmosome (D) between lateral cell borders. **A & B**: Note lateral interdigitations of the cell membranes (dashed lines). **B –** Golgi apparatus (yellow arrow), granular endoplasmic reticulum (red arrows).
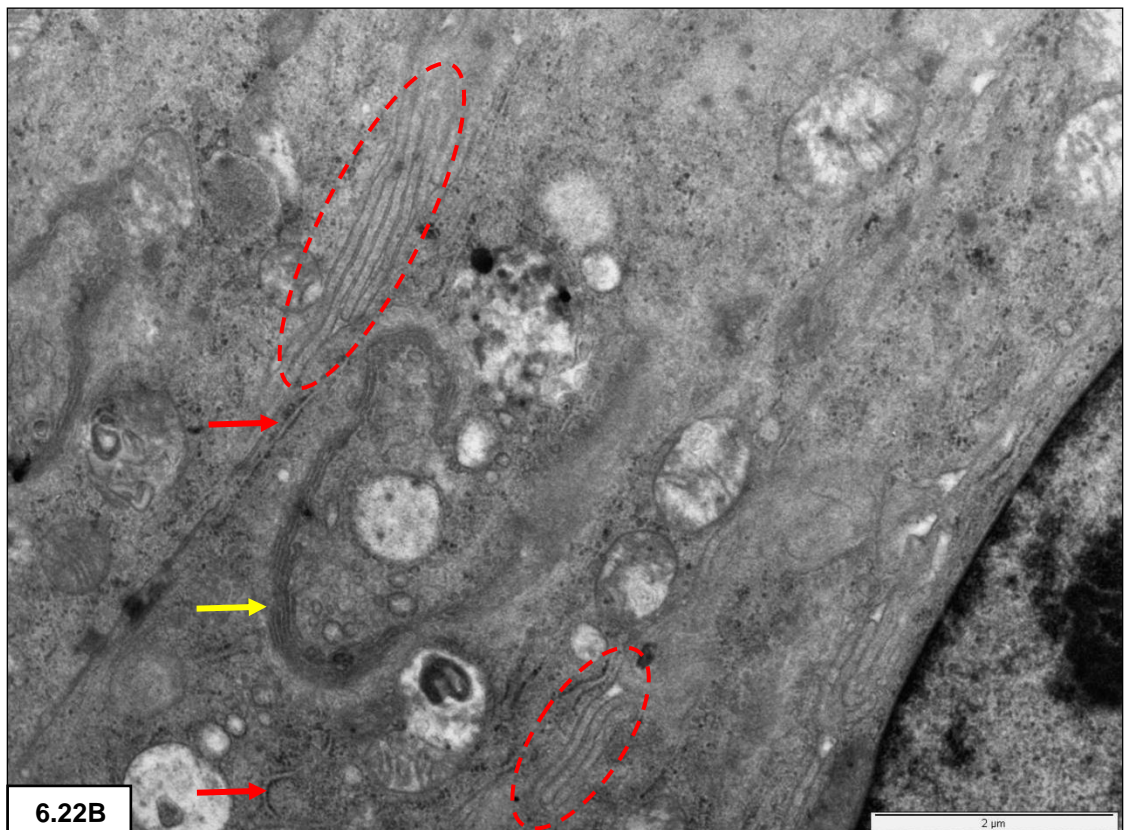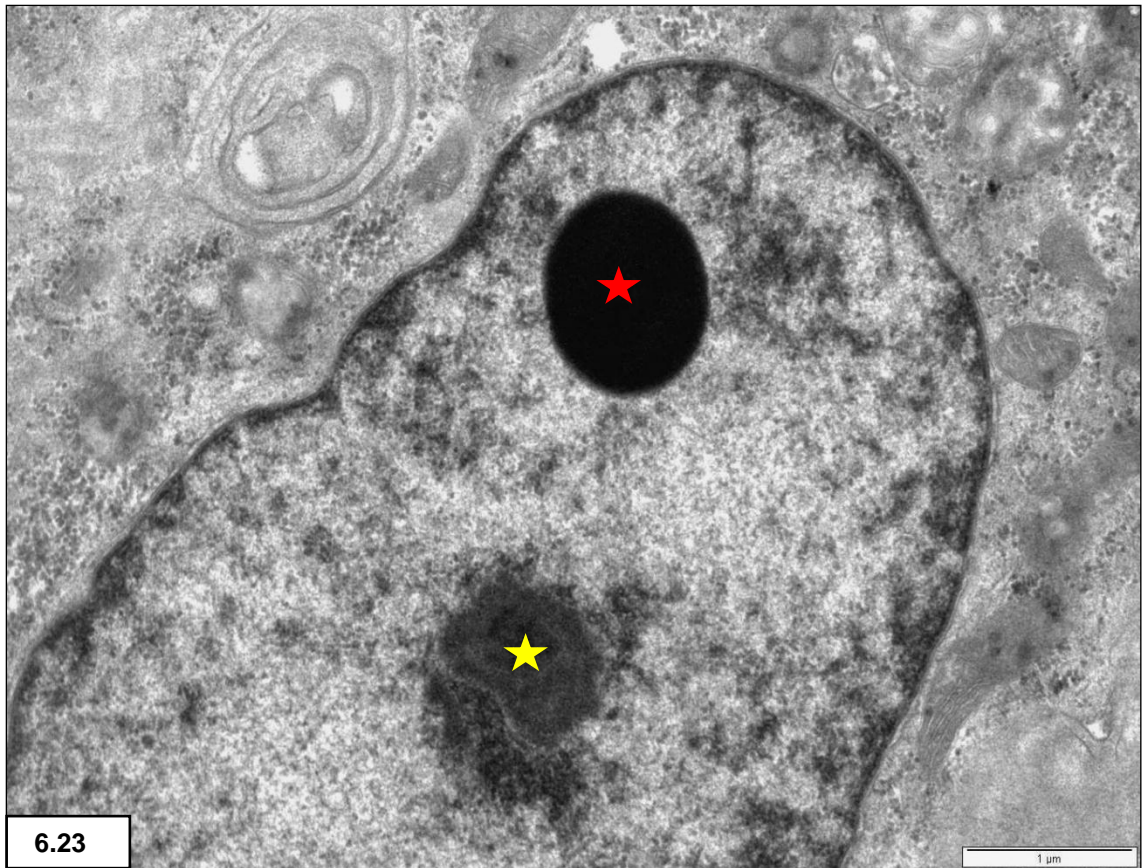
Figure 6.23: Two nucleoli – note the prominent circular electron-dense nucleolus (red star) and the more typical amorphous nucleolus (yellow star).
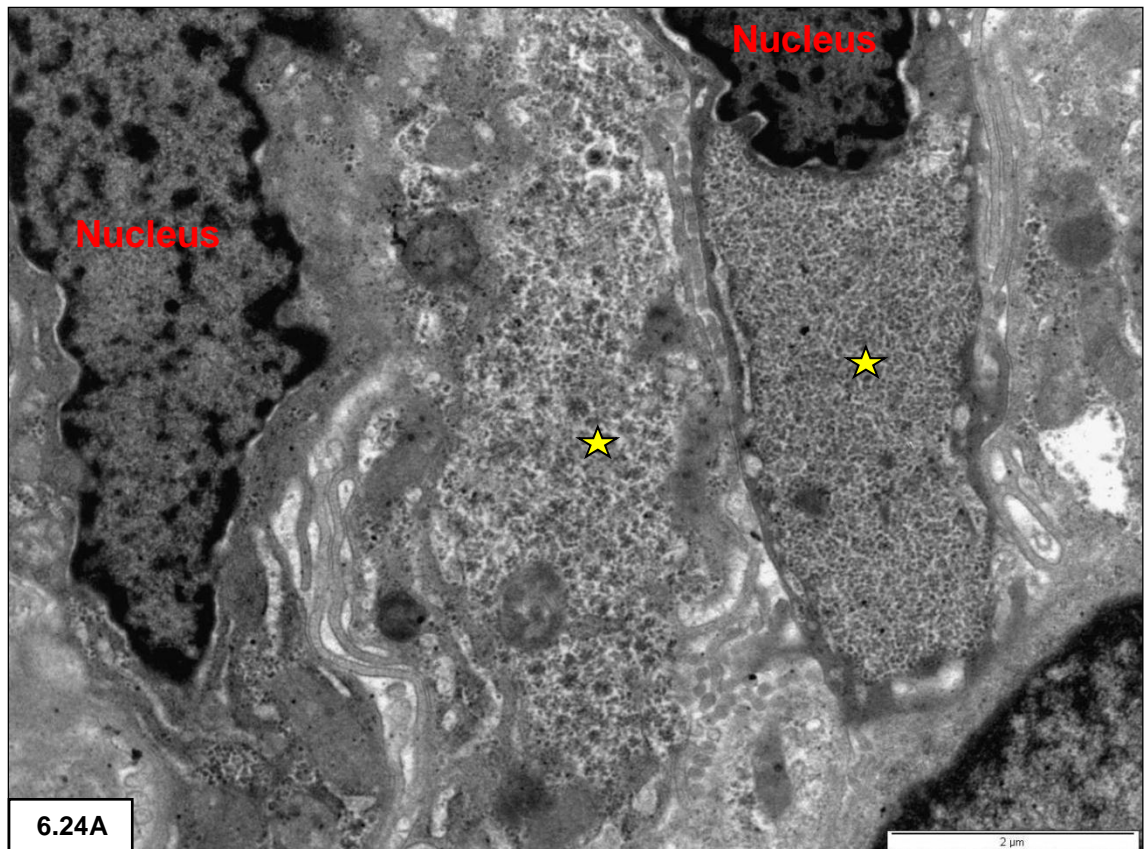
Figure 6.24 A: Collections of glycogen granules (stars) at the base of adjacent cells.
B: Intermediate filaments (yellow arrows), mitochondria (red arrows).
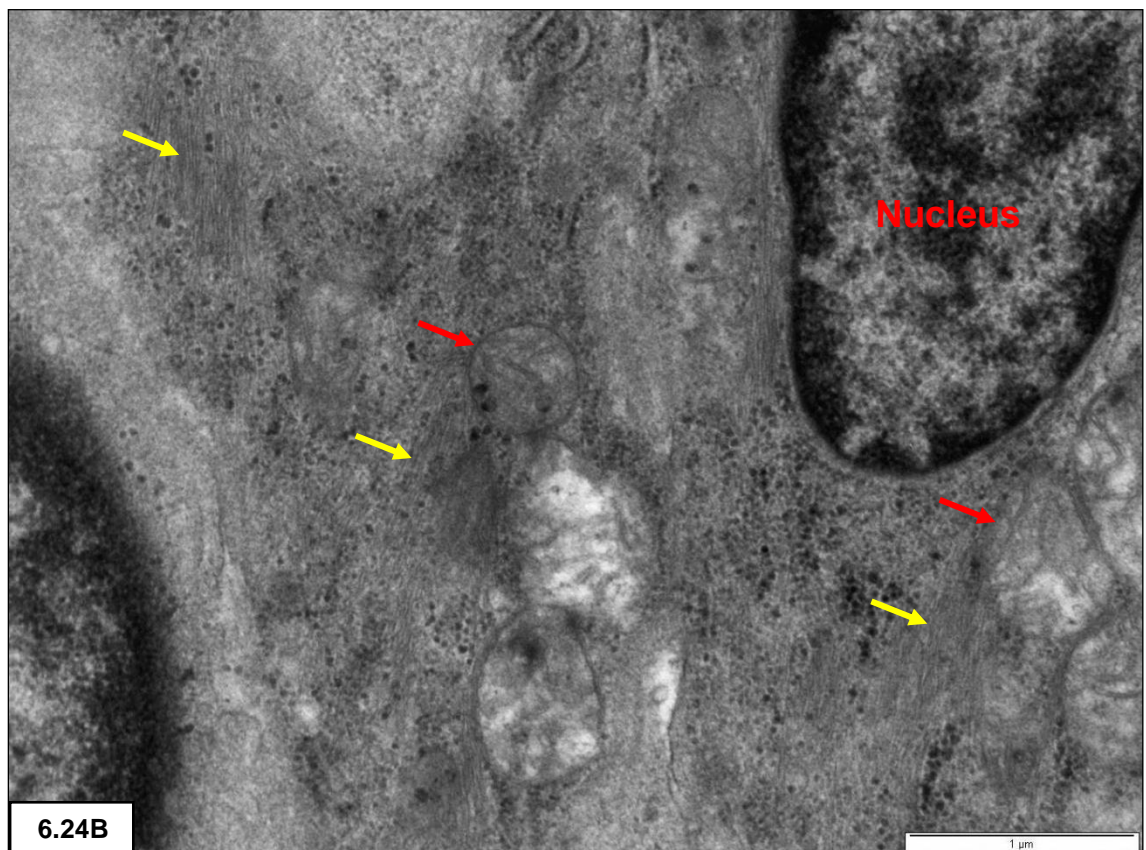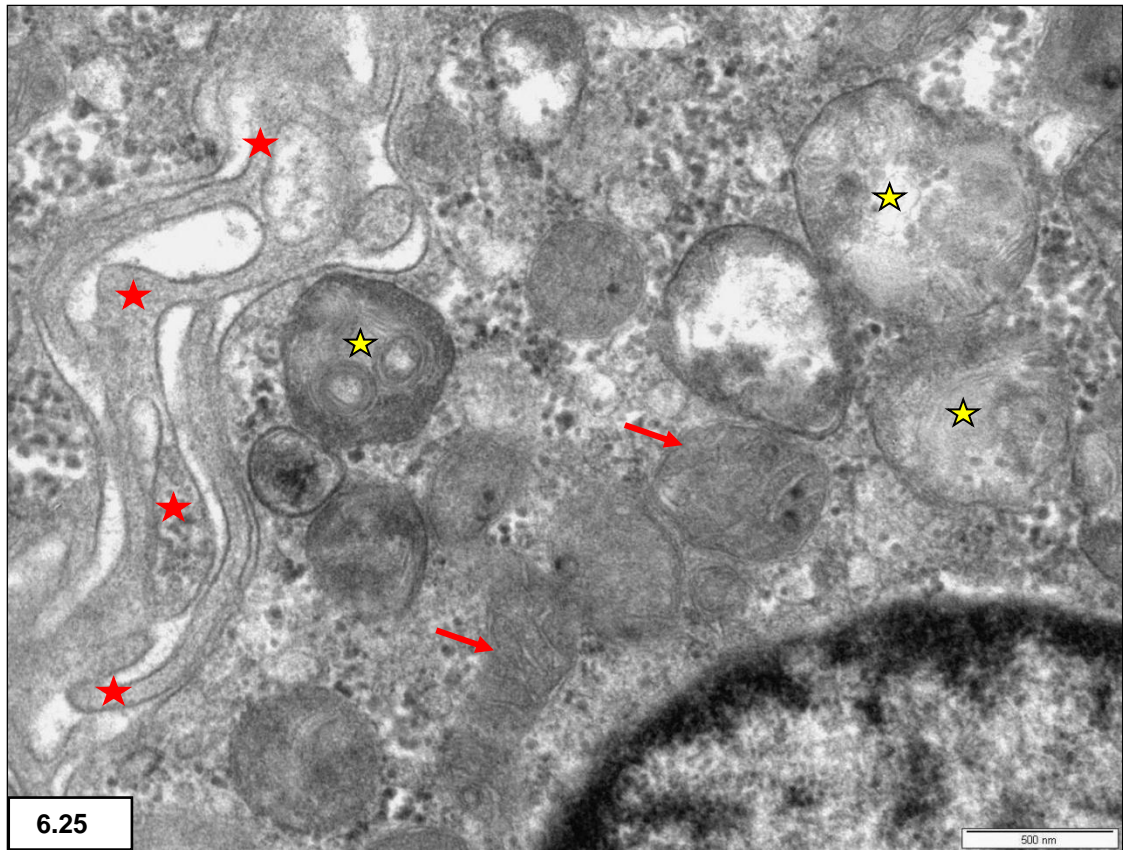
Figure 6.25: Lysosomes with whorled membranes (yellow stars).
Note mitochondria (arrows) and interdigitating cell membranes (red stars).
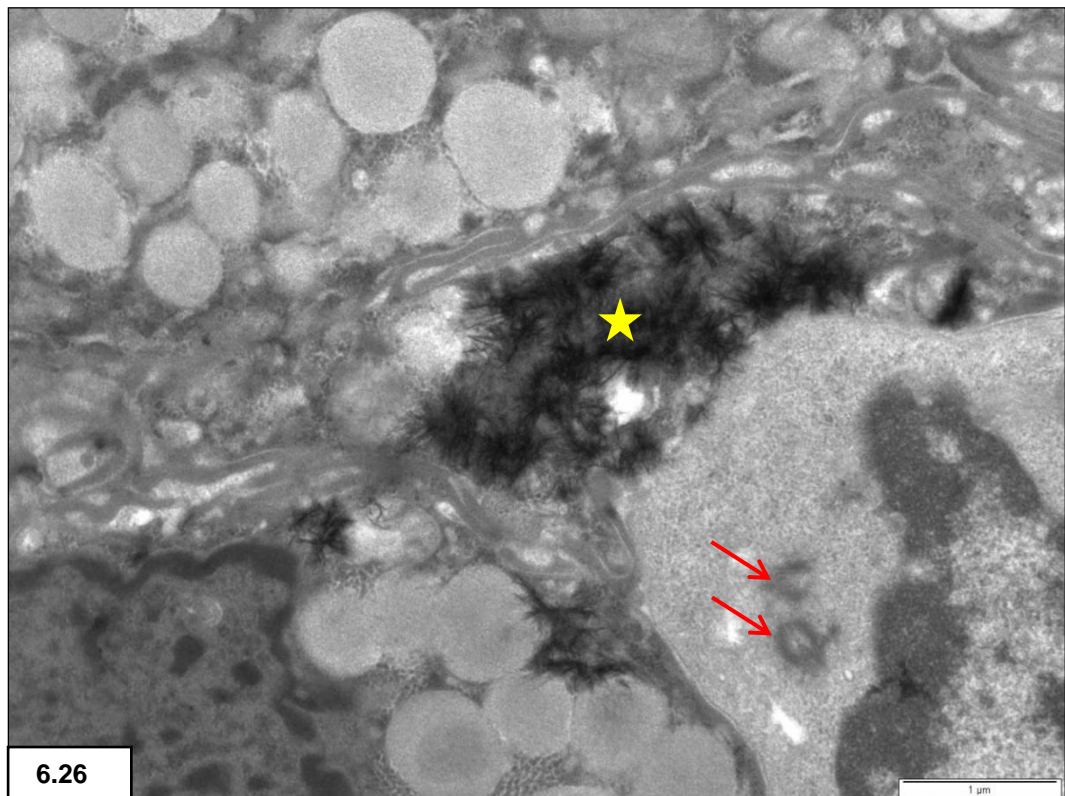
Figure 6.26: Electron-dense calcium deposits (yellow star). Note centrioles (arrows).
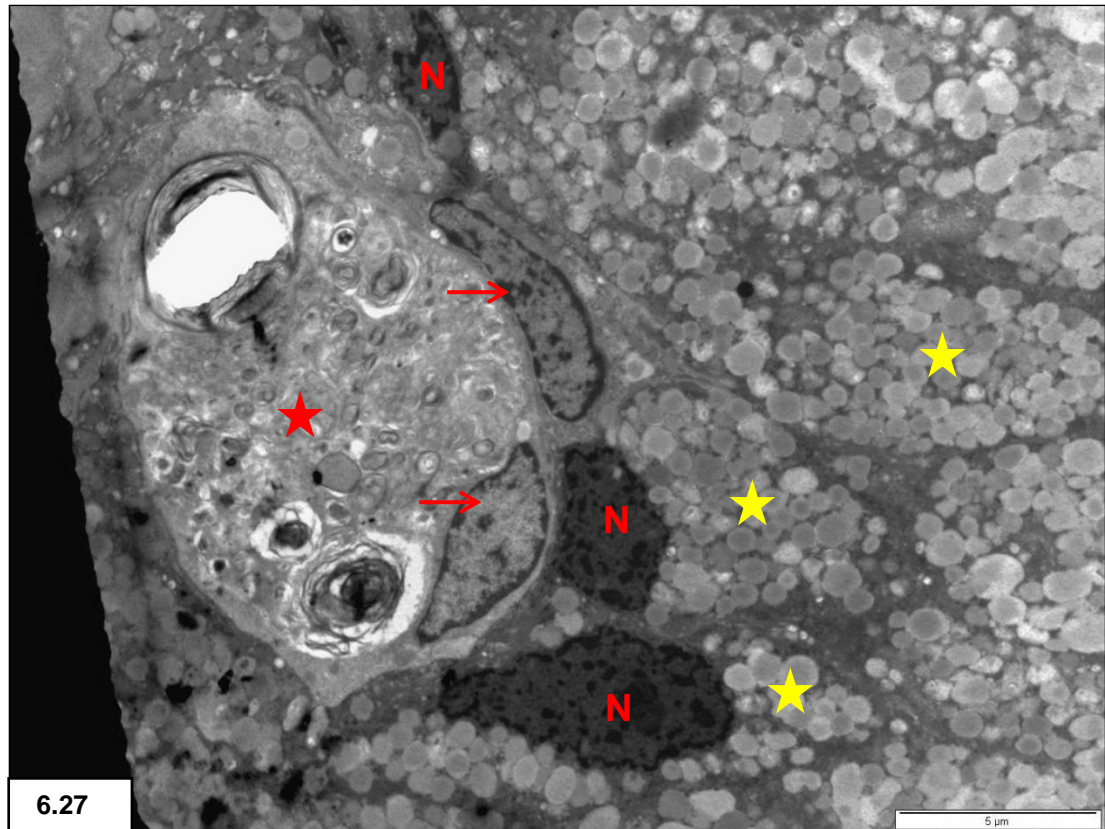
Figure 6.27: Cytoplasmic vacuoles filled with membranous debris (red star) present in macrophages between the pseudostratified columnar epithelial cells. Macrophage nuclei (arrows). Secretory granules (yellow stars) and nuclei (**N**) of epithelial cells.
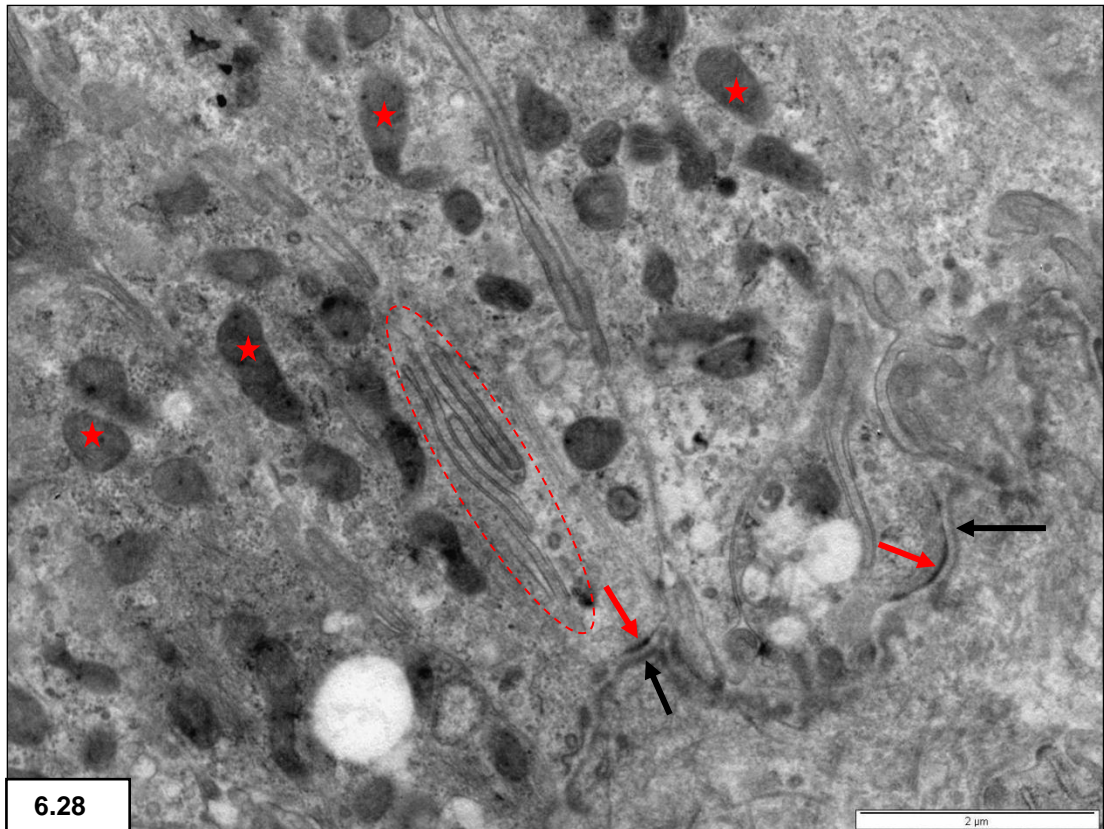
Figure 6.28: Undulating basal lamina (black arrows), hemidesmosomes (red arrows), basolateral interdigitations (dashed line). Note mitochondria (stars).
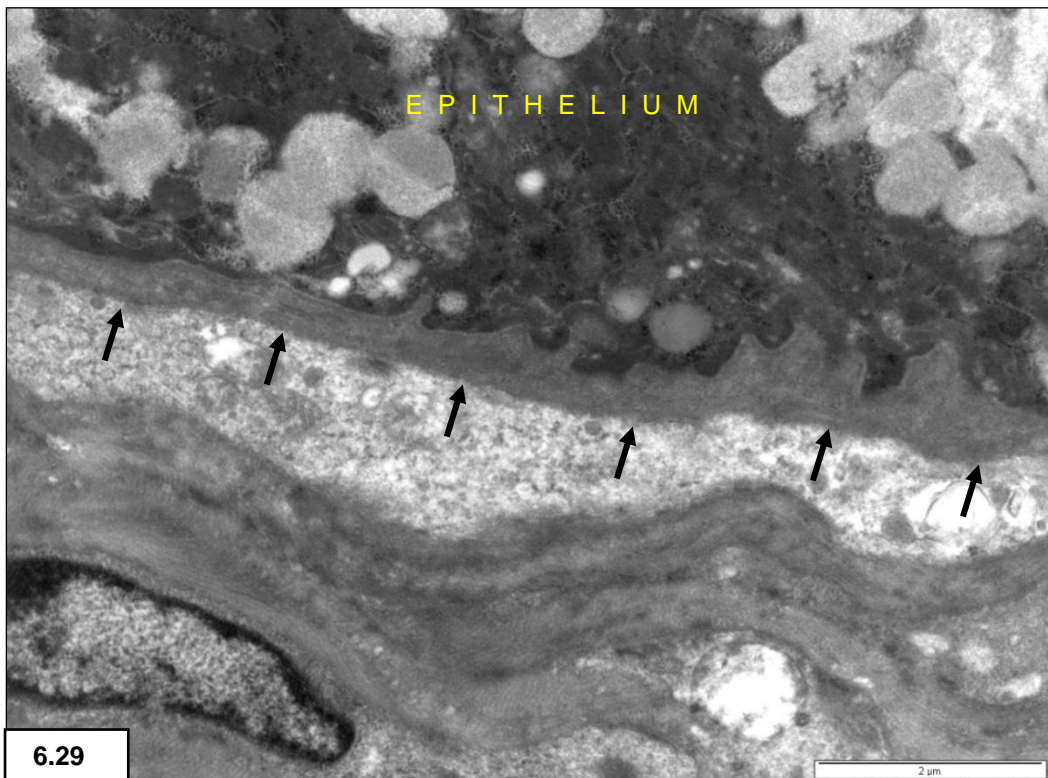
Figure 6.29: Thickened basal lamina (arrows) beneath a cell displaying apical loss of cytoplasm.
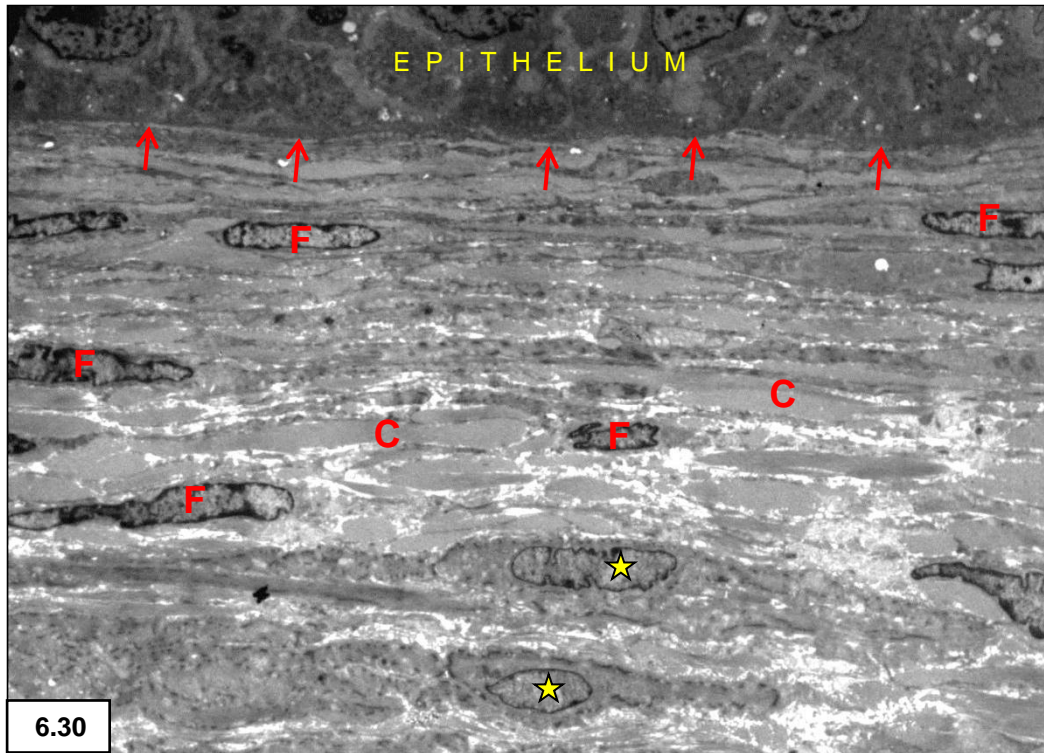
Figure 6.30: *Lamina propria* - smooth muscle cells (stars) relatively near basal lamina (arrows). Fibroblasts (**F**) with intervening collagen (**C**) also present.
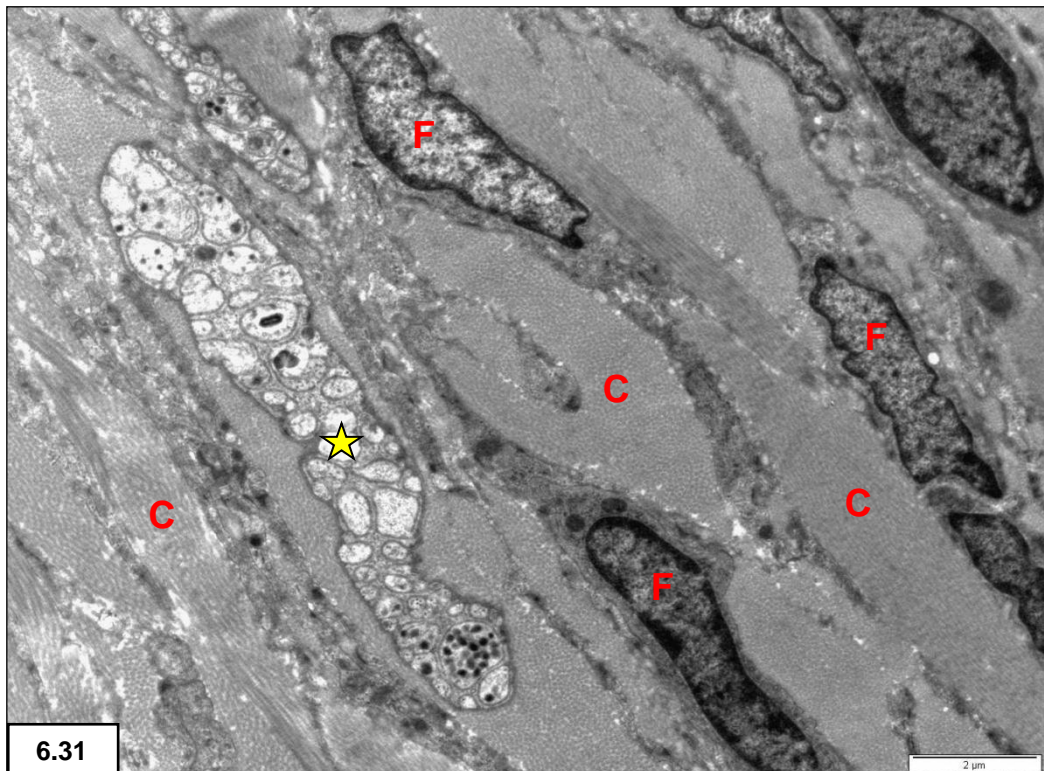
Figure 6.31: A nerve ganglion (star) among sheets of collagen fibres (**C**) and accompanying fibroblasts (**F**) in the *lamina propria.*
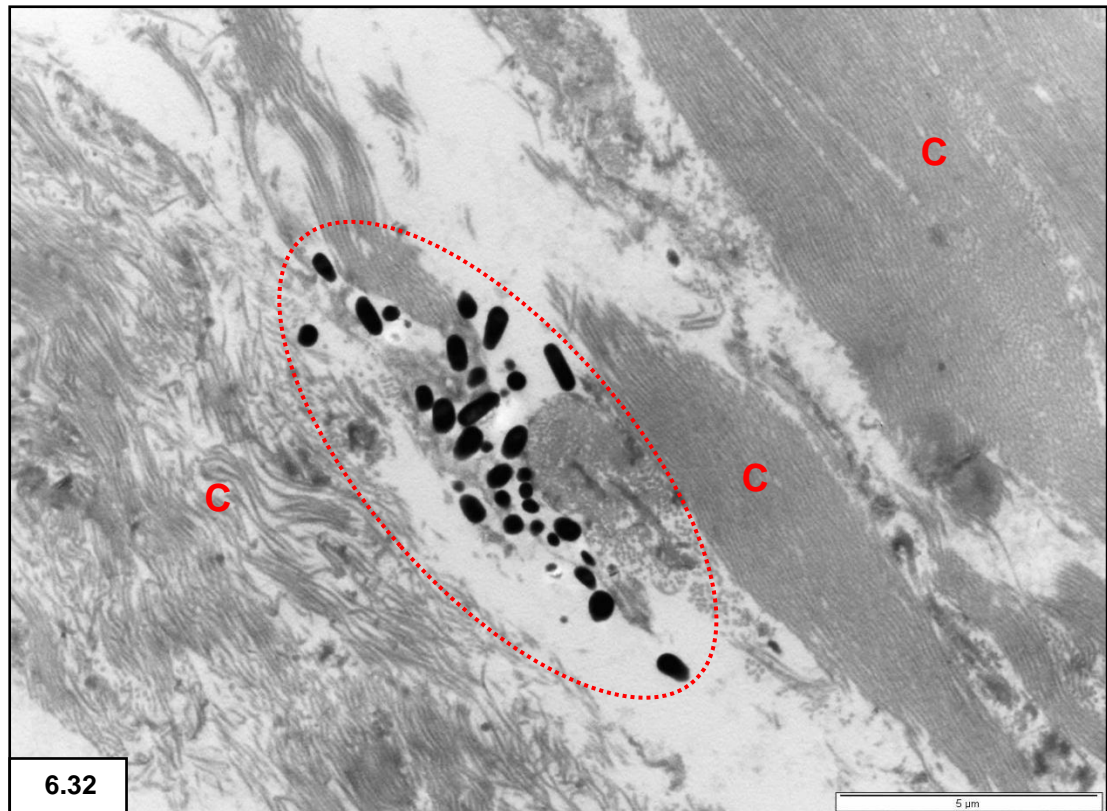
Figure 6.32: Loose lying melanin granules (dashed circle) between collagen fibres (**C**) in the *lamina propria*.

MUSCULARIS EXTERNA
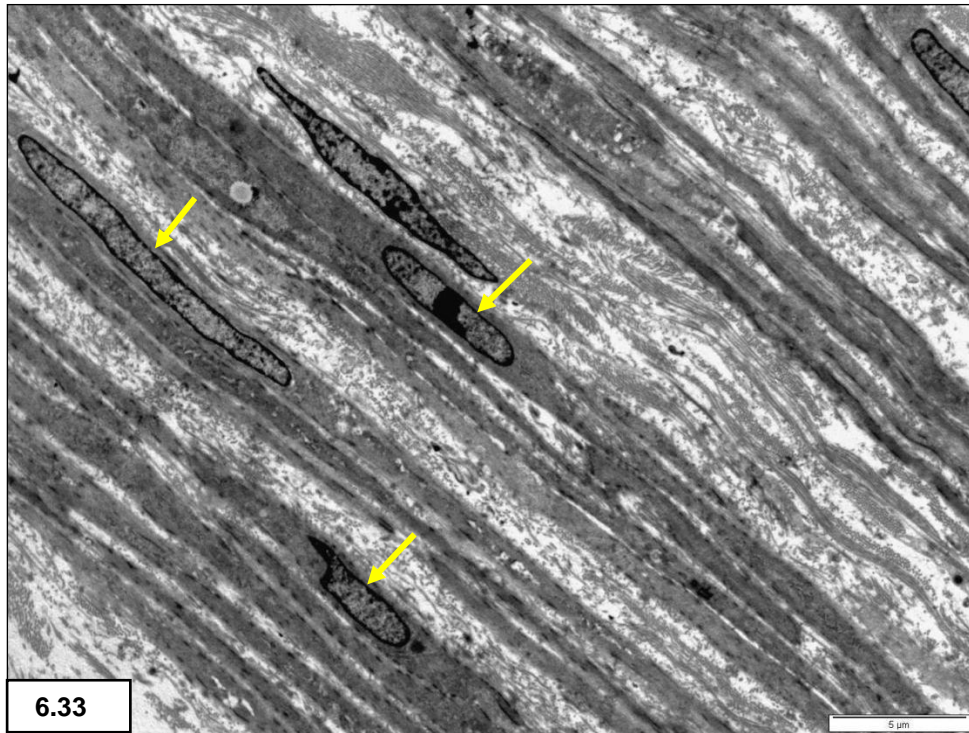
Figure 6.33: *Muscularis externa - s*mooth muscle cells and collagen fibre layers. Note smooth-contoured nuclear membranes (arrows) of muscle cells.
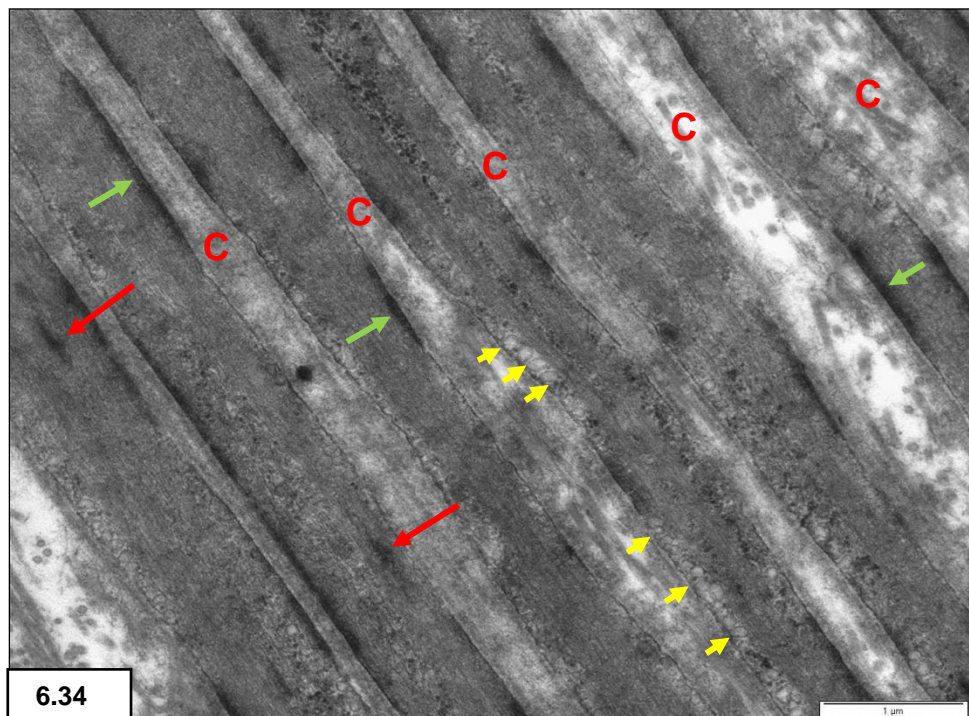
Figure 6.34: Intermediate filaments forming dense bodies (red arrows) and subplasmalemmal dense plaques (green arrows) in smooth muscle cells. Note cell surface pinocytotic vesicles (yellow arrows).Intervening collagen fibres (**C**).
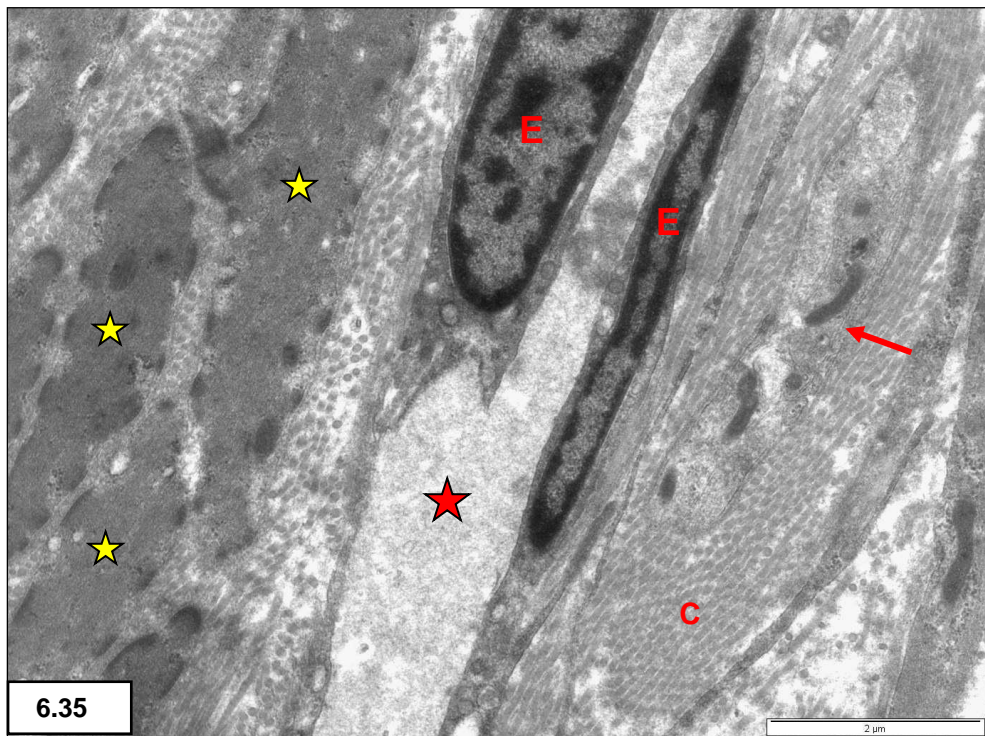
Figure 6.35: *Muscularis externa* - lymphatic vessel (red star), endothelial cells (**E**) smooth muscle cells (yellow stars) fibroblast (arrow). Collagen fibre (**C**).
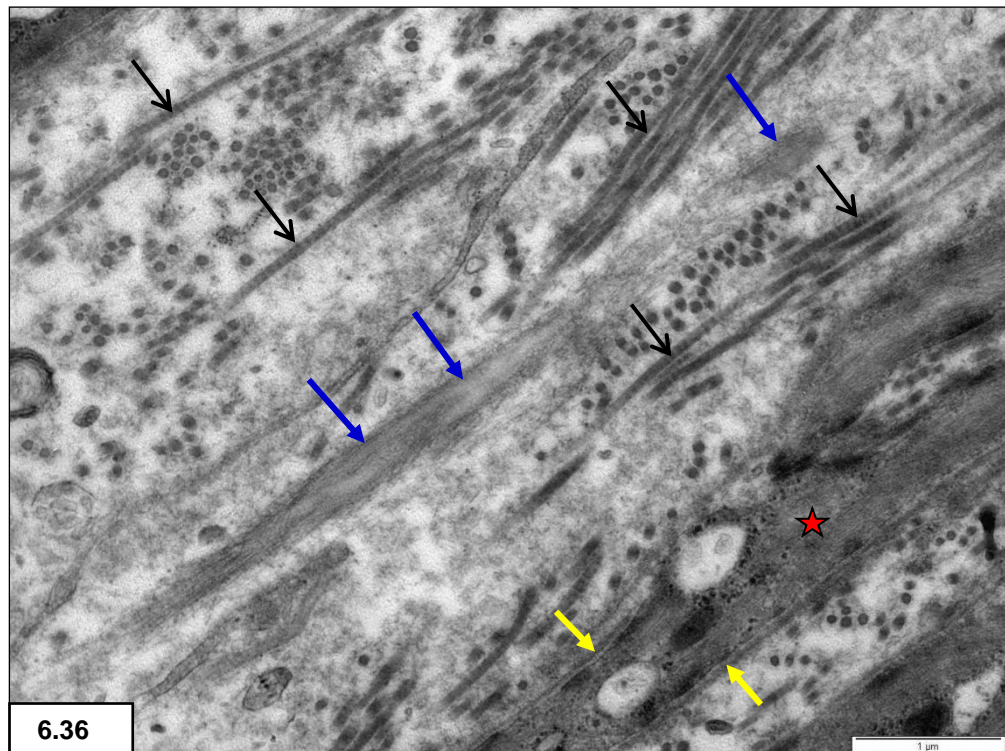
Figure 6.36: Elastic fibre (blue arrows), smooth muscle cell (star) surrounded by an external lamina (yellow arrows). Collagen fibrils (black arrows).
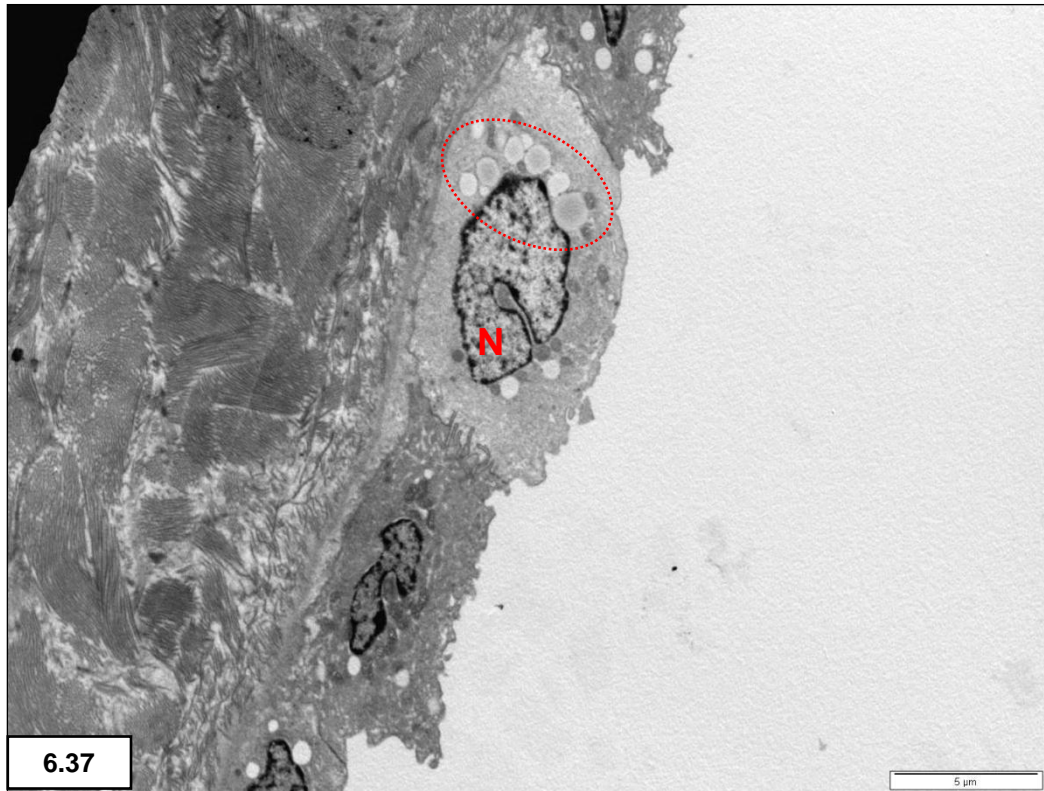
Figure 6.37: Serosa - dark and light staining mesothelial cells with clefted nuclei (**N**) and lipid droplets (dashed circle).
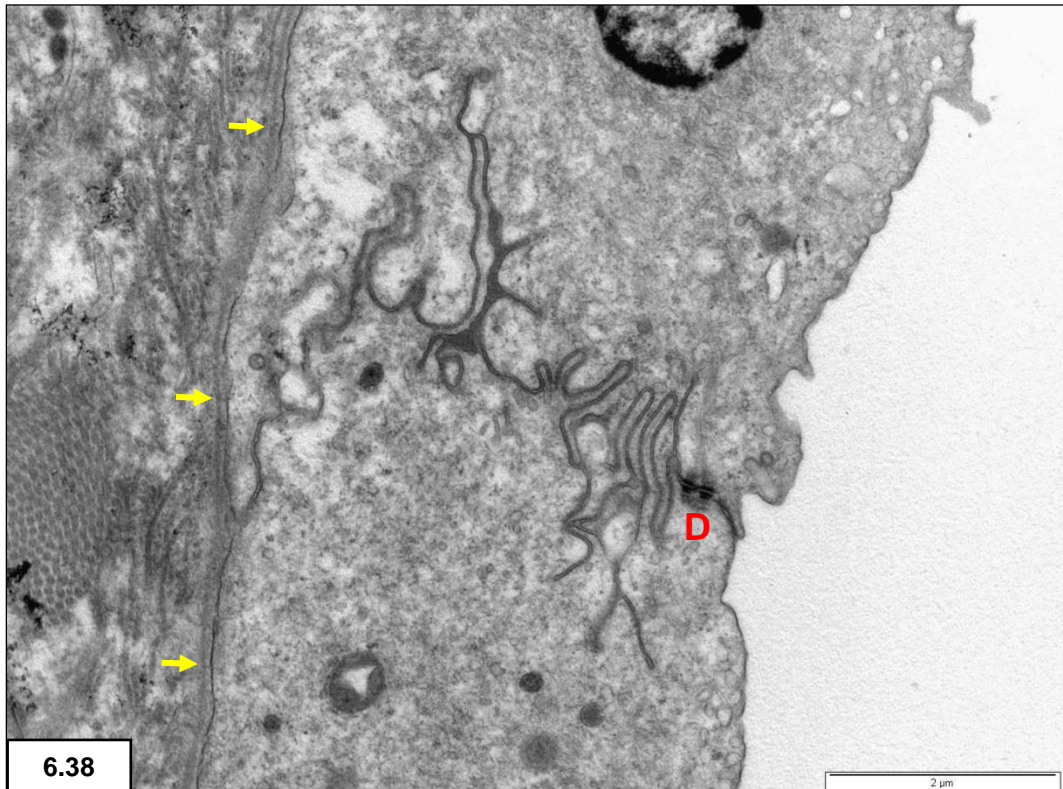
Figure 6.38: Interdigitations and desmosomes (D) between neighbouring mesothelial cells. Note the prominent basal lamina (arrows).
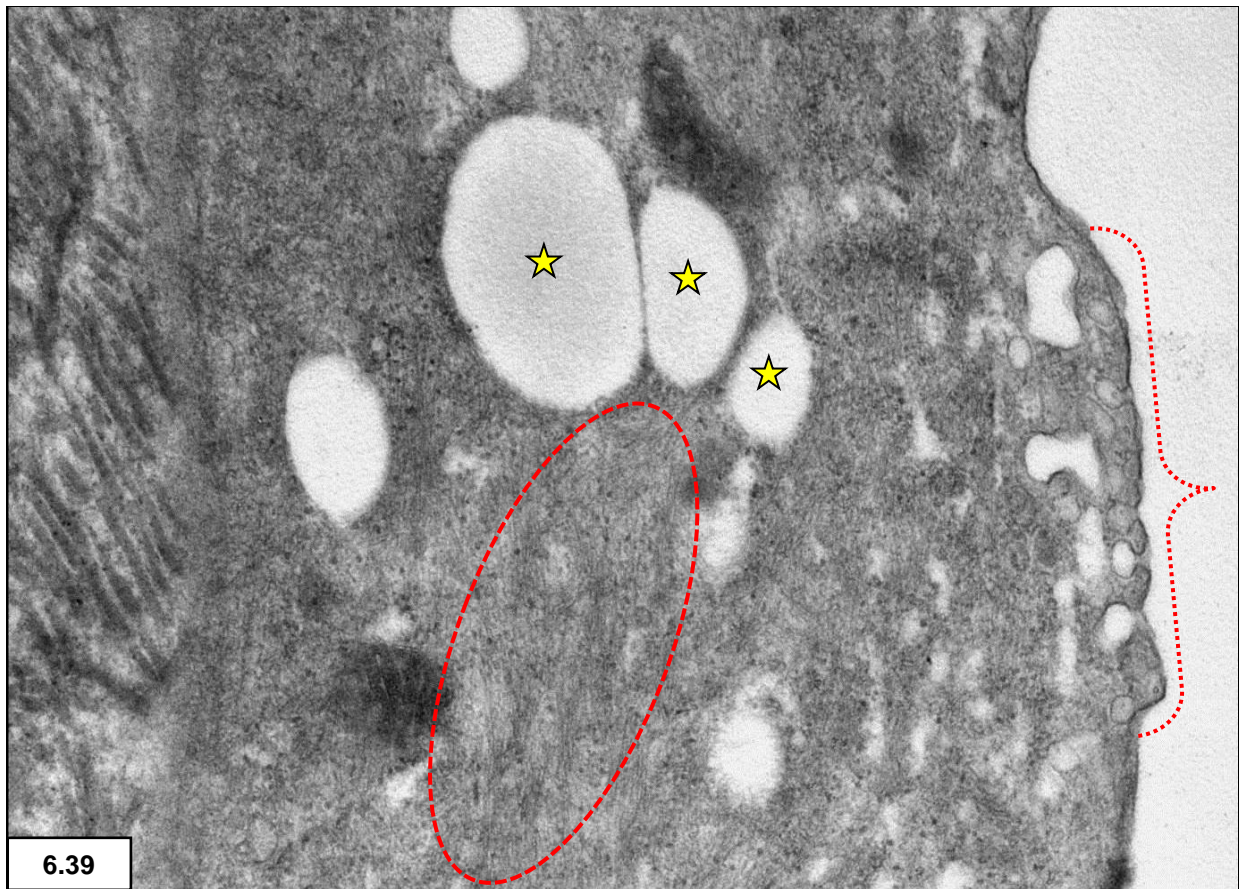
Figure 6.39: Serosa - large pinocytotic vesicles at the cell surface (bracket). Note lipid droplets (stars) and intermediate filaments (dashed circle).

CHAPTER 6
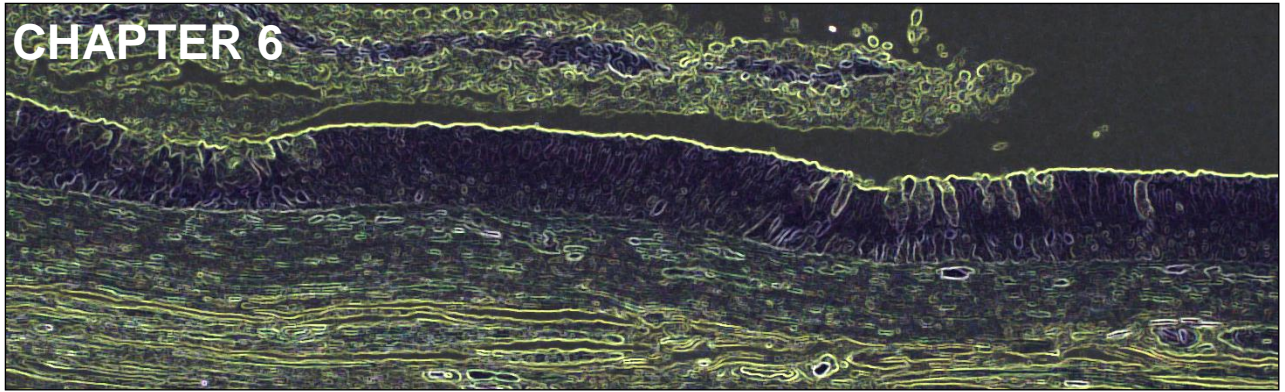
LIGHT MICROSCOPY AND TRANSMISSION ELECTRON MICROSCOPY OF THE GALLBLADDER

6.1 INTRODUCTION

Histology textbooks and internet websites cover the histology and transmission electron microscopy of the vertebrate gallbladder adequately (Ross *et al.* 2003; Junqueira *et al.* 1975; www.pathologyoutlines.com). A few publications contain merely superficial information regarding reptilian gallbladder histology (Schaffner 1998; Moura *et al.* 2009; McClellan-Green *et al.* 2006; Jacobson 2007). Silveira & Mimura (1999) gave more insight into the histology of the gallbladder of the snake *Bothrops jararaca.* Oldham-Ott & Gilloteaux (1997) reviewed the morphology, including light microscopy, transmission and scanning electron microscopy, of the gallbladder in amphibians, fish, reptiles (excluding crocodiles), birds and mammals. The authors found that although some morphological differences were present between vertebrates, their gallbladders were essentially similar and that reptilian gallbladders were morphologically the closest to the mammalian gallbladder. The literature is clearly lacking in microscopical descriptions of the gallbladder in crocodiles and observations on the Nile crocodile gallbladder will therefore unavoidably have to be compared to findings in other vertebrates.

6.2 LIGHT MICROSCOPY

6.2.1 MATERIALS AND METHODS

The gallbladders were separated from the perfused livers of five juvenile Nile crocodiles and their walls sampled from three different areas for immersion fixation in, namely near the cystic duct (neck), from the body and at the blind end (fundus). The samples were fixed in 10% acqueous buffered formalin for 24 hours to two weeks before dehydrating through a graded ethanol series, clearing in xylene and infiltrating with paraffin wax in a Shandon Excelsior Thermo Electron Corporation Tissue Processor. The samples were then embedded using a Thermolyne Histo Center 2 Embedding Unit and 3 to 5 micron thick sections were cut with a Reichert Jung rotary microtome. The following stains were used to demonstrate gallbladder architecture: haematoxylin & eosin (H/E; n=8), Periodic Acid-Schiff reaction (PAS; n=1) and PAS with diastase treatment (PAS-D; n=1) (Bancroft & Stevens 2003). Semi-thin toluidine blue stained resin sections (0.3 µm; n=54) were also examined to evaluate the appearance of the gallbladder at the light microscopy level (refer to section 6.3.1).

6.2.2 IMAGE CAPTURING & PROCESSING

Slides (n=64) were examined by brightfield illumination with an Olympus BX63 (Hamburg, Germany) compound microscope and images were recorded by an Olympus DP72 digital camera. The Olympus CellSense software, version 1.5, was used to adjust the brightness and contrast, and a sharpening filter was applied where required.

6.2.3 RESULTS

The gallbladder wall comprised three layers, namely, a mucosa that was subdivided into an epithelium and a *lamina propria*, a *muscularis externa* and a serosa, including a subserosa (Fig. 6.1).

The **mucosal epithelial layer** lined the gallbladder lumen and irregular shallow folding (Fig. 6.2) was apparent. In all three sampling zones the epithelium appeared to be composed of a mixture of simple and pseudostratified columnar epithelium. A single layer of basal nuclei indicated the presence of a simple columnar epithelium in certain areas whereas simple columnar epithelium merging with pseudostratified columnar epithelium

was present in other areas (Figs. 6.3 A & B). The epithelium presented with a combination of light and dark cells staining with the dark cells being slimmer and at times shorter than the neighbouring light cells (Fig. 6.4). The apical and basal cytoplasm was filled with PAS-positive (pink-staining) granules, giving these cells the appearance of slender goblet cells (Fig. 6.5). The fine granular PAS-positivity in the basal cytoplasm disappeared after diastase treatment (PAS-D) indicating the presence of glycogen (Fig. 6.6). The pink-staining apical granules remained, however, demonstrating their mucinous nature. Semi-thin toluidine blue resin sections revealed a faint pink metachromasia in the cytoplasm confirming the presence of mucin and glycogen (Fig. 6.7 B). Bulging of the epithelial cell apices (Figs. 6.8 A & B) were noted in some regions and other areas presented with exocytosis of secretory granules (Fig. 6.7 B) or a total loss of cell apices (Figs. 6.9 A & B). More dark cells were present in the areas where secretion or recovery was seen to be taking place (Fig. 6.7 A), and in one gallbladder large lipid-like globules (Fig. 6.9 B) were seen in the lumen next to the epithelium. Nuclei in the pseudostratified portions were arranged at different levels (Fig.6.10) in the basal third of the epithelium. Nucleoli, sometimes more than one per nucleus, were evident and a few had a distinctive red colour (Fig. 6.10). A few lymphocytes were present, mostly in the basal layer, with only some traversing the epithelium. Basal lymphocyte numbers were increased in areas of apical loss. Scanty large vacuolar areas were noted throughout the epithelium (Fig. 6.8 A). A PAS-positive basement membrane (Fig. 6.6) separated the epithelium from the *lamina propria* (Fig. 6.1) that consisted of blood vessels, lymphocytes and plasma cells in a collagenous stroma containing fibroblasts, collagen fibres and nerve ganglia. No glands were seen in this layer.

A ***muscularis externa*** (Fig. 6.1) was found external to the *lamina propria.* Smooth muscle cells (Fig. 6.9 B), with intervening collagen and fibroblasts, were seen at this level. Nerve ganglia, lymphatic and blood vessels were also present throughout the muscular layer.

The **serosa** (Fig. 6.11) consisted of a layer of simple squamous epithelium, the mesothelium, supported by a subserosa comprising connective tissue. Some mesothelial cells occasionally displayed a darker cytoplasm than others. Collagen fibres and blood vessels were present in the underlying connective tissue.

6.3 TRANSMISSION ELECTRON MICROSCOPY

6.3.1 MATERIALS AND METHODS

Parallel samples (n=15) of the three gallbladder zones were fixed in 2.5% glutaraldehyde in Millonig's buffer (pH 7.2), rinsed in Millonig's buffer, post-fixed in 1% osmium tetroxide in the same buffer, rinsed again and dehydrated through a series of graded ethanol before being infiltrated with propylene oxide and an epoxy resin and finally embedded in absolute epoxy resin. Tissue blocks were sectioned with a Reichert-Jung Ultramicrotome. Semi-thin resin sections (0.3 µm) were stained with 1% toluidine blue in borax and ultra-thin (50-90 nm) sections were collected onto copper grids (n=36) and stained with Reynold's lead citrate and an acqueous saturated solution of uranyl acetate (Hayat 2000).

6.3.2 IMAGE CAPTURING & PROCESSING

The grids (n=36) were examined with a Philips CM 10 transmission electron microscope (Eindhoven, Netherlands) operated at 80 kV. A Megaview III side-mounted digital camera was used to capture the images and the iTEM software (Olympus Soft Imaging System, GMBH) to adjust the brightness and contrast.

6.3.3 RESULTS

The **pseudostratified columnar epithelial cells** (see Figures 6.12 A & B) of the mucosa, revealed the following morphological features:

- Irregularly arranged apical microvilli, mostly uniform in shape and size, but a few with a staghorn, branching or club-shaped configuration (Fig. 6.14) and some being longer than others. Individual microvilli were covered by a glycocalyx.
- Apical junctional complexes (Figs. 6.15 & 6.17 B)
- Scanty cilia in a few cells, a single cilium per cell (Fig. 6.16)
- Desmosomes between deeper lateral cell borders (Fig. 6.22 A)
- Secretory granules (Figs. 6.13 & 6.17 A & B) containing mucus glycoproteins, mostly of medium electron density, but some more electron dense – found mostly in the apical cytoplasm, but also present in the basal portions of the cells

- Protrusions of the cytoplasm (Figs. 6.17 A & B), decapitation (pinching off) of apical cytoplasm (Figs. 6.19 A & B) and secretion of granule content into lumen (Figs. 6.18 A & B) – the microvilli were reduced or absent in these cells (Fig. 6.17 A & B)

- Lysosomes – some containing whorled membranes (Fig. 6.25)

- Apical and basal concentrations of mitochondria (Figs. 6.13 & 6.25) - the apical mitochondria was obscured in certain cells due to accumulations of secretory granules

- Golgi & granular endoplasmic reticulum (Fig. 6.22 B)

- Lipid-like globules in close association with the epithelial surface (Fig. 6.21)

- Monoparticulate glycogen particles, mostly seen in the basal cytoplasm (Fig. 6.24 A), but in a few instances (evident after release of secretory granules) in the subapical regions

- Scanty cytoplasmic calcium deposits (Fig. 6.26)

- Lateral (Figs. 6.22 A & B) and basolateral (Fig. 6.28) cell membrane interdigitations

- Intermediate filaments (Fig. 6.24 B)

- Large oval-shaped nuclei with smooth contours (Fig. 6.13)(in the resting phase), corrugated contours in active phase (Figs. 6.20 A & B)

- Distinctive round electron-dense nucleoli (comparable to red nucleoli seen in Figure 6.10) in some nuclei, in addition to 'normal' nucleoli – often the two different nucleoli were present in the same nucleus (Fig. 6.23)

Darker staining cells (Figs. 6.12 A & B), containing secretory granules and large collections of glycogen granules (Fig. 6.24 A), were present between lighter staining epithelial cells. The dark cells were slimmer than the light cells and some of them lacked secretory granules. The epithelial cells resembled slender goblet cells due to the accumulation of the subapical secretory granules (Fig. 6.13). The presence of the granules resulted in bulging of the cell apices into the gallbladder (Figs. 6.17 A & B). The luminal surface of these cells was almost devoid of microvilli. The secretory granules were seen to merge with the cytoplasmic membrane with release of their contents into the lumen (Figs. 6.18 A & B). In certain instances fusion of granules with resultant formation of large vacuoles seemed to take place before luminal release (Fig. 6.17 B). Loose-lying apical cellular structures containing secretory granules were similarly evident in the lumen (Fig. 6.19 B). Some cell apices were completely disrupted with the resultant loss of

cytoplasmic structures, leaving gaps in the epithelial lining (Figs. 6.20 A & B). Dark cells increased in number in areas of apical loss (Figs. 6.20 A & B) with the epithelium on occasion displaying only a single layer of dark basal nuclei. This finding dispelled the light microscopical impression that simple columnar epithelium co-existed with pseudostratified columnar epithelium. Occasional large cytoplasmic vacuoles, also seen light microscopically in the epithelium, filled with membranous debris (Fig. 6.27), were present in macrophages. A few lymphocytes were found in the basal epithelium and were also observed traversing the epithelium, with an increase of lymphocytes being noted in the regions of apical loss (Figs. 6.20 A & B). The epithelial cells rested on a continuous basal lamina that was mostly undulating (Fig. 6.28). Hemidesmosomes were identified where the cell membrane and basal lamina abutted (Fig. 6.28). The basal lamina seemed to be thickened underneath regions of apical loss (Fig. 6.29).

In the *lamina propria,* below the basal lamina, blood vessels and nerve ganglia (Fig. 6.31), surrounded by fibroblasts and sheets of collagen fibres, were present. The occasional eosinophil, plasma cell or lymphocyte was also found. Lymphocytes were more numerous in the vicinity of the basal lamina beneath areas of apical loss (Fig. 6.20 B). A few smooth muscle cells (Fig. 6.30), containing filaments forming densities and subplasmalemmal plaques, were seen between the collagen fibres. A small number of melanin granules (Fig. 6.32) were scattered among the collagen fibres in one gallbladder.

Subjacent to the *lamina propria* were prominent layers of alternating smooth muscle cells and collagen fibres (Fig. 6.33) which constituted the bulk of the **muscular layer**. However, the chief components were the smooth muscle cells that were mainly sectioned in the longitudinal plane. These cells were each surrounded by a thin, distinct external lamina and contained numerous intermediate filaments forming focal densities and subplasmalemmal dense plaques (Fig. 6.34). Elongated nuclei with mainly smooth contours were noted in the smooth muscle cells (Fig. 6.33). Many pinocytotic vesicles were identified at the cell surfaces. Scattered fragments of elastic fibres (Fig. 6.36), as well as lymphatic (Fig. 6.35) and blood vessels, were found lying between the smooth muscle cells and the collagen fibres. Nerve ganglia that occasionally included myelinated nerve fibres were present among the muscle cells.

The **serosa** consisted of a single layer of mesothelial cells (Fig.6.37) resting on an even basal lamina (Fig. 6.38). The cells contained indented nuclei and showed prominent

cytoplasmic interdigitations and desmosomes (Fig. 6.38) between neighbouring cells. Numerous large pinocytotic vesicles were located at the cell surfaces (Fig. 6.39). Cytoplasmic lipid droplets, mitochondria and intermediate filaments were present (Fig. 6.39).The cytoplasm of some cells was more electron-dense than others (Fig. 6.37) even though their ultrastructural features were similar. A connective tissue subserosa consisting of blood vessels surrounded by a collagenous stroma supported the basal lamina.

6.4 DISCUSSION

The gallbladder wall of reptiles is organised into an epithelial layer, a *lamina propria,* a muscular and a serosal layer (Gilloteaux 1997; Oldham-Ott & Gilloteaux 1997; Silveira & Mimura 1999) and was identical to that found in the juvenile Nile crocodile. As in other vertebrates a *muscularis mucosae* and submucosa (Junqueira *et al.* 1975; Ross *et al.* 2003; www.pathologyoutlines.com) were absent in the Nile crocodile gallbladder.

Several authors agree that the gallbladder **mucosa** of vertebrates, including reptiles, consists of either a simple or a pseudostratified columnar epithelium (Gilloteaux 1997; Oldham-Ott & Gilloteaux 1997; Schaffner 1998; Silveira & Mimura 1999; Moura *et al.* 2003; Mcclellan-Green *et al.* 2006; Jacobson 2007). Simple columnar epithelium could not be demonstrated in the juvenile Nile crocodile - the single layer of basal nuclei observed with the light microscope was seen with the electron microscope to be due to the loss of the apical cytoplasm. In higher vertebrates there is maturation of the gallbladder epithelium from pseudostratified in the embryo to simple high columnar epithelium in the adult (Silveira & Mimura 1999). Adult Nile crocodile gallbladders will need to be examined to establish whether the pseudostratified epithelium found in juveniles is merely a developmental stage.

Surface microvilli, junctional complexes and basolateral interdigitations correspond to the normal features of absorptive cells (Ross *et al.* 2003). The microvilli in this study were not as numerous or regular as those found in typical brush borders – the reason for the decrease in microvilli in the bulging apices is conceivably to allow for cell membrane permeability during exocytosis as described in the rabbit (Frederiksen *et al.* 1979). Single long microvilli were also found by Oldham-Ott and Gilloteaux (1997) in their study of the lizard gallbladder to which they ascribed a possible mechano- or chemo-sensory function. The scanty columnar brush cells found in the mouse (Luciano & Reale 1997) and in some

reptilian (Oldham-Ott and Gilloteaux 1997) gallbladders were not evident in the ultra-thin sections of the Nile crocodile gallbladder. Scanning electron microscopy however may reveal the presence of brush cells in this species. The cilia on the cell surface and the desmosomes situated between the deeper lateral cell borders observed in the present study were not mentioned in the cited publications. The fact that a single cilium per cell was seen in only a few cells may suggest a sensory role for these sparse cilia (Ross *et al.* 2003). Lipids are known to be absorbed from bile in human gallbladders (Hopwood & Ross 1997). In the present study the luminal lipid globules seen were possibly being absorbed by the epithelial cells and the large debris-filled vacuoles within the epithelium were perhaps a transient phase in the clearing of cellular remnants from the gallbladder lumen.

The goblet cell is not a normal constituent of the gallbladder epithelium in some mammals (Hayward 1962; www.pathologyoutlines.com), but its existence was briefly mentioned in reptiles (Oldham-Ott & Gilloteaux 1997; Schaffner 1998). The gallbladder epithelium of the juvenile Nile crocodile in the resting phase of the secretory cycle consisted in its entirety of slender goblet cells. The clustering of secretory granules in the subapical region of the Nile crocodile gallbladder epithelium is the first phase of the secretory cycle and comparable with the situation mentioned by Kuver *et al.* (2000) in the mouse gallbladder. The apical bulging, exocytosis of mucous granules and the stripping of the apical structures into the lumen are further sequential stages of the mucus secretory cycle (Lee 1980; Gilloteaux 1997; Oldham-Ott & Gilloteaux 1997; Kuver *et al.* 2000). There seems to be a combination of merocrine (exocytosis), apocrine (pinching off of apical cell cytoplasm) and to some extent holocrine (shedding of the whole cell containing cell product) secretion occurring in the Nile crocodile gallbladder epithelium. The lysosomes containing whorled membranes in the present study appeared similar to the myelinosomes described by Ghadially (1988). This author also refers to the secretory granules in alveolar cells as myelinosomes and perhaps the 'lysosomes' in the current study are rather precursor secretory granules. Glands, probably responsible for the mucus component in bile, were found in the *lamina propria* of mammals (Gilloteaux 1997) and in some reptiles (Oldham-Ott & Gilloteaux 1997), but were absent in Nile crocodile. The function of mucus production most likely belongs to the surface epithelial cells of the Nile crocodile gallbladder. The Nile crocodile gallbladder epithelium clearly has both absorptive and

secretory functions. This was also found to be true for mammalian gallbladders (Madrid *et al.* 1997).

Dark cells are known to appear in the normal human gallbladder epithelium and there is speculation that this is due to cellular dehydration (Ghadially 1998). The finding of dark cells among the lighter epithelial cells in the Nile crocodile epithelium is in agreement with this inference as active fluid transport for bile concentration supposedly occurs from the lumen across the gallbladder epithelium. Dark cells may also be a forerunner of dying cells (Ghadially 1998) and in the present study this may be the reason for the proliferation of dark cells in areas of secretory activity, i.e. perhaps the dark cells die off after secretion. In contrast to this deduction, large areas of the epithelium consisted only of dark basal nuclei in sections of total apical loss – possibly these cells act as stem cells to balance cell turnover. Ross *et al.* (2003) explained that in certain pseudostratified epithelia the basal cells are stem cells that produce the functional epithelial cells thus balancing cell turnover. Lamote & Willems (1997) found that the normal gallbladder has a low cell turnover rate, but that abnormal circumstances could trigger proliferative activity. The nucleoli found in the nuclei of human gallbladder epithelium were described as indistinct (www.pathologyoutlines.com), but those of the Nile crocodile were very distinctive in their round shape and intense, uniform electron-density.

The increase of lymphocytes in the basal epithelium as well as in the underlying *lamina propria* in regions of apical loss may be a defense mechanism in a compromised epithelium. Concomitant with this deduction is the thicker basal lamina in these regions that may serve to strengthen the gallbladder wall. The presence of a thicker basal lamina was not cited by other authors, but Hopwood & Ross (1997) mentioned the importance of basement membranes allowing the movement of regenerating cells during tissue renewal.

Gilloteaux (1997) mentioned the presence of nerve ganglia between the fibromuscular and the subserosal layers in the vertebrate gallbladder – in the Nile crocodile nerve ganglia were also present in the ***lamina propria***. Melanin is known as a free radical trap in reptilian livers (McClellan-Green *et al.* 2006) and the free-lying melanin granules found between the collagen fibrils in this study may function in this regard. Glands that are variably present in this layer in other vertebrates (Gilloteaux 1997) were not seen in the Nile crocodile.

The present ultrastructural report of the smooth muscle cells in the **muscular layer** of the Nile crocodile gallbladder is almost identical to the description of smooth muscle cells given by Ghadially (1998), the only exception being the smooth-contoured nuclear outline. Ghadially (1998) also described these nuclei as folded, notched or showing many invaginations. Fragmented elastic fibres were found between the muscle-collagen layers in the *muscularis externa*, but their existence was not specified in other reptiles. In humans elastic tissue was noted in the subserosal layer (www.pathologyoutlines.com). Rokitansky-Aschoff crypts and the Canals of Luschka seen in the fibromuscular layer of other vertebrates (Gilloteaux 1997) were absent in the Nile crocodile gallbladder sections examined.

Descriptions (Junqueira *et al.* 1975; Ross *et al.* 2003) of the **serosa** are limited to the mere mentioning of connective tissue, blood and lymphatic vessels covered by a simple squamous epithelium. The serosa and subserosa in the Nile crocodile gallbladder is similar to the general vertebrate pattern.

6.5 REFERENCES

BANCROFT, J.D. & STEVENS, A. 2003. *Theory and practice of histological techniques.* Churchill Livingstone, New York.

FREDERIKSEN, O., MØLLGÅRD, K. & ROSTGAARD, J. 1979 Lack of correlation between transepithelial transport capacity and paracellular pathway ultrastructure in alcian blue-treated rabbit gallbladders. *Journal of Cell Biology,* 83: 383-393.

GHADIALLY, F.N. 1988. *Ultrastructural pathology of the cell and matrix.* Butterworths, London.

GILLOTEAUX, J. 1997. Introduction to the biliary tract, the gallbladder, and gallstones. *Microscopy Research and Technique,* 38: 547-551.

HAYAT, M.A. 2000. *Principles and techniques of electron microscopy: biological applications.* Cambridge University Press, Cambridge, UK.

HAYWARD, A. F. 1962. Aspects of the fine structure of the gallbladder epithelium of the mouse. *Journal of Anatomy,* 96: 227-236.

HOPWOOD, D. & ROSS, P.E. 1997. Biochemical and morphological correlations in human gallbladder with reference to membrane permeability. *Microscopy Research and Technique,* 38: 631– 642.

JACOBSON, E.R. 2007. Overview of reptile biology, anatomy, and histology, in *Infectious diseases and pathology of reptiles,* edited by E.R. Jacobson. CRC Press, Taylor & Francis Group, 6000 Broken Sound Parkway NW, Suite 300, Boca Raton, FL 33487-2742, pp. 1-130.

JUNQUEIRA, L.C., CARNEIRO, J & CONTOPOULUS, A.N. 1975. *Basic histology.* Lange Medical Publications, Los Altos, California.

KUVER, R., KLINKSPOOR, J.H., OSBORNE, W.R.H. & LEE, S.P. 2000. Mucous granule exocytosis and CFTR expression in gallbladder epithelium. *Glycobiology,* 10: 149-157.

LAMOTE, J. & WILLEMS, G. 1997. DNA synthesis, cell proliferation index in normal and abnormal gallbladder epithelium. *Microscopy Research and Technique,* 38: 609–615.

LEE, S. P. 1980. The mechanism of mucus secretion by the gallbladder epithelium. *British Journal of Experimental Pathology*, 61: 117-119.

LUCIANO, L. & REALE, E. 1997. Presence of brush cells in the mouse gallbladder. *Microscopy Research and Technique,* 38:598–608.

MADRID, J.F., HERNANDEZ, F. & BALLESTA, J. 1997. Characterization of glycoproteins in the epithelial cells of human and other mammalian gallbladder. A review. *Microscopy Research and Technique,* 38: 616–630.

MCCLELLAN-GREEN, P., CELANDER, M. & OBERDÖRSTER, E. 2006. Hepatic, renal and adrenal toxicology, in *Toxicology of reptiles,* edited by S.C. Gardner & E. Oberdörster. CRC Press, Taylor & Francis Group, 6000 Broken Sound Parkway NW, Suite 300, Boca Raton, FL 33487-2742, pp. 123-148.

MOURA, L.R., SANTOS, A.L.Q., BELLETI, M.E., VIEIRA, L.G., ORPINELLI, S.R.T. & DE SIMONE, S.B.S. 2009. Morphological aspects of the liver of the freshwater turtle *Phrynops geoffroanus* Schweigger, 1812 (Testudines, Chelidae). *Brazilian Journal of Morphological Science,* 26: 129-134.

OLDHAM-OTT, C.K. & GILLOTEAUX, J. 1997. Comparative morphology of the gallbladder and biliary tract in vertebrates: variation in structure, homology in function and gallstones. *Microscopy Research and Technique,* 38: 571-597.

ROSS, M.H., KAYE, G.I. & PAWLINA, W. 2003. *Histology: a text and atlas.* 4th ed. Lippincott Williams & Wilkens, Baltimore, USA.

SCHAFFNER, F. 1998. The hepatic system, in *Biology of reptilia: volume 19, Morphology G: Visceral organs,* edited by C. Gans & A.B. Gaunt. Society for the Study of Amphibians and Reptiles, Missouri, pp. 485-531.

SILVEIRA, P.F. & MIMURA, O.M. 1999. Concentrating ability of the *Bothrops jararaca* gallbladder. *Comparative Biochemistry and Physiology,* Part A, 123: 25–33.

WWW site references:

www.pathologyoutlines.com

CHAPTER 7

GENERAL CONCLUSIONS

The micro-morphology of the juvenile Nile crocodile liver and gallbladder has not previously been described. Selected information is available on reptiles in general and more specifically on the Saltwater crocodile, the West African crocodile and the caiman. It is essential to have a thorough knowledge of the normal histology and ultrastructure of the liver and gallbladder in order to properly evaluate the pathology of disease in these organs of the Nile crocodile. Due to the shortage of information on the subject matter, this study had to rely on findings in other vertebrates for assessment and comparison. The study illustrated the topography, gross anatomy, histology and ultrastructure of the liver and gallbladder of *Crocodylus niloticus.* The emphasis was on distinguishing the different cell populations by using light microscopy and transmission electron microscopy.

The two liver lobes were connected dorso-medially by an isthmus, which also consisted of liver tissue, and were located in the coelomic cavity demarcated by the post-pulmonary and post-hepatic membranes. The right lobe was larger than the left lobe, with both lobes having a triangular shape. The isthmus in this species may be a developmental adaptation to allow for the inclusion of other organs in the body cavity.

The **light microscopical features** of the liver in this study confirmed the findings in most reptiles and in the few crocodilians investigated, namely, that the classic lobular growth pattern could not be identified and was indeed absent from the juvenile Nile crocodile. Instead, a haphazard sinusoidal and portal tract arrangement determined the parenchymal growth pattern. The cross-sectional parenchymal tubular structures were similar to the descriptions in four non-mammalian vertebrate classes and in the two crocodilian species, *Caiman latirostris* and *Osteoleamus.* The tubules consisted of four to five pyramidal hepatocytes surrounding a central lumen. In the longitudinal sectioning plane the tubules consisted of two-cell-thick plates with an elongated lumen. The liver cords were seen to

branch and anastomose. The nuclei of the hepatocytes were eccentrically located nearest to the sinusoidal lumen as in some reptiles and in the West African crocodile. Peribiliary cytoplasmic granules were positive for hemosiderin and variably sized lipid droplets and glycogen were present.

The non-parenchymal component of the liver consisted of sinusoids lined by flat endothelial cells, accompanied by Kupffer cells and extrasinusoidal stellate cells. The shape of the sinusoids were intermediary between sacculosinusoidal and tubulosinusoidal, i.e. irregular and angular, and therefore the same as that of young alligators. Many single Kupffer cells were found in different locations in the liver, namely, in the sinusoid, in the space of Disse and forming part of groups of hepatocytes. This differs from other reptiles where the Kupffer cell was either bound to the sinusoidal wall or prominent Kupffer cell collections were noted or the cell was a rare finding. The cells contained large inclusions consisting of melanin, hemosiderin and a third component that stained pink with the PAS reaction.

The liver was enclosed by a noticeable fibrous covering, Glisson's capsule, which extended fibrous trabeculae into the parenchyma with the trabeculae traversing the parenchyma in a haphazard manner. The fibrous trabeculae are suggested to prevent damage to the liver during trashing movements of the crocodile. A prominent collagenous sheath containing fibroblasts, plasma cells, lymphocytes and phagocytes surrounded the portal tract areas. A delicate network of reticular fibers existed around the parenchymal tubules.

The architectural components of the juvenile *Crocodylus niloticus* liver were further clarified by **transmission electron microscopical examination**. The large polygonal hepatocytes contained eccentric nuclei displaying compact nucleoli consisting of variably arranged electron-dense material. The cytoplasm was filled with alpha or beta glycogen particles and contained variable numbers and sizes of lipid droplets. Many mitochondria with matrix granules, peroxisomes with an amorphous content, peribiliary lysosomes containing hemosiderin granules and cholesterol slits, were present. Occasional centrioles, melanin granules and prominent bile pigments were exhibited. Granular and smooth endoplasmic reticulum and pericanalicular Golgi complexes were identified. The apical surfaces extended microvilli into bile canalicular lumina that were sealed off by junctional complexes. Unlike in mammals, bile canaliculi were absent between the lateral borders of

the hepatocytes in the juvenile Nile crocodile. Desmosomes and microvilli were present between lateral cell membranes. Certain reptiles display a basal lamina around hepatocyte groups, but in the Nile crocodile a basal lamina was only present in support of hepatocyte groups next to Glisson's capsule. Most groups of hepatocytes were surrounded by reticular fibres and scanty collagen fibres instead.

Endothelial cells with flattened nuclei and long, thin fenestrated cytoplasmic extensions lined the sinusoids. When active their nuclei and cytoplasm bulged into the sinusoidal spaces. Numerous pinocytotic vesicles and lysosomes attested to the transmembranous activity of the endothelial cells. The basement membrane normally surrounding blood vessels was absent around the sinusoids – instead the space of Disse consisting of a clear area displaying microvilli extending from the base of the hepatocyte, and cytoplasmic projections of stellate and myofibroblastic cells, was present.

The Kupffer cells of *Crocodylus niloticus* were highly mobile cells found in different locations in and around the sinusoids and as part of hepatocyte groups. This differs from other vertebrates where these cells were described as fixed cells or resident in the sinusoidal lumen. Large phagosomes contained three different elements, notably melanin, hemosiderin and ceroid. Melanin is synthesised by the Kupffer cells and traps the potentially harmful superoxides formed by iron as a defensive reaction. Ceroid was the third 'pink' component seen with the PAS reaction as these crocodiles were too young to have accumulated the 'wear and tear' pigment lipofuscin. Lipid droplets were a normal constituent of most Kupffer cells in contrast to mammalian Kupffer cells where they were absent. The vermiform processes found in other vertebrates were absent. The most conspicuous structure, namely the 'tubulosomes', found in the Nile crocodile Kupffer cells, have not been described in other reptiles. These organelles may have the tripartite function of breaking down phagosome contents, melanin synthesis and promoting cell mobility. The melanomacrophages seen forming part of hepatocyte groups were also designated Kupffer cells due to their analogous cytoplasmic content.

Stellate cells, regarded as the storage site for vitamin A, were located in the space of Disse and contained a few large non-membrane bound lipid droplets sometimes displacing and indenting the nucleus. This differs from the numerous lipid droplets found in the stellate cells of the West African crocodile. The cells extended long subendothelial cytoplasmic processes and were in close contact with the endothelial cells, as well as

Kupffer cells and myofibroblastic cells in the space of Disse. Some stellate cells exhibited a solitary cilium protruding into the space of Disse and a chemoreceptor or sensory function was ascribed to these immotile cilia. Sparse multivesicular bodies were found in contrast to the West African crocodile that showed a consistent presence of these bodies. Stellate cell cytoplasm contained filaments, microtubules, coated and pinocytotic vesicles.

Another type of cell was found in the same location in the space of Disse as the stellate cells – the two cells sometimes occurred simultaneously. This cell displayed features of both fibroblasts and smooth muscle cells and was called a myofibroblastic cell. Lipid droplets were absent and filaments forming densities and subplasmalemmal plaques as well as dilated granular endoplasmic reticulum were noted. The myofroblastic cells may be responsible for regulating the sinusoidal blood flow and for maintaining the extracellular connective tissue component. Previous reports stated that hepatic stellate cells lose their vitamin A content and transform into myofibroblasts during detrimental circumstances. However, both the stellate cell and the myofibroblastic cell were present simultaneously in the same location – perhaps these are two different cell populations with different functions. Another explanation is that differentiation from stellate into myofibroblastic cell occurs in the same region where stellate cells already reside.

The liver-specific natural killer cells, pit cells, were found in the sinusoidal lumen and in close association with endothelial and Kupffer cells. Pit cells act as the first line of defence in the liver and destroy target cells by bringing about apoptosis and necrosis. They contained numerous small electron-dense membrane-bound granules and larger vesicles that were either electron-lucent or contained an amorphous electron-dense interior. The latter feature differed from other reports as they did not have the distinctive internal rod bridging the diameter of the vesicle. Another difference was the demonstration of single pinocytotic vesicles in the pit cells of the juvenile Nile crocodile giving them a pinocytotic function as well.

Intercalated cells with an electron-lucent cytoplasm, due to the lack of organelles, were present in groups of hepatocytes and in the space of Disse. They resembled lymphocytes, although with more abundant cytoplasm, and are reported to have an immune function.

The structure of the portal triad correlated with other descriptions and consisted of a portal vein, hepatic artery and bile duct, sometimes accompanied by a lymphatic vessel.

Additionally, concentrations of lymphoid tissue were found in this area, perhaps for increased immunity.

Plasma cells are antibody-producing cells and were regularly found in the portal tracts where antigens may enter the liver.

The isthmus consisted of the same components as the liver lobes. However, due to it being immersion-fixed and the sinusoidal contents not being removed, cytoplasmic remnants of hepatocytes were found in the sinusoids. One author explained the reason for the presence of cellular debris in the sinusoids as being a way of eliminating redundant cellular waste or to provide the body with essential substances.

The fully distended pouch-like **gallbladder** was attached caudally to the right liver lobe in the dorso-medial region by the hepatocystic ligament which is in accordance with the situation in other crocodilians. Three anatomical regions, the neck area closest to the hepatocystic ligament, the middle area constituting the body of the organ, and the blind end, were recognised. The layers of the gallbladder wall were separated into an epithelial layer, a *lamina propria,* a muscular and a serosal layer. The epithelial layer consisted of pseudostratified columnar epithelium and exhibited the normal features of absorptive cells, namely, surface microvilli, junctional complexes and basolateral interdigitations. Desmosomes were also present between the deeper lateral cell membranes. Microvilli were decreased in numbers in areas of apical bulging to allow for cell membrane permeability during exocytosis. The scanty long microvilli observed may have a possible mechano- or chemo-sensory function. Sparse cilia were also present in the epithelial cells and could have a sensory function. The presence of single cilium has not been described in other reptiles. The appearance of the epithelium depended on the current phase of the secretory cycle. Slender goblet cells represented the resting phase, the clustering of secretory granules in the subapical region signified the start of the secretory phase, followed by apical bulging, exocytosis of mucous granules and the stripping of the apical structures into the lumen being the final stages of the mucus secretory cycle. A combination of merocrine, apocrine and holocrine secretion was observed to take place. The juvenile Nile crocodile gallbladder thus has both absorptive and secretory functions. Proliferation of dark cells were present in areas of secretory activity and this is ascribed to their probable role as stem cells in balancing cell turnover. They may also represent dying cells. Glycogen granules were present. Lymphocytes were increased in number in the

basal epithelium and in the underlying *lamina propria* in areas where the epithelium was compromised and the basal lamina was thickened underneath the same regions pointing to a defense and strengthening function. The *lamina propria* consisted of a collagenous stroma containing fibroblasts, collagen fibers, nerve ganglia, blood vessels, lymphocytes and plasma cells. Smooth muscle cells with intervening collagen and fibroblasts constituted the *muscularis externa* that also contained nerve ganglia, lymphatic and blood vessels. The even nuclear profiles of these smooth muscle cells contrasted with the invaginated nuclear membranes described in other smooth muscle cells. Slivers of elastic fibers were present between the muscle-collagen layers in the *muscularis externa.* The serosal layer comprised mesothelial cells supported by a basal lamina with the cells containing prominent pinocytotic vesicles, lipid droplets, intermediate filaments and mitochondria. Cytoplasmic interdigitations and desmosomes existed between neighbouring cells. A collagenous stroma consisting of blood vessels and connective tissue supported the basal lamina and constituted the subserosa. The macroscopic and microscopic features of the juvenile Nile crocodile gallbladder are similar to that of mammals.